THE AMERICAN JOURNAL OF PATHOLOGY

VOLUME XXXIV NOVEMBER–DECEMBER, 1958 NUMBER 6

EFFECTS OF ANTIHYPERTENSIVE TREATMENT ON THE EVOLUTION OF THE RENAL LESIONS IN MALIGNANT NEPHROSCLEROSIS*

LAWRENCE J. MCCORMACK, M.D.; JEAN E. BÉLAND, M.D.; ROLAND E. SCHNECKLOTH, M.D., and ARTHUR C. CORCORAN, M.D.

From the Division of Pathology and the Division of Research, The Cleveland Clinic Foundation and The Frank E. Bunts Educational Institute, Cleveland, Ohio.

Malignant nephrosclerosis is a well-characterized renal vascular lesion, first described by Fahr[1] in 1919. It is nearly always associated with severe, persistent elevation of average levels of resting diastolic arterial pressure and with other symptoms and signs of the syndrome of malignant hypertension. It usually appears in patients less than 50 years of age, in whom it is often a complication of pre-existing, less severe hypertensive disease.[2] If treatment does not restore arterial pressure to normal levels, the course of the disease is usually marked by rapidly progressing renal failure, terminating in death of some 80 per cent of patients within one year of the onset, and of virtually all by the end of 5 years. It has now been abundantly demonstrated that remissions of this syndrome can be brought about by a variety of measures — lumbodorsal sympathectomy, treatment with bacterial pyrogens or tissue extracts and, during the past 6 years, the administration of one of a variety of potent antihypertensive drugs that have in common the capacity to lower diastolic arterial pressure. In one group of patients treated with these drugs a retrospective study[3] at 4 years showed that the incidence of survival had been increased from 3 to about 30 per cent. With present techniques it is anticipated that this survival can be doubled.

At necropsy, patients who had been under intensive antipressor therapy showed hitherto undescribed changes in the evolution of the renal lesions of malignant nephrosclerosis. The purpose of this report is to describe these changes and to contrast them with lesions of necropsied patients who had had little or no effective antihypertensive treatment.

* Presented at the Fifty-fourth Annual Meeting of the American Association of Pathologists and Bacteriologists, Washington, D.C., April 13, 1957.

Received for publication, February 7, 1958.

Material and Methods

One hundred patients with the clinical diagnosis of severe essential or malignant hypertension were studied at necropsy. All demonstrated various stages in the evolution of the renal lesions of malignant nephrosclerosis. Multiple blocks of the kidneys were fixed, usually in a modified Zenker's or a 4 per cent formalin solution, and multiple paraffin sections were prepared. These were stained with hematoxylin-eosin-methylene blue (HEM), Mallory's phosphotungstic acid hematoxylin (PTAH), Mallory-Heidenhain (MH), Masson's trichrome (MT), and Verhoeff's and Gomori's elastic tissue stains. Frozen sections prepared from formalin-fixed blocks of tissue were stained with Sudan IV.

The initial microscopic study of these sections was made without reference to or knowledge of the clinical course, although the sections of treated cases had been recognized as such prior to this critical evaluation. To enhance further the objectivity of the review, sections considered to show the influence of effective antihypertensive therapy were intermingled with those from other patients with arteriolar nephrosclerosis, untreated malignant nephrosclerosis, and with sections from patients who had no renal lesions. Repeated evaluations of the intermingled sections showed that the several groups could be recognized with a high degree of accuracy and, especially, that the sections showing the changes indicative of treated malignant nephrosclerosis were distinguishable.

Clinical Observations

Of the 100 cases, 19 were found to show evidences of "healing" or regression of the acute, destructive lesions of malignant nephrosclerosis. All 19 patients had been under treatment with potent antipressor drugs, the majority with ganglionoplegic agents (hexamethonium, pentolinium bitartrate, chlorisondamine, or mecamylamine, alone or in combination with reserpine), while some had been treated with hydralazine, alone or in combination with other drugs.

The lesions in 14 of the 19 treated patients differed greatly from those of untreated patients. The 14 constitute our group I. These patients had been under treatment for periods of 4 to 48 months, and 10 of them for more than 12 months. Their mean age was 44 years; the range from 28 to 66 years. The remaining 5 cases (group II) revealed microscopic evidences of moderate regression of lesions. Correspondingly, the duration of antihypertensive treatment in these was found to be relatively short, ranging from 3 days to 15 weeks. The shortest period of treatment consisted of an infusion of sodium nitroprusside which had maintained an average diastolic pressure of 97 mm.

of Hg for 3 days before death. The age range in group II was 44 to 55 years; the mean, 48 years. The 81 cases in group III showed typical lesions of active malignant nephrosclerosis. The age range here of 27 to 68 years (mean age 44 years) was comparable to that of the other two groups. Group III served as a control, since none of the patients had received effective antihypertensive treatment. Some had been given bacterial pyrogens or had been subjected to lumbodorsal sympathectomy or even total adrenalectomy, but these procedures had not resulted in significant, sustained lowering of diastolic pressure.

In order to detect the association between the efficacy of treatment and the nature of the renal vascular lesions, responses to treatment were graded as "good" (average supine diastolic pressure less than 100 mm. of Hg and evidence of clinical improvement), "fair" (moderate decrease in supine diastolic average pressure but to levels greater than 100 mm. of Hg and some clinical improvement) and "poor" (no decrease in blood pressure or a decrease only in standing diastolic pressure, often in association with remission of the syndrome of malignant hypertension and minor improvement). Of the 19 patients in groups I and II, 17 had maintained diastolic pressure averages of more than 126 mm. of Hg prior to treatment. Good responses occurred in 7 and were maintained for from 5 to 26 months; 11 showed only fair responses for periods of 1 to 24 months; 1 patient had a poor response. At the time of death, while still under treatment, only 4 of the 7 patients responding well initially continued to do so, and at that time 7 of the 19 patients were responding poorly to therapy.

In 14 of the 19 treated patients, papilledema was present when treatment was started. All, however, had evidences of progressive, severe hypertensive vascular disease, compatible with a diagnosis of malignant hypertension. At the time of death, papilledema was present in 6 and absent in 13 patients.

Of the 19, 6 had pretreatment evidences of moderate to severe renal damage, manifested by proteinuria and by urea or creatinine retention. At the time of death, 15 had severe renal failure and most of these demonstrated the uremic syndrome. Pretreatment blood urea levels of these 19 patients averaged 59 mg. per 100 ml., with levels of more than 100 mg. per 100 ml. in 3 patients. Progression of renal damage can be inferred from the fact that at the time of death the mean blood urea nitrogen value for the group was 199 mg. per 100 ml., and the level was greater than 100 mg. in 15. Renal failure was the primary cause of death of 14 patients; one patient each died of cardiac failure, pulmonary fibrosis, meningitis, hypertensive encephalopathy, and dissecting aortic aneurysm.

Morphologic Observations

The kidneys of treated patients (groups I and II) did not differ appreciably in gross appearance from those of patients who had not received treatment or in whom treatment had been ineffective in lowering arterial pressure (group III).

However, as noted above, the histologic sections showed substantial differences between groups I and II on the one hand and group III on the other (Table I). These were most strikingly delineated in sections stained with PTAH. In panoramic scanning under low power, a greater amount of tissue staining brown was present in groups I and II than in group III. The difference was due to an apparent increase in connective tissue in the renal parenchyma in groups I and II. While in some this change was focal only (Fig. 1), in most cases it was diffusely distributed (Fig. 2). Focal fibrosis occurred in association with parenchymal tubular atrophy, whereas diffuse fibrosis was accompanied by a less severe but generalized reduction in the total mass of renal tubules. In addition, large amounts of purple-staining intratubular cast material were only rarely demonstrable in the treated groups. Instead, the tubules appeared dilated and lined by flattened epithelium. This appearance of tubular atrophy was most pronounced in both the proximal and distal convoluted segments. If the term "tranquillity" may be applied to a morphologic pattern, it describes the over-all histologic appearance seen in treated malignant nephrosclerosis when contrasted with the violent aspect of sections from the control group.

The most significant differences were in the renal arteries and arterioles. Thus, renal hilar and interlobar arteries in group III showed few abnormalities (Fig. 3) while, in contrast, corresponding vessels in groups I and II exhibited extensive subintimal fibrosis (Fig. 4) and, occasionally, complete occlusion. The arcuate and interlobular arteries in group III were thickened, with fragmentation, reduplication of the elastica, and some proliferation. The musculature contained many foci of necrosis which took a brilliant red stain with MH and stained positively for fibrin with PTAH (Fig. 5). Some of these vessels showed evidence of recent and, occasionally, old thrombosis, with hemorrhage extending through the vascular wall. Corresponding vessels in groups I and II revealed a considerable reduction in the extent of vascular damage. Indeed, in group I, the only common residua of this damage were the occurrence of thickened vascular walls and, here and there, of luminal obliteration by fibrous tissue, at times resembling healed lesions of polyarteritis nodosa (Fig. 6). Sections stained with PTAH contained rare foci exhibiting intramural deposition of fibrin; the red

masses observed in group III sections stained with MH were rare. Lesions in group II were intermediate in degree between those of groups I and III.

The intralobular arteries and arterioles (less than 100 μ in diameter)

TABLE I

Summary of Renal Arterial and Glomerular Lesions in 100 Patients with Malignant Nephrosclerosis

Type of lesion	Treated patients (19)		Untreated patients (81)
	Group I No. of cases	Group II No. of cases	Group III No. of cases
Necrotic arterioles per 100 arterioles			
None	3	0	2
1 – 5	11	3	14
6 – 10	—	2	21
11 – 20	—	—	23
21 – 30	—	—	16
31 – 40	—	—	5
	(Maximum–2)	(Maximum–10)	(Maximum–34)
Necrotic glomeruli per 100 glomeruli			
None	9	0	8
1 – 5	5	4	26
6 – 10	—	0	12
11 – 20	—	1	33
21 – 30	—	—	2
	(Maximum–2)	(Maximum–14)	(Maximum–28
Atheroma of arterioles per 100 arterioles			
None	14	2	55
1	—	2	11
2	—	1	9
3	—	—	6
Arteriosclerosis of large arteries			
Absent	0	1	12
Slight	2	2	57
Moderate	4	1	9
Marked	8	1	3

in group III invariably showed extensive and typical changes of malignant nephrosclerosis. Corresponding vessels in groups I and II differed in several respects, although the so-called "onion peel" or lamellar fibroelastic hyperplastic lesions were present also in group III. One difference was that the hyperplastic vessels seemed less

swollen and edematous in groups I and II. A greater difference, however, was in the frequency of arteriolar necrosis and occlusion. Thrombosis and thrombonecrosis occurred with an average incidence of 12 in 100 counted arterioles in each case in group III, but was detected in fewer than 2 in 100 arterioles and often in none at all in group I. There was an average maximum incidence of 9 lesions in 100 vessels in group II. The smaller arterioles were often visualized with difficulty in groups I and II; occasionally all that could be seen was thickening of their walls.

Small focal accumulations of lipid-laden histiocytes were evident within the interstices of the thickened walls of small arteries and arterioles in 33 of the 81 cases in group III, but were not manifest in any of the vessels in groups I and II. This lesion is believed to represent an initial phase of atheroma formation. The fact that it was not seen in groups I and II is evidence that the process is reversible.

Necrosis of preglomerular arterioles observed in group III was commonly associated with glomerular lesions of focal or total necrosis (Fig. 7). This occurred with an average incidence of 7 per 100 glomeruli in group III; in one case the incidence was 28 in 100. Glomeruli in groups I and II showed a high incidence of scarring (Fig. 8), but the frequency of necrosis was low, varying from 0 to 2 per 100 counted. Over-all glomerular hyalinization was not associated with arteriolar lesions; when it was present, clusters of glomeruli were affected and the lesion was often traced to old thrombosis in an adjacent interlobular artery.

Discussion

The data demonstrate that the clinical remission effected in patients with malignant nephrosclerosis by intensive treatment with antihypertensive drugs is associated with a corresponding remission in the histologic lesions of renal vascular disease and with a change in their nature. The most obvious alteration was cessation of activity and regression in both arteriolar necrosis and thrombonecrosis. This was associated with disappearance of most of the foci of fibrin accumulation and of the evidence of acute vascular damage. The change was best demonstrated in the patients in group I, all of whom had shown at least an initially favorable response to treatment. In most of these patients treatment had been continued for longer periods than in the case of patients in group II.

A second major difference in lesions was the appearance of parenchymal and perivascular fibroplasia with focal or diffuse renal parenchymal atrophy in treated patients. These were not manifest in the ineffectually treated controls.

A third, highly significant difference was in the distribution of vascular lesions. In group III the lesions appeared primarily in arterioles and small arteries, leaving large arteries intact; in groups I and II the large arteries showed extensive subintimal fibrosis which, in some instances, progressed to vascular occlusion. Medium-sized arteries, such as the arcuate and interlobular vessels, of the treated groups showed regression of the manifestations of acute vascular injury. Here, again, in some lesions there were evidences of fibrous vascular occlusion which resembled healed periarteritis nodosa. As observed elsewhere,[4] these lesions resembled those encountered in hypertensive vascular disease induced in rats which were subsequently treated with an antipressor agent.

In a previous paper,[3] which included many of the patients listed in groups I and II, it was emphasized that the severely hypertensive patient when treated effectively does not die as the result of the hypertensive disease *per se,* but succumbs to complications of progressive atherosclerosis. Among these were listed cerebral hemorrhage and thrombosis, myocardial infarction, dissecting aneurysm, and slowly progressive renal failure. These complications usually occurred in patients with the more severe forms of hypertension prior to treatment and in those whose responses to treatment were poor. The nature of the renal lesion leading to failure has been described in the present paper. Although the acute lesions of malignant hypertension may be almost completely reversible and proceed to healing, the hypertensive state results in damage to large and medium-sized arteries. This may, in part, contribute to the subsequent appearance of atherosclerosis and fibrous intimal hyperplasia even though arterial pressure is more or less controlled. This lesion, which affects renal vessels diffusely, would account for the progressive renal failure occurring in the majority of the patients in the treated group. Moreover, since in some patients treatment was not wholly suppressive, minimal active lesions of malignant nephrosclerosis persisted and were apparently progressive, although at a much slower rate than in cases not treated with antihypertensive drugs. This, too, might eventuate in renal failure. Lastly, the data compiled support the conclusion derived from experimental studies[4] that the acute destructive vascular lesions of malignant nephrosclerosis are caused by increased arterial pressure.

Summary and Conclusions

1. Treatment of malignant hypertension with potent antihypertensive drugs greatly alters the evolution of renal vascular lesions in this disease.

2. The lesions were studied in large numbers of sections procured from kidneys of 100 necropsied patients who had had malignant nephrosclerosis. Nineteen of these had been under treatment with antipressor drugs.

3. Treated patients, especially those who had been under therapy for long periods of time, almost always exhibited remission and healing of the acute arteriolar lesions: thrombosis, thrombonecrosis and glomerular necrosis.

4. These patients also showed a noteworthy alteration in the nature of the vascular disease. Large and medium-sized renal arteries revealed subintimal fibroplasia with progression to occlusion in some vessels. It is this lesion which presumably leads to the slowly progressive renal failure which was the cause of death in a majority of the treated patients in the group.

5. The observations substantiate the clinical inference that patients with therapeutically induced remission of malignant hypertension exhibit an increased incidence of arteriosclerosis and its complications. This presumably reflects the damage inflicted upon the arteries during the pretreatment period of uncontrolled hypertension. The lesions observed in treated patients correspond to those encountered in hypertensive rats receiving a potent antipressor agent.

REFERENCES

1. Fahr, T. Über Nephrosklerose. *Virchows Arch. path. Anat.*, 1919, 226, 119–178.

2. Keith, N. M.; Wagener, H. P., and Barker, N. W. The problem of prognosis in essential hypertension: a follow-up study in 219 cases. *Tr. A. Am. Physicians*, 1938, 53, 81–87.

3. Corcoran, A. C.; Dustan, H. P., and Page, I. H. Antidiuresis and other renal responses to piperoxan in pheochromocytoma. *Circulation*, 1956, 14, 221–226.

4. Masson, G. M. C.; McCormack, L. J.; Dustan, H. P., and Corcoran, A. C. Hypertensive vascular disease as a consequence of increased arterial pressure. Quantitative study in rats with hydralazine-treated renal hypertension. *Am. J. Path.*, 1958, 34, 817–833.

LEGENDS FOR FIGURES

FIG. 1. Renal cortex showing focal but severe atrophy with interstitial fibrosis. Note tubular dilatation and lack of casts. Phosphotungstic acid hematoxylin (PTAH) stain. × 40.

FIG. 2. Diffuse atrophy of renal cortex with interstitial fibrosis and loss of tubules. PTAH stain. × 40.

FIG. 3. Interlobar artery in patient with untreated malignant nephrosclerosis showing no major histologic lesions. PTAH stain. × 65.

FIG. 4. Interlobar artery in patient with treated malignant nephrosclerosis. Subintimal fibrosis and marked narrowing of the lumen are present. Mallory-Heidenhain stain. × 65.

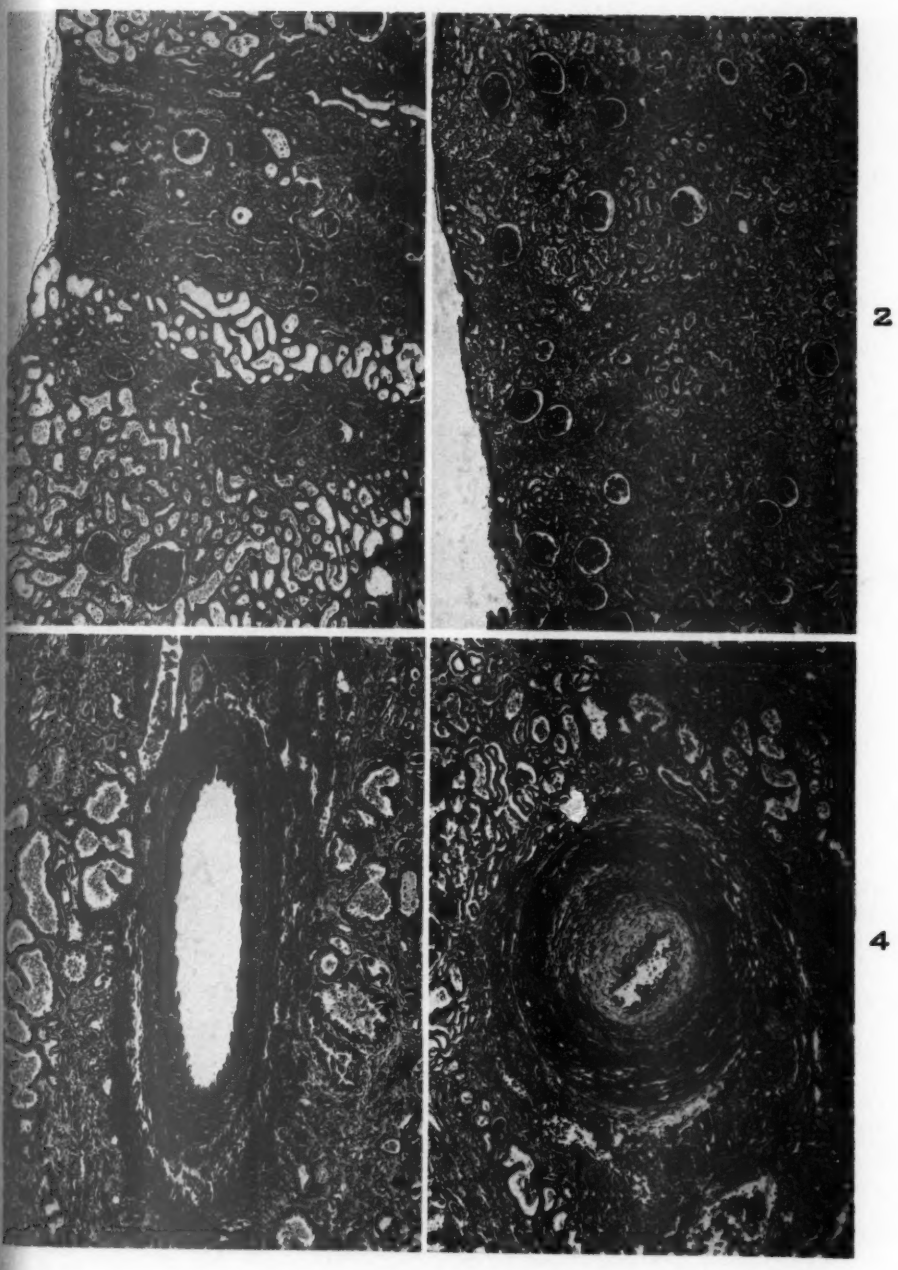

2

4

FIG. 5. Interlobular artery in patient with untreated malignant nephrosclerosis showing mural necrosis and subintimal accumulation of fibrin. PTAH stain. × 170.

FIG. 6. Interlobular artery in treated malignant nephrosclerosis. The arterial wall is partially destroyed with resultant dilatation. The lumen is filled by an organized thrombus. PTAH stain. × 170.

FIG. 7. Afferent arteriolar and lobular glomerular necrosis in untreated malignant nephrosclerosis. Fibrin deposition is prominent. A small juxtaglomerular arteriole is also affected. Note the absence of tubular dilatation and the partial retention of tubular architecture in proximal convoluted segments. PTAH stain. × 170.

FIG. 8. Lobular glomerular sclerosis believed to result from healing of lobular necrosis. Note the tubular dilatation and marked flattening of tubular epithelium. PTAH stain. × 170.

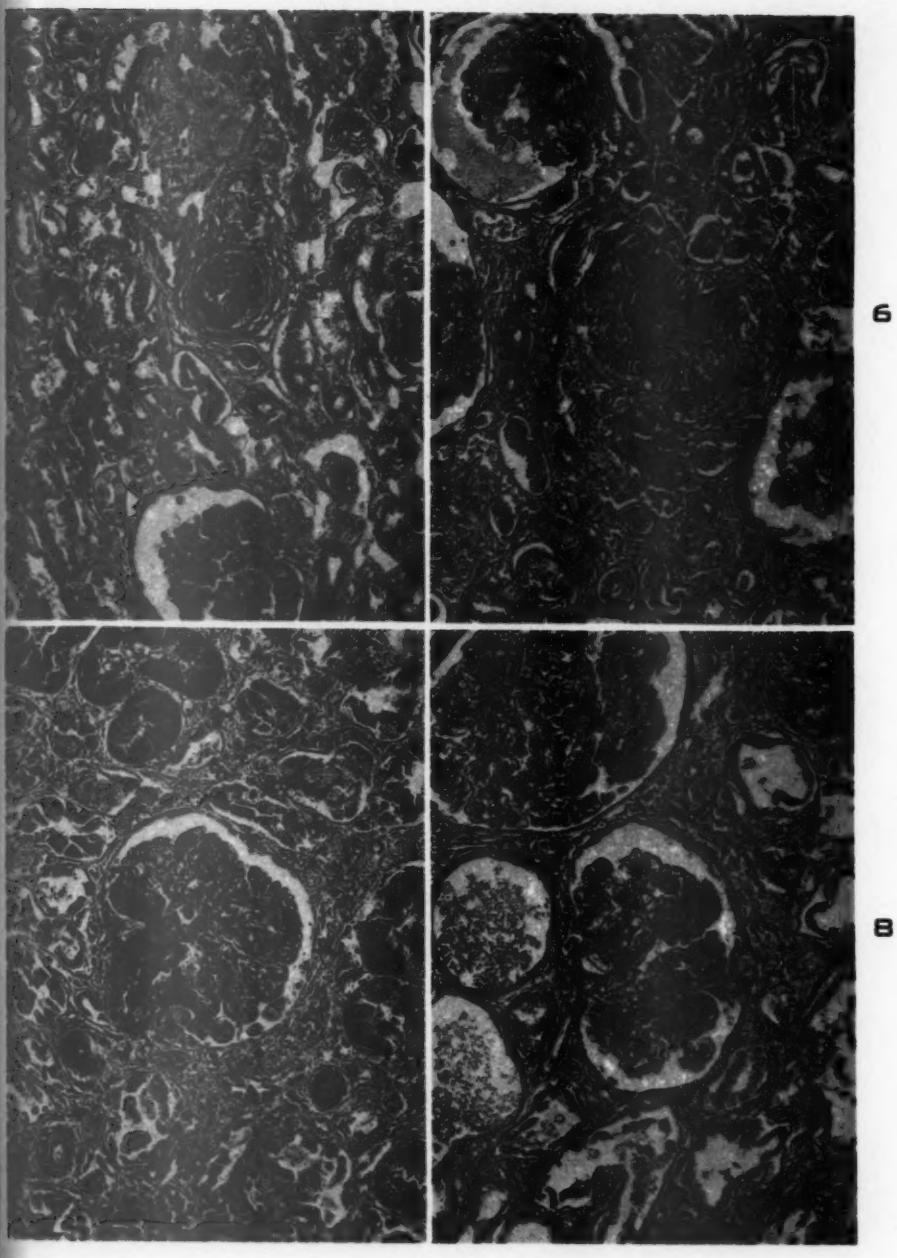

6

8

THE DIFFUSE INTIMAL THICKENING OF THE HUMAN AORTA WITH AGING *

HENRY Z. MOVAT, M.D., Ph.D.;† ROBERT H. MORE, M.D., and M. DARIA HAUST, M.D.
From the Department of Pathology, Queen's University and Kingston General Hospital, Kingston, Canada.

As a preliminary to studies on arteriosclerosis of the aorta, it was essential for us to establish the normal structure of the vessel. The lesions of arteriosclerosis are generally regarded as being focal.[1] Preceding these focal lesions there is, however, a diffuse thickening occurring in the intima, which increases with age and is more marked in the lower than in the upper aorta. These changes were well described by Jores.[2] Some investigators[3] have stated that this diffuse thickening is more prominent in the dorsal than in the ventral part of the vessel. A sex difference in the incidence of this lesion has been shown to exist in coronary arteries,[4] but Prior[5] did not collect enough material to draw a definite conclusion regarding a similar sex difference in the aorta. It is important to bear these changes in mind because they pre-exist the superimposed focal arteriosclerotic lesions.

The aim of the present study is to investigate the structure and development of the diffuse intimal thickening of the aorta in order to achieve a better understanding of the superimposed focal arteriosclerotic lesions.

MATERIAL AND METHODS

From 92 human aortas obtained at necropsy, 200 sections were prepared for study from areas which appeared grossly normal. Each aorta was opened longitudinally along the lesser curvature of the arch and along the line of origin of the right intercostal arteries. If normal areas were present, blocks were taken from the ascending (or arch), upper and lower thoracic and upper and lower abdominal aorta, from both the ventral and dorsal walls. All blocks were fixed for 72 hours either in Lillie's buffered 10 per cent formalin (pH 7)[6] or for 24 hours in formol sublimate acetic solution. Following fixation, each of the specimens was bisected, one part being placed in 70 per cent ethanol (for embedding in paraffin), the other being left in the fixative for embedding in carbowax. The following stains were carried out: he-

* Supported by grants-in-aid from The Bickell Foundation of Toronto, Canada, and the Public Health Research Grants of Canada.
Received for publication, March 24, 1958.
† Present Address: Department of Pathology, University of Toronto, Banting Institute, Toronto, Canada.

malum, phloxine, saffron; pentachrome II (omitting elastica); elastica (Weigert-Hart, nuclear fast red, metanil yellow); Fettrot and hematoxylin. Additional stains for other purposes were made, as described in another publication.[7]

Results

In the fetus, the endothelium was intimately adherent to the internal elastic lamina (Fig. 1). Occasionally, however, some splitting of the internal elastic lamina was encountered. Most newborn infants showed some splitting of the internal elastic lamina resulting in a minimal thickening of the intima (Fig. 2). If the aorta of a newborn infant was coiled and embedded as a whole, patches of splitting of the elastica were detected throughout the vessel. A microscopically distinguishable intima was demonstrable between the age of 6 months to one year. The intima was thicker in the distal than in the proximal parts of the aorta. One could see either two elastic membranes with smooth muscle cells between them and the endothelium covering the innermost elastic membrane; or a prominent internal lamina and an intima composed of several delicate elastic fibers and membranes, intermingled with smooth muscle cells (Fig. 3). Collagen fibers were few in this early intima but metachromatic ground substance was abundant (Fig. 4).

During the second decade of life, a well developed intima was present throughout the aorta, being much thicker in the distal (Fig. 6) than in the proximal (Fig. 5) part. When this intima had attained considerable thickness, one could, as a rule, distinguish a musculo-elastic layer and an elastic-hyperplastic layer[8] (Fig. 6). In the musculo-elastic layer smooth muscle cells were arranged longitudinally, i.e., parallel to the long axis of the aorta. The layer was usually well separated by the internal elastic lamina from the media, in which the smooth muscle cells had a circular arrangement. The elastic-hyperplastic layer was composed of irregularly arranged smooth muscle cells, occasional histiocytes and fibroblasts, delicate elastic fibers, and ground substance. Not infrequently, smooth muscle cells were oriented as if migrating from the media through openings in the internal elastic lamina into the intima (Fig. 7). The smooth muscle cells of the intima were sometimes small, delicate, and difficult to recognize as such. Often, however, they had typical elongated, somewhat wavy, chromatin-rich nuclei and slender, tapering, acidophilic cytoplasm containing several myofibrils. The myofibrils were best demonstrable as dark purplish-blue when stained with phosphotungstic acid hematoxylin stain (PTAH) (Fig. 6), and as red with the trichrome stain.

Differences between proximal and distal parts of the aorta were most

constant from the first to the fourth decades. In older ages the diffuse intimal thickening varied considerably from case to case. In the aorta of a 24-year-old individual, for instance, one could clearly recognize a progressive thickening from the proximal to the distal portions. Whereas in the upper thoracic aorta (Fig. 8) the intima was quite thin, in the upper abdominal part (Fig. 9) it had attained 2 to 3 times, and in the lower abdominal part (Fig. 11) it often measured 8 to 10 times the thickness of the intima of the thoracic aorta. Differences between the ventral and dorsal portions were not constant. Sometimes the intima of the dorsal aorta was thicker than the ventral and vice versa. (Figs. 9 and 10). Three layers were frequently discernible, particularly in the abdominal aorta (Fig. 11). External to the internal elastic lamina lay the musculo-elastic layer with longitudinally arranged smooth muscle cells and elastic fibers. A hyperplastic elastic layer, composed mainly of irregularly arranged smooth muscle cells and elastic fibers, was situated between the musculo-elastic layer and the innermost connective tissue layer. The latter was at times well demarcated by a thick elastic membrane and consisted of ground substance, delicate collagen and elastic fibers, and a few cellular elements.

After the fifth decade, but particularly in old age, the intima often had attained a considerable thickness. The thick intima of old age frequently showed a pattern of three layers (Figs. 13 to 15), but sometimes only two layers were present in spite of a considerable thickness. The various elements could be best distinguished in pentachrome I stained sections (Fig. 12) in which red smooth muscle cells and black elastic fibers were found embedded in a blue staining ground substance. In addition, yellow collagen fibers were found in the elastic-hyperplastic and connective tissue layer. Increased amounts of acid mucopolysaccharide (Fig. 15) could be demonstrated in the elastic-hyperplastic layer, particularly when there was some fragmentation of elastic fibers (Fig. 14). The connective tissue layer contained less acid mucopolysaccharide than in the younger age group and often had a hyalinized appearance (Fig. 15).

In the ascending aorta and arch, the splitting of the internal elastic lamina permitted, at times, a clear separation of the intima from the underlying media. In other cases, splitting caused a broadening of the internal elastic lamina (Fig. 16).

The diffuse thickening of the intima in the lower abdominal aorta was sometimes considerable and was associated with collagenization of the musculo-elastic and elastic-hyperplastic layers and atrophy of smooth muscle and elastic elements. This also affected the inner por-

tions of the media (Fig. 17). The connective tissue layer in such cases occasionally contained a number of foam cells (Fig. 17).

Whereas, in regions which appeared normal grossly, intracellular accumulation of lipids seldom occurred, extracellular accumulation was found in some aortas after the third and fourth decades and was quite frequent after the fifth decade. The lipid, which was not visible grossly, was found mainly along the internal elastic lamina as a single thick band or several thinner bands (Figs. 18 and 19). Small amounts of finely dispersed lipid was at times distributed diffusely throughout the intima, but it always showed a tendency to accumulate along the elastic fibers and membranes. When the internal elastic lamina showed a band-like splitting, as seen in Figure 16, one had the impression that lipid had precipitated not only along but also within or between the split delicate elastic fibrils (Fig. 18).

Discussion

Transitions from the diffuse alterations which we have described to arteriosclerotic lesions are often very gradual.[9] Jores[2] considered the diffuse changes to be normal because they occurred in all individuals. According to him, they were not physiologic because of their irregular development and distribution in the various portions of the vascular system, their gradual transition to pathologic lesions, and their absence in animals. Jores believed that functional and mechanical stress during life, particularly of hydrodynamic nature, was responsible for the development of the diffuse intimal thickening. That the stress which occurs in hypertension caused marked thickening has been shown recently by Wilens.[8]

We are in agreement with Jores that the most marked thickening appears in the first 3 decades of life, i.e., during the period of vascular growth (*"erste oder aufsteigende Periode des Gefasswachstums"*).[2] It is true also that this first period is followed by a second, extending into the middle or end of the fourth decade, during which no considerable further change occurs. During a third or declining (*"absteigende"*) period, there seems to be not only collagenization as believed by Jores and Aschoff, but also some further increase in thickness. Collagenization is associated with an alteration in the structure of the elastic elements.[10] Often these undergo atrophy in both the intima and the media (Fig. 17). It is this loss in the functional capacity of elastic tissue, associated with atrophy of the smooth muscle and increase of collagenous tissue, which, in our opinion, predisposes to the development of focal arteriosclerotic lesions.

These studies confirm the earlier findings of Jores that the intima increases in thickness with age, and also that the increase is more marked in the distal than in the proximal portions of the vessel. Arteriosclerosis is most severe in regions where the diffuse intimal thickening is most marked. On the other hand, arteriosclerotic lesions seldom occur in the absence of diffuse intimal thickening, i.e., in young individuals and in the proximal portions of the aorta. These relationships and the absence of spontaneous arteriosclerosis in animals, which show no age changes in the intima, strongly suggest that diffuse intimal thickening predisposes to the development of arteriosclerosis.

It will be the scope of subsequent publications to deal with the various focal arteriosclerotic lesions which are superimposed on the diffuse intimal changes described in this paper.

SUMMARY

The structure of the diffuse intimal thickening of the aorta, which develops in postnatal life, is described.

This thickening increases with age and is more marked in the distal than in the proximal portion of the aorta. During the first 3 decades there is little individual variation, but in old age the degree of diffuse intimal thickening may vary from case to case. The diffusely thickened intima may be composed of 1, 2, or 3 layers, a musculo-elastic, an elastic-hyperplastic, and a connective tissue layer.

The diffuse thickening of the aorta is considered to be a normal developmental and aging process and not a part of arteriosclerosis although it undoubtedly represents one of the local factors which predisposes to the inception of arteriosclerosis. The focal arteriosclerotic lesions are superimposed on the diffuse intimal thickening.

REFERENCES

1. Duff, G. L., and McMillan, G. C. Pathology of atherosclerosis. *Am. J. Med.*, 1951, 11, 92–108.
2. Jores, L. Arterien. In: Handbuch der Speziellen Pathologischen Anatomie und Histologie. Band II, Herz und Gefässe. Henke, F., and Lubarsch, O. (eds.). Julius Springer, Berlin, 1924, pp. 608–786.
3. Wilens, S. L. The nature of diffuse intimal thickening of arteries. *Am. J. Path.*, 1951, 27, 825–839.
4. Dock, W. The predilection of atherosclerosis for the coronary arteries. *J. A. M. A.*, 1946, 131, 875–878.
5. Prior, J. T., and Jones, D. B. Structural alterations within the aortic intima in infancy and childhood. *Am. J. Path.*, 1952, 28, 937–951.
6. Lillie, R. D. Histopathologic Technic and Practical Histochemistry. The Bakiston Co., Inc., New York and Toronto, 1954, 501 pp.

7. Movat, H. Z., and More, R. H. The nature and origin of fibrinoid. *Am. J. Clin. Path.*, 1957, 28, 331–353.

8. Gross, L.; Epstein, E. Z., and Kugel, M. A. Histology of the coronary arteries and their branches in the human heart. *Am. J. Path.*, 1934, 10, 253–274.

9. Langhans. Quoted by Jores.[2]

10. Schwarz, W. Elektronenmikrospische Untersuchungen der Altersveränderungen in der Media der menschlichen Aorta. *Virchows Arch. path. Anat.*, 1954, 324, 612–628.

LEGENDS FOR FIGURES

FIG. 1. Aorta of 7-month-old fetus. Endothelium is firmly adherent to the internal elastic lamina (A); no intima is present. Weigert-Hart elastica, nuclear fast red, and metanil yellow stains. × 307.

FIG. 2. Aorta of newborn infant. There is splitting of the internal elastic lamina at (A) with formation of minimal diffuse thickening of the intima. Stain and magnification as in Figure 1.

FIG. 3. Aorta of 6-month-old infant. The intima above the internal elastic lamina (A) is composed of longitudinally arranged elastic fibers with smooth muscle cells between them. Stain and magnification as in Figure 1.

FIG. 4. Aorta of 5-year-old child. Internal elastic lamina shows splitting. Newly formed intima contains abundant metachromatic ground substance (gray in photomicrograph). Toluidine blue stain. × 307.

FIG. 5. Upper thoracic aorta of 16-year-old male. The intima is thin, and there are longitudinally arranged smooth muscle cells internal to the internal elastic lamina (A). Heidenhain's azan stain. × 307.

FIG. 6. Abdominal segment of the aorta shown in Figure 5. There are two layers: the musculo-elastic layer between (A) and (B) and the elastic-hyperplastic layer above (A). Phosphotungstic acid hematoxylin stain. × 307.

FIG. 7. This illustration shows the growth or migration of smooth muscle cells from the media through an opening in the internal elastic lamina (A) into the musculo-elastic layer of the intima. Trichrome stain. × 307.

FIGS. 8 to 10. Aorta of 24-year-old female. A thin intima is present above the internal elastic lamina (A) in the posterior upper thoracic aorta (Fig. 8). In the posterior upper abdominal aorta (Fig. 9), splitting of the internal elastic lamina (B), formation of a *lamella* (or *membrana*) *interna* (A), and several longitudinally arranged elastic fibers are seen. Formation of an internal elastic lamina (B) and membrane (A) is seen in Figure 10, representing the anterior abdominal aorta; this is thicker than the posterior wall. Stain as in Figure 1. × 184.

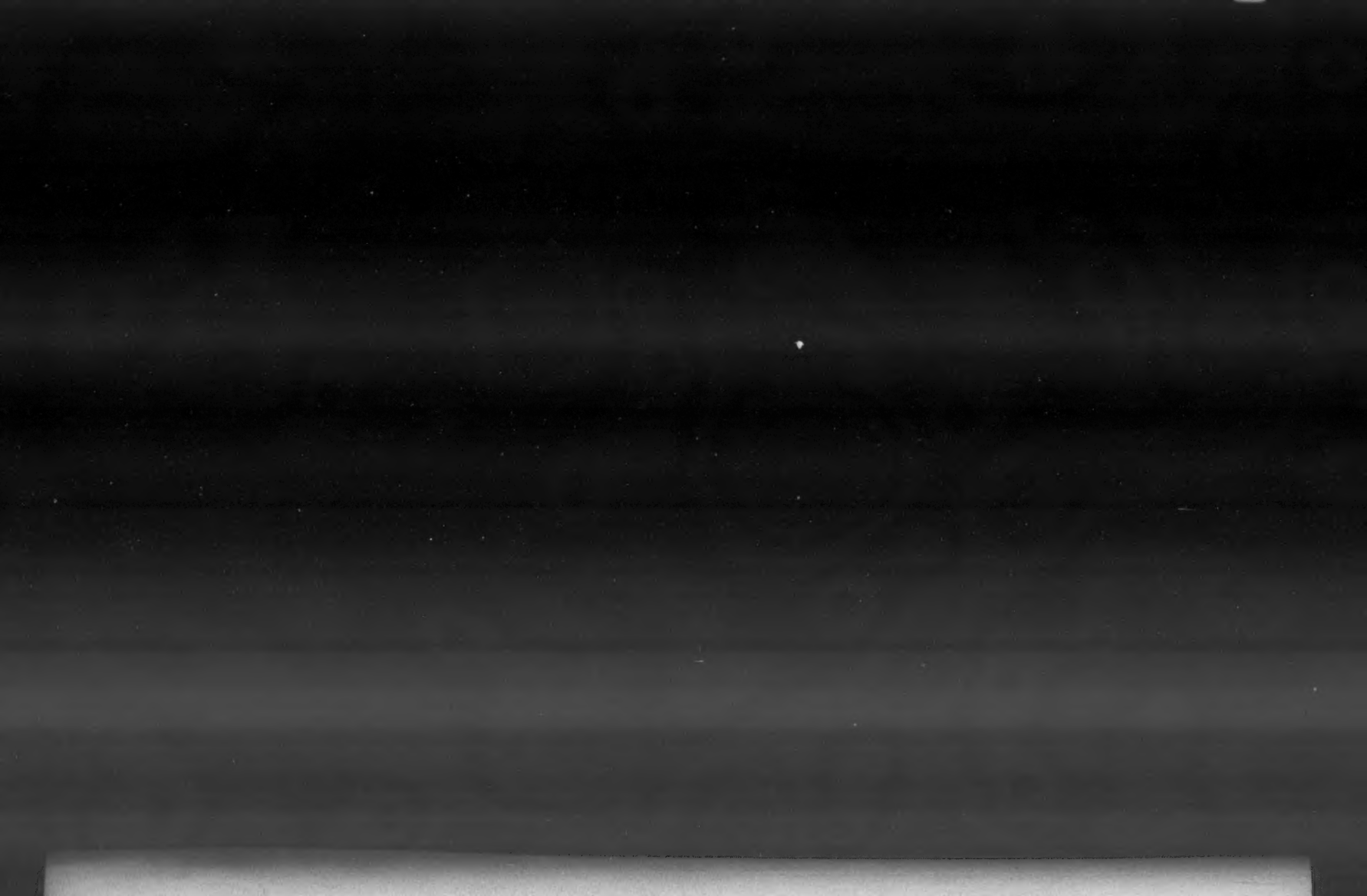

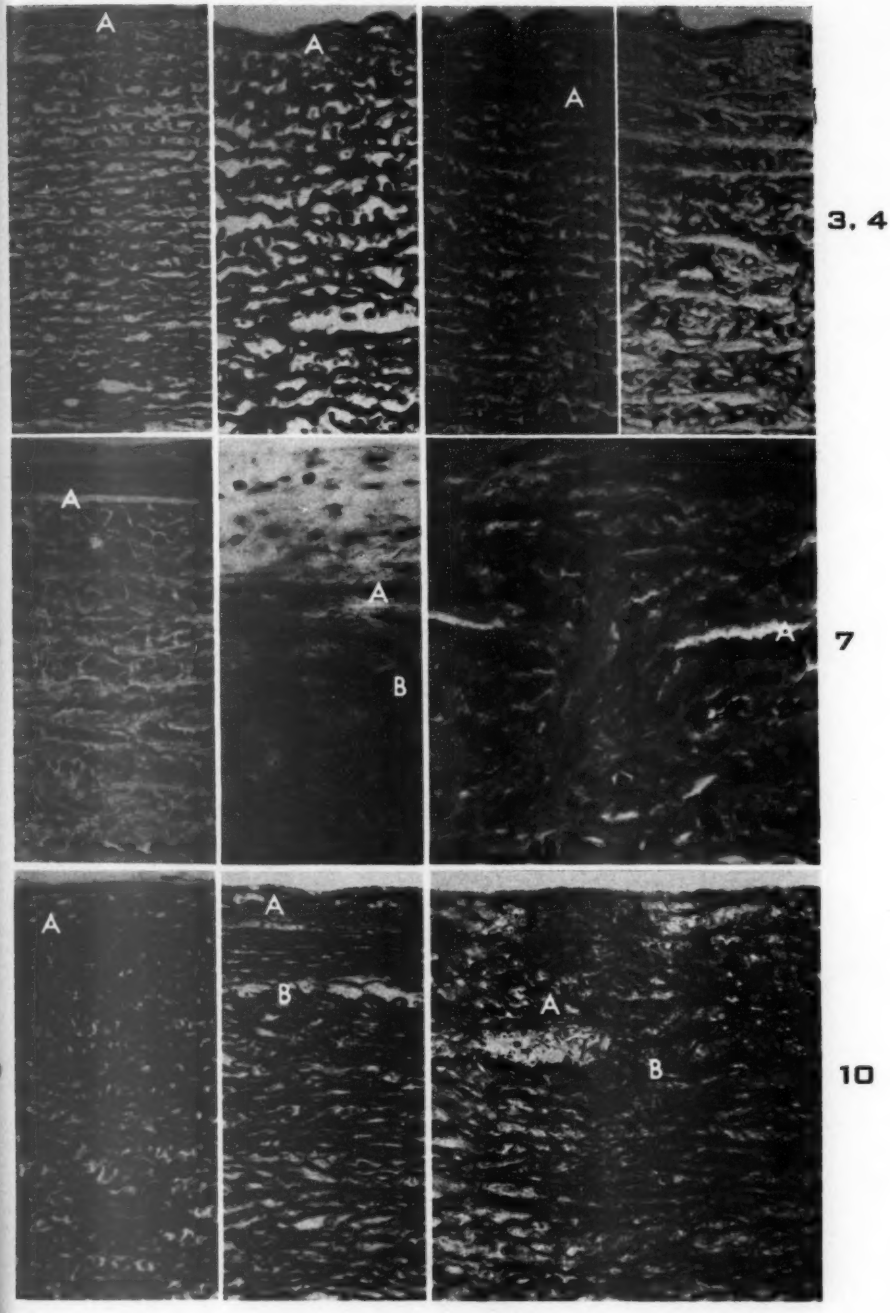
A
A
A
2
3, 4
A
A
B
6
7
A
B
A
B
9
10

FIG. 11. The abdominal aorta from case shown in Figures 8 to 10. There are 3 layers: a connective tissue layer, from lumen to (A); an elastic-hyperplastic layer (A to B); and a musculo-elastic layer (B to C). Weigert-Hart, nuclear fast red, and metanil yellow stains. × 184.

FIG. 12. Upper abdominal aorta of 49-year-old male. A markedly thickened intima appears above the prominent internal elastic lamina (B). The musculo-elastic layer can be recognized between (A) and (B). In spite of marked thickening there is no clear distinction between the 3 layers. Pentachrome I stain. × 184.

FIG. 13. Upper thoracic aorta, anterior wall, of a 59-year-old male. There is a clear separation between the 3 layers: connective tissue layer (lumen to A), elastic-hyperplastic layer (A to B) and musculo-elastic layer (B to C). Stain as in Figure 11. × 184.

FIG. 14. Lower abdominal aorta of a 67-year-old male. Intima is composed mainly of connective tissue (from lumen to A) and elastic-hyperplastic (A to B) layers. The musculo-elastic layer (B to C) is thin. Stain as in Figure 11. × 184.

FIG. 15. Lower abdominal aorta shown in Figure 14, stained to demonstrate acid mucopolysaccharide and PAS-positive structures. Acid mucopolysaccharide (blue in slide, pale gray in photograph) is increased in the elastic-hyperplastic layer (A to B). Smooth muscle cells in the elastic-hyperplastic (A to B) and musculo-elastic (B to C) layers are seen to be surrounded by reticulin fibers (purplish-red in slide, and black in photograph). The connective tissue layer (A) appears somewhat homogeneous. It stained faintly with both Alcian blue and periodic acid-Schiff stains. Alcian blue, PAS, hematoxylin, and orange G stains. × 184.

FIG. 16. Arch (anterior) of 59-year-old male. Splitting of the internal elastic lamina (A) causes a band-like appearance. The intima above it appears homogeneous and acellular. Stain as in Figure 11. × 184.

FIG. 17. Lower abdominal aorta of a 60-year-old male showing early arteriosclerosis. There is collagenization of the elastic-hyperplastic and musculo-elastic layer (A to B), and atrophy of smooth muscle cells in both the intima and media. Foam cells are present in the connective tissue layer. Stain as in Figure 11. × 92.

FIG. 18. Upper abdominal aorta, posterior wall, of a 69-year-old male. Lipid (black in the photograph) is seen deposited along the internal elastic lamina. Fettrot and hematoxylin stains. × 184.

FIG. 19. Another region in the upper abdominal aorta a few centimeters distal to the area shown in Figure 18. Lipid is deposited along the frayed internal elastic lamina. Fettrot and hematoxylin stains. × 184.

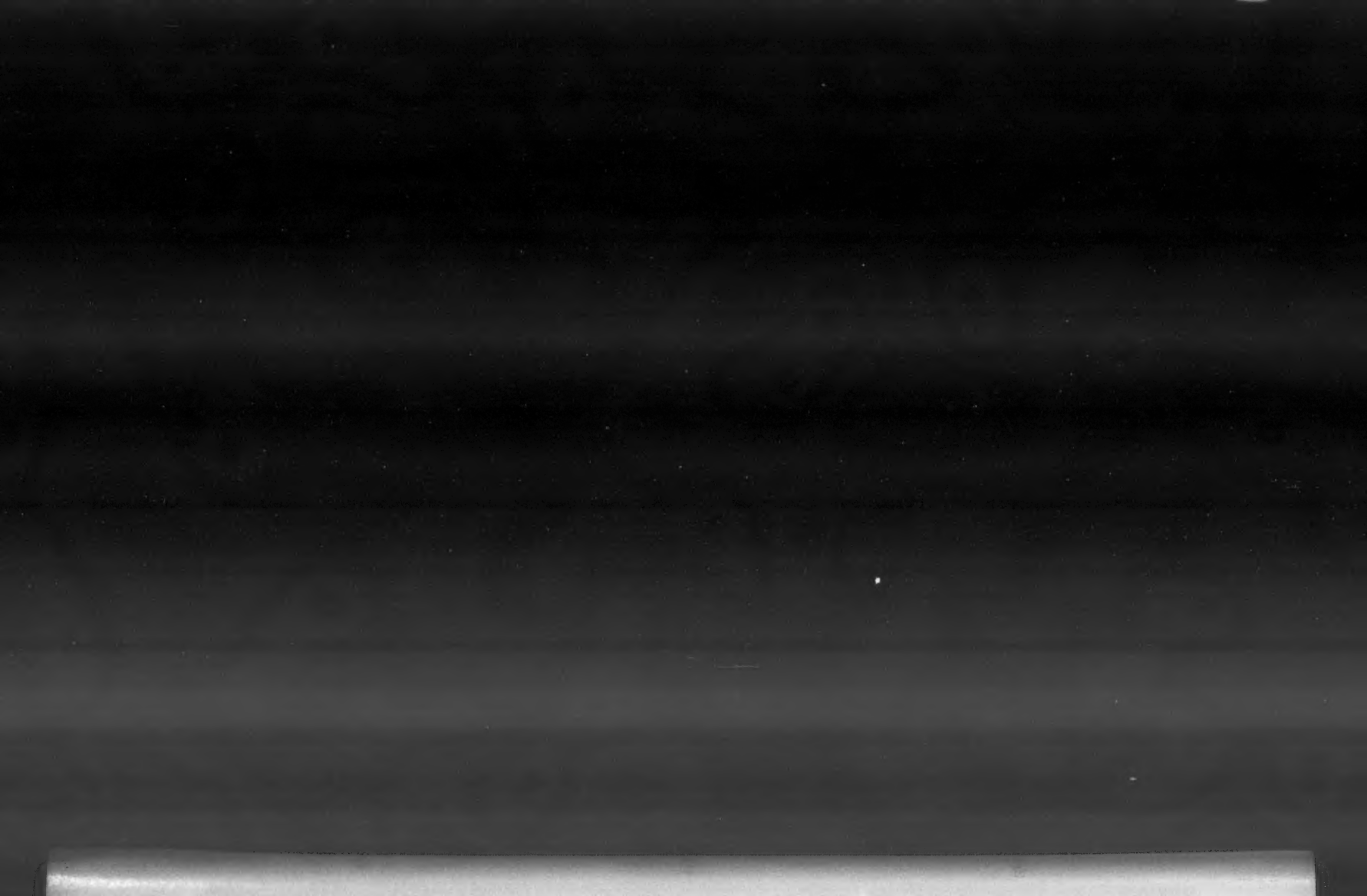

12

14

17

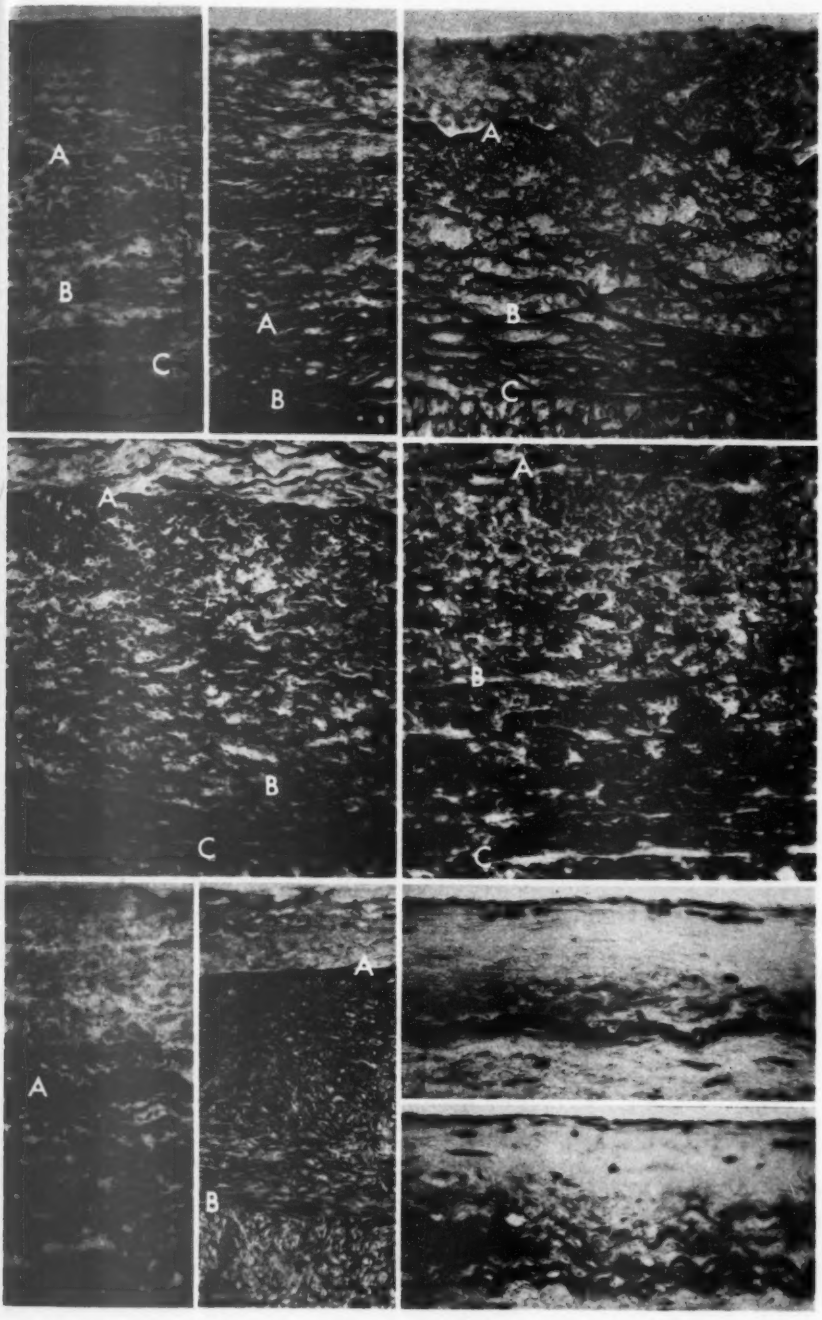
12
A
B
C
A
B
13
A
B
C
14
A
B
C
15
A
B
C
17
A
A
B
18
19

PULMONARY CAPILLARY PROLIFERATION INDUCED BY OXYGEN INHALATION *

PHILIP C. PRATT, M.D.

From the Ohio Tuberculosis Hospital, and the Department of Pathology, Ohio State University College of Medicine, Columbus, Ohio.

Pulmonary physiologists have long known that a progressive alteration in pulmonary function occurs during prolonged exposure to inhalation of atmospheres containing high concentrations of oxygen. Not only is there a progressive loss of vital capacity over a period of several days' exposure, but recovery of the original vital capacity is slow and may require several days.[1,2] Examination of pulmonary tissue from animals sacrificed after days or weeks of exposure to increased oxygen has revealed such features as "hyperemia,"[1,3,4] "engorgement and hemorrhage,"[5] "fibrinous pneumonia and congestion,"[6,7] and "damage to capillary walls."[2]

On several occasions the author has had opportunity to examine pulmonary tissue from persons who had died following prolonged progressive pulmonary disease, and who had had oxygen therapy for considerable periods before death. A peculiar similarity in the appearance of several such lungs, even though the causes of the pulmonary insufficiency were different, gave rise to the suspicion that oxygen might be contributing to the terminal structural abnormality. In essence, the lesion appeared to be an overgrowth of capillaries in the alveolar septums. Since a search of the literature revealed scattered descriptions of this type of reaction but none in which it was attributed to oxygen inhalation, a number of necropsy cases were reviewed with specific attention to the possible influence of oxygen upon pulmonary tissue.

MATERIAL AND METHODS

Two groups of cases were chosen for study. Group I was selected by examination of a series of clinical records from the University Hospital, Columbus, Ohio. A consecutive series of 10 necropsied patients was selected on the basis of their having received oxygen therapy during the hospital stay. The microscopic sections of pulmonary tissue were re-examined in order to determine the presence or absence of capillary proliferation. In this laboratory it is customary to prepare at least 3 sections from different lobes of the lungs, and often a section from each lobe is available. All slides in each case were reviewed and were similar to each other in appearance except in those instances

* Received for publication, April 16, 1958.

where one or two lobes were the seat of pneumonia or carcinoma. Stains for elastic tissue and reticulum were made on new sections prepared from the original tissue blocks.

Group II consisted of a consecutive series of 22 necropsy cases culled from the records of the University Hospital Pathology Department. The microscopic sections of pulmonary tissue were simply removed from the file, examined, and an opinion was formed as to whether or not capillary proliferation was present. The clinical records were then checked. In addition to this material, a few specimens of surgically resected pulmonary tissue and others showing pulmonary edema and atelectasis were studied in order to substantiate the belief that the lesions ascribed to oxygen exposure were specific for this condition.

Results

The clinical and histologic data in group I are arranged in order of the duration of oxygen inhalation. The observations in group II are summarized in Table I.

Group I

Case 1. Male, 57 years. Old and recent cerebrovascular accidents. There were no preceding respiratory complaints, but nasal catheter oxygen was begun on admission because of Cheyne-Stokes respiration. Oxygen administration was continued for 19 days at 7 liters per minute, ending 5 days before death. Progressive respiratory impairment was noted and was considered the probable cause of death. The total lung weight at necropsy was 870 gm.; grossly the lung tissue was "congested."

Five sections of lung tissue were available for study. All showed generalized slight to moderate alveolar septal thickening with increased numbers of congested capillaries (Fig. 1). In many small foci, alveolar structure was obscured, and in these areas fibrocytes and distinct delicate collagen fibers were noted (Fig. 2). A few foci of purulent lobular pneumonia were readily distinguished.

Case 2. Male, 77 years. Old and recent cerebrovascular accidents. There were no preceding respiratory complaints, but nasal catheter oxygen was begun on admission because of "moderate respiratory distress." It was continued for 16 days, until death, at the rate of 4 to 5 liters per minute. Progressive respiratory impairment was the probable cause of death. The total lung weight at necropsy was 990 gm.; the lungs were dark red, firm, and a "small amount of red fluid" could be expressed.

Three sections of lung tissue were available for study. All showed almost complete obliteration of alveolar spaces, with marked thickening of the remaining recognizable septums (Fig. 3A). In many regions only "sheets" of closely packed capillaries could be seen. In those areas where alveoli could still be discerned, capillary tufts were observed to project into the alveolar lumens (Figs. 4 and 6). A distinct scarring obscured the pulmonary structure in scattered areas (Fig. 5). Most of the smaller bronchi contained mucoid material in which neu-

trophils were suspended, but no evidence of leukocytic reaction was seen elsewhere.

Case 3. Male, 79 years. Generalized arteriosclerosis with cerebral thrombosis. There were no preceding respiratory complaints, but nasal catheter oxygen was given because of "moderate dyspnea." It was continued for 8 days at 6 liters per minute. Death resulted from a massive cerebral hemorrhage. The lungs weighed 780 gm. and were purplish-blue in color.

Three sections of lung tissue were available for study, and two of these showed partial consolidation by purulent bronchopneumonia. In nonpneumonic areas capillary congestion and irregular thickening of alveolar septums were seen (Fig. 8). A few intra-alveolar tufts could be found, but in general the changes were relatively inconspicuous.

Case 4. Male, 79 years. Pulmonary emphysema with cor pulmonale and congestive heart failure. Because of dyspnea, oxygen was administered by nasal catheter at 6 liters per minute for 6 days. Treatment was discontinued 4 days prior to death, which was attributed to edema. The lungs weighed 1,390 gm. and showed congestion. On section there were red patches from which oozed foamy material.

Five sections of lung tissue were available for study, and all showed evidence of pulmonary edema. In addition there was a generalized thickening of alveolar septums with an increased prominence of capillaries. Occasional intra-alveolar tufts were present. Inflammatory cells were absent except in relation to bronchioles. Here, there was usually lymphocytic infiltration which was interpreted as an indication of chronic bronchitis related to the emphysema. Even the affected bronchioles showed numerous prominent capillaries in their walls and subepithelial regions (Fig. 9), and in many respiratory bronchioles, capillaries appeared in the lumens (Fig. 10). The latter lesion was not prominent in any other cases in group I but was seen in some of those in group II.

Case 5. Female, 40 years. Subarachnoid hemorrhage. Nasal catheter oxygen was given because of unexplained hyperpnea. The rate was 7 liters per minute for 6 days, and this was terminated 6 days before death. The lungs weighed 430 gm.

Two sections of lung tissue were available. In each the alveolar septums were uniformly thin and the spaces empty. The capillary lesion noted in the other cases was not apparent, but it is possible that it may have regressed subsequent to interruption of oxygen exposure. The clinical record was not sufficiently detailed to permit a conclusion on this point.

Case 6. Female, 80 years. Arteriosclerotic cardiovascular disease with congestive failure. Because of dyspnea, cyanosis, and pleural effusion, nasal catheter oxygen was given for 3 days at 4 liters per minute, until death. Death was attributed to congestive failure. The lungs weighed 610 gm. and were dark red, congested and atelectatic.

Three sections of lung tissue were available. All showed generalized capillary congestion and proliferation; in many regions the septal tissue occupied more area than the air spaces. There were no definite

examples of intra-alveolar capillary tuft projection. There were occasional foci of fresh hemorrhage which may have been either ante or post mortem.

Case 7. Male, 66 years. Myocardial infarction. Because of marked dyspnea, nasal catheter oxygen was given at 6 liters per minute for about 24 hours, ending 2 days before death. The latter was the result of pulmonary embolism. The lungs weighed 630 gm. and showed generalized congestion with patchy dark red areas measuring 3 to 4 cm. in diameter.

Three sections of lung tissue were available. All showed generalized evidence of capillary congestion and dilatation, but there was no significant degree of septal thickening or capillary tuft formation (Fig. 11).

Cases 8, 9 and 10. Each received oxygen for less than 24 hours and showed only minimal capillary congestion, or none at all. The lungs weighed 720, 630, and 650 gms., respectively.

Group II

Examination of Table I which lists the patients in group II reveals a high frequency of oxygen administration to terminally ill patients; 15 of the 22 consecutive cases reviewed had been so treated. It is apparent that each of the 6 cases considered to have a slight degree (+) of capillary proliferation had had prolonged oxygen therapy, the briefest period being 36 hours (case 8345). On the other hand there were 3 cases (8338, 8342 and 8344) in which oxygen had been administered for 2 to 4 days, but no capillary proliferation was manifest.

Summary of Pathologic Observations

In this study, the gross appearance of the lungs was determined only by review of the necropsy protocols. In all instances the descriptions indicated a generally uniform appearance of the two lungs and the various lobes. When the changes were described as "patchy," the patches were noted in all lobes and appeared similar everywhere. The lungs were never described as collapsed or small, and the terms "excessively red" and "congested" appeared in most of the protocols. It is significant that all of the lungs showing capillary proliferation were unusually heavy. Those patients having the longest oxygen exposure had the heaviest lungs except in instances where pulmonary edema was also present because of congestive failure (cases 4 and 6).

Microscopically, the rate of development of the capillary alterations appeared to be variable in different persons. Thus in some instances proliferation was as prominent after only 2 to 3 days of exposure (cases 8337 and 8345) as after 7 days (case 8350). On the other hand, a few cases showed only capillary congestion after as much as 4 days' exposure (cases 5, 8338 and 8344).

Despite these variations, the sequence of events in the development of the lesion can be reconstructed. The first change presumably consists of congestion and dilatation of the alveolar septal capillaries (Fig. 11). The dilatation becomes progressively more pronounced and the septal walls thicker until the stromal tissue, rather than air spaces,

TABLE I

Group II. Correlation of Capillary Proliferation and Oxygen Therapy

Case no.	Age	Clinical diagnosis	Alveolar septums*	Duration of oxygen therapy
8330	68	Miliary tuberculosis	±	1 hour
8331	19	Granulomatous infection	o	o
8332	74	Bronchopneumonia	o	24 hours
8333	63	Thrombocytopenic purpura	o	o
8334	27	Carcinoma of colon with metastases	o	1 hour
8335	70	Bronchogenic carcinoma	+++	7 days
8336	2	Pneumonia; enteritis	o	o
8337	42	Lobar pneumonia	++	3 days
8338	35	Intestinal obstruction; septicemia	±	4 days
8339	78	Carcinoma of breast with metastases	+	2 days
8340	73	Bronchogenic carcinoma	o	12 hours
8341	47	Nutritional cirrhosis; massive hemorrhage	o	o
8342	77	Pyelonephritis	o	3 days
8343	70	Coronary occlusion	o	15 hours
8344	48	Acute pancreatitis	±	2 days
8345	60	Traumatic injuries (automobile)	++	36 hours
8346	6	Monocytic leukemia	±	8 hours
8347	64	Carcinoma of prostate	o	o
8348	—	Stillborn	o	o
8349	64	Carcinoma of uterus	±	o
8350	74	Subdural hemorrhage	++	7 days
8351	64	Hodgkin's disease	o	o
8352	68	Emphysema and cor pulmonale	++	4 days

* Key
o = thin septums; inconspicuous capillaries.
± = thin septums; capillaries congested; no proliferation.
+ = thin septums; capillaries congested; slight proliferation.
++ = thickened septums; capillaries congested; moderate proliferation.
+++ = thickened septums; capillaries congested; marked proliferation; early fibrosis.

occupies the major portion of each microscopic field. In such instances any given field has the appearance of collapsed lung, but the generalized character of the lesion in a lung of normal size and increased

weight is not consistent with mere atelectasis. A further distinction may be made by the fact that in atelectasis it is possible to make out the individual thin alveolar septums apposed to each other (Fig. 7). In the lesion induced by oxygen exposure one would be forced to postulate an actual fusion of adjacent septums to explain the appearance on the basis of collapse alone (Fig. 6). It seems clear that when the degree of change is such that the amount of stroma equals or exceeds the volume of air space, there has been capillary proliferation in addition to the opening of all existing vessels. Additional features provide unmistakable evidence of capillary proliferation in the form of papillary tufts projecting into the lumens of alveolar spaces (Figs. 1 and 4) and bronchioles (Fig. 10).

In early lesions, examples of this condition are difficult to detect. After 4 or more days of exposure, however, many intra-alveolar capillary tufts are present. There is also increase in the number of capillaries in the submucosa and walls of bronchioles (Fig. 8). Finally, after one to two weeks or more of continuous exposure to oxygen, fibrocytes appear among the proliferated capillaries and a diffusely distributed deposition of delicate collagen fibers occurs (Figs. 2 and 5).

Evidence of inflammatory reaction in these lungs is quite inconspicuous. The dark staining cells seen in the septums in most of the illustrations suggest a lymphocytic infiltration, but close inspection reveals that most of them are erythrocytes. Often the erythrocytes in the septums are arranged in rows; this is taken to indicate that they lie in longitudinally cut capillaries even if the vessel walls are not clearly visible in every instance. Nuclei of endothelial cells are numerous and usually rather large. The persisting alveolar spaces are generally empty except for a small number of phagocytes. Occasionally moderate numbers of extravasated erythrocytes are seen, and these presumably represent capillary hemorrhage, although extravasation during sectioning of the lung may also occur. There is, in some instances, slight edema of the alveolar septums.

Intra-alveolar fibrin, neutrophils, and edema fluid are absent except in the few cases having pneumonic consolidation or congestive failure (cases 1, 3, 4, 8337, 8352). In case 8337 (lobar pneumonia) capillary proliferation was present only in the nonpneumonic lobes.

Discussion

The observations are considered to indicate that oxygen causes not only pulmonary alveolar capillary congestion, but a marked proliferation of the capillaries as well. This is accompanied by thickening of alveolar septums and even papillary projections of capillary tufts into

the alveolar spaces. The lesions are occasionally accompanied by capillary hemorrhage or slight pulmonary edema. They are present in all lobes but are often patchy in distribution. A few apparently uninvolved septums are almost invariably found near those showing capillary proliferation. It is important to note also that the affected lungs are generally exceedingly heavy and are often described as being excessively red in color.

The observations in an unselected series of consecutive necropsied patients (group II) reveal a surprisingly high frequency of oxygen administration during terminal illnesses. The related alterations in pulmonary septal capillaries are thus probably so common as to have escaped specific comment heretofore. Many of the specimens reviewed had been described as showing "patchy atelectasis" with or without "pulmonary edema and hemorrhage."

There are various reasons for the failure of certain patients to develop capillary changes even though exposed to oxygen inhalation. Among these is the chance that for technical reasons or because of shallow respirations, administration of the gas may not actually have appreciably raised the pulmonary oxygen concentration. For example, some of these patients were placed in an oxygen tent, an inefficient method of administration. Another possible explanation is the fact that oxygen has been found to have a more pronounced effect when administered to the normal individual than to the patient with a pathologic state accompanied by hypoxemia.[2]

The lesions described seem entirely compatible with the observation that there is progressive loss of pulmonary function when oxygen exposure is continuous over a period of days. This has been attributed to the "irritant" effect of oxygen[2,6,8] which was considered to result in edema and hemorrhage. It is difficult to see why such responses, if they are indeed inflammatory, should be so slow in developing, since oxygen should be just as irritating on the first as on the fifth day. Similarly, it seems logical that simple inflammation should resolve promptly on discontinuation of oxygen administration; yet physiologists have shown that recovery of normal function may be delayed for two weeks after cessation of oxygen exposure. In view of these discrepancies and, in addition, the absence of fibrin deposit and neutrophil infiltration, and the paucity of edema, it is believed that oxygen specifically provokes capillary proliferation and does not excite inflammation as in the case of an ordinary irritant. The mechanism of this action remains to be investigated although the first step is probably already known since physiologists have shown that capillary dilatation occurs within minutes after inception of oxygen exposure.[8]

If one examines the illustrations in papers describing the results of exposure of normal animals to oxygen, one finds several examples of the same type of capillary lesions in the alveolar septums of these animals (Fig. 3, ref. 4; Figs. 5 and 6, ref. 5).

It might be suggested that oxygen does not itself cause capillary proliferation, but merely prolongs life so that another factor has time to produce the lesion. On the other hand, many patients with similar diseases, though untreated with oxygen, have lived as long and did not show the capillary alteration.

In certain respects the lesions are reminiscent of interstitial pneumonitis or of diffuse interstitial fibrosis. It was for this reason that two consecutive groups of cases were reviewed. Since both of these conditions are rather infrequent, it is scarcely possible they would occur with the observed frequency by chance in these randomly selected consecutive groups of patients receiving oxygen therapy for a wide variety of conditions.

The appearance of diffuse pulmonary fibrosis in some of the patients with the most prolonged exposure to oxygen is of importance in that this may well indicate the possibility of irreversible alteration. There is reason to believe that capillary proliferation alone may be reversible since various reports[2,6,8] state that human volunteers who show changes in pulmonary function after several days' exposure in oxygen chambers regain original functional capacity within a week or so after returning to normal atmosphere. However, this matter requires further study; it would be desirable to make actual observations of the regression of the lesion. Moreover, patients receiving oxygen should be followed during life, with subsequent correlation of necropsy lesions and clinical manifestations. The same procedure should be used to clarify the significance of pulmonary fibrosis. Since cases of this nature will obviously be rare, investigations with experimental animals should be planned.

The observations reported are not necessarily presented to emphasize the hazards of oxygen administration. These are becoming generally appreciated and are less frequent as increasing care is exercised in the administration of this gas. The morphologic expression of toxicity may serve as an explanation for the development of "dependence" upon oxygen administered to persons with respiratory impairment. The thickened alveolar septums would interfere with oxygen diffusion into blood. Thus, on return to normal atmospheric oxygen concentration the patient would be expected to have greater difficulty than before oxygen therapy was begun. The need for "weaning" the patient from oxygen is also clarified.

Mention should be made of the possibility that the pulmonary lesions described may have a more general systemic significance. The effects of high concentrations of oxygen upon retinal capillary development, especially in premature infants are well documented.[7,9] It is also now recognized that cutaneous angiomas are more common in premature infants than in normal children, and that the incidence has decreased as oxygen administration in early infancy has been curtailed.[10]

Finally, attention is directed to the fact that the pulmonary changes induced by oxygen often have been erroneously considered to be manifestations of certain obscure pulmonary diseases. Thus capillary proliferation is mentioned in the original article[11] and in numerous subsequent publications concerning the Hamman-Rich syndrome.[12,13] Similar lesions have also been described in other chronic progressive pulmonary disorders characterized by respiratory insufficiency.[14,15] Since most patients with these conditions receive oxygen therapy during the final stages of their ailments, the likelihood that septal capillary proliferation may be a reflection of oxygen inhalation requires consideration. So-called "plasma cell pneumonia of premature infants"[16] is said to be characterized by generalized septal thickening without clinical or morphologic evidences of infection, but with progressive pulmonary insufficiency. This may also be a manifestation of oxygen toxicity.

Summary

Evidence has been presented to show that with oxygen inhalation for as little as two days, pulmonary alterations consisting of capillary congestion and proliferation may be observed. After continuous inhalation for approximately two weeks, diffuse fibrosis has been encountered. Alveolar concentrations of oxygen obtained during administration by nasal catheter are believed to be sufficient to cause these alterations.

The capillary lesions are thought to be responsible for the development of "oxygen dependence" and for the variations in pulmonary function which occur during and after inhalation of high concentrations of oxygen. They are presumably reversible at least until the time fibrosis supervenes.

Failure of previous recognition of the effect of oxygen upon pulmonary tissue is attributed to the high frequency of its administration. The lesion has thus been so commoplace as to be considered a normal variation in pulmonary structure.

The importance of appreciating the potential effect of oxygen on pulmonary parenchyma and of differentiating the lesions induced from those of various obscure pulmonary diseases is emphasized.

REFERENCES

1. Comroe, J. H., Jr.; Dripps, R. D.; Dumke, P. R., and Deming, M. Oxygen toxicity. The effect of inhalation of high concentrations of oxygen for twenty-four hours on normal men at sea level and at a simulated altitude of 18,000 feet. *J. A. M. A.*, 1945, **128**, 710–717.
2. Ohlsson, W. T. L. A study on oxygen toxicity at atmospheric pressure. *Acta. med. scandinav.*, 1947, Suppl. 190, 93 pp.
3. Smith, F. J. C.; Heim, J. W.; Thomson, R. M., and Drinker, C. K. Bodily changes and development of pulmonary resistance in rats living under compressed air conditions. *J. Exper. Med.*, 1932, **56**, 63–78.
4. Paine, J. R.; Lynn, D., and Keys, A. Observations on the effects of prolonged administration of high oxygen concentration to dogs. *J. Thoracic Surg.*, 1941, **11**, 151–168.
5. Binger, C. A. L.; Faulkner, J. M., and Moore, R. L. Oxygen poisoning in mammals. *J. Exper. Med.*, 1927, **45**, 849–864.
6. Stadie, W. C.; Riggs, B. C., and Haugaard, N. Oxygen poisoning. *Am. J. M. Sc.*, 1944, **207**, 84–114.
7. Patz, A.; Eastham, A.; Higginbotham, D. H., and Kleh, T. Oxygen studies in retrolental fibroplasia. II. The production of the microscopic changes of retrolental fibroplasia in experimental animals. *Am. J. Ophth.*, 1953, **36**, 1511–1522.
8. Comroe, J. H., Jr., and Dripps, R. D. The Physiological Basis for Oxygen Therapy. Charles C Thomas, Springfield, Ill., 1950, p. 16.
9. Ashton, N.; Ward, B., and Serpell, G. Role of oxygen in the genesis of retrolental fibroplasia. A preliminary report. *Brit. J. Ophth.*, 1953, **37**, 513–520.
10. Wagener, H. P. Diseases of the retina and optic nerve. *A. M. A. Arch. Ophth.*, 1956, **55**, 699–746.
11. Hamman, L., and Rich, A. R. Acute diffuse interstitial fibrosis of the lungs. *Bull. Johns Hopkins Hosp.*, 1944, **74**, 177–212.
12. White, R. B., and Craighead, J. T. Hamman-Rich syndrome (diffuse interstitial pulmonary fibrosis). *Dis. Chest*, 1957, **31**, 335–340.
13. Golden, A., and Bronk, T. B. Diffuse interstitial fibrosis of lungs; a form of diffuse interstitial angiosis and reticulosis of lungs. *A. M. A. Arch. Int. Med.*, 1953, **92**, 606–614.
14. Walford, R. L., and Kaplan, L. Pulmonary fibrosis and giant-cell reaction with altered elastic tissue. Endogenous "pneumoconiosis." *A. M. A. Arch. Path.*, 1957, **63**, 75–90.
15. Wiese, E. R., and Hall, W. E. B. Asbestosis: report of a case. *Dis. Chest*, 1956, **30**, 229–230.
16. Manschot, W. A. Etiology of retrolental fibroplasia. *A. M. A. Arch. Ophth.*, 1954, **52**, 833–845.

[*Illustrations follow*]

LEGENDS FOR FIGURES

FIG. 1. Case 1. Oxygen, 19 days. Some pulmonary aveolar septums are thin; others, especially one in the lower left, are thickened. Capillaries are prominent everywhere and a capillary tuft occupies the lumen of the alveolar space in the center of the field. Several capillaries can be traced from the septum into the alveolar lumen. Hematoxylin and eosin stain. × 400.

FIG. 2. Case 1. Septal thickening and increased numbers of thin-walled capillaries are seen. In addition, fibrocytes and a few strands of collagen are present. Hematoxylin and eosin stain. × 400.

FIG. 3. Distribution and pattern of the pulmonary lesions in patients exposed to oxygen. Hematoxylin and eosin stain. × 4.

A. Case 2. Oxygen exposure, 16 days. The alveolar spaces are almost completely obscured by septal thickening. For detail see Figure 4.

B. Case 3. Oxygen exposure, 8 days. This illustrates the effect of squeezing on the pattern produced by the septal thickening.

C. Case 8335. Oxygen exposure, 7 days. Some alveolar spaces are obscured by septal thickening. Those which remain show minor variability in size. This pattern is often interpreted as patchy atelectasis or as the result of rough handling of tissue at necropsy.

D. Case 4. Oxygen exposure, 3 days. The pattern is entirely similar to that in Figure 3C.

E. Lobar atelectasis in a patient not receiving oxygen. For detail see Figure 7.

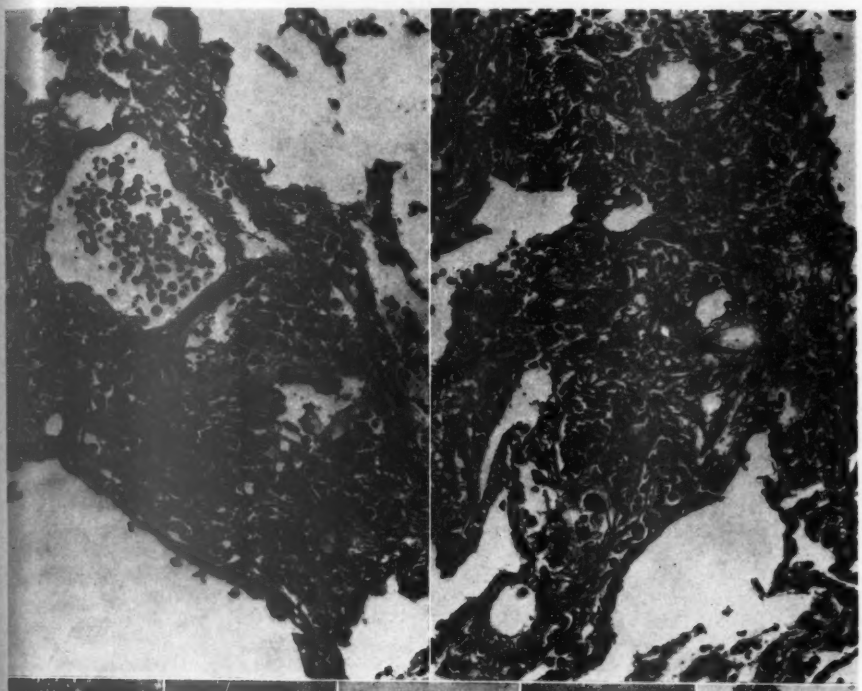

2

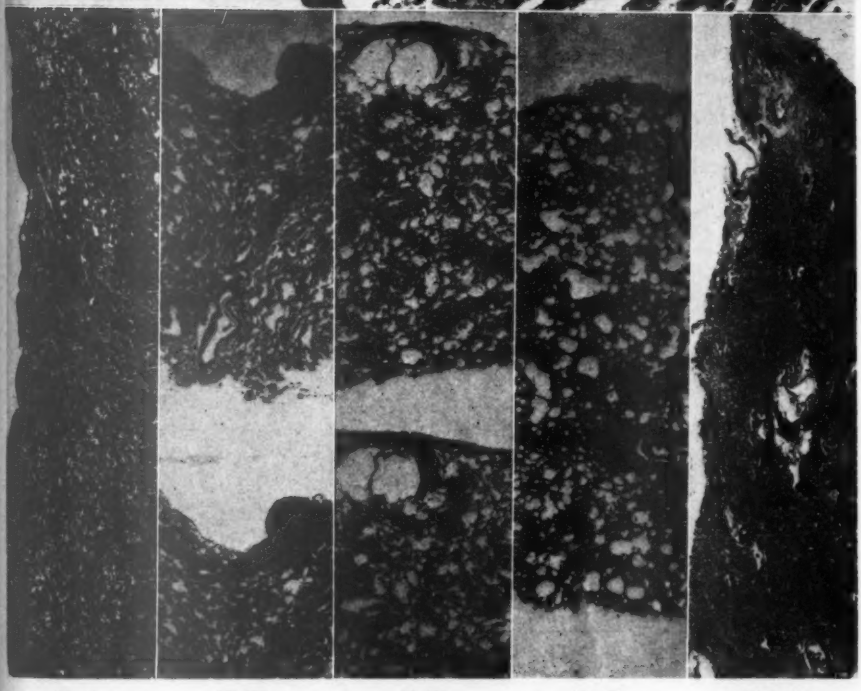

3A 3B 3C 3D 3E

FIG. 4. Case 2. Oxygen, 16 days. There is thickening of all alveolar septums, producing a pattern superficially resembling atelectasis. Close inspection will reveal many thin-walled capillaries, with lumens often packed with erythrocytes. There is a tuft of capillaries in the lumen of the alveolus at the center. Hematoxylin and eosin stain. × 400.

FIG. 5. Case 2. Photograph illustrates the widespread character of the lesion present in Figure 4. Note also the scattered strands of collagen. Hematoxylin and eosin stain. × 100.

FIG. 6. Case 2. The pattern of reticulum in the walls of the proliferated capillaries is shown. Note tufts projecting into alveolar spaces. Compare with Figure 7. Foot's modification of the Bielschowsky stain for reticulum. × 400.

FIG. 7. Reticulum stain of atelectatic lung tissue for comparison with Figure 6. Although apposed, individual septums are uniformly thin and readily distinguishable. Foot's modification of the Bielschowsky stain for reticulum. × 400.

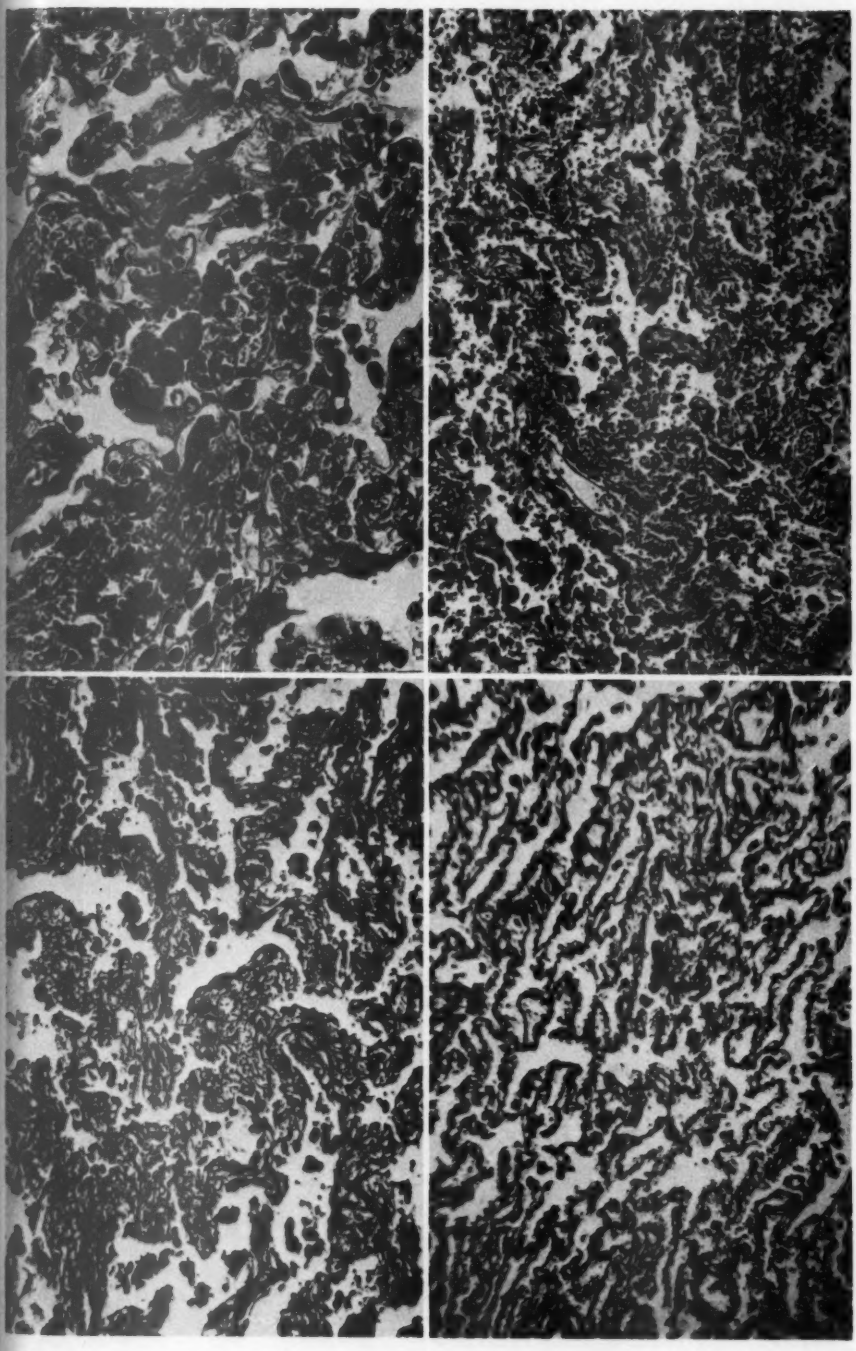

5

7

FIG. 8. Case 3. Oxygen, 8 days. Alveolar septal thickening, with congested and numerous capillaries. Most of the dark-staining cells are erythrocytes, and they can often be seen in rows. Hematoxylin and eosin stain. × 400.

FIG. 9. Case 4. Oxygen, 6 days. The epithelium of a respiratory bronchiole is shown at the bottom. The lumen of the bronchiole is distended by capillaries. Hematoxylin and eosin stain. × 400.

FIG. 10. Case 4. The wall of a small bronchus contains increased numbers of capillaries in the submucosa. These are also evident outside the muscular layer. Note the numerous capillaries in the adjacent pulmonary tissue, at the bottom. Hematoxylin and eosin stain. × 400.

FIG. 11. Case 7. Oxygen, 1 day. The capillaries are prominent and rather congested, but there is no evidence of proliferation. These changes are nonspecific and this field may be considered as a normal control for comparison with other illustrations. Hematoxylin and eosin stain. × 400.

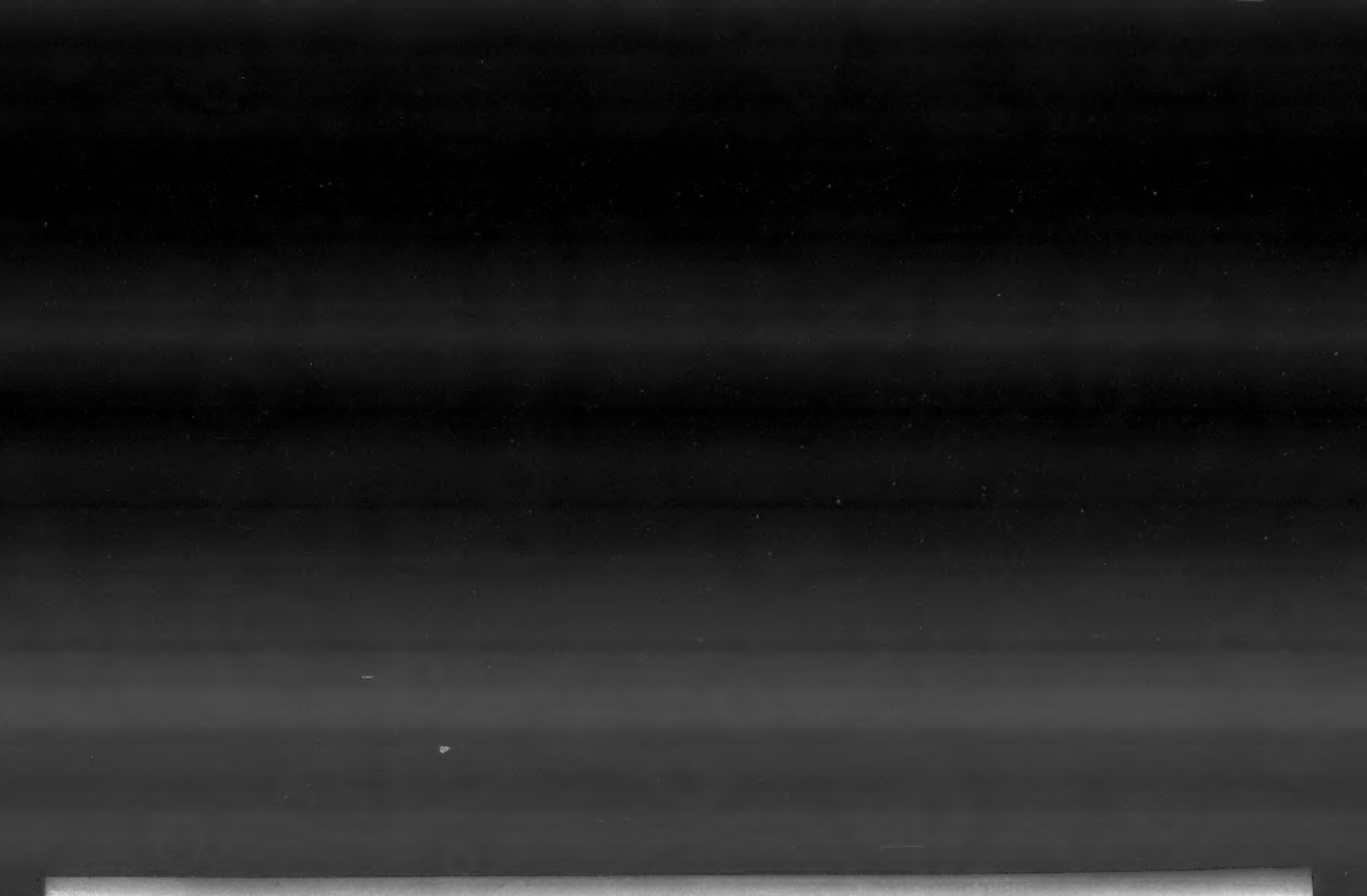

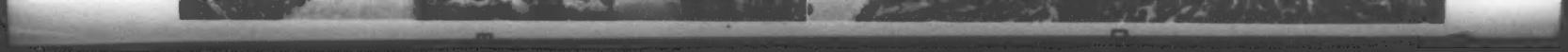

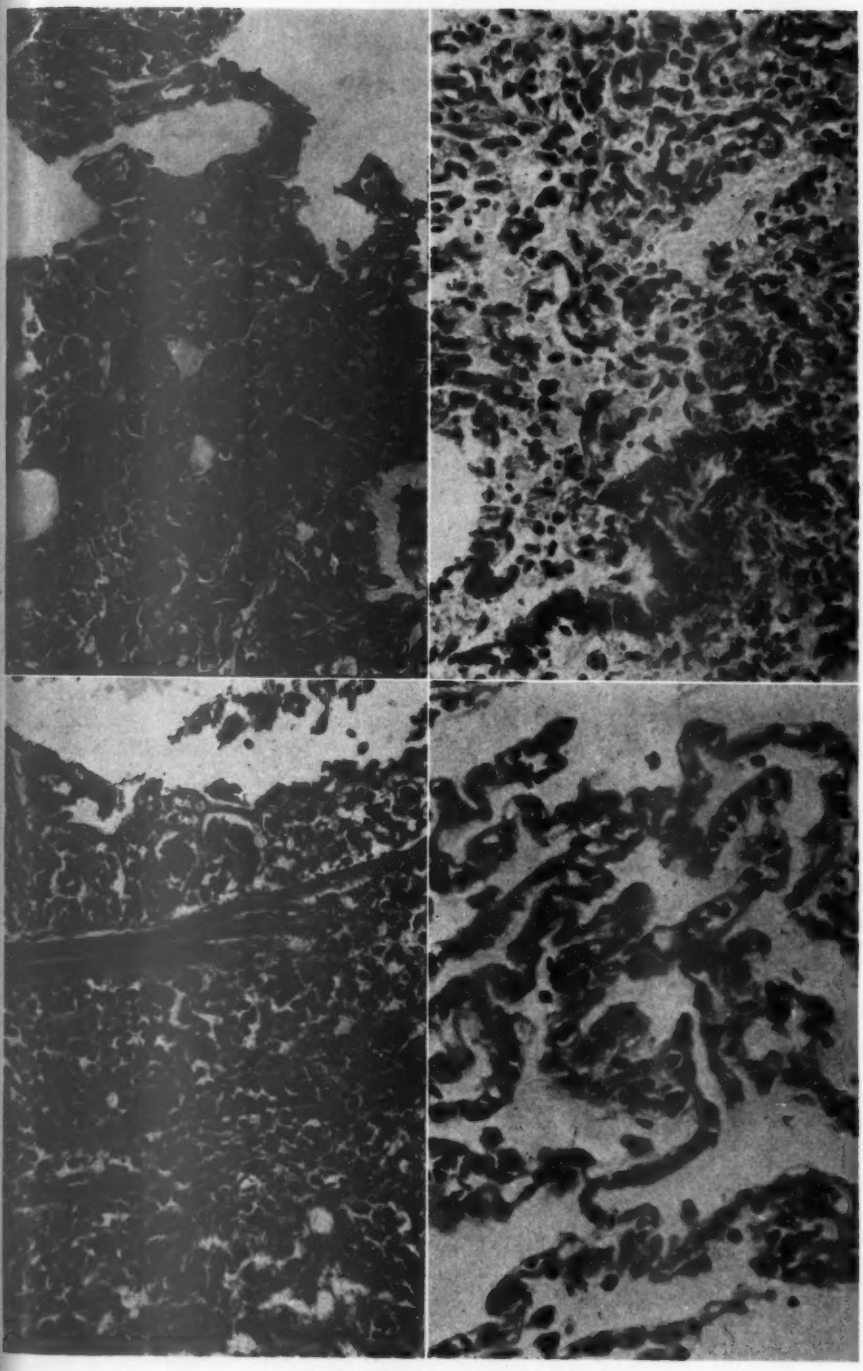

9

11

THE EFFECTS OF STAPHYLOCOCCAL TOXIN ON THE LUNGS OF RABBITS*

J. R. JACKSON, M.R.C.S.; R. J. GIBBONS, M.D., and DESMOND MAGNER, M.D.
From the Departments of Pathology and of Bacteriology, University of Ottawa, Ottawa, Canada.

Although the action of staphylococcal toxin in certain tissues has been thoroughly studied, little has been recorded concerning its effects on the lung. From both the clinical and pathologic viewpoints, however, staphylococcal pneumonia in the human subject often presents findings which serve to distinguish it from pneumonia due to other causes. It may exhibit hemorrhagic, necrotizing lesions, comparable to those caused in other organs by the experimental use of staphylococcal toxin. Moreover, Evans and Evans[1] have shown that staphylococcal pneumonia may bring about complete neutralization of the circulating antibody to staphylococcal alpha hemolysin, whereas this was not the case in patients suffering from staphylococcal infections elsewhere in the body. The observation of the Evanses suggests that large quantities of toxin may be produced in the lungs. For these reasons it seemed that a study of the action of staphylococcal toxin in the pulmonary tissues of rabbits might yield information concerning the pathogenesis of human staphylococcal pneumonia, and also the mechanism whereby the toxin produces its characteristic effects in other tissues as well.

MATERIALS AND METHODS

Toxin was prepared from pyogenic staphylococci of the "Wood" strain. The organisms were inoculated in brain-heart infusion with 0.3 per cent agar added, and incubated at 37° C. in an atmosphere of 75 per cent oxygen and 25 per cent carbon dioxide. After 40 hours, the broth culture was passed through cheesecloth, through Whatman filter paper, and spun in a centrifuge at 2,000 r.p.m. for 45 minutes. The supernatant was sterilized by passage through a Seitz filter. The resultant toxin was found to be rapidly lethal to rabbits in doses of 0.3 ml. per kg. of body weight, was actively dermonecrotic, and produced hemolysis of a 1 per cent suspension of rabbit blood cells in a dilution of 1:512.

Twelve male and 14 female albino rabbits were used, the weights

* This work was assisted by a grant from the Province of Ontario under the National Health Grants program of the Department of National Health and Welfare.
Presented at the Fifty-fourth Annual Meeting of the American Association of Pathologists and Bacteriologists, Washington, D.C., April 11, 1957.
Received for publication, April 21, 1958.

ranging from 2,275 gm. to 3,860 gm. In 22 animals staphylococcal toxin was injected into the trachea, and in 3 a direct intrabronchial injection was made, using a polyethylene tube introduced via the trachea. In one of the animals India ink was mixed with the staphylococcal toxin. Details of the dosages of toxin used are summarized in Tables I to IV. All intratracheal injections were standardized to a

TABLE I

Group I. Survival after Intratracheal Injection of Staphylococcal Toxin

No.	Sex	Wt. (gm.)	Mode of death	Toxin		Survival
				Dose per kg. of body wt.	Dilution	
R24	F	3860	Sacrificed	0.26 ml.	Undiluted	20 min.
R25	F	3320	Sacrificed	0.03 ml.	1:4	40 min.
R23	F	2800	Sacrificed	0.29 ml.	Undiluted	55 min.
R27	M	3800	Sacrificed	0.05 ml.	1:3	55 min.
R28	F	3450	Sacrificed	0.14 ml.	1:1	60 min.
R3	F	3860	Sacrificed	0.23 ml.	Undiluted	1¼ hr.
R37	M	2100	Sacrificed	0.25 ml.	1:1	1½ hr.

TABLE II

Group II. Survival after Intratracheal Injection of Staphylococcal Toxin

No.	Sex	Wt. (gm.)	Mode of death	Toxin		Survival
				Dose per kg. of body wt.	Dilution	
R2	M	2702	Died	0.37 ml.	Undiluted	1¾ hr.
R22	F	3600	Died	0.22 ml.	Undiluted	2 hr.
R10	M	2460	Died	0.05 ml.	1:7	2½ hr.
R5	F	2702	Died	0.075 ml.	1:4	3 hr.
R21	F	3700	Sacrificed	0.27 ml.	Undiluted	4 hr.
R4	M	2850	Died	0.15 ml.	1:1	5 hr.

volume of 1.0 ml. with normal saline. The intrabronchial injections were similarly standardized to 0.5 ml. No attempt was made to obtain uniformity in the dilution of toxin used or in the dose of toxin per kilogram, but these were adjusted to permit the infliction of maximum pulmonary damage compatible with survival of the animal for the desired period of observation. Usually no anesthetic was required, but in some cases Nembutal® or Nembutal supplemented by ether was employed. In 6 instances 20 ml. of 1 per cent solution of trypan blue in normal saline was injected into the inferior vena cava 10 minutes before the animal was sacrificed.

In 5 unselected control animals (Table IV) the toxin was neutralized

prior to introduction by incubation with an equal or larger quantity of staphylococcal antitoxin (supplied by the Connaught Laboratories, Toronto, for therapeutic purposes) for 1 hour at 37° C. The antitoxin contained approximately 800 units per ml. In one animal the sterile broth culture medium itself was used.

Animals died or were sacrificed by a blow on the back of the neck,

TABLE III

Group III. Survival after Intratracheal or Intrabronchial Injection of Staphylococcal Toxin

No.	Sex	Wt. (gm.)	Mode of death	Toxin		
				Dose per kg. of body wt.	Dilution	Survival
R11	F	3375	Sacrificed	0.035 ml.	1:8	24 hr.
R19	M	3200	Sacrificed	0.024 ml.	1:4	25 hr.
R12	F	2875	Sacrificed	0.025 ml.	1:13	48 hr.
R20	M	2975	Sacrificed	0.025 ml.	1:6	72 hr.
R13	M	3000	Sacrificed	0.020 ml.	1:15	4 days
R18	M	3025	Sacrificed	0.010 ml.	1:32	4 days
R15	M	2550	Sacrificed	0.020 ml.	1:19	7 days

TABLE IV

Group IV. Controls

No.	Sex	Wt. (gm.)	Mode of death	Toxin ml./kg.	Antitoxin ml./kg.	Broth	Dilution of toxin	Time of sacrifice
R26	F	3450	Sacrificed	0.029	0.029		1:9	55 min.
R29	F	3300	Sacrificed	0.075	0.150		1:3	2 hr.
R30	F	3325	Sacrificed	0.075	0.150		1:3	4 hr.
R8	F	2275	Sacrificed			0.5 ml.	1:1	7 hr.
R9	M	2275	Sacrificed	0.05	0.05		1:8	24 hr.
R14	M	2950	Sacrificed	0.02	0.02		1:6	4 days

at periods varying from 20 minutes to 7 days after instillation of the toxin. A complete necropsy was performed in all animals. An increase in the weight of the lungs was a frequent finding. The weight of the lungs in each case was calculated in terms of a percentage of the total body weight. Since in none of the controls did the right lung exceed 0.20 per cent or the left 0.13 per cent of the total body weight, ratios in this range were taken as approximately normal. Tissues were fixed in 10 per cent neutral formalin or Zenker's solution. Multiple blocks of lung were embedded in paraffin, and sectioned. In addition, sections were made of brain, thymus, trachea, heart, liver, pancreas, spleen, adrenals, and kidneys. Sections were stained with hematein, phloxine,

and saffron. In special instances Weigert's stain for elastic tissue, Gomori's and Weigert's stains for iron, Mallory's phosphotungstic acid hematoxylin stain for fibrin, Cowdry's mucicarmine method for mucin and Giemsa's stain for blood cells were also used. Frozen sections were stained with Sudan IV for neutral fat.

Results

Symptomatic Effects of the Toxin

Injection of the toxin produced no immediate reaction, but in about 10 minutes the pupils became contracted. Shortly afterwards respirations became slow, deep, and labored, and cyanosis often developed. In surviving animals partial recovery ensued, but some degree of dyspnea usually remained. In no animal surviving the first 24 hours did the toxin produce injury sufficient to cause death within the period of observation.

Pathologic Observations

The alterations of major importance were in the tracheobronchial tree, lungs, and pleural cavities. The animals were divided into 3 groups for purposes of description. Group I consisted of 7 rabbits that died or were sacrificed up to 90 minutes after introduction of staphylococcal toxin into the trachea (Table I). Group II was comprised of 6 rabbits surviving for 105 minutes to 5 hours after the injection of the toxin (Table II). In group III were 7 rabbits living for 24 hours to 7 days after injection (Table III).

Gross Necropsy Findings. The animals in group I showed only slight injection of tracheal mucosa and slight increase in lung weights. In group II, the tracheal mucosa was considerably injected, and frothy fluid, often blood-stained, was present in the trachea and bronchi. One or more lobes in every rabbit contained glistening red areas of jelly-like consolidation, usually situated centrally and peribronchially and sometimes occupying most of the lobe. Edema was often present in the unconsolidated lung, and lung weights were moderately increased. In group III tracheobronchial changes were still more marked. Centrilobar peribronchial zones of brownish consolidation (Fig. 1) were present in all animals, save one that had received very dilute toxin. Portions of lung remote from the consolidated zones were edematous or manifested a diffuse pale yellow firmness. In this group the increase in lung weights was marked, ranging up to 5 times the estimated normal weight. Straw-colored or blood-stained pleural effusions were present in some animals. Findings in the other organs were not considered relevant. No significant gross alterations were noted in the lungs or other organs of the 7 control rabbits.

Microscopic Observations. In group I the alterations in the trachea were inconstant and minimal. In groups II and III, the animals living for from 2 to 25 hours after exposure to toxin showed mucosal congestion, edema, focal hemorrhage and occasional light neutrophil infiltrations (Fig. 2). Rabbits surviving over 48 hours showed an absence of significant tracheal alterations.

Significant lesions in the lungs were noted only in one rabbit in group I that survived for 55 minutes. In this animal there was a centrilobar zone of vascular dilatation and alveolar edema (Fig. 3).

The centrilobar consolidations present in the rabbits in group II consisted of areas of intense capillary congestion and alveolar edema, with alveolar hemorrhage of mild to moderate degree. An acute inflammatory exudate was present in perivascular and peribronchial connective tissue, and one animal showed acute inflammation marginal to the consolidation. Polymorphonuclear leukocytes were constantly absent in consolidated alveolar areas. A feature in 4 of the 6 animals in this group was tremendous dilatation and recent thrombosis of larger pulmonary blood vessels (Fig. 4). Two rabbits showed an acute vasculitis. Areas of lung remote from the central lesions were normal or showed alveolar edema.

Microscopic examination of the brownish consolidations in group III showed zones of hemorrhagic necrosis (Figs. 5 and 6). The majority of lesions manifested an acute vasculitis and perivasculitis (Fig. 7). Portions of lung marginal to necrotic zones were the sites of a heavy neutrophil and fibrinous inflammatory exudation. In a few animals focal or diffuse bronchopneumonia was present in lobes free from centrilobar necrosis. After 3 days, reparative changes became manifest, with "epithelialization" of alveoli and growth of young fibroblasts into alveolar exudate and necrotic tissue (Fig. 8), as well as in the connective tissue about bronchi and blood vessels.

Bacteriologic Findings. Bacteriologic studies were not made in the rabbits sacrificed within 5 hours of the injection of toxin. Swabs or tissue were taken from each of the lungs of those surviving for 24 hours or longer. In 2 animals surviving for 4 and 7 days a growth of short, gram-negative bacilli was obtained on blood agar, the colonies and bacteria having the gross and microscopic characteristics of bacilli of the Alcaligenes group. The organisms did not ferment sugar or liquefy gelatin, and were not found to be pathogenic to rabbits on intravenous injection. It was concluded that they were probably saprophytic organisms derived from the gastrointestinal tract. Swabs from the other animals grew no organisms on culture.

Observations with Intravenous Injection of Trypan Blue. In order

to investigate the role of vascular stasis in the production of the pulmonary alterations, 20 ml. of a 1 per cent solution of trypan blue in normal saline was introduced into the inferior vena cava in 5 animals (R24, R25, R28, R23, R21) at intervals of 20 minutes to 4 hours following the intratracheal injection of various dilutions of toxin. The animals were sacrificed after 10 minutes and necropsy performed immediately. A sixth animal (R26) which received neutralized toxin was used as a control.

In the control animal (R26) and at 20 minutes (R24), the lungs were uniformly blue. At 40 minutes (R25) and 60 minutes (R28) the lungs, otherwise grossly unremarkable, showed complete exclusion of the dye from numerous, irregular, peripherally situated, fan-shaped regions measuring up to 1.0 cm. in diameter (Fig. 10). Microscopic examination failed to show differences between stained and unstained areas.

With undiluted toxin (R23), after 55 minutes there was complete exclusion of trypan blue from the right superior lobe and adjacent portions of the middle and infero-lateral lobes (Fig. 9). Present elsewhere were patchy, peripherally situated zones devoid of dye, resembling those described in the previous paragraph. Microscopically, the central portions of the right superior, middle, and infero-lateral lobes showed vascular dilatation, congestion, and edema (Fig. 3). After 4 hours (R21), there was complete failure of trypan blue to penetrate any portion of the right lung. In the left, however, only a few small peripheral unstained areas were seen. These measured less than 0.2 mm. in diameter. Firm hemorrhagic lesions occupied the lobes of the right lung. Microscopically, there was intense dilatation of capillaries and larger pulmonary vessels, with thrombosis in some of the latter. Many venules had ruptured, and alveoli were packed with erythrocytes.

Discussion

The means by which staphylococcal toxin produces its necrotizing effects in various tissues has been the subject of speculation and experimental investigation. In particular, renal cortical necrosis produced by the intravenous injection of the toxin has interested a number of workers. Several have attributed the renal necrosis to a local vascular disturbance produced by the toxin. Thrombosis of regional blood vessels,[2,3] dilatation and rupture of glomerular capillaries,[4] and obstructive vascular stasis following injury to intralobular arteries and afferent arterioles[5] or spasm of renal veins[6,7] have all been considered as the vascular lesions leading to renal necrosis. On the other hand, it has

been held[4,8] that the toxin acts directly on endothelial and epithelial cells of the glomerular tufts and on the epithelium of the renal tubules.

Concerning the pathogenesis of the necrotic lesions produced by staphylococcal toxin in nonrenal tissues, Rigdon[9] was of the opinion that those which occurred in the intestine and elsewhere following the intravenous injection of toxin were due to direct injury to cells. Thal and Egner,[10] studying staphylococcal dermal necrosis in rabbits, noted an absence of neutrophils and an exclusion of intravenously injected trypan blue from lesions that became necrotic. This led them to consider the lesions to be essentially dermal infarctions secondary to vascular spasm. They observed spasm directly in small mesenteric arteries and veins about which staphylococcal toxin had been infiltrated. Thal and Molestina[11] observed local venous spasm in rabbits developing severe hemorrhagic pancreatic necrosis following the injection of staphylococcal toxin into the main pancreatic duct.

In the respiratory system various effects of staphylococcal toxin have been described in studies not specifically concerned with this problem. Russ[12] observed pulmonary edema and hypertension and right heart failure following the intravenous administration of toxin. Burnet and his associates,[13,14] using heart-lung, lung-pump, and heart-artificial lung preparations as well as experimental animals, observed a rise in pulmonary arterial pressure and a fall in systemic arterial pressure following the injection of staphylococcal toxin. They postulated a nonspecific, tonic contraction of pulmonary arterioles as well as a direct cardiac action of the toxin. No recent inquiries into the pulmonary effects of staphylococcal toxin appear to have been undertaken. However, Thal and Egner,[15] investigating the mechanism of shock produced by the toxin in rabbits, noted that the intravenous injection of alpha toxin led to aggregations of leukocytes along the endothelium of the small pulmonary vessels, and the occasional occurrence of pulmonary edema.

In our experiments a striking result of the introduction of staphylococcal toxin into the bronchial tree was the appearance of large peribronchial zones of hemorrhagic consolidation, usually situated in the central and posterior portions of the lungs. These lesions rapidly proceeded to complete necrosis of pulmonary tissue. Marginal areas showed an acute inflammatory reaction. Two aspects of this observation seem worthy of consideration: first, the pathogenesis of the pulmonary lesions; and, second, the relevance of our experimental results to findings in human staphylococcal pneumonia.

Vascular alteration played an important role in the development of

the pulmonary lesions. Initial intense congestion of larger blood vessels and alveolar capillaries was followed by edema, then rupture of capillaries and venules, and hemorrhage. Later, complete necrosis of pulmonary tissue occurred. That these lesions in fact represented classical infarcts due to spasm of larger pulmonary arteries does not seem likely since they lacked pyramidal configuration and peripheral location. Their location, however, corresponded to the distribution of India ink in the bronchial tree, when this was mixed with the injected toxin. There appears to be no strong argument against the view that staphylococcal toxin, diffusing through bronchial walls, produced the lesions by a direct effect on pulmonary capillaries and venules. Apparently paralytic dilatation and increased permeability of capillary blood vessels, with alveolar edema and hemoconcentration, led to stagnation of circulation, an effect sometimes enhanced by actual thrombosis of larger vessels. Whether such stagnation hyperemia, equivalent in terms of function to ischemia, was the sole mechanism producing pulmonary necrosis remains undecided. The possibility that the toxin also caused necrosis of cells by direct action does not seem unlikely.

The intravenous injection of trypan blue solution shortly before death gave additional evidence for the existence of a severe pulmonary circulatory disturbance. In animals sacrificed shortly after the injection of staphylococcal toxin, in which the lungs were free of zones of consolidation, there were peripheral wedge-shaped areas devoid of trypan blue. This appeared to indicate that spasm of smaller pulmonary blood vessels, presumably of transitory nature, did occur. However, for the reasons given above, spasm was not believed to have been responsible for the zonal pulmonary necrosis. In rabbits allowed to survive for longer periods after the injection of toxin, in which central zones of consolidation were found at necropsy, trypan blue solution was excluded from whole lobes or major portions of them. If the circulatory alteration thus indicated occurred initially in all animals receiving toxin, the circulation evidently became re-established peripherally beyond the central necrotic zone, since peripheral portions of the lung rarely became necrotic.

Absence of an acute inflammatory exudate in the foci of pulmonary consolidation is noteworthy. In our opinion, this was attributable to the inhibition of the vascular response following early focal circulatory arrest. Acute inflammation in marginal zones and in perivascular and peribronchial connective tissue within the necrotic lesions probably represented a reaction to staphylococcal toxin of tissues in which circulation persisted, or was re-established. The occurrence of acute

pneumonitis in some animals in areas remote from the centrilobar hemorrhagic and necrotic lesions is more difficult to explain. Possibly staphylococcal toxin, diffusing in and diluted by edema fluid, was present in concentrations insufficient to cause vascular stasis but nevertheless was capable of evoking an inflammatory response.

Staphylococcal pneumonia has been encountered as a complication during outbreaks of influenza[16,17] and has been observed in epidemic[18] and sporadic[19] form predominantly in infants. The disease in infancy may be rapidly fatal, death occurring sometimes within a matter of hours.[20] In such patients pathologic lesions in the lungs may be confined to hemorrhagic consolidation and spreading alveolar edema.[21] With longer survival the picture usually is that of a progressive hemorrhagic necrotizing pneumonia proceeding to multiple abscess formation.[22] The similarity of the earlier changes seen in this type of pneumonia to the lesions produced initially in the rabbit by the intratracheal injection of staphylococcal toxin are striking and indicate that the former may be due, at least in part, to a local production of exotoxin. Reference has already been made to the observation of Evans and Evans,[1] suggesting that relatively large quantities of toxin are in fact being produced in the lung in staphylococcal pneumonia. The hemorrhagic necrotic components of the full-blown disease and the frequency of venous thrombosis resemble the later lesions encountered in our experimental animals, and may also be attributed to the effect of the toxin.

The exclusion of large portions of lung from effective circulation was demonstrated in animals receiving intratracheal staphylococcal toxin by means of the intravenous injection of trypan blue. If a similar large scale pulmonary circulatory disturbance occurs in human staphylococcal pneumonia, it may well contribute to the occurrence of early and sudden death.

Summary and Conclusions

Staphylococcal toxin introduced into the tracheobronchial tree of rabbits produced large peribronchial zones of hemorrhagic consolidation which proceeded to complete necrosis of pulmonary tissue. Evidence is presented indicating that a vascular disturbance characterized by stagnation hyperemia with functional ischemia is important in the production of the lung necrosis. However, the possibility that the toxin may also cause necrosis of pulmonary tissue by direct action has not been excluded. Histologic features of the experimental lesions are similar to certain of those observed in fatal staphylococcal pneumonia in human patients.

REFERENCES

1. Evans, A. D., and Evans, M. Staphylococcal infection of the lower respiratory tract in adults with influenza. *Lancet*, 1956, 1, 771–773.
2. Neisser, M., and Wechsberg, F. Ueber das Staphylotoxin. *Ztschr. Hyg.*, 1901, 36, 229–349.
3. Von Glahn, W. C., and Weld, J. T. The effect of *Staphylococcus aureus* toxin on the kidney. *J. Exper. Med.*, 1935, 61, 1–8.
4. Glynn, J. H. The pathogenesis of cortical necrosis of the kidneys in rabbits following the injection of staphylococcus toxin. *Am. J. Path.*, 1937, 13, 593–604.
5. De Navasquez, S. Experimental symmetrical cortical necrosis of the kidneys produced by staphylococcus toxin: a study of the morbid anatomy and associated circulatory and biochemical changes. *J. Path. & Bact.*, 1938, 46, 47–65.
6. Thal, A. P. Selective spastic occlusion of the renal vascular system produced with staphylococcal toxin. (Abstract.) *Fed. Proc.*, 1951, 10, 372–373.
7. Thal, A. Selective renal vasospasm and ischemic renal necrosis produced experimentally with staphylococcal toxin. Observations on the pathogenesis of bilateral cortical necrosis. *Am. J. Path.*, 1955, 31, 233–259.
8. Rigdon, R. H.; Joyner, A. L., and Ricketts, E. T. A study of the action of a filtrable staphylococcal toxin on the kidneys of normal rabbits. *Am. J. Path.*, 1934, 10, 425–434.
9. Rigdon, R. H. Early lesions following intravenous administration of a filtrable staphylococcus toxin. A study on the dog and rabbit. *Arch. Path.*, 1935, 20, 201–208.
10. Thal, A., and Egner, W. Local effect of staphylococcal toxin. Studies on blood vessels with particular reference to phenomenon of dermonecrosis. *A. M. A. Arch. Path.*, 1954, 57, 392–404.
11. Thal, A., and Molestina, J. E. Studies on pancreatitis. III. Fulminating hemorrhagic pancreatic necrosis produced by means of staphylococcal toxin. *A. M. A. Arch. Path.*, 1955, 60, 212–220.
12. Russ, V. K. Die Toxine und Antitoxine der pyogenen Staphylokokken. *Ztschr. f. exper. path. u. Therap.*, 1916, 18, 220–250.
13. Burnet, F. M., and Kellaway, C. H. Recent work on staphylococcal toxins, with special reference to the interpretation of the Bundaberg fatalities. *M. J. Australia*, 1930, 2, 295–301.
14. Kellaway, C. H.; Burnet, F. M., and Williams, F. E. The pharmacological action of the exotoxin of *Staphylococcus aureus*. *J. Path. & Bact.*, 1930, 33, 889–912.
15. Thal, A. P., and Egner, W. The mechanism of shock produced by means of staphylococcal toxin. *A. M. A. Arch. Path.*, 1956, 61, 488–495.
16. Tytler, W. H.; Janes, R. M., and Dobbin, G. M. Pathological and Bacteriological Findings in Fatal Cases of Pneumonia During the Influenza Epidemic of October and November 1918. In: Studies of Influenza in Hospitals of the British Armies in France, 1918. Great Britain, National Health Insurance Joint Committee. Medical Research Committee. Special Report, Series No. 36. His Majesty's Stationery Office, Oxford, 1919, pp. 77–87.
17. Wollenman, O. J., Jr., and Finland, M. Pathology of staphylococcal pneumonia complicating clinical influenza. *Am. J. Path.*, 1943, 19, 23–42.

18. DePape, A. J., and McEwen, D. S. Staphylococcal pneumonia and pyoderma in infancy. *Canad. M. A. J.*, 1951, 65, 439–447.

19. Kanof, A.; Kramer, B., and Carnes, M. Staphylococcus pneumonia. A clinical, pathologic, and bacteriologic study. *J. Pediat.*, 1939, 14, 712–724.

20. McLetchie, N. G. B. Staphylococcal pneumonia in childhood. *Canad. M. A. J.*, 1949, 60, 352–356.

21. Guthrie, K. J., and Montgomery, G. L. Staphylococcal pneumonia in childhood. Pathological considerations. *Lancet*, 1947, 2, 752–755.

22. Magner, D., and Kussner, N. Staphylococcal pulmonary infection in infancy. *Am. J. Clin. Path.*, 1954, 24, 1391–1401.

[*Illustrations follow*]

LEGENDS FOR FIGURES

All photomicrographs were prepared from sections stained with hematein, phloxine and saffron.

FIG. 1. R11. Survival 24 hours. Lung. A cross section of the left inferior lobe shows an area of consolidation.

FIG. 2. R4. Survival 5 hours. Trachea. The blood vessels of the submucosa are dilated. There is edema and hemorrhage in the lamina propria of the mucosa and in the submucosa. × 70.

FIG. 3. R23. Survival 55 minutes. Lung. The alveolar capillaries and thin-walled pulmonary blood vessels are markedly dilated, and there is alveolar edema. × 90.

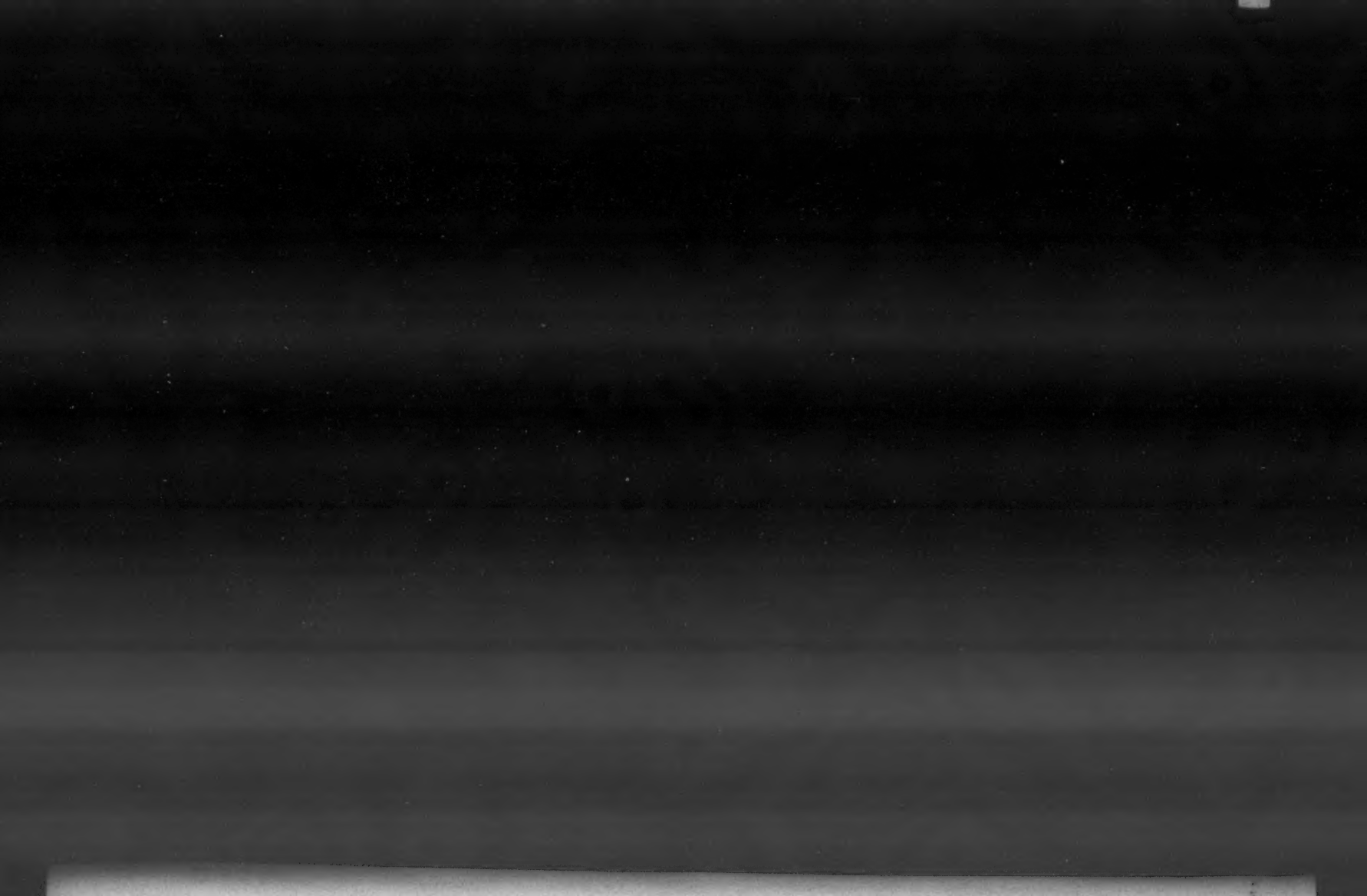

1

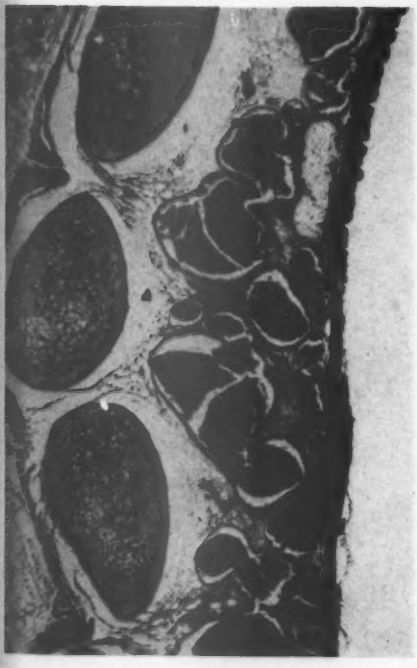

2

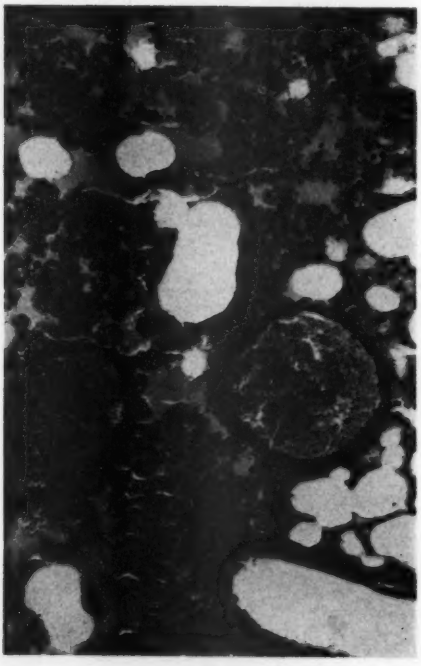

3

FIG. 4. R2. Survival 1 hour and 45 minutes. Lung. A greatly dilated pulmonary blood vessel contains a thrombus. There are endothelial swelling and collections of leukocytes along the endothelial surface. × 100.

FIG. 5. R12. Survival 48 hours. Lung. There is a large zone of hemorrhagic necrosis about a central bronchus. × 15.

FIG. 6. R12. Survival 48 hours. Lung. Surrounding the bronchus is a zone of edema and hemorrhagic necrosis. In the lower part of the photograph the outlines of alveolar walls can be seen. There is an acute inflammatory exudate in the peribronchial connective tissues. × 70.

FIG. 7. R11. Survival 24 hours. Lung. A parabronchial blood vessel shows an infiltration of neutrophils, principally in the subendothelial, adventitial, and periadventitial regions. × 300.

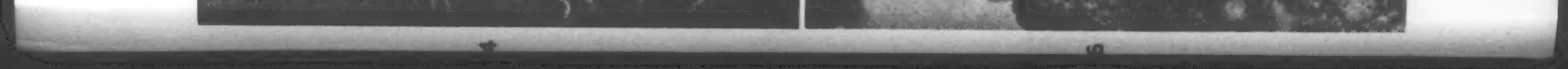

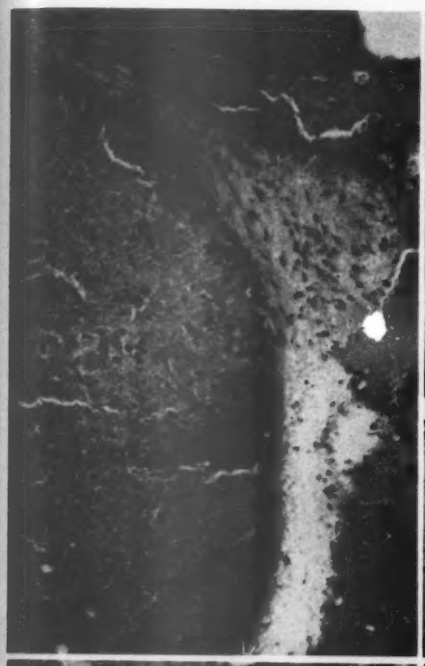

5

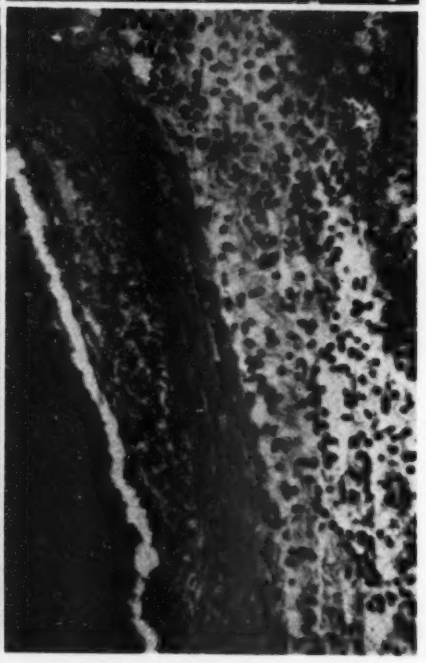

7

FIG. 8. R13. Survival 4 days. Lung. A field at the margin of a zone of hemorrhagic necrosis shows evidence of repair. The alveoli are lined by plump cells giving the appearance of epithelialization. × 300.

FIG. 9. R23. Survival 55 minutes after injection of undiluted toxin. A solution of trypan blue was introduced into the inferior vena cava 10 minutes before death. Trachea and lungs, posterior aspect. There is complete exclusion of the dye from the right superior and middle lobes and much of the right inferolateral lobe.

FIG. 10. R28. Survival after intratracheal injection of dilute toxin. A solution of trypan blue was introduced into the inferior vena cava 10 minutes before death. Portion of trachea and lungs, posterior aspect. There are small, clearly demarcated, peripheral regions unstained by the dye.

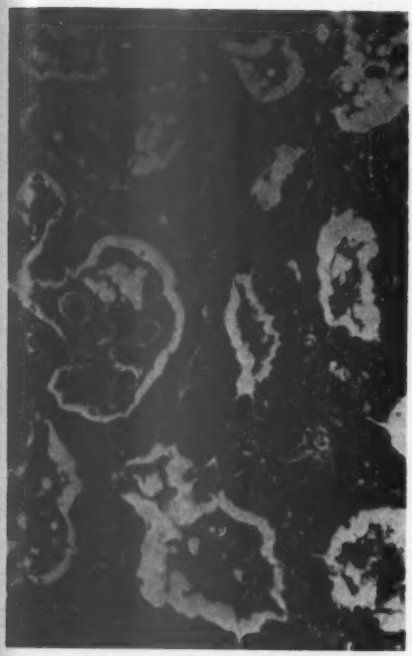

9

10

ENHANCED SUSCEPTIBILITY OF PROLIFERATING ENDOTHELIUM TO SALIVARY GLAND VIRUS UNDER NATURALLY OCCURRING AND EXPERIMENTAL CONDITIONS*

F. Stephen Vogel, M.D.

From the Department of Pathology, The New York Hospital-Cornell Medical Center, New York, N.Y.

The endothelial cells of proliferating capillaries in a chronic peritonitis of a youth, herein described with disseminated salivary gland virus disease, were enlarged and contained numerous inclusion bodies. This was in conspicuous contrast to the absence of cytomegaly and inclusions in the endothelium elsewhere and to the extreme rarity of this phenomenon in other cases of disseminated salivary gland virus disease.[1,2] The observation suggested the possibility that proliferating endothelial cells have enhanced susceptibility to the salivary gland virus. This possibility was tested experimentally.

Report of a Case

A 10-year-old schoolboy developed fever, sore throat, enlargement of the cervical lymph nodes, malaise, and epistaxis. During the subsequent 10 weeks there were intermittent episodes of fever, anorexia, and malaise with a 20 pound weight loss.

An examination performed upon admission to the hospital 20 days prior to death showed a cachectic child with icterus of the skin and sclera. The nasal septum was covered with dried blood. There was cheilosis. Peripheral lymph nodes were enlarged, firm, and discrete, measuring up to 1.5 cm. across. The lungs were clear. The heart was not enlarged, and a soft, nontransmitted, systolic murmur was audible at the apex. The abdomen was protuberant. The liver edge was firm and extended 9 cm. below the costal margin. The border of the spleen was 21 cm. beneath the left costal margin. The neurologic examination was normal.

Laboratory studies disclosed a white blood count of 4,500 per cm.^{3} with 76 per cent lymphocytes, 13 per cent neutrophils, 2 per cent band forms, and 9 per cent monocytes. The hemoglobin was 10 gm. per 100 ml. The urine had a specific gravity of 1.013 and gave no reaction for protein or sugar. L.E. preparations, Coombs's test, and heterophile, Brucella, and Weil-Felix agglutination reactions were all negative. A blood culture was also negative. The serum bilirubin level was 7.6 mg. per cent. The serum albumin was 2.7 gm. per cent; the globulin 1.0 gm. per cent. The serum alkaline phosphatase was 37.5 Bodansky units, and a cephalin flocculation test was negative. The prothrombin time was greater than 2 minutes; the bleeding time, 11.5 minutes, and the clotting time, 10 minutes. The stool was negative to the guaiac test. A bone marrow examination revealed mild erythroid hyperplasia.

The patient weakened progressively with frequent temperature elevations to 39°C. A splenectomy and liver biopsy were performed on the tenth hospital day. The liver showed periportal lymphocytic infiltrations with intranuclear inclusions

* This investigation was supported by a research grant B-803 from the National Institute of Neurological Disease and Blindness of the National Institutes of Health, United States Public Health Service.

Received for publication, May 8, 1958.

in parenchymal cells. The spleen weighed 1,900 gm. It contained many small hemorrhages and foci of necrosis but no demonstrable inclusions. On the third day following operation the patient became febrile, and the surgical incision exuded purulent material from which hemolytic *Staphylococcus aureus* was cultured. The abdomen became protuberant, and 3,600 cc. of sanguinous fluid was removed by paracentesis. Signs and roentgenologic evidence of bronchopneumonia developed and death occurred on the 20th hospital day.

Necropsy Observations

The body was that of an extremely cachectic white youth weighing 29 kg. The abdomen was protuberant and contained 500 cc. of serosanguinous fluid.

The submaxillary glands were not grossly altered but on microscopic examination showed focal lymphocytic infiltrations. Some acinar cells in these areas and lesser numbers of free-lying cells in the ducts were enlarged and contained conspicuous intranuclear inclusion bodies. Most affected cells had a single nucleus, but some were binucleated and a few were multinucleated. The intranuclear inclusions measured 10 to 12 μ across. They were weakly acidophilic and had a finely granular and somewhat ordered architecture. A clear halo was present about each, and in this zone the chromatin material was marginated toward the nuclear membrane. The cytoplasm was regularly abundant (Fig. 1). In some cells there were zones of cytoplasmic rarefaction which contained small, pale, granular inclusion bodies. These stained positively with periodic acid.

The lungs weighed 1,190 gm. There were numerous, widely dispersed and confluent, gray, indurated areas of consolidation. These showed, on microscopic examination, an intra-alveolar exudate of fibrin with numerous macrophages and lesser numbers of lymphocytes, neutrophils, and erythrocytes. There were multitudes of enlarged mononucleated and binucleated cells containing prominent, deep-staining, intranuclear inclusion bodies. These were most abundant in the alveolar exudate adjacent to the alveolar septums. Lesser numbers were present in the exudate that filled many of the small bronchi and bronchioles (Fig. 2).

The heart weighed 210 gm. It was not grossly abnormal. Many histologic sections from representative portions showed small, discrete, focal lymphocytic infiltrations at all depths of the myocardium. There was minimal necrosis. However, several myocardial cells were notably enlarged and their rounded nuclei contained conspicuous inclusion bodies.

The liver weighed 1,700 gm. Throughout the parenchyma and most marked in the periportal regions there were dense lymphocytic infiltrations. Many of the parenchymal cells were enlarged with abundant

coarsely granular cytoplasm and rounded nuclei that frequently contained conspicuous inclusion bodies. The pancreatic acinar tissue was also focally infiltrated by lymphocytes. Several acinar cells were notably enlarged and showed intranuclear and intracytoplasmic inclusion bodies.

The adrenal glands weighed 7.3 gm. together. The cortices contained small nodular foci of necrosis measuring up to 0.5 cm. across. These were characterized histologically by dense infiltrations of granulocytes and lesser numbers of lymphocytes and macrophages. There was much necrosis of the parenchyma, and many of the cortical cells were enlarged and contained intranuclear inclusion bodies. The medullary tissues were unaffected.

The kidneys were symmetrically enlarged and together weighed 370 gm. They contained moderately dense, focal and linear, interstitial leukocytic infiltrations that were most marked in the outer margins of the cortex. Several tubular epithelial cells were enlarged and contained intranuclear inclusions. The capsule of the left kidney was thickened by loose fibrous tissue, and several of the fibroblasts showed elongated intranuclear inclusion bodies.

The mucosa of the distal esophagus and stomach was ulcerated in multiple discrete areas measuring less than one cm. across. Fibroblasts at the base of the esophageal ulcers contained fusiform intranuclear inclusion bodies; similar inclusions were also present in enlarged smooth muscle cells of the adjacent muscularis. Numerous intranuclear inclusions were present throughout the gastric mucosa. They were most abundant within the cardia and particularly at the bases of the glands. Individual cells were enlarged, and their abundant cytoplasm stained more intensely than that of adjacent normal glandular epithelium. The chromatin in the enlarged nuclei was coarse and clumped, and in many nuclei there were prominent inclusion bodies. In lesser numbers, the interstitial cells of the mucosa were also enlarged and contained intranuclear inclusions. Both the glandular and interstitial cells of the duodenum, jejunum, and ileum were similarly affected but in lessening degrees. The mucosal epithelium of the appendix, cecum, and colon contained no demonstrable inclusions. However, enlarged, inclusion-bearing, interstitial cells were present sparsely throughout the colon.

The striated muscles of the diaphragm and of the psoas region were examined. Each contained nodular lymphocytic infiltrations. Many muscle cells in these regions were enlarged and often multinucleated. Some contained characteristic intranuclear inclusion bodies.

The brain was edematous and weighed 1,350 gm. There were patchy

perivascular lymphocytic infiltrations in the cerebral and cerebellar tissues. These were most conspicuous in the infundibular, hypothalamic, and mural regions of the third ventricle. Several poorly-formed intranuclear inclusions were present in the infundibulum. The host cells had rounded nuclei with inconspicuous nucleoli and scant cytoplasm. They most closely resembled astrocytes. Larger and entirely characteristic intranuclear inclusions were contained within glial cells of the posterior lobe of the pituitary. The choroid plexus of each ventricle was densely infiltrated by lymphocytes and large mononuclear cells. Several of the latter contained intranuclear inclusion bodies.

The entire peritoneum, most conspicuously that covering the stomach and diaphragm, was moderately thickened by a mesh of fibroblasts and small blood vessels. This was lightly but diffusely infiltrated by large monocytes and lymphocytes. The outer surfaces were thickly covered with fibrin. Many of the endothelial cells of the capillaries and small blood vessels were conspicuously enlarged and contained prominent intranuclear inclusions (Fig. 4). Lesser numbers of fibroblasts and mesothelial cells were also enlarged and contained rounded or elongated intranuclear inclusion bodies.

Experimental Study

Materials and Methods

The experimental study was carried out by injecting the mouse strain of salivary gland virus intraperitoneally in mice with focal granulomatous peritonitis induced by means of sterile sand. The susceptibility of proliferating endothelium in the granulomas and of the nonproliferating endothelium in other sites of the peritoneum were determined by microscopic study.

Animals. Young Swiss mice weighing 18 to 20 gm. were used.

Virus. The mouse strain of salivary gland virus was procured from Dr. Margaret Smith, St. Louis. Intraperitoneal injections of 0.2 cc. of a 1:10 suspension of the salivary gland tissue in saline regularly induced extensive necrosis in the livers and spleens of the young mice. There were multitudes of intranuclear inclusions in these organs, and death of the host ensued within 4 to 6 days. Comparable subcutaneous injections induced latent infections in the salivary glands with development of cytomegaly and intranuclear inclusions after 7 to 14 days.

Production of Granulomas. Sterile sand was ground vigorously with a mortar and pestle in small quantities of sterile saline. The finely particulate material, in a cloudy suspension, was used for intraperitoneal injection in amounts of 0.5 cc. To study the development of the granulomas, pairs of mice were sacrificed daily for 14 days.

Induction of Viral Infection. Mice in groups of 20, with granulomas 5 and 10 days old, received 0.2 cc. of a 1:10 saline suspension of mouse salivary gland tissue intraperitoneally. This, as proven by histologic examination, contained numerous pathognomonic, cytomegalic, inclusion-bearing cells. Comparable groups of mice without sand granulomas received similar injections for control purposes. All animals were sacrificed just prior to death after 4 to 6 days.

Histologic Preparations. As routine, small portions of tissue from the peritoneal granulomas and from many additional sites in the peritoneum, liver, and spleen of animals in the experimental and control groups were fixed in Bouin's solution. The paraffin embedded tissues were sectioned at 4 μ and stained by hematoxylin and eosin.

The Susceptibility of the Mouse Endothelium to the Mouse Strain of Salivary Gland Virus

Sand Granulomas. The sterile sand granulomas were often localized immediately beneath the anterior abdominal wall at the injection site, encased by loops of small intestine and omentum. Smaller nodules were regularly distributed elsewhere, particularly in the omentum and over the capsules of the liver and spleen. The silica was abundant in the central portions of the nodule, encapsulated by large fibroblasts and macrophages. There were numerous medium-sized blood vessels and blood-filled capillaries. The endothelial cells had plump, slightly pleomorphic, elongated nuclei. None contained inclusion bodies. The vascular proliferation was pronounced in 5-day-old granulomas; it was more conspicuous in lesions examined during the subsequent 5 days, and was thereafter obscured somewhat by fibroblastic proliferation and early deposition of collagen.

Granulomas with Virus. The proliferating endothelium of the capillaries and small blood vessels in the sand granulomas of mice which received both sand and salivary gland virus were notably more pleomorphic than those in animals receiving sand alone. The nuclei and cytoplasm of very many proliferating endothelial cells were approximately twice the expected size, and great numbers contained conspicuous, deep-staining, intranuclear inclusion bodies (Fig. 5). Young fibroblasts of the granulomas were also affected to a lesser degree. The intensity of the leukocytic infiltration and the amount of necrosis in these tissues were notably greater than in sand granulomas not harboring the virus. As was true also in control animals without granulomas, the liver and spleen regularly contained multitudes of intranuclear inclusions and much necrosis. The mesothelial cells of all animals contained few inclusion bodies. The endothelial cells in the

peritoneum of control animals without granulomas which received the virus, and the nonproliferating endothelial cells at a distance from the granulomas in the peritoneum of mice in the experimental groups, as well as the endothelial cells in the livers and spleens of all animals regularly failed to show cytomegaly or intranuclear inclusions.

Discussion

The observations make it clear that proliferating endothelium of mice manifests an enhanced susceptibility to the mouse strain of the salivary gland virus. The presence of widely disseminated lesions in the livers and spleens of the same animals provides evidence of a viremia and makes it seem unlikely that the preferential localization in the inflammatory sites is solely a manifestation of greater accessibility of these tissues to the virus. The cause of the enhanced cellular susceptibility remains wholly obscure. However, the findings are in general agreement with previous observations that proliferating epithelial cells show a greater susceptibility to the Shope papilloma virus than does normal epithelium.[3] They have added interest since it has been clearly shown that in one instance proliferating neoplastic cells manifested a decreased susceptibility to the salivary gland virus. Mice bearing methylcholanthrene-induced carcinomas of the acinar epithelium of the salivary glands, when inoculated subcutaneously with the salivary gland virus, have failed to show cytologic evidence of viral localization in the neoplastic tissue while cytomegaly and intranuclear inclusions were present in abundance in the contiguous parotid gland.[4]

The human strain of the salivary gland virus has generally exhibited wide infectivity but low virulence. Routine postmortem examinations of the salivary tissues of fetuses and infants below the age of 2 years have disclosed cytologic[5] and cultural[6] evidences of latent infections in up to 30 per cent of cases. The host resistance is notably less during these periods, and many examples of fatal disseminated disease are recorded.[1] By contrast, infections have been rarely noted in children above the age of 2 years or in adults.[7] Characteristic cytomegaly and intranuclear inclusions have been observed in the lung, adrenal, and gastrointestinal tract, but in most instances the viral infection is superimposed upon and terminates another chronic illness. Spontaneous infections by species specific viral strains[8] have also been noted in chimpanzees,[9] monkeys,[10] and rodents.[11]

The viral dissemination and cellular localization was unusually widespread in the present case. As in others,[1] the salivary glands, heart, lungs, liver, pancreas, adrenals, kidneys, stomach, small and large intestine, pituitary, and central nervous system contained lesions.

In addition, and uniquely, the mesothelium and proliferating endothelium of the peritoneum, the smooth muscle of the esophagus, and the skeletal musculature of the diaphragm and psoas regions were also affected. This fatal infection in an otherwise healthy youth broadens the concepts of the host and cellular susceptibility to the salivary gland virus.

Summary

A 10-year-old boy with a fatal disseminated salivary gland virus infection showed characteristic cytomegaly with intranuclear and intracytoplasmic inclusions in the salivary gland, heart, lung, liver, pancreas, adrenals, kidney, esophagus, gastrointestinal tract, central nervous system, smooth and skeletal muscle, and conspicuously in the endothelium and mesothelium of a chronic proliferative peritonitis.

The presence of cytomegaly and intranuclear inclusions in the proliferating endothelial cells of the peritoneum and their absence elsewhere in nonproliferating endothelium suggested that these cells have increased susceptibility to the salivary gland virus during maturation. Experimental studies made it clear that proliferating endothelial cells of the blood vessels in sand granulomas of mice have a notably greater susceptibility to the mouse strain of salivary gland virus than does nonproliferating endothelium elsewhere in the same animal. The findings broaden previous observations on the effect of cellular state upon the susceptibility to viruses.

REFERENCES

1. Wyatt, J. P.; Saxton, J.; Lee, R. S., and Pinkerton, H. Generalized cytomegalic inclusion disease. *J. Pediat.*, 1950, **36**, 271–294.
2. Worth, W. A., Jr., and Howard, H. L. New features of inclusion disease of infancy. *Am. J. Path.*, 1950, **26**, 17–35.
3. Friedewald, W. F. Cell state as affecting susceptibility to a virus. Enhanced effectiveness of the rabbit papilloma virus on hyperplastic epidermis. *J. Exper. Med.*, 1942, **75**, 197–220.
4. Bauer, W. H., and Grand, N. G. Interaction of a salivary gland virus and experimentally produced carcinoma of mouse salivary gland. *Cancer Res.*, 1954, **14**, 768–774.
5. Farber, S., and Wolbach, S. B. Intranuclear and cytoplasmic inclusions ("protozoan-like bodies") in the salivary glands and other organs of infants. *Am. J. Path.*, 1932, **8**, 123–136.
6. Smith, M. G. Propagation in tissue cultures of a cytopathogenic virus from human salivary gland virus (SGV) disease. *Proc. Soc. Exper. Biol. & Med.*, 1956, **92**, 424–430.
7. Wyatt, J. P.; Hemsath, F. A., and Soash, M. D. Disseminated cytomegalic inclusion disease in an adult with primary refractory anemia and transfusional siderosis. Report of a case. *Am. J. Clin. Path.*, 1951, **21**, 50–55.
8. Rivers, T. M. (ed.). Viral and Rickettsial Infections of Man. J. B. Lippincott Co., Philadelphia, 1952, ed. 2, p. 674.

9. Vogel, F. S., and Pinkerton, H. Spontaneous salivary gland virus disease in chimpanzees. *A.M.A. Arch. Path.*, 1955, 60, 281–285.

10. Covell, W. P. The occurrence of intranuclear inclusions in monkeys unaccompanied by specific signs of disease. *Am. J. Path.*, 1932, 8, 151–158.

11. Kuttner, A. G., and Wang, S.-H. Problem of the significance of the inclusion bodies found in the salivary glands of infants, and the occurrence of inclusion bodies in the submaxillary glands of hamsters, white mice, and wild rats (Peiping). *J. Exper. Med.*, 1934, 60, 773–791.

LEGENDS FOR FIGURES

Sections illustrated are all stained with hematoxylin and eosin.

FIG. 1. A cytomegalic cell lying free in a duct of the submaxillary gland of a 10-year-old boy dying of disseminated salivary gland virus disease. The nucleus is greatly enlarged and occupied by a huge intranuclear inclusion body. This has a somewhat ordered vesiculated structure. A few chromatin granules are marginated toward the pale nuclear membrane within the halo about the inclusion body. The abundant cytoplasm is finely granular. × 1,900.

FIG. 2. The alveolar exudate in the lung is formed of fibrin, leukocytes, and red blood cells. Many enlarged cells with prominent intranuclear inclusions are present. × 450.

FIG. 3. In the bases of the gastric glands there are two enlarged epithelial cells without inclusion bodies and two that show characteristic intranuclear inclusions. × 650.

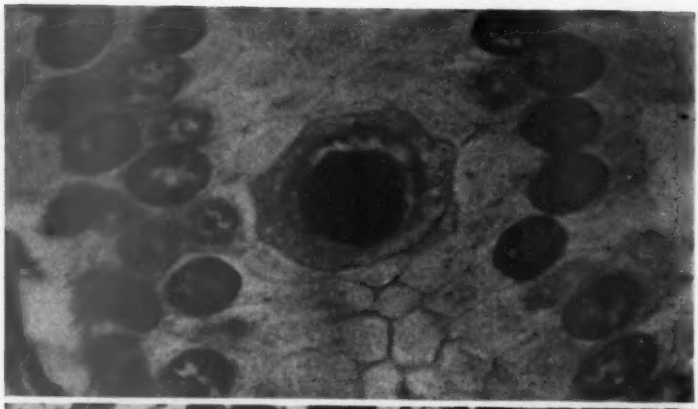

1

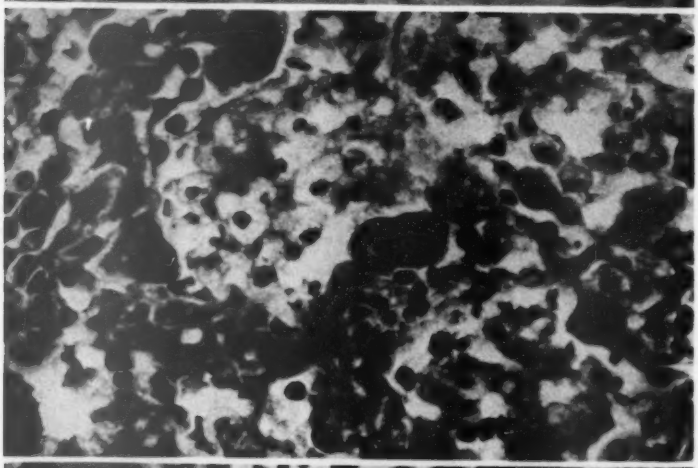

2

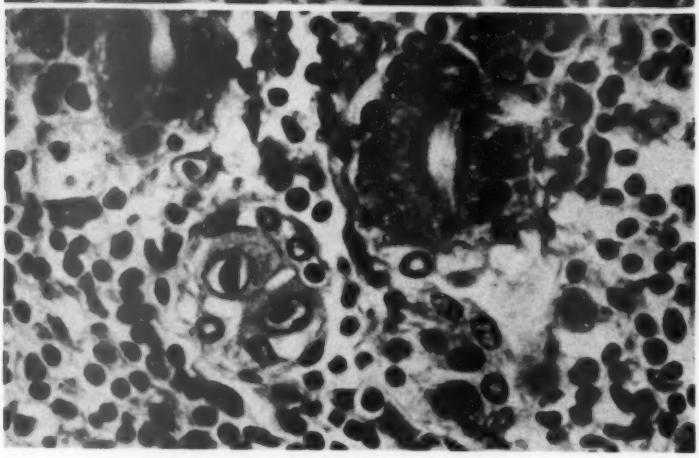

3

FIG. 4. The serosa of the stomach shows a chronic proliferative peritonitis that is formed of fibroblasts, fibrin, and round cells. The proliferating capillary endothelium is pleomorphic and one cell contains a conspicuous intranuclear inclusion. × 275.

FIG. 5. Section of a sand granuloma of a mouse harboring the salivary gland virus. There are numerous enlarged, pleomorphic endothelial cells lining the proliferating blood vessels. Many of these have conspicuous intranuclear inclusions. There is excessive necrosis and leukocytic infiltration in the granulomatous tissue. × 450.

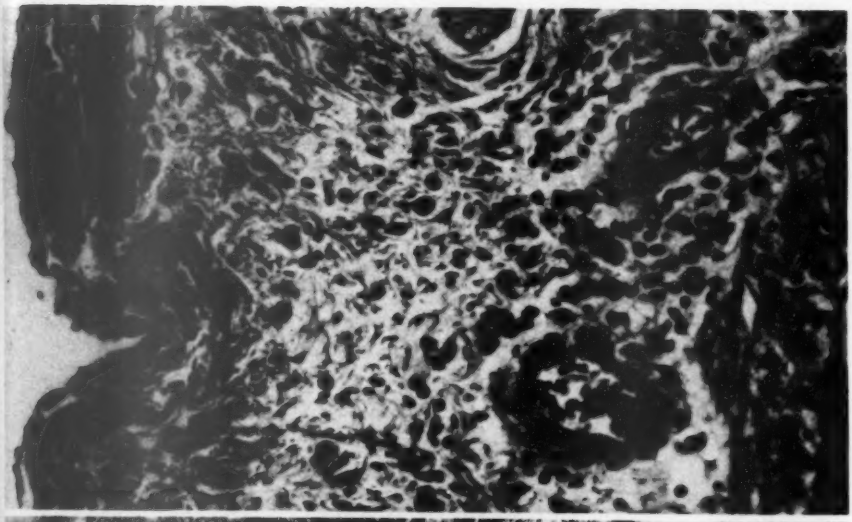

4

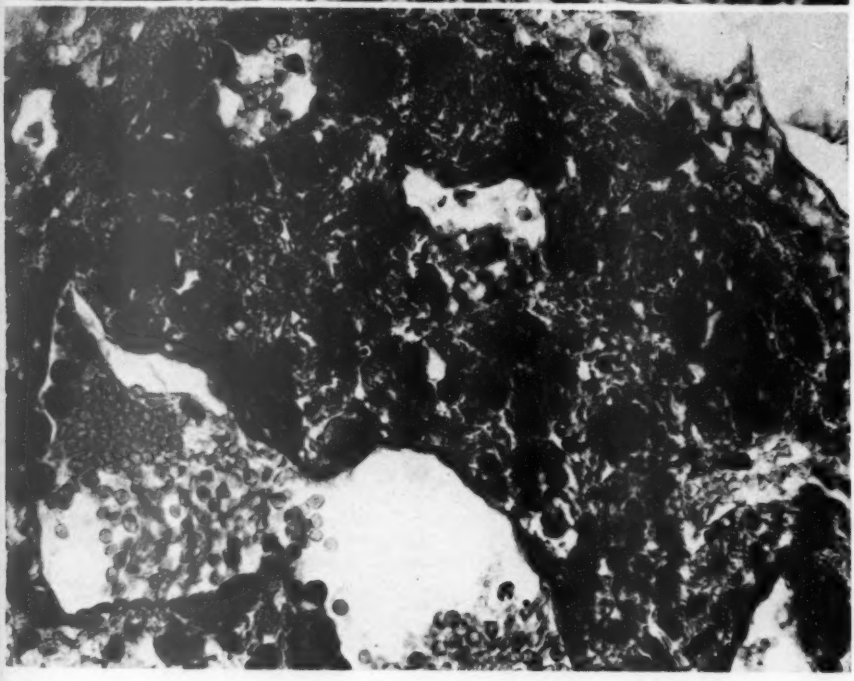

5

ISOTHIOCYANATE COMPOUNDS AS FLUORESCENT LABELING AGENTS FOR IMMUNE SERUM *

J. L. Riggs, M.A.; R. J. Seiwald, Ph.D.;† J. H. Burckhalter, Ph.D.; C. M. Downs, Ph.D., and T. G. Metcalf, Ph.D.‡

From the Department of Bacteriology and the Laboratory of Pharmaceutical Chemistry, University of Kansas, Lawrence, Kans.

Since the use of fluorescein labeled antibodies for the selective staining of homologous antigens was introduced by Coons and associates,[1,2] the technique has received wide use and has proved to be a valuable tool in immunologic and microbiologic studies. In addition to the use of fluorescein isocyanate as a labeling agent, as described by Coons, the use of an orange fluorescing isocyanate of rhodamine B has been reported by Silverstein, Eveland and Marshall.[3] By using the rhodamine B labeled antibody simultaneously with a different antibody labeled with fluorescein isocyanate, they were able to differentiate between two organisms of unlike antigenic composition in the same smear preparation, one organism appearing red-orange and the other yellow-green when viewed in the ultraviolet microscope.

Because of the difficulty in preparation, the danger in the use of phosgene, and the instability of the isocyanates described by Coons and Silverstein, we have undertaken studies to determine if the synthesis of the labeling agents could be simplified and if a chemically active group other than isocyanate could be used in coupling the fluorescent dyes with immune globulin. Recently Goldman and Carver[4] overcame the instability of fluorescein isocyanate by absorption to filter paper and have described a simple method of labeling the antiserum.

The present report deals with the synthesis of stable, solid iso*thio*cyanates of fluorescein and rhodamine B and the use of these two compounds in "labeling" antibodies for the specific staining of antigens. The dyes have been used in both the direct method of Coons[2] and the indirect method of staining as given by Weller and Coons,[5] and have shown satisfactory fluorescence when labeled antibody is applied to bacterial smears, bacteria in tissue, and to rickettsiae, bacteria, and viruses in cultured cells.

* This work was supported in part by a grant from the National Institutes of Health, United States Public Health Service; and from the general Research Fund of the University of Kansas.

Received for publication, March 15, 1958.

† Present Address: Department of Chemistry, University of San Francisco, San Francisco, Calif.

‡ Present Address: Department of Bacteriology, University of New Hampshire, Durham, N.H.

Materials and Methods

Organisms

Bacillus anthracis strain Ax 16 was grown in Burdon's modification of Thorne's medium[6] to favor capsule formation. *Pasteurella tularensis* was grown in glucose cysteine blood agar and in mouse fibroblast (L cells).[7] *Rickettsia typhi*, Wilmington strain, was cultivated in chick entodermal cells. Adenovirus RI-67 was grown in human liver cells.[8]

Antiserums

Anti-anthrax and anti-tularemia serums were prepared in rabbits by the injection of formalinized suspensions of the respective bacteria. Antiserum for *R. typhi* was convalescent serum from a human source and had a complement fixation titer of 1:32. Serum against RI-67 was prepared by the injection of virus into rabbits. Anti-rabbit serum was used in the indirect test and was prepared by the injection of rabbit serum into a goat. Anti-human serum was prepared by the injection of human serum into rabbits. The globulin-containing antibodies were precipitated from the whole antiserums by 3 precipitations with one half saturated ammonium sulphate. The ammonium sulphate was removed by dialysis and the precipitated globulin dissolved in buffered saline, pH 7.2. Before conjugation, the protein content of the globulin antibody was determined, and the conjugation with the fluorescent dyes carried out as given below.

Application of Labeled Antibody

All slides prepared from bacteria were dried and fixed with gentle heating. Rickettsia or virus infected cells grown on cover slips were washed in buffered saline, fixed in cold acetone for 15 minutes and stored in the refrigerator until treated with labeled antiserum.

Direct Procedure

In this method the slides were treated with a labeled antiserum corresponding to the antigen used to prepare the slide. The length of time for application of the antibody and the time of washing must be worked out individually for each type of antigen used. As a rule, antiserum was applied for 20 minutes at 37° C. The slides were then washed in 4 changes of buffered saline for 20 minutes and mounted in buffered glycerol. The glycerol used for mounting fluorescein isothiocyanate stained slides was buffered at pH 8.0, that for rhodamine B, at pH 7.2.

Indirect Procedure

The slides were reacted with unlabeled specific antiserum for 15 minutes at 37° C., then washed for 10 minutes in 3 changes of buffered saline. The preparation was then treated with labeled antiserum corresponding to the specific antiserum.

Controls

The specificity of the reactions was shown by lack of staining with labeled normal serum or by the blocking technique described by Coons,[2] in which unlabeled specific antiserum was applied prior to treatment with labeled antiserum. No staining was evident in these controls as the normal serum was readily removed by washing, and in the blocking technique antibody sites were already occupied by unlabeled antibody.

Microscope

The ultraviolet microscope consisted of the Reichert-Hacker "Lux" X equipment, fitted with a maximum-pressure mercury vapor arc lamp, type HBO 200. The ultraviolet filter used was the Reichert UV pass filter No. BG 12, thickness 1.5 mm. This ultraviolet source was used in conjunction with a standard Leitz monocular research microscope fitted with the normal glass optical system of lenses. A Leitz Euphos protective filter, thickness 1.5 mm., was fitted in the ocular. The condenser was an aplanatic darkfield condenser used without a funnel stop in the objective.

Experimental Results

The Synthesis of Fluorescein Isothiocyanate I *

Nitrofluorescein Diacetate I. Nitrofluorescein and its two isomeric diacetates were prepared according to the method of Coons.[2] Only the diacetate isomer I was used in the following preparation.

Aminofluorescein Diacetate I. A suspension of 5.0 gm. (0.011 mole) of finely divided nitrofluorescein diacetate I and 1 gm. of Raney nickel catalyst in 200 ml. of absolute ethanol was hydrogenated at 50 pounds pressure until hydrogen ceased to be taken up. Application of heat to the reaction vessel by means of a heat lamp greatly accelerated the reaction. The solution gradually assumed a bright blue fluorescence during the hydrogenation. The reaction mixture was filtered to remove

* The chemical syntheses reported are reproducible and give reproducible biological results. However, as in the case of the isocyanates, the analytically pure isothiocyanates are difficult to obtain. Further chemical studies are being carried out.

the catalyst, the solution was evaporated to a volume of about 30 ml., and the residue poured into 1 liter of ice water. The light tan solid product was collected on a filter, washed with water and dried. It weighed 4.3 gm. (88 per cent yield) and melted over a range, 145° to 160° C.

Analysis: Calculated for $C_{24}H_{17}NO_7 \cdot H_2O$: C, 64.14; H, 4.26; N, 3.12; H_2O, 4.01. Observed: C, 64.02; H, 4.46; N, 3.01; H_2O, 3.84.

Fluorescein Isothiocyanate I. A solution of 5 gm. of aminofluorescein diacetate I in 20 ml. of acetone was added by drops to a stirred solution of 4 ml. of thiophosgene (Rapter Laboratories, P.O. Box 4050, Chicago 54, Illinois) in 20 ml. of acetone at 40° C. The solution was then heated at reflux temperature for 4 hours. The solvent and excess

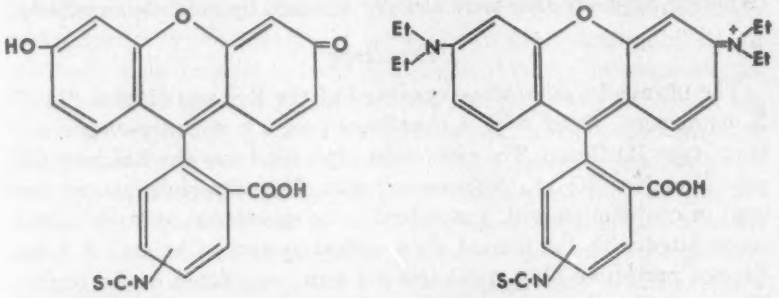

Text-figure 1. Fluorescein isothiocyanate (left); rhodamine B isothiocyanate (right).

thiophosgene were removed under reduced pressure, the residue dissolved in 20 ml. of acetone, and the solution added by drops to 1,200 ml. of rapidly stirred Skellysolv B.* The precipitated orange solid was collected on a filter washed with Skellysolv B and dried. It weighed 4.3 gm. The product decomposed upon heating: it did not melt.

The infra-red spectrum resembled that of fluorescein except that a strong isothiocyanate peak[9] occurred near 2,100 cm^{-1}. It appeared that at least one and probably both of the acetate groups had been removed during the reaction with thiophosgene. In contrast to fluorescein isocyanate obtained from Coon's deacetylated aminofluorescein I, this product was very soluble in acetone and acetone water mixtures. It was at least as fluorescent as the Coons isocyanate, and it was stable in solid form. Occasionally, batches gave a lighter or darker product, but the color of the isothiocyanate did not appear to influence the fluorescence of the protein conjugate.

* Skellysolv B, which has a boiling point of 60° to 70° C., is principally n-hexane but also contains n-pentane and n-heptane. It was obtained from the Skelly Oil Company, 605 West 47th St., Kansas City, Mo.

The Synthesis of Rhodamine B Isothiocyanate *

4-Nitrophthalic Acid. This material (Eastman Kodak Company, Rochester, New York) was used without further purification.

4-Nitrophthalic Anhydride. The anhyride was prepared by heating the acid for 2 hours at 170° to 175° C. After cooling, the light tan solid was powdered and was used without further purification; melting point, 115° to 117° C.

Nitrorhodamine B. The plan for this preparation was suggested by German patent 85931 (1897) although the procedure is quite different.

A suspension of 4.8 gm. (0.0025 mole) of the finely powdered anhydride in 100 ml. of xylene was heated with vigorous stirring until reflux temperature was reached. While the mixture was maintained at just below reflux temperature, a solution of 8.2 gm. (0.005 mole) of *m*-diethylaminophenol (Eastman) in 50 ml. of xylene was added by drops over a period of 30 minutes. At this point, the solution was usually red, and it might also contain a finely divided solid. The mixture was kept at reflux temperature for 18 hours, although stirring was usually discontinued after 2 hours.

The dark purple solution was distilled at slightly diminished pressure until the remaining volume was abqut 30 ml. On cooling, a thick gum precipitated. The xylene layer was decanted, the residual gum washed with 30 ml. of cold xylene and then dissolved in 200 ml. of boiling chloroform. The solution was filtered, cooled, and poured into 800 ml. of cold, rapidly stirred Skellysolv B. The precipitated solid was washed with Skellysolv B and dried. The magenta powder weighed 9.15 gm. (75 per cent yield) and melted over a wide range.

Aminorhodamine B. A suspension of 2.0 gm. (0.004 mole) of nitrorhodamine B and 1 gm. of Raney nickel in 200 ml. of absolute ethanol was hydrogenated at 50 pounds pressure and 35° C. temperature for 16 hours. During this time, the nitrorhodamine completely dissolved and absorbed the theoretic amount of hydrogen. The solution was filtered to remove the catalyst, evaporated to a volume of 30 ml., and poured in a thin stream into 400 ml. of cold Skellysolv B. The precipitated solid was collected, washed with Skellysolv B and dried. It weighed 1.45 gm. (78 per cent yield) and exhibited a brilliant red fluorescence when dissolved in slightly acidulated alcohol.

Rhodamine B Isothiocyanate. One gm. of aminorhodamine B was suspended in 15 ml. of acetone and the suspension added by drops to a solution of 1 gm. of thiophosgene in 5 ml. of acetone contained in a

* The chemical syntheses reported are reproducible and give reproducible biologic results. However, as in the case of the isocyanates, analytically pure isothiocyanates are difficult to obtain. Further chemical studies are being carried out.

50 ml. Erlenmeyer flask equipped with a magnetic stirrer. The resultant slurry was stirred at 40° C. for 8 hours, cooled, filtered, and the filtrate concentrated to a gum. The gum was redissolved in 5 ml. of acetone and the solution poured into 200 ml. of Skellysolv B. The magenta solid weighed 0.85 gm. and melted over a wide range. The substance exhibited a bright orange-red fluorescence and possessed a characteristic isothiocyanate absorption band at approximately 2,100 cm^{-1}. in the infra-red.[9]

Conjugation Procedure

The protein content of the immune globulin to be conjugated was determined by either the standard micro-Kjeldahl procedure or by the modification of Folin's method reported by Lowry, Rosebrough, Farr and Randall.[10]

The following reagents were combined in an Erlenmeyer flask fitted with a mechanical stirrer: 10 ml. saline (0.85 per cent NaCl), 3 ml. carbonate-bicarbonate buffer (0.5 M, pH 9.0), 2 ml. acetone (reagent grade). The mixture was cooled in an acetone-dry ice bath until crystals of ice formed. To this cooled mixture was then added, with stirring, 10 ml. of the diluted globulin fraction of known protein concentration. This mixture was again cooled in the cold bath until crystals of ice formed, and to this cooled, stirred solution was added slowly 1.5 ml. of acetone containing the required amount of fluorescein isothiocyanate or rhodamine B isothiocyanate (0.05 mg. of dye per mg. of protein). After addition of the solution of the dye in acetone, the mixture was transferred to the cold room (4° C.) and stirring was continued for 18 hours. The mixture was then transferred to a mechanical dialyzer, and dialyzed against phosphate buffered saline (0.01 M, pH 7.2) until the dialysate showed no fluorescence when viewed with a small portable ultraviolet light.

The conjugate was then filtered through a Millipore filter, put up in 2 ml. aliquots, shell frozen, and stored in the dry ice chest until used. Before using, all antiserums were adsorbed with mouse liver powder prepared by Coon's method.[11]

Use of Labeled Antiserum

Bacillus anthracis. Antiserum prepared against *B. anthracis* as described was used in the indirect method originated by Coons.[5] Slides thinly inoculated with the organisms grown on Burdon's modification of Thorne's medium were prepared, fixed with heat, and treated with specific antiserum prepared in the rabbit. After washing, the slide was treated with anti-rabbit serum prepared in the goat and conjugated

with fluorescein isothiocyanate. Under the microscope the organisms were well seen, and the capsule was brilliantly outlined by green fluorescence (Fig. 1). The same procedure, with the use of the goat anti-rabbit serum conjugated with rhodamine B isothiocyanate, gave a fluorescence of an orange-red color (Fig. 6).

Pasteurella tularensis. The direct procedure was used in this experiment with the antiserum obtained from the rabbit as described. The slides were prepared as for *B. anthracis* and treated with the labeled anti-*P. tularensis* serum. The organisms appeared in the fluorescent microscope as small coccoid to oval bodies fluorescing a bright yellow-green (Fig. 2).

The specificity of the staining of *B. anthracis* and *P. tularensis* was demonstrated by treatment of smears with labeled normal serum. Such smears, after washing and mounting in glycerin, show no fluorescence. Blocking of the specific reaction was shown by application of unlabeled specific antiserum. The prior application of the unlabeled serum prevented the attachment of the labeled antiserum and no, or only slight, fluorescence was seen upon examination under ultraviolet light.

Double Staining with Red and Green Dyes

In this experiment, smears were made containing both *B. anthracis* and *P. tularensis.* Anti-anthrax serum labeled with the rhodamine B isothiocyanate and anti-tularemia serum labeled with fluorescein isothiocyanate were applied *ad seriatum* and the slide washed and mounted as before. The contrast between the specifically stained red *B. anthracis* rods and the green coccoid *P. tularensis* was well seen.

Demonstration of Specific Staining of Infected Cultured Cells

P. tularensis, R. typhi, and adenovirus (RI-67) were all well demonstrated by the use of specific labeled antiserum. *P. tularensis* was grown in the mouse fibroblast (L cell) in Scherer's medium[12] containing horse serum.[13] Cover slips were removed and fixed in cold acetone for 15 minutes, stained with labeled anti-tularensis serum and examined after mounting in glycerin (Fig. 3).

Entodermal cells of chick embryos were cultivated on cover slips following the method of Weiss and Pietryk.[14] They were infected with *R. typhi* and 8 days after infection were treated with fluorescein labeled human convalescent serum. The rickettsiae appeared as bright fluorescent rods within the cytoplasm of the infected cells (Fig. 4).

Adenovirus RI-67 was grown in liver cells and cover slips removed at 12, 24, 48, and 72 hour intervals after infection. The immune serum

was conjugated with fluorescein isothiocyanate used as described above. The virus was demonstrated in the nuclei of liver cells 48 hours after infection with 10^3 $TCID_{50}$ of adenovirus (Fig. 5). Fluorescence was observed 24 hours after infection, but not after 12 hours, and the fluorescence increased to confluent masses as the cells rounded. No fluorescent areas could be observed clearly in the cytoplasm.

Demonstration of P. tularensis in the Infected Mouse

White mice were inoculated by subcutaneous injection in the left inguinal region. The inoculum consisted of 25 and 250 organisms of *P. tularensis* as shown by plate count. Normal mice and infected mice were sacrificed at 18, 42, and 66 hours. Impression smears and cultures were made from the left inguinal lymph node, peritoneal fluid, spleen, liver, and heart blood. The impression smears were fixed in acetone and stained with fluorescein isothiocyanate labeled anti-tularensis serum. The lymph node, spleen and liver impressions first gave positive reactions at 42 hours in the mouse receiving 250 organisms (Fig. 7). At 66 hours, the mouse receiving 25 organisms showed fluorescent rods in the lymph node and spleen but not in the other smears examined. At this time all smears from the mouse which had received 250 organisms were positive. A faint fluorescence could be seen in impressions of normal tissue but was never confusing. Table I indicates the time at which *P. tularensis* was demonstrable by fluorescence in the tissues of infected mice as compared to the time of appearance of characteristic colonies in glucose cysteine blood agar inoculated with infected tissues. The advantage in the use of fluorescent antibody as a diagnostic tool is readily seen.

Discussion

One of the major difficulties encountered in the utilization of the fluorescent antibody technique is the synthesis of the labeling compound itself. The results obtained by the use of fluorescein isothiocyanate and rhodamine B isothiocyanate as described indicate that some of these difficulties have been successfully overcome. The use of highly toxic phosgene gas in the synthesis of a reactive group was avoided by replacing it with thiophosgene, a less toxic liquid with a low boiling point. The products obtained were the isothiocyanates which were as reactive under the conditions used as was the isocyanate. Moreover, the isothiocyanate of fluorescein was obtained as an amorphous yellow-orange powder, which was shown to be reactive 6 months after preparation, with no special care being taken to insure the

stability of the compound. The isothiocyanate of rhodamine B was a reddish-purple solid with stability paralleling that of fluorescein isothiocyanate.

The specificity of the staining was demonstrated by a variety of controls; all of these proved to be negative, with no fluorescence in the control slides. The delicacy of staining can be seen in the accompanying illustrations. The structure of the organism *B. anthracis* was clearly manifested in the rhodamine B and fluorescein stained preparations.

TABLE I

Demonstration of Fluorescence versus Growth of Colonies of P. tularensis (In Mice and Culture Medium)

No. of organisms introduced	Time* (hr.)	Demonstration of organisms by fluorescent antibody				
		Spleen	Lymph node	Liver	Peritoneal fluid	Blood
25	18	–	–	–	–	–
	42	–	–	–	–	–
	66	+	+	–	–	–
	90	+	+	+	+	+
250	18	–	–	–	–	–
	42	+	+	+	–	–
	66	+	+	+	+	+
	90	+	+	+	+	+
		Demonstration of colonies by plate culture				
25	90	–	–	–	–	–
	144	–	+	–	–	–
	114	1 col.	+	–	–	–
	114	+	+	+	+	+
250	90	–	+	–	–	–
	144	+	+	+	–	+
	114	+	+	+	+	+
	114	+	+	+	+	+

* Time elapsed after inoculation of mice.

The capsules, cell walls, and septums between cells were all discernible. In tissue culture preparations the specificity of the technique was also evident in comparing the staining characteristics of slides from uninfected cultures with those prepared from infected tissues. Nonspecific fluorescence was absorbed by treatment of the serum with mouse liver powder prior to staining; uninfected cells then had only vague outlines when observed with the fluorescent microscope, while

the organisms or virus masses were clearly fluorescent in infected cells.

Preliminary study of the orange-red fluorescence of rhodamine B dye indicated that there were many instances in which this dye could be used alone or in conjunction with the yellow-green fluorescence of fluorescein. Moody, Goldman and Thomason[15] showed that antiserum labeled with fluorescein isocyanate was a valuable adjunct to conventional diagnostic methods in the identification of micro-organisms. Silverstein and co-workers[3] proposed that a scheme of identification could be established by using two fluorescent dyes simultaneously. The specific staining of the dye-labeled antiserum makes this method a valuable tool where mixed cultures are encountered as shown by Moody and associates.[15] The indirect method of Weller and Coons[5] may create many possibilities in diagnostic methodology since a micro-organism, after treatment with specific antiserum, may then be stained with a labeled serum directed against the species used for the preparation of the bacterial antiserum, thus utilizing one labeled antiserum against a variety of micro-organisms. The use of two dyes to study dual infection by two different viral agents and the interference phenomenon among animal viruses could be profitably investigated.

Coons, Snyder, Cheever and Murray,[16] Watson,[17] Buckley,[18] and many others have used antiviral serums labeled with fluorescein isocyanate. Our results have indicated that the isothiocyanate labeled serums would be equally useful.

Fluorescein isothiocyanate and rhodamine B isothiocyanate have the advantage over the isocyanates since they may be prepared with a less toxic substance, thiophosgene; the dyes themselves are stable as a dry powder over a period of 6 months. The preparation of the dyes is readily accomplished, different batches giving equally reliable products. The stability of the labeled and frozen or dried antiserum has been tested over a period of many months, and its staining qualities have remained reliable. Judging from the results reported in this paper, the fluorescein isothiocyanates and rhodamine B isothiocyanates should be applicable to any of the staining procedures in which the isocyanates have been utilized.

Summary

Two fluorescent isothiocyanate dyes have been synthesized for use in labeling antibodies. The advantages of these isothiocyanates over the corresponding isocyanates depend upon their stability in a solid form which allows their storage and use directly when needed. The substitution of a less toxic substance, thiophosgene, for the highly toxic phosgene gas offers added advantage.

The dyes were successfully conjugated with antiserums against different antigens.

Specific staining of the following antigens was carried out, using the direct and indirect techniques: *B. anthracis, P. tularensis, R. typhi,* and adenovirus RI-67.

REFERENCES

1. Coons, A. H.; Creech, H. J.; Jones, R. N., and Berliner, E. The demonstration of pneumococcal antigen in tissues by the use of fluorescent antibody. *J. Immunol.*, 1942, 45, 159–170.
2. Coons, A. H., and Kaplan, M. H. Localization of antigen in tissue cells. II. Improvements in a method for the detection of antigen by means of fluorescent antibody. *J. Exper. Med.*, 1950, 91, 1–13.
3. Silverstein, A. M.; Eveland, W. C., and Marshall, J. D., Jr. Rapid identification of organisms with fluorescent antibodies of contrasting colors. (Abstract.) Bacteriological Proceedings. The Society of American Bacteriologists, 1957, p. 147.
4. Goldman, M., and Carver, R. K. Preserving fluorescein isocyanate for simplified preparation of fluorescent antibody. *Science,* 1957, 126, 839–840.
5. Weller, T. H., and Coons, A. H. Fluorescent antibody studies with agents of varicella and herpes zoster propagated *in vitro*. *Proc. Soc. Exper. Biol. & Med.*, 1954, 86, 789–794.
6. Burdon, K. L. Useful criteria for identification of *Bacillus anthracis* and related species. *J. Bact.*, 1956, 71, 25–42.
7. Downs, C. M.; Coriell, L. L.; Chapman, S. S., and Klauber, A. The cultivation of *Bacterium tularense* in embryonated eggs. *J. Bact.*, 1947, 53, 89–100.
8. Chang, R. S-M. Continuous subcultivation of epithelial-like cells from normal human tissues. *Proc. Soc. Exper. Biol. & Med.*, 1954, 87, 440–443.
9. Gilman, H. (ed.) Organic Chemistry. John Wiley & Sons, Inc., New York, Vol. 3, 1953, p. 145.
10. Lowry, O. H.; Rosebrough, N. J.; Farr, A. L., and Randall, R. J. Protein measurement with the Folin phenol reagent. *J. Biol. Chem.*, 1951, 193, 265–275.
11. Coons, A. H.; Leduc, E. H., and Connolly, J. M. Studies on antibody production. I. A method for the histochemical demonstration of specific antibody and its application to a study of the hyperimmune rabbit. *J. Exper. Med.*, 1955, 102, 49–60.
12. Syverton, J. T.; Scherer, W. F., and Elwood, P. Studies on the propagation *in vitro* of poliomyelitis viruses. V. The application of strain HeLa human epithelial cells for isolation and typing. *J. Lab. & Clin. Med.*, 1954, 43, 286–302.
13. Merriott, J. W., and Downs, C. M. Growth of *Pasteurella tularensis* in cultured cells. To be published.
14. Weiss, E., and Pietryk, H. C. Growth of *Coxiella burnetii* in monolayer cultures of chick entodermal cells. *J. Bact.*, 1956, 72, 235–241.
15. Moody, M. D.; Goldman, M., and Thomason, B. M. Staining bacterial smears with fluorescent antibody. I. General methods for *Malleomyces pseudomallei*. *J. Bact.*, 1956, 72, 357–361.

16. Coons, A. H.; Snyder, J. C.; Cheever, F. S., and Murray, E. S. Localization of antigen in tissue cells. IV. Antigens of rickettsiae and mumps virus. *J. Exper. Med.*, 1950, 91, 31–38.

17. Watson, B. K. Distribution of mumps virus in tissue cultures as determined by fluorescein-labeled antiserum. *Proc. Soc. Exper. Biol. & Med.*, 1952, 79, 222–224.

18. Buckley, S. M. Visualization of poliomyelitis virus by fluorescent antibody. *Arch. f. Virusforsch.*, 1955, 6, 388–400.

Grateful acknowledgment is made to Dr. Eric Brown, Mr. John Merriott and Miss Virginia Hocker.

LEGENDS FOR FIGURES

FIG. 1. *Bacillus anthracis* grown in Burdon's medium. Photograph of a smear treated with anti-anthrax serum prepared in the rabbit and stained with goat anti-rabbit serum labeled with fluorescein isothiocyanate. Prepared from a Superanscochrome color transparency. × 1,000.

FIG. 2. *Pasteurella tularensis* grown on glucose cysteine blood agar. Photograph of a smear stained with anti-tularensis serum labeled with fluorescein isothiocyanate. Prepared as in Figure 1. × 1,000.

FIG. 3. *P. tularensis* growing intracellularly in mouse fibroblast (L cell) 96 hours after inoculation. The cover slip was stained with anti-tularensis serum labeled with fluorescein isothiocyanate. Prepared as in Figure 1. × 1,000.

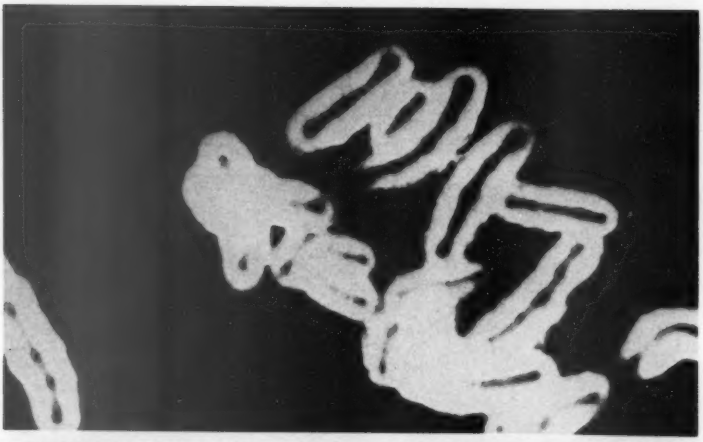

1

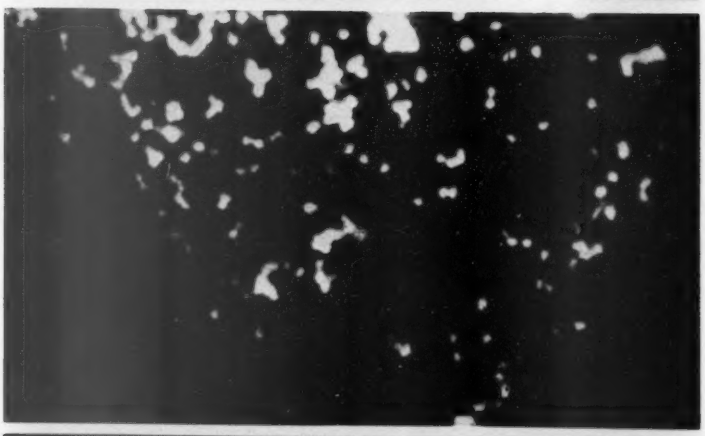

2

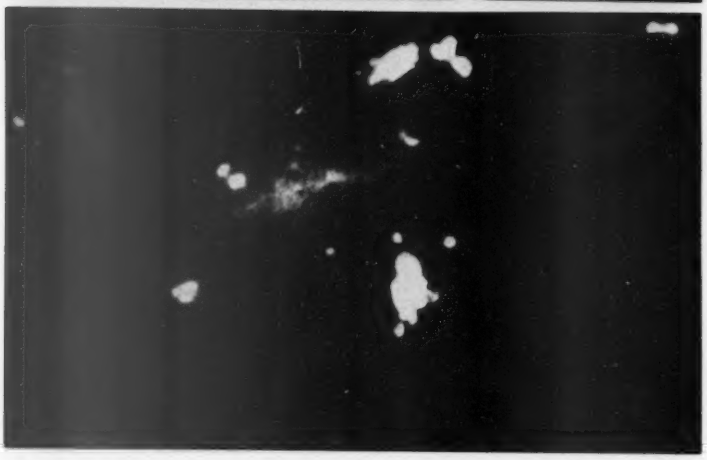

3

FIG. 4. *Rickettsia typhi* growing intracellularly in giant cell from chick entoderm cultivated *in vitro*. Stained with convalescent human serum labeled with fluorescein isothiocyanate. Prepared as in Figure 1. × 1,000.

FIG. 5. Adenovirus RI 67 grown in Chang's liver cell tissue culture and stained with rabbit anti-RI 67 serum labeled with fluorescein isothiocyanate. Prepared as in Figure 1. × 1,000.

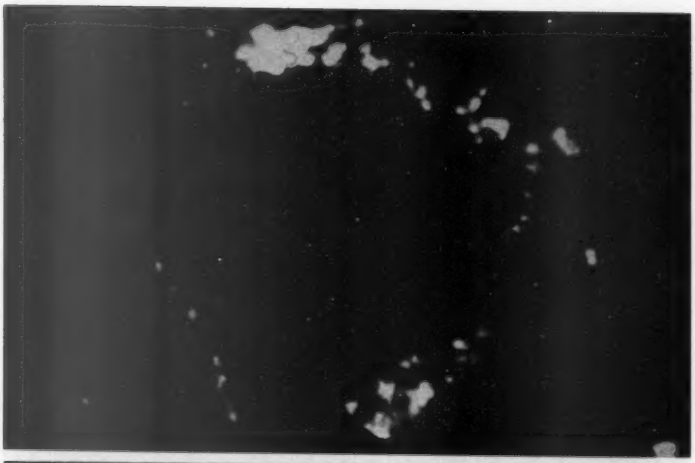

4

5

FIG. 6. *B. anthracis* treated with anti-anthracis serum, followed by staining with anti-rabbit serum labeled with rhodamine B isothiocyanate (indirect method). Superanscochrome. × 1,000.

FIG. 7. *P. tularensis* in impression smear of mouse spleen 42 hours after subcutaneous inoculation of 250 organisms. Stained with anti-tularensis serum labeled with fluorescein isothiocyanate. Superanscochrome. × 1,000.

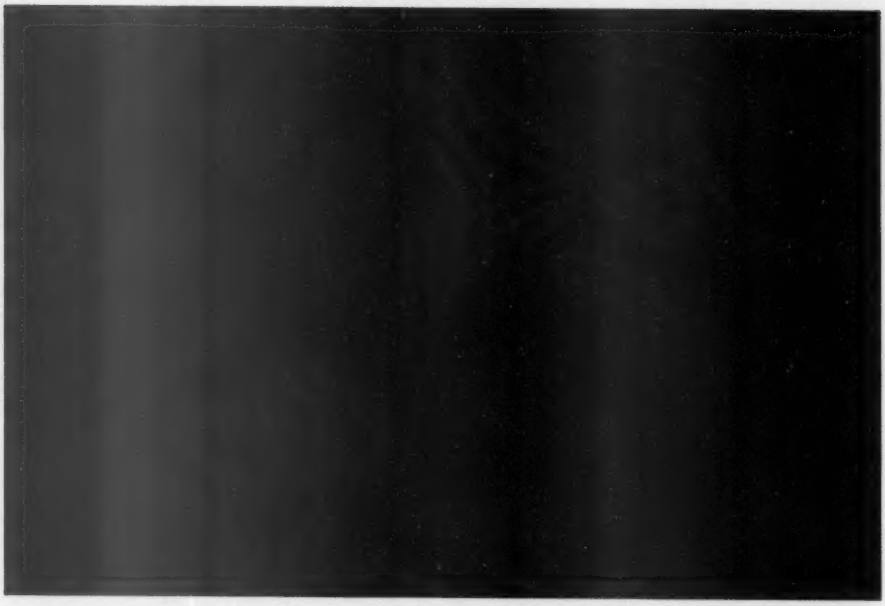

6

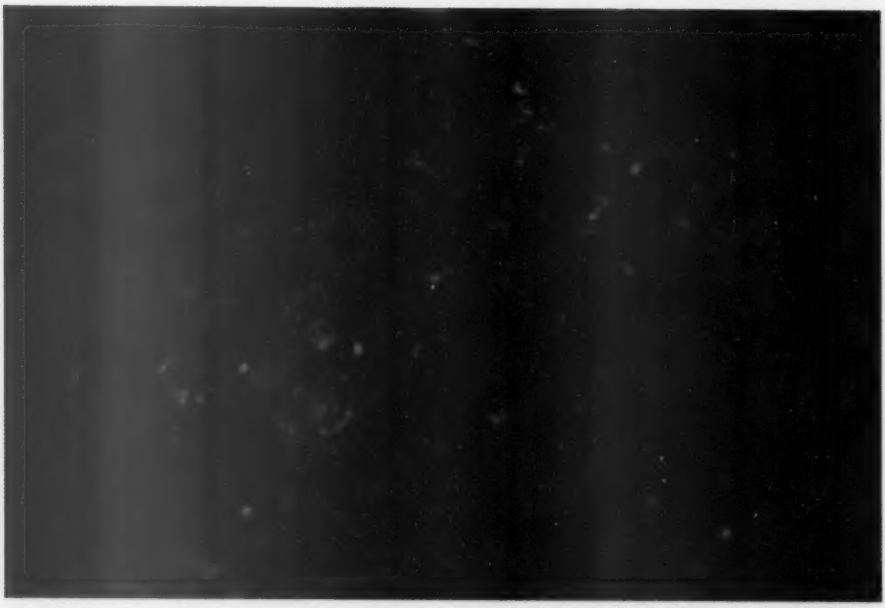

7

MELIOIDOSIS: PATHOGENESIS AND IMMUNITY IN MICE AND HAMSTERS

II. Studies with Avirulent Strains of Malleomyces pseudomallei *

Arthur M. Dannenberg, Jr., M.D.,† and Eva M. Scott, A.B.

From the Naval Medical Research Unit No. 1 and the Naval Biological Laboratory, Department of Bacteriology, University of California, Berkeley, Calif.

A previous report[1] described the pathogenesis of melioidosis caused by virulent strains of *Malleomyces pseudomallei*.‡ The present report describes the pathogenesis of melioidosis caused by two relatively avirulent strains of *M. pseudomallei*. In mice and hamsters, high but sublethal doses of these avirulent strains produced nonprogressive lesions and a generalized infection, which resulted in the development of significant immunity to challenge by virulent strains.[2] The bacteriologic and pathologic aspects of this nonprogressive form of melioidosis are herein presented, in order to show the nature of resistance to this disease and the character of the virulence of this species of organism.

Materials and Methods

Bacterial Strains

Strains of *M. pseudomallei* designated in this laboratory as 102-7 and 102-8 were derived as single colony isolates from an avirulent stock culture obtained from the Walter Reed Army Institute of Research and designated at that laboratory as No. 295. On 4 per cent glycerin beef extract agar, strain 102-7 formed rough, cream-colored, flat colonies, and strain 102-8 formed rough, slightly raised, yellow-orange colonies. The intraperitoneal LD_{50} of strain 102-7 for mice and hamsters was approximately 1×10^8 organisms, that of strain 102-8 was approximately 5×10^8. Both strains were therefore considered relatively avirulent. They produced similar pathologic lesions.

Determination of Number of Viable Bacteria in Whole Organs

Whole organs were washed with 4 per cent glycerin beef extract broth (glycerin broth), and their volume determined by fluid displace-

* This work was supported by the Bureau of Medicine and Surgery, Navy Department, and the Office of Naval Research. Opinions contained in this report are not to be construed as reflecting the views of the Naval Service (Article 1252, United States Naval Regulations, 1948).

Received for publication, April 7, 1958.

† Lieutenant Commander, Medical Corps, United States Naval Reserve.

‡ Melioidosis was first described by Whitmore and Krishnaswami in Rangoon, Burma, and not in the Malay States as stated in the first paper in this series.[1] It was the classical study of Stanton and Fletcher[3] which came from the Malay States.

ment in a graduated 15 ml. centrifuge tube. The tissues were then ground with mortar and pestle without abrasive. Ten per cent suspensions were made by adding 9 volumes of glycerin broth to 1 volume of tissue. Polymyxin (100 units per ml.) was useful in avoiding contamination. At the concentration used, it had no apparent effect on bacterial viability. The number of viable organisms per ml. of tissue suspension, determined by plating 10-fold serial dilutions, was used to calculate the total number of organisms contained in the entire organ.

Other materials and methods were the same as those in the preceding report.[1]

Behavior of Avirulent Strains of M. pseudomallei in Mice

Stanton and Fletcher[3] found that repeated introduction of killed cultures of *M. pseudomallei* into laboratory animals conferred little immunity against parenteral infection. Unpublished work in this laboratory[4] not only confirmed these observations but also indicated that vaccines prepared from dead organisms were even less effective against respiratory challenge. On the other hand, as will be demonstrated in a succeeding paper,[2] vaccination of mice and hamsters with live avirulent strains induced significant protection against this type of challenge. The behavior of these avirulent strains in the tissues of the host was therefore studied in the hope of determining some of the factors responsible for their immunizing capacity.

Three groups of mice were inoculated with large doses of live avirulent organisms by the subcutaneous (s.c.), intraperitoneal (i.p.) and respiratory routes respectively. The number of viable bacteria in the mouse organs was determined at various intervals thereafter. Following infection by the s.c. and i.p. routes (Tables I and II), the bacterial titers were maintained more or less at the 3 to 4 hour level for about 3 days and then declined, possibly due to the development of immunity. Following respiratory exposure (Table III), the pulmonary bacterial titers dropped between 6 and 12 hours and then remained more or less constant for several weeks. No decline in titer was observed by the fifth day, in spite of histologic evidence indicating resolution of pulmonary lesions at this time.

The immunizing capacity of these avirulent strains is therefore probably the result of their ability to create a generalized infection persisting at least 3 days following all 3 routes of administration. Although the quantitative data do not support the interpretation of bacterial multiplication, the persistence of bacteria for 6 and 11 weeks

following inoculation by both inhalation and i.p. injection, as well as the development of lesions as described below, would indicate that some reproduction must have occurred.

Pathogenesis of Respiratory Melioidosis Produced by Avirulent Strains in Mice and Hamsters

The pathogenesis of lesions resulting from single or small numbers of other bacteria[5,6] has been best studied in the lung following the inhalation of aerosols. Eighteen mice were therefore allowed to inhale

Table I

Titers of Avirulent M. pseudomallei in Mice Following Subcutaneous Inoculation

Inoculum: strain and dose	Interval after inoculation	Organisms per organ*					
		Liver	Lung	Spleen	Kidney	Axillary lymph nodes	Inguinal lymph nodes
102–8 3.5×10^7	3–4 hrs.	5×10^3	0	3.5×10^3	1×10^1	1×10^1	2×10^3
		5×10^3	4×10^0	2.6×10^3	1×10^1	1×10^1	8.8×10^2
	1 day	1×10^1	0	1×10^1	1×10^1	1.2×10^3	2.8×10^3
		0	0	0	0	5×10^0	5×10^1
	2 days	5×10^2	5×10^1	1×10^1	5×10^1	2.0×10^3	1.2×10^4
		5×10^2	3×10^0	6×10^1	3×10^3	1.9×10^3	1.2×10^4
	3 days	2×10^3	1×10^1	0	5×10^1	1×10^3	0
		1×10^2	0	8×10^1	0	5.1×10^3	1.2×10^4
	6 days	0	0	0		1×10^1	1×10^1
		0	0	0		0	1×10^1
	10 days	0	0	0	0	0	0
	15 days	0	0	0	0	0	0
102–7 7.5×10^6	24 days	0	0	0		0	0
	42 days	0	0	0		0	0

* Each horizontal row represents observations on one mouse.

Note: Two days after inoculation of 7.5×10^6 bacteria (strain 102–8) in another experiment, the local subcutaneous lesions of two mice were removed and cultured. There were 1.3×10^6 organisms in one lesion, and 4.8×10^6 organisms in the other.

5.3×10^6 organisms of strain 102-7 and were sacrificed in groups of 3 on days 1, 2, 3, 4, 5, and 8.

On gross examination all the organs appeared normal except for the livers, which were pale yellow during the first few days. Microscopic examination, however, revealed both the development and resolution of pulmonary lesions. On the first day these lesions consisted of small

TABLE II

Titers of Avirulent M. pseudomallei in Mice Following Intraperitoneal Inoculation

Inoculum		Time after inoculation of bacteria	Organisms per organ*						
Strain	Dose (organisms)		Liver	Lung	Spleen	Blood (1 ml.)	Peritoneal washings†	Abdominal lymph nodes‡	Peritoneal abscesses
102–7	1.1×10^{8}	3–4 hours	4.8×10^{6}	2.3×10^{4}	6.1×10^{6}	9.2×10^{4}	1.0×10^{6}	—	—
102–7	1.1×10^{8}	1 day	7.1×10^{7}	2.1×10^{6}	1.5×10^{7}	2.3×10^{4}	5.1×10^{7}	—	—
			1.5×10^{6}	3.9×10^{4}	2.1×10^{6}	4.4×10^{3}	1.3×10^{4}	—	—
102–7	1.1×10^{8}	2 days	4.0×10^{7}	3.6×10^{5}	2.5×10^{6}	2.9×10^{3}	1.0×10^{6}	—	—
			8.5×10^{6}	1.8×10^{5}	1.4×10^{6}	1.4×10^{3}	7.7×10^{5}	—	—
102–7	1.1×10^{8}	3 days	2.6×10^{6}	3.2×10^{6}	3.8×10^{7}	1.9×10^{5}	7.0×10^{6}	—	—
			8.4×10^{6}	1.3×10^{5}	2.7×10^{5}	1.8×10^{3}	7.0×10^{5}		
102–7	1.1×10^{8}	6 days	3.1×10^{3}	0	1.1×10^{3}	0	1.0×10^{1}	—	—
102–7	2.7×10^{7}	2 weeks	0	0	0	—	—	0	§
102–8	2.8×10^{8}	2 weeks	—	—	5.5×10^{3}	—	—	—	1.0×10^{4}
102–7	2.7×10^{7}	9 weeks	0	0	0	—	—	5.0×10^{1}	§
102–8	2.8×10^{8}	9 weeks	1.0×10^{1}	1.0×10^{1}	1.0×10^{3}	—	—	1.0×10^{3}	1.0×10^{3}
102–7	2.7×10^{7}	11 weeks	0	0	1.0×10^{3}	—	—	1.0×10^{1}	§
102–8	2.8×10^{8}	11 weeks	1.0×10^{3}	0	1.0×10^{3}	—	—	1.0×10^{2}	§

* Each horizontal row represents findings on one mouse.

† The peritoneal cavities were washed 3 times with 1 ml. of glycerin broth. The total number of organisms in the washings is indicated.

‡ Periportal, mesenteric, aortic and iliac lymph nodes.

— Not examined.

§ No peritoneal abscesses found.

TABLE III

Titers of Avirulent M. pseudomallei, Strain 102–7, in Mice Following Inhalation

Time after inhalation of bacteria	Inoculum dose (organisms)	Organisms per organ*			
		Lung		Spleen	
		No. of organisms	Logarithmic average	No. of organisms	Logarithmic average
2 hours	1.6×10^6	1.5×10^5	9.5×10^4		
	1.6×10^6	6.0×10^4			
	1.7×10^7	9.5×10^4			
6 hours	1.6×10^6	2.2×10^4	2.3×10^4		
	1.6×10^6	2.0×10^4			
	1.7×10^7	2.0×10^4			
	1.7×10^7	3.3×10^4			
12 hours	1.6×10^6	4.8×10^3	3.7×10^3		
	1.6×10^6	4.2×10^3			
	1.7×10^7	4.3×10^3			
	1.7×10^7	2.2×10^3			
1 day	1.6×10^6	2.0×10^3	1.7×10^3		
	1.6×10^6	1.2×10^3			
	1.7×10^7	1.1×10^3			
	1.7×10^7	2.8×10^3			
2 days	1.6×10^6	5.0×10^2	8.2×10^2	1.0×10^3	1.0×10^1
	1.6×10^6	9.5×10^2		1.0×10^3	
	1.7×10^7	4.0×10^2		0	
	1.7×10^7	2.4×10^2		0	
3 days	1.6×10^6	5.0×10^0	2.2×10^2	1.0×10^1	3.0×10^1
	1.6×10^6	2.4×10^2		1.0×10^1	
	1.7×10^7	5.0×10^1		1.0×10^2	
	1.7×10^7	4.1×10^2		1.0×10^2	
4 days	1.6×10^6	4.2×10^2	1.2×10^2	0	
	1.6×10^6	5.0×10^2		0	
	1.7×10^7	1.0×10^2		0	
	1.7×10^7	1.1×10^2		0	
5 days	5.5×10^6	4.3×10^2	1.4×10^2	1.0×10^1	3.0×10^1
		4.6×10^2		1.0×10^2	
8 days	1.6×10^6	1.0×10^2	4.2×10^2		
	1.6×10^6	0			
	1.7×10^7	2.0×10^2			
	1.7×10^7	1.5×10^4			
11 days	5.5×10^6	1.0×10^4	3.0×10^2		
	5.5×10^6	1.0×10^2			
	1.6×10^6	3.0×10^1			
	1.7×10^7	2.0×10^2			
17 days	5.5×10^6	5.2×10^2	4.0×10^2		
	5.5×10^6	3.0×10^2			
24 days	5.5×10^6	5.0×10^2	5.0×10^2		
6 weeks	5.5×10^6	5.0×10^0	2.0×10^0		
	5.5×10^6	0			

* Each figure represents findings on one mouse.

intra-alveolar accumulations of neutrophils and a few mononuclear cells. On the second and third days an exudate of varying proportions of neutrophils and mononuclear cells filled several of the alveolar spaces (Fig. 1). Bacteria, though rare, were found in both types of exudative cells, a fact which provides some evidence supporting the belief that reproduction occurred among the few bacteria that lodged in that site. The alveolar septums, thickened by mononuclear cells, did not undergo necrosis. On the fourth and fifth days thickening of several of the alveolar walls occurred in focal manner. The alveolar exudate had disappeared except for an occasional dust phagocyte, and no bacteria were seen. On the eighth day the lesions had apparently resolved, for none could be found.

A few hamsters were similarly infected with approximately the same doses of the same strain. Only a 2 and an 8-day old lesion were found. The former is shown in Figure 2. These lesions resembled respectively the 2 and the 5-day lesions in mice.

No focal lesions were observed in any other organ of either species of animal, but certain systemic toxic effects were nevertheless manifest in mice. Their livers showed mild fatty infiltration which was most severe on the first day and had practically disappeared by the fifth day. Their kidneys generally showed cloudy swelling for two days.

Recapitulating, the inhalation of this avirulent strain by mice and hamsters resulted in focal pulmonary lesions that showed little or no necrosis. In a few days these lesions seemed to resolve completely, and no secondary lesions arose. Evidence of some transient systemic toxicity was, however, apparent in mice.

The results enumerated above and those which follow suggest that avirulent strains 102-7 and 102-8 might produce a more virulent form of disease if they were better able to accumulate in the tissues of the host. The following experiment, using procedures known to decrease the ability of the host to destroy or inhibit bacteria,[7-11] was designed to test this hypothesis.

Eighteen mice, 6 weeks old, were divided into 3 groups. One group served as controls, one group was fasted for about 20 hours before infection and given only vegetables thereafter, and one group was given 2.5 mg. of cortisone acetate (Merck) intramuscularly (i.m.) 2 days prior to infection, the day of infection, and 3 days after infection. All 3 groups were inoculated with 4.4×10^6 avirulent organisms, strain 102-7, by the respiratory route. Two animals of each group were sacrificed on the second, fifth, and eleventh days after infection and their lungs prepared for histologic study. The fasted mice continued to lose weight throughout the experimental period.

In another experiment, cortisone was administered in similar dosages to 10 mice that were sacrificed at a time corresponding to the fifth day above. This experiment was performed in order to rule out the possibility of pulmonary lesions arising from the normal bacterial flora of mice under the influence of cortisone.

The results were most striking on the fifth day after infection. At this time no gross or microscopic lesions were found in either control group, whereas in both the fasted and the cortisone-treated infected animals, microscopic focal lesions were seen which consisted of alveolar plugs of partially necrotic neutrophils and other cells with little or no necrosis of the alveolar septums (Figs. 3 and 4). Bacteria were seen in moderate numbers.* A comparison of these photomicrographs with Figure 1, which resembles the control lesions at their height 2 days after respiratory exposure, indicates that more necrosis was present in the lesions of the fasted and cortisone-treated animals. In fact, the lesions of the latter animals had some of the characteristics of lesions caused by virulent strains (see Figs. 11 and 12 of the preceding paper.[1]) Thus two procedures known to lower the resistance of mice enabled avirulent strains to produce a more severe disease. By analogy, it is conceivable that acute melioidosis of human beings may represent an enhancement of a subclinical disease occurring in a debilitated host.

Factors Responsible for the Avirulence of Strains 102-7 and 102-8 in Mice

Avirulence of micro-organisms may be defined as a relative inability to create a distinct clinical disease in a given host. Under this definition 3 different explanations of avirulence are possible: (1) a relative inability of the organism to establish an infection; (2) a relative inability of the organism to accumulate in the tissues of the host; and (3) a relative inability of the organism to produce substances injurious to the host. Combinations of the 3 factors are common, but the following examples illustrate that any one of the 3 alone can suffice to account for avirulence. An example of the first is plague in mice where at least 10^4 organisms of *Pasteurella pestis,* strain 139L, were necessary to establish an infection by the respiratory route, but, once established, the infection was usually fatal.[12] An example of the second is tuberculosis caused by the human type of tubercle bacillus in natively resistant rabbits: A moderately low dose caused infection[13] and development of lesions, but there was no generalized multiplication of bacteria, and

* In other experiments the spleens of cortisone-treated mice which had been inoculated i.p. with avirulent strains, were found by cultural methods to contain 10 to 1,000 times more bacteria than the spleens of control animals.

healing occurred. An example of the third, suggested by Dr. K. F. Meyer, is typhus in the rat.[14,15] These animals were easily infected. The rickettsiae multiplied extensively in this host, and yet a completely inapparent disease was usually produced. Dubos[16] has cited other examples. In the following studies the nature of the avirulence of *M. pseudomallei*, strain 102-7, is analyzed.

TABLE IV

Number and Size of Pulmonary Lesions in Mice Two Days after Inhalation of 5.5×10^6 M. pseudomallei, Strain 102–7

Mouse no.	Average no. of lesions per section	Average diameter of lesions (μ)
1	0.5	100
2	1.8	150
3	0.2	130
4	2.6	150
5	0.6	130
6	0.2	110
7	2.8	100
8	4.0	130
9	2.6	140
10	3.0	110
11	1.4	140
12	0.8	160
Average	1.7	130

Relative Inability of Avirulent Strain 102-7 to Establish a Melioidotic Infection

If a large number of organisms of a given strain are required to generate a single lesion, then such a strain may be said to possess a relative inability to establish infection. This number was determined for strain 102-7 as follows:

Twelve mice were infected with 5.5×10^6 bacteria by the respiratory route. They were sacrificed 2 days after exposure, and their lungs, fixed by the intratracheal injection of FU 48 (Technicon), averaged 3.9 ± 0.3 mm. in thickness after allowance was made for their curved surfaces. Histologic sections of the lung were cut at 7 μ thickness and 300 μ apart. In each section there was an average of 1.7 lesions with an average diameter of 130 μ (Table IV).

From these data the average number of lesions per lung was estimated. Specifically, it required 19 sections $\left(\frac{130\ \mu}{7\ \mu}\right)$ to enclose one lesion, and it was estimated that there were 560 sections $\left(\frac{3.9\text{ mm.}}{7\ \mu}\right)$ per mouse lung. If there was one lesion per section, there would be 29 lesions $\left(\frac{560}{19}\right)$ in the lung. But since there was an average of 1.7 lesions seen in each section, an average of 49 lesions (29×1.7) must have been present in the whole lung. Since the inhaled dose was 5.5×10^6 organisms, the number of organisms required to establish one pulmonary lesion was 110,000 $\left(\frac{5.5 \times 10^6}{49}\right)$. With the virulent

strain 103-67, only about 30 organisms were required to establish one pulmonary lesion.[2,17] These data demonstrate the relative inability of avirulent strain 102-7 to establish melioidotic infection.

Because inhaled bacterial aggregates from the aerosolized suspensions would fail to reach the alveoli to generate lesions,[5,6,18] an experiment was performed to ascertain whether or not the 3,000-fold difference in the ability of the virulent and avirulent strains to establish melioidosis could be due to differences in aggregation.

Suspensions of the virulent strain 103-67 and avirulent strain 102-7 were examined microscopically as unstained wet preparations made by placing a cover slip over a drop of a 1 to 10 dilution of broth cultures. The suspensions of each strain, both before and after the aerosolizing procedure, consisted almost entirely of isolated bacteria with far less than one clump of 2 to 20 bacteria for each 100 single organisms.

Thus the marked difference in the ability of these two strains to produce melioidotic lesions can not be attributed to differences in bacterial dispersion in the aerosolized suspensions, but is apparently due to factors intimately concerned with the interaction between the host and the parasite.*

Relative Inability of Avirulent Strains to Accumulate in the Tissues of the Host

Tables I, II, and III clearly indicate that avirulent strains of *M. pseudomallei* had a relative inability to accumulate in the tissues of the host. In fact, no increase in the number of bacteria over their initial levels could be detected. On the other hand, similar studies with virulent strains[2,19] showed a continued rapid increase in the number of bacteria in the various organs from the time of inoculation to the time of death.

For example, 4 days after the inhalation of 10^6 to 10^7 avirulent organisms, strain 102-7, each of 4 mice had about 10^3 organisms in its lungs (Table III). By comparison, each of 5 mice inhaling approximately 2.5×10^3 virulent organisms, strain 103-67, had about 10^8 organisms per lung at 4 days.[2] Thus the avirulent strains did not accumulate in the tissues of the host while the virulent strains did.

Ability of Avirulent Strains 102-7 and 102-8 to Injure the Host

Equal numbers of avirulent and virulent bacteria must be present in the tissues in order to compare their abilities to injure the host. Large numbers of avirulent organisms, strains 102-7 and 102-8, were therefore

* We are indebted to Dr. Clara Nigg and Mr. Walter R. Leif of this Laboratory for performing this experiment and interpreting the observations.

inoculated s.c. and i.p. into mice to produce local injury and i.p. into mice and hamsters to produce systemic injury.

Local Injury. When 10^6 to 10^8 avirulent bacteria were injected s.c., a local abscess sometimes formed (Fig. 5). This persisted several weeks and eventually healed. When 10^8 avirulent bacteria were injected i.p., local abscesses also formed in rare instances in the omentum, mesentery, or broad ligament and were frequently adherent to one or more of the abdominal organs. The abscesses induced by s.c. and i.p. inoculation showed the same characteristics as the chronic abscesses caused by the virulent strains introduced i.p.: a central necrotic core of dead neutrophils surrounded by granulation tissue which frequently contained plasma cells. However, the abscesses caused by the avirulent strains never gave rise to generalized disease.

It is conceivable that the local abscesses were the result of nonspecific factors and did not reflect the multiplication of the inoculated bacteria. No experiments were performed to determine this, but evidence suggesting that avirulent organisms were capable of reproducing in the tissues has been given above.

Systemic Injury. When 10^9 avirulent bacteria were injected i.p., mice and hamsters usually died within 24 hours. They exhibited evidence of a fulminating septicemia and toxemia which resembled that caused by the introduction of 10^9 organisms of the virulent strain 103-67. In both instances bacteria were found in the cells of the pulmonary alveolar walls and in the Kupffer cells of the liver. Occasionally organisms were encountered in phagocytic cells of renal glomeruli and in circulating neutrophils. Bacteria were sometimes extremely numerous within the phagocytes (Figs. 6 and 7).

Pathologic alterations were most marked in the spleen, because this organ evidently filtered out a relatively high percentage of the circulating bacteria. The red pulp was usually loaded with intact and disintegrating phagocytes containing many micro-organisms, and the white pulp frequently showed the same "pitted" appearance (Fig. 8) that was ascribed to the direct or indirect toxic effects of virulent organisms in a previous report.[1]

Mice necropsied one day after inoculation had mild to moderate fatty degeneration of the liver. Hamsters were not thus affected, but occasional hepatic cells exhibited hyaline degeneration. The rarity of distinct necrotic foci at this time was due conceivably to the rapid death of the host. In animals that lived slightly longer, focal necrosis resembling that produced by virulent strains was found in the liver and spleen (Fig. 9). These lesions are of interest in that they developed

spontaneously during the course of a generalized infection rather than as a result of the employment of artificial experimental procedures.

A few experiments were performed in order to determine the cause of death following the i.p. injection of large doses of avirulent organisms. Was death merely due to the exotoxins and endotoxins present in the bacterial culture medium, or were these toxic substances produced or released by avirulent bacteria *in vivo*? To answer this question, the bacteria were washed 3 times with 1 per cent peptone solution before their intraperitoneal injection into mice and hamsters. The pathologic and bacteriologic effects were then compared to those found with unwashed cultures. As shown in Table V, the mortality of the animals and the bacterial titers in the spleen were similar in the two groups. The pathologic findings were also similar and resembled those described above. It seems, therefore, that any exotoxins or endotoxins responsible for the death of mice and hamsters inoculated with avirulent strains were produced or released *in vivo*.

The data presented in Table V are also of interest in that they confirm bacteriologically the existence of the large numbers of organisms which were observed histologically in the tissues. Similar studies with washed and unwashed cultures of the virulent strain 103-67 produced results that quantitatively resembled those found with the avirulent strains (Table V). It is therefore likely that comparable numbers of virulent and avirulent organisms in the tissues caused comparable local and systemic injury to the host.

Discussion

The results of the foregoing experiments suggest that the avirulence of strains 102-7 and 102-8 was due to a relative inability to establish a melioidotic infection and a relative inability to accumulate in the tissues of the host. It did not appear to be due to a relative inability to injure the host.

These studies with avirulent strains of *M. pseudomallei* have furthered our understanding of the nature of resistance to the disease and of the virulence of the organism. Resistance to the disease reflects a failure of bacterial accumulation in the host tissues. The resistance is increased by vaccination[2] with avirulent *M. pseudomallei*, strains 102-7 and 102-8. These have been shown to create a generalized infection which persists for at least several days, provided that very large infecting doses are used. Avirulent strains of *Bacillus anthracis*[20] and *Pasteurella pestis*[21] have also been employed for vaccination against their respective diseases. The nature of the protective or im-

TABLE V

Number of Bacteria in Tissues One Day after Intraperitoneal Inoculation with M. pseudomallei

Inoculum: strain, dose (organisms) and treatment	No. and type of animals	Mortality and average day of death*	Tissue cultured	No. of bacteria in entire organ†
102-7 (avirulent)	10 mice	100%	spleen	1.8×10^{8}
2.5×10^{3}		1.6 days	spleen	8.1×10^{7}
unwashed			lung	3.6×10^{6}
(1:10 dilution			lung	1.6×10^{8}
of broth culture)			blood	6.1×10^{5}/ml.
			blood	1.9×10^{6}/ml.
102-7 (avirulent)	8 mice	100%	spleen	8.7×10^{7}
5.0×10^{3}		1.4 days	spleen	6.9×10^{8}
washed				
102-8 (avirulent)	8 mice	100%	spleen	9.2×10^{8}
3.6×10^{9}		1.3 days	spleen	6.0×10^{8}
washed			spleen	2.8×10^{9}
103-67 (virulent)	7 mice	100%	spleen	2.8×10^{8}
3.9×10^{3}		1.1 days	spleen	2.5×10^{8}
washed			spleen	4.8×10^{8}
102-7 (avirulent)	10 hamsters	100%	spleen	5.7×10^{9}
2.5×10^{9}		1.0 days	spleen	3.3×10^{9}
unwashed			lung	3.2×10^{9}
(undiluted			lung	3.1×10^{6}
broth culture)			blood	3.1×10^{6}/ml.
			blood	3.7×10^{6}/ml.
102-7 (avirulent)	9 hamsters	100%	spleen	4.2×10^{9}
3.7×10^{9}		1.2 days	spleen	5.7×10^{9}
washed			spleen	1.7×10^{9}
102-8 (avirulent)	7 hamsters	86%	spleen	5.7×10^{9}
5.5×10^{9}		1.5 days	spleen	4.5×10^{9}
washed			spleen	6.6×10^{9}
103-67 (virulent)	10 hamsters	100%	spleen	4.2×10^{8}
8.0×10^{3}		1.0 days	spleen	1.2×10^{8}
unwashed			lung	1.0×10^{8}
(1:10 dilution			lung	1.0×10^{8}
of broth culture)			blood	9.0×10^{6}/ml.
			blood	4.2×10^{4}/ml.
103-67 (virulent)	8 hamsters	100%	spleen	4.8×10^{8}
3.9×10^{3}		1.0 days	spleen	3.6×10^{8}
washed				

* When a moribund animal was sacrificed, it was considered for statistical purposes to have died on that day. Dead animals were collected once or twice a day.

† Each figure represents findings on one moribund animal. Blood is expressed in bacteria per ml.

munizing antigens of these species is known in part,[22-30] but the character of the immunizing antigens of *M. pseudomallei* remains to be investigated. It is possible that a surface antigen[31-33] constitutes a significant factor.

Virulence in *M. pseudomallei* stems from factors which enable the bacteria to accumulate in the tissues of the host. These factors, e.g., toxins, antiphagocytic substances, enzyme inhibitors, etc., are sometimes called aggressins and have been partially characterized for *B. anthracis*[26,27,34-36] and *P. pestis*.[28-30,37,38] They may or may not be toxic[22,26,30,35] and may or may not be protective or immunizing antigens.[26,30,35,36] Some of these aggressins may also exist in avirulent strains.[39,40] Similar characterizations for *M. pseudomallei* are not yet available. It has, however, been shown that both virulent and avirulent strains of *M. pseudomallei* produce toxins *in vitro* which are lethal to both mice and hamsters.[41,42] Moreover, the pathologic studies with avirulent strains reported in this paper as well as the bacteriologic studies reported by Chambon and Fournier[31,32] suggest that factors in addition to toxins contribute to the virulence of this bacterial species.

Summary

Bacteriologic studies have indicated that certain relatively avirulent strains of *Malleomyces pseudomallei* produced a generalized, though inapparent, infection in mice following introduction of large doses by the subcutaneous, intraperitoneal or respiratory routes.

Pathologic studies demonstrated that these strains produced a hitherto undescribed type of respiratory melioidosis in mice and hamsters, manifested by nonprogressive microscopic pulmonary lesions which showed little or no necrosis and were accompanied, in mice, by limited evidence of systemic toxicity.

Procedures, known to decrease the ability of the host to inhibit the accumulation of bacteria, e.g., starvation or cortisone administration, increased the severity of the respiratory melioidosis caused by these strains. This was indicated by the presence of focal necrotic pulmonary lesions exhibiting some of the characteristics of lesions produced by virulent strains.

The avirulence of the strains seemed to be due to a relative inability to establish lesions and a concomitant failure to accumulate in the tissues of the host. However, the ability of the avirulent strains to injure the host seemed comparable to that of virulent strains when similar numbers of organisms were present in the tissues.

References

1. Dannenberg, A. M., Jr., and Scott, E. M. Melioidosis: Pathogenesis and immunity in mice and hamsters. I. Studies with virulent strains of *Malleomyces pseudomallei*. *J. Exper. Med.*, 1958, 107, 153–166.

2. Dannenberg, A. M., Jr., and Scott, E. M. Melioidosis: Pathogenesis and immunity in mice and hamsters. III. The effect of immunization with avirulent strains of *Malleomyces pseudomallei* on melioidosis caused by virulent strains. (In preparation.)
3. Stanton, A. T., and Fletcher, W. Melioidosis. Studies from the Institute for Medical Research, Federated Malay States, 1932, No. 21, 59 pp.
4. Smart, K., and Main, O. (Personal communication.)
5. Wells, W. F.; Ratcliffe, H. L., and Crumb, C. On the mechanics of droplet nuclei infection. II. Quantitative experimental air-borne tuberculosis in rabbits. *Am. J. Hyg.*, 1948, 47, 11–28.
6. Lurie, M. B.; Heppleston, A. G.; Abramson, S., and Swartz, I. B. An evaluation of the method of quantitative airborne infection and its use in the study of the pathogenesis of tuberculosis. *Am. Rev. Tuberc.*, 1950, 61, 765–797.
7. Dubos, R. J.; Smith, J. M., and Schaedler, R. W. Metabolic disturbances and infection. *Proc. Roy. Soc. Med.*, 1955, 48, 911–918.
8. Smith, J. M., and Dubos, R. J. The effect of nutritional disturbances on the susceptibility of mice to staphylococcal infections. *J. Exper. Med.*, 1956, 103, 109–118.
9. Schaedler, R. W., and Dubos, R. J. Reversible changes in the susceptibility of mice to bacterial infections. II. Changes brought about by nutritional disturbances. *J. Exper. Med.*, 1956, 104, 67–84.
10. Miner, R. W. (ed.). Mechanism of corticosteroid action in disease processes. *Ann. New York Acad. Sc.*, 1953, 56, 625–814.
11. Shwartzman, G. (ed.). The Effect of ACTH and Cortisone Upon Infection and Resistance. Columbia University Press, New York, 1953, 204 pp.
12. Smith, P. N. (Personal communication.)
13. Lurie, M. B.; Abramson, S., and Heppleston, A. G. On the response of genetically resistant and susceptible rabbits to the quantitative inhalation of human type tubercle bacilli and the nature of resistance to tuberculosis. *J. Exper. Med.*, 1952, 95, 119–134.
14. Nicolle, C., and Lebailly, C. Les infections expérimentales inapparentes. Exemples tirés de l'étude du typhus exanthématique. *Arch. Inst. Pasteur, Tunis*, 1919, 11, 1–5.
15. Maxcy, K. F. Endemic typhus of the Southeastern United States. The reaction of the white rat. *Pub. Health Rep.*, 1929, 44 (2), 1935–1943.
16. Dubos, R. J. The Bacterial Cell. In Its Relation to Problems of Virulence, Immunity and Chemotherapy. Harvard University Press, Cambridge, 1945, pp. 188–228.
17. Dannenberg, A. M., Jr., and Scott, E. M. Determination of respiratory LD_{50} from number of primary lesions as illustrated by melioidosis. *Proc. Soc. Exper. Biol. & Med.*, 1956, 92, 571–575.
18. Hatch, T. F. Behavior of Microscopic Particles in the Air and in the Respiratory System. In: Aerobiology. Moulton, F. R. (ed.). American Association for the Advancement of Science, Washington, D. C., 1942, No. 17, 102–105.
19. Colling, M., and Nigg, C. (In preparation.)
20. Pasteur, L. De l'atténuation des virus et de leur retour à la virulence. *Compt. rend. Acad. d. Sc., Paris*, 1881, 92, 429–435.
21. Otten, L. Immunization against plague with live vaccine. *Indian J. M. Res.*, 1936, 24, 73–101.

22. Watson, D. W.; Cromartie, W. J.; Bloom, W. L.; Kegeles, G., and Heckly, R. J. Studies on infection with *Bacillus anthracis*. III. Chemical and immunological properties of the protective antigen in crude extracts of skin lesions of *B. anthracis*. *J. Infect. Dis.*, 1947, **80**, 28–40.

23. Belton, F. C., and Strange, R. E. Studies on a protective antigen produced *in vitro* from *Bacillus anthracis:* Medium and methods of production. *Brit. J. Exper. Path.*, 1954, **35**, 144–152.

24. Strange, R. E., and Belton, F. C. Studies on a protective antigen produced *in vitro* from *Bacillus anthracis:* Purification and chemistry of the antigen. *Brit. J. Exper. Path.*, 1954, **35**, 153–165.

25. Wright, G. G.; Hedberg, M. A., and Slein, J. B. Studies on immunity in anthrax. III. Elaboration of protective antigen in a chemically-defined non-protein medium. *J. Immunol.*, 1954, **72**, 263–269.

26. Smith, H., and Gallop, R. C. The chemical basis of the virulence of *Bacillus anthracis*. VI. An extracellular immunising aggressin isolated from exudates of infected guinea-pigs. *Brit. J. Exper. Path.*, 1956, **37**, 144–155.

27. Smith, H.; Tempest, D. W.; Stanley, J. L.; Harris-Smith, P. W., and Gallop, R. C. The chemical basis of the virulence of *Bacillus anthracis*. VII. Two components of the anthrax toxin. Their relationship to known immunising aggressins. *Brit. J. Exper. Path.*, 1956, **37**, 263–271.

28. Baker, E. E.; Sommer, H.; Foster, L. E.; Meyer, E., and Meyer, K. F. Studies on immunization against plague. I. The isolation and characterization of the soluble antigen of *Pasteurella pestis*. *J. Immunol.*, 1952, **68**, 131–145.

29. Englesberg, E.; Chen, T. H.; Levy, J. B.; Foster, L. E., and Meyer, K. F. Virulence in *Pasteurella pestis*. *Science*, 1954, **119**, 413–414.

30. Keppie, J.; Smith, J., and Cocking, E. C. Lethality for guinea pigs of ultrasonic extracts of *Pasteurella pestis:* Its relationship to death of guinea pigs from plague. *Nature, London*, 1957, **180**, 1136.

31. Chambon, L., and Fournier, J. Constitution antigénique de *Malleomyces pseudomallei*. I. Caractères morphologiques, culturaux, biochimiques et variations de type immunologique. *Ann. Inst. Pasteur*, 1956, **91**, 355–362.

32. Chambon, L., and Fournier, J. Constitution antigénique de *Malleomyces pseudomallei*. II. Démonstration de l'existence des antigènes *M*, *K* et *O* et étude de leurs propriétés immunologiques. *Ann. Inst. Pasteur*, 1956, **91**, 472–485.

33. Chambon, L.; Staub, A. M., and Bourdet, M. Constitution antigénique de *Malleomyces pseudomallei*. III. Mode d'extraction et premiers essais de purification de l'antigène d'enveloppe K. *Ann. Inst. Pasteur*, 1957, **93**, 376–389.

34. Watson, D. W.; Cromartie, W. J.; Bloom, W. L.; Heckly, R. J.; McGhee, W. J., and Weissman, N. Studies on infection with *Bacillus anthracis*. V. The isolation of an inflammatory factor from crude extracts of lesions of *B. anthracis* infection and its biological and chemical relationship to glutamyl polypeptide. *J. Infect. Dis.*, 1947, **80**, 121–136.

35. Smith, H.; Zwartouw, H. T., and Harris-Smith, P. W. The chemical basis of the virulence of *Bacillus anthracis*. VIII. Fractionation of the intracellular material of *Bacillus anthracis*. *Brit. J. Exper. Path.*, 1956, **37**, 361–371.

36. Zwartouw, H. T., and Smith, H. Polyglutamic acid from *Bacillus anthracis* grown *in vivo:* Structure and aggressin activity. *Biochem. J.*, 1956, **63**, 437–442.

37. Burrows, T. W., and Bacon, G. A. The basis of virulence in *Pasteurella pestis:* The development of resistance to phagocytosis *in vitro*. *Brit. J. Exper. Path.*, 1956, 37, 286–299.

38. Burrows, T. W., and Bacon, G. A. The basis of virulence in *Pasteurella pestis:* An antigen determining virulence. *Brit. J. Exper. Path.*, 1956, 37, 481–493.

39. Smith, H., and Keppie, J. Studies on the chemical basis of the pathogenicity of *Bacillus anthracis* using organisms grown *in vivo*. In: Mechanisms of Microbial Pathogenicity. Fifth Symposium of the Society for General Microbiology Held at the Royal Institution, London, April, 1955. Howie, J. W., and O'Hea, A. J. (eds.). Cambridge University Press, Cambridge, 1955, pp. 126–151.

40. Burrows, T. W. The basis of virulence for mice of *Pasteurella pestis*. In: Mechanisms of Microbial Pathogenicity. Fifth Symposium of the Society for General Microbiology Held at the Royal Institution, London, April, 1955. Howie, J. W., and O'Hea, A. J. (eds.). Cambridge University Press. Cambridge, 1955, pp. 152–175.

41. Nigg, C.; Heckly, R. J., and Colling, M. Toxin produced by *Malleomyces pseudomallei*. *Proc. Soc. Exper. Biol. & Med.*, 1955, 89, 17–20.

42. Nigg, C. (Personal communication.)

We wish to express our appreciation to Dr. Clara Nigg for her help and advice during this study; to Dr. Max B Lurie of the University of Pennsylvania for his critical review of the results; to J. Brand Brickman and Margaret Colling for assistance; to Robert E. Bevis and William F. Hetrick for the photographs; and to Henry Stokes, Glen L. Iley, Hospital Corpsman, first class, and Alan J. Davidson for the preparation of the sections.

LEGENDS FOR FIGURES

FIG. 1. Mouse, 2 days after inhalation of 5.3×10^6 *M. pseudomallei*, avirulent strain 102–7. Lesion located at the periphery of the lung. Neutrophils and some mononuclear cells fill 4 alveoli in the center and have overflowed into neighboring alveoli, the walls of which are thickened with mononuclear cells. There is no significant evidence of necrosis. Two bacteria, not visible in the photograph, were found in the central cellular mass. This represents the respiratory lesion at its height. Methylene blue stain. × 300.

FIG. 2. Hamster, 2 days after inhalation of 1.5×10^5 *M. pseudomallei*, avirulent strain 102–7. This exudate is similar to that found in mice (Fig. 1) and consists of neutrophils in the alveolar spaces. These occasionally contain one or two bacteria (not shown). Hematoxylin and eosin stain. × 300.

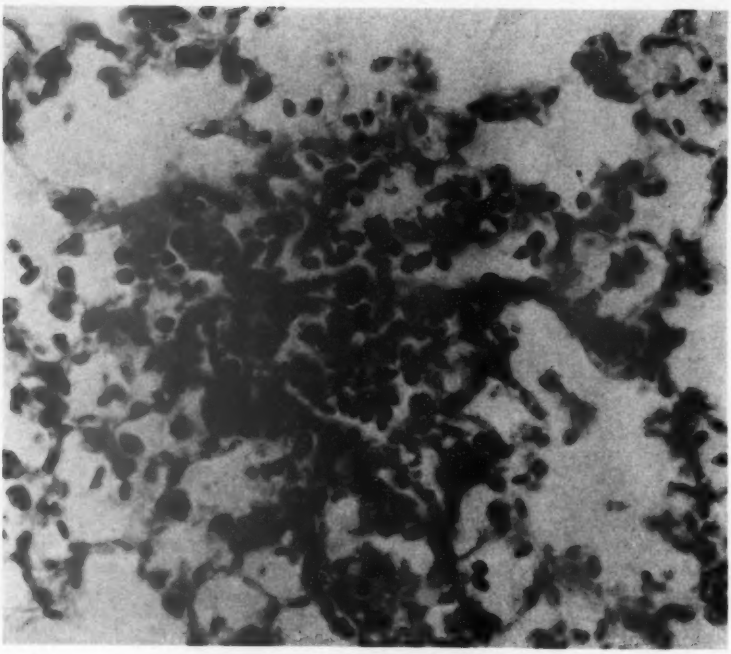

1

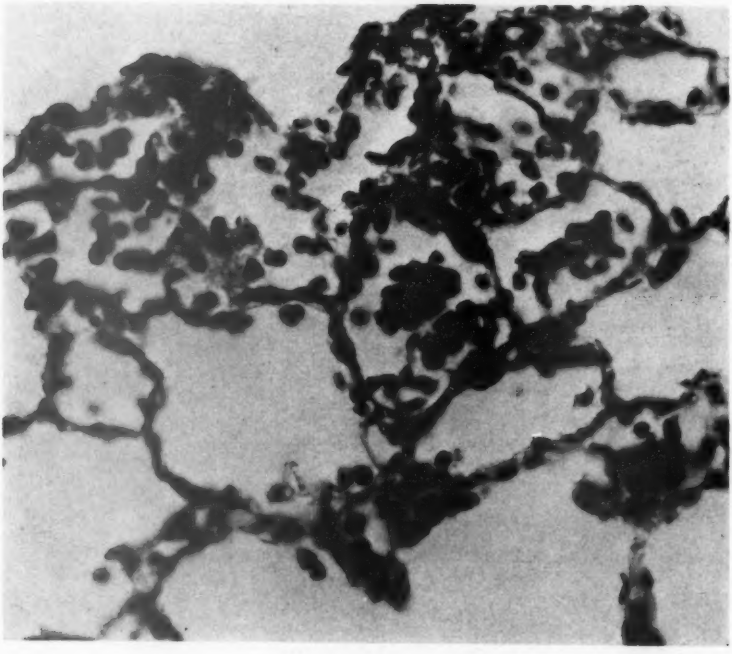

2

FIG. 3. Fasted mouse, 5 days after inhalation of 4.4×10^6 *M. pseudomallei*, avirulent strain 102–7. Pulmonary alveolar plugs of partially necrotic neutrophils and other cells are characteristic of lesions caused by virulent strains. The alveolar septums remain essentially intact. This photograph is to be compared with Figure 1 which resembles the control lesions two days after respiratory exposure. (Compare also with lesions caused by virulent organisms in Figures 11 and 12 of preceding paper.[1]) Giemsa stain. × 350.

FIG. 4. Lung, cortisone-treated mouse, 5 days after inhalation of 4.4×10^6 *M. pseudomallei*, avirulent strain 102–7. Histologic characteristics are identical with the lesion observed in the fasted mouse (Fig. 3). Giemsa stain. × 350.

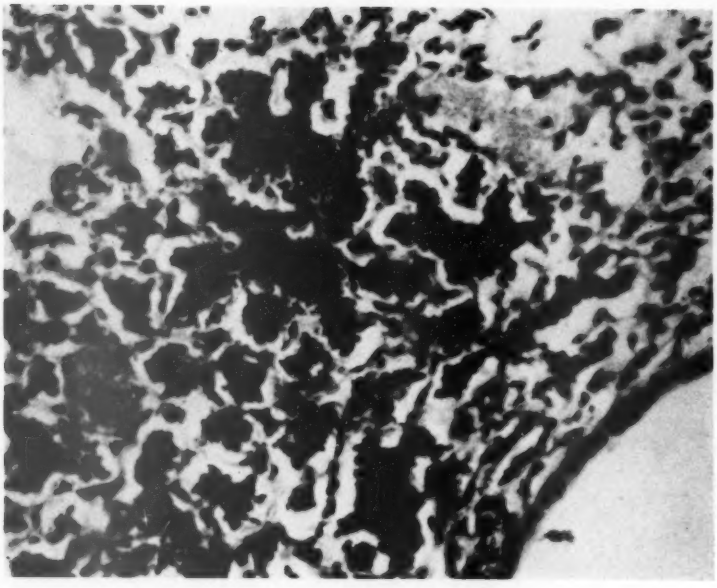

3

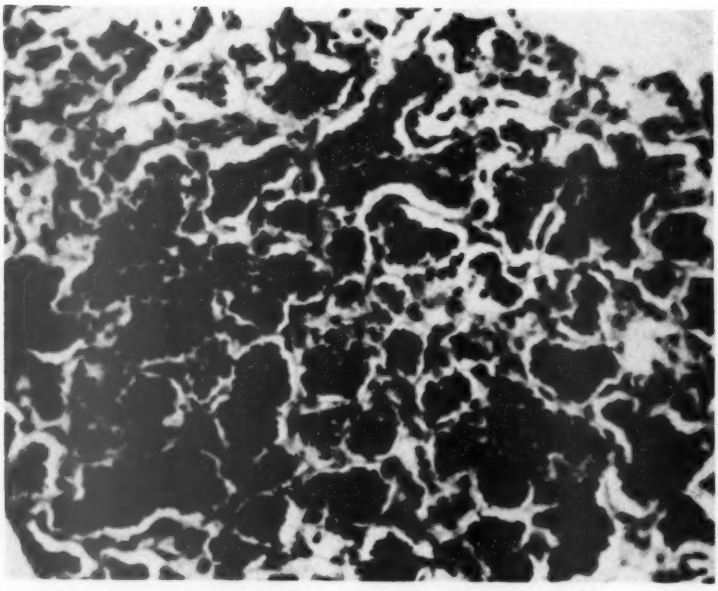

4

FIG. 5. Subcutaneous (s.c.) abscess, mouse, 13 days after s.c. inoculation of 3.9×10^7 *M. pseudomallei*, avirulent strain 102–8. A suppurative focus with ulceration above and delimitation by granulation tissue and fibroblasts at the left. Giemsa stain. × 50.

FIG. 6. Lung, hamster, 2 days after intraperitoneal (i.p.) inoculation of 2.7×10^8 *M. pseudomallei*, avirulent strain 102–7. Phagocytes, which were constituents of a disrupted alveolar septum, contain many bacteria. The hemorrhage, shown in the alveolar spaces, is a rather rare occurrence. Giemsa stain. × 1,200.

FIG. 7. Lung, hamster, one day after i.p. inoculation of 8.0×10^8 *M. pseudomallei*, virulent strain 103–67. Alveolar phagocytes contain many bacteria. This is similar to lesion shown in Figure 6 where an avirulent strain was used. Giemsa stain. × 1,030.

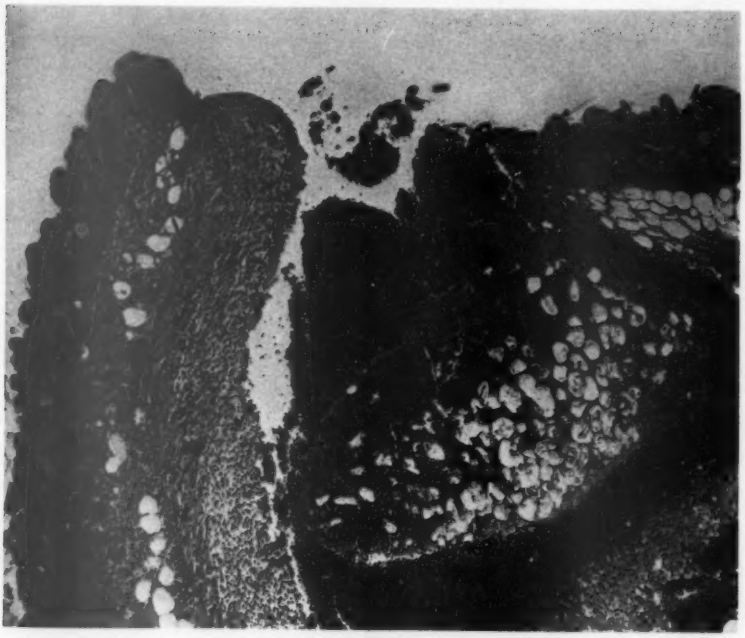

5

6

7

FIG. 8. Spleen, hamster, one day after i.p. inoculation of 2.7×10^8 *M. pseudomallei*, avirulent strain 102–7. In the red pulp (right) are many intracellular and extracellular bacteria. In the white pulp (left) are two "pitted" areas (arrows). These contain large phagocytes lining the branches of the central artery and frequently swollen with nuclear debris. (Compare with Figure 22, reference 1.) Giemsa stain. × 1,030.

FIG. 9. Spleen, hamster, 3 days after the i.p. inoculation of 5.0×10^8 *M. pseudomallei*, avirulent strain 102–8. A rather diffuse though focal necrotic lesion contains many disintegrating neutrophils in its center. Bacteria (not seen in the photograph) are numerous. The abscess, which resembles those produced by virulent strains, resulted from a generalized infection with the avirulent strain. Giemsa stain. × 160.

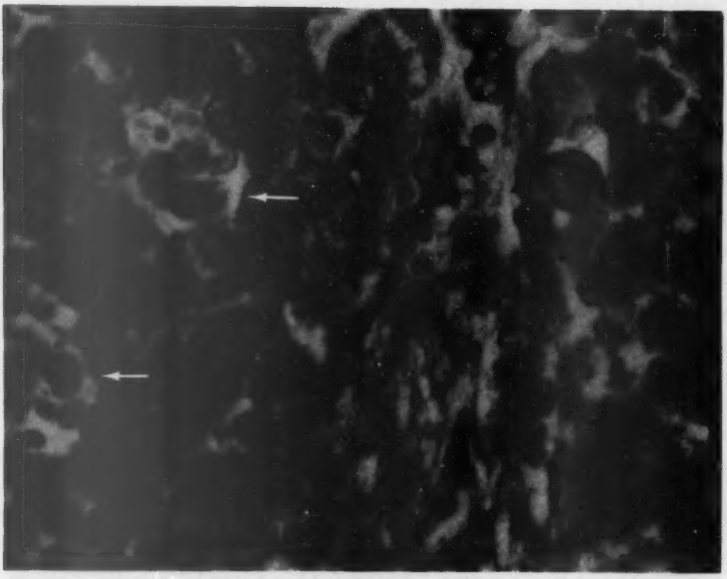

8

9

FOLLICULAR LIPIDOSIS OF THE SPLEEN

A Study of the Mode of Lipid Transport with Reference to the Lymphatics of the Spleen *

Gil M. Goldberg, M.D., and Otto Saphir, M.D.
From the Department of Pathology, Michael Reese Hospital, Chicago, Ill.

In previous studies[1-4] it was shown that a deep parenchymal lymphatic system exists in the human spleen. Fine, endothelial-lined spaces were observed beneath the intima of veins and along the courses of arterioles of the white pulp.[3] From these studies it appeared that lymphatics existed in the spleen along the splenic arteries and veins. The presence of such lymphatics was further substantiated by the observations of tumor cells within this system in instances of metastatic carcinoma to the spleen.[1] Comparable to an injection of these lymphatics by particulate matter, carcinoma cells were found along arteries and veins, sometimes bulging into their lumens, but still being confined within thin lymphatic walls. Similar lymphatics were also encountered along the follicular arterioles of the white pulp and the malpighian corpuscles.

The accumulation of lipids in excessive amounts in the spleen and their localization in the lymphoid follicles is not rare and has been repeatedly commented upon by various authors.[5-9] However, the route of transport of such lipids has not been settled. As a matter of fact, Richter[8] very recently stated that "the mode of transport to the spleen is not known." Wiland and Smith,[9] who studied the incidence of lipid globules in the lymph follicles of the human spleen, thought that the lipids were brought to the spleen by a hematogenous route. They gave no explanation as to their distribution in various parts of the spleen. The feeding of animals with lipids and oils[10] and the aspiration of lipids[11] resulted in their deposit in mesenteric and pulmonary hilar lymph nodes, as well as in the portal spaces of the liver and malpighian follicles of the spleen.[10-11] Since the mode of transport to the spleen in experimental animals was likewise not ascertained,[8] the significance of the distribution of lipids along the arterioles, trabeculae, and capsule, and of their presence in lymphoid follicles merits investigation.

Goldberg,[1-4] in a previous study on the distribution of lymph vessels in the human spleen, showed that these vessels bore a constant relation to blood vessels. Lymphatics were found in the adventitia of the

* This study was supported in part by the Byron C. Sharpe Fund and in part by the Lebold Memorial Fund.
Received for publication, April 21, 1958.

splenic artery and vein, subintimally in smaller trabecular veins, and along trabecular arteries. Arterioles of the white pulp, which are not accompanied by trabeculae, showed the presence of lymphatic vessels between their walls and the white pulp. It was brought out that the lymphatic vessels in the spleen formed an integral part of the walls of blood vessels, as in any other blood vessel of the body (*vasa lymphatica vasorum sanguinorum*). However, because the arteries and the veins within the spleen have two mural components—namely, the wall itself and the dense trabecular connective tissue, the lymphatic vessels which are located between these two components are usually compressed and not visible. They were observed in the normal spleen only in places where they were not compressed by dense connective tissue.[3] They were also clearly visible when they contained cellular elements, as in cases of metastatic mucin-producing carcinoma.[1]

It is the purpose of this study to evaluate the location, distribution, and mode of transport of lipids in the spleen in the light of recent observations of a deep lymphatic system existing in the human spleen.[1-4]

Material and Method

This study is based on the histologic examination of 3 spleens which contained lipid vacuoles along blood vessels and within the malpighian follicles. In the first instance the spleen was from a 61-year-old white man whose necropsy diagnosis was generalized arteriosclerosis and myocardial infarction. The second patient was a 49-year-old white woman with nutritional cirrhosis of the liver. The third patient was a 28-year-old Negro with miliary tuberculosis of the lungs, kidneys, and suprarenal glands. Blocks were cut from the hilar region as well as from the deep parenchyma of the spleen, and from the splenic arteries and veins along their respective courses. The tissue was fixed in 10 per cent formalin. Multiple sections from these blocks were cut at 8 μ and stained with hematoxylin and eosin, and by the van Gieson and Weigert methods for elastic fibers. Frozen sections from the various locations were also stained with Sudan IV.

Results

Splenic Artery

Sudanophilic vacuoles were encountered in the adventitia of the arteries (Fig. 1). Sometimes the vacuoles were surrounded by an infiltration of lymphocytes. The location of the vacuoles corresponded to that of the lymphatics demonstrated by the presence of carcinoma cells in cases studied previously.[1]

Trabecular Arteries

Vacuoles were found in slit-like spaces within the walls of these arteries. Sometimes a prominent endothelial lining could be made out in the slits. These corresponded to the location of lymphatics in which carcinoma cells had been found in other cases[1] (Figs. 2 and 3).

Follicular Arterioles

These arterioles, the walls of which are devoid of a trabecular component, exhibited irregular vacuoles along their walls. The vacuoles were also observed along the walls of arterioles in the white pulp and in the malpighian corpuscles (Fig. 4). This location, likewise, corresponded to that of the lymphatics observed in the carcinoma specimens (Fig. 5). However, in some instances, groups of vacuoles could be seen extending into the surrounding white pulp and even into the region bordering the red pulp (Fig. 6). This phenomenon is undoubtedly due to the escape of lipid from the smallest lymphatic vessels and corresponds to the invasion of the neighboring white and red pulp by carcinoma cells after they too have escaped the lymphatics (Fig. 7).

Malpighian Follicles

Single (Fig. 8) or multiple vacuoles, which sometimes fused to form voluminous vacuoles, were observed on the outer margins of the central arterioles (Fig. 9). Again, the location was remarkably similar to that of the lymphatics made visible by the presence of cancer cells (Fig. 10).

Splenic Vein

This vein was surrounded by fat tissue which made it difficult to distinguish the lipid-engorged lymphatics. However, when the tributaries of the splenic vein were examined at the hilus of the spleen, vacuoles located subintimally could be easily observed in the walls (Fig. 11). The subintimal location of the lymphatics had been particularly stressed in previous observations;[1-4] the outer part of the venous wall is formed by the trabecular component (Fig. 12).

Trabecular Veins

These veins, as stated above, have been found to have a thin wall, and an outer, thick, dense, connective tissue support formed by the accompanying trabeculae. Lymphatics have been demonstrated in the subintimal region of the venous wall proper. Multiple small vacuoles could be observed in our specimens in exactly the same location (Fig. 13). The vacuoles were surrounded by collections of lymphoid

elements (Figs. 13 and 15), and occasionally the entire process bulged into the lumen of the vein. The accumulation of carcinoma cells, confined within the lymphatic walls (Fig. 14) was a significant finding in carcinoma cases.[1]

Vacuoles

All the vacuoles, wherever seen in the spleen and along the vessels, stained red with Sudan IV. They could be observed either singly (Figs. 4 and 8) or in groups (Figs. 6 and 9). When found in groups, they were irregular in size, replacing the lymphoid elements of the white pulp. Solitary vacuoles within the adventitia of an arteriole often demonstrated an endothelial lining (Fig. 8). Vacuoles were not found in the lumens of blood vessels.

Granulomas

Lipid granulomas were encountered. These consisted of multiple irregular vacuoles, always staining with Sudan IV. Between the voluminous vacuoles, lymphoid elements, macrophages and foreign body giant cells were found. These contained minute vacuoles (Fig. 16). The granulomas seemed to develop only after breakdown of minute lymphatics permitted the lipids to reach the tissues.

Discussion

The question presented itself as to whether the sudanophilic vacuolated material observed along the blood vessels of the spleen, in malpighian corpuscles, and in the granulomas, consisted of adipose tissue or represented a deposition of lipid globules.

The vacuoles were non-nucleated, irregular in size, and generally did not bear any uniform histologic relationship to the surrounding tissue. When such a relationship was observed, it was only in the form of a foreign body granuloma reaction characterized by giant cells and macrophages. These observations parallel the results of experiments carried out by Stryker,[10] and suggest that the sudanophilic vacuolated material is a noncellular lipid substance which has been transported to the spleen.

It has been thought by some investigators[9-12] that lipid droplets were carried to the spleen by means of blood vessels, even though this mechanism could never be satisfactorily demonstrated. If the droplets were transported to the spleen via the blood circulation, one would expect to see fat emboli in the arteries and in the sinusoids of the red pulp. However, this could not be demonstrated in our specimens. Only the evidences of chronicity, characterized by granulomas, were

observed in the red pulp. None of the sections gave any evidence of a transport of lipids into the spleen by the blood.

From necropsy material[10,11] and experimental study,[10] it appears that lymph nodes in the mesenteric and splenic hilar regions may show a deposition of lipid droplets. Animals fed with lipids exhibited fat in intestinal lymphatics in a proportion similar to that in the emulsion which had been fed to them.[10]

As stated above, it has been demonstrated that the human spleen has a well developed, deep, parenchymal lymphatic system.[1-4] The lipid droplets located along trabecular arteries, follicular arterioles of the white pulp (malpighian follicles), and veins, create a pattern with unique resemblance to the lymphatic vessels brought into view by the presence of carcinoma cells. The lipid droplets observed in the distribution of the lymphatics present features of a systematic sequence of events. A minimal, very early lesion is characterized by lipid vacuoles located within the lymphatics. In the more advanced lesion where lipids have reached the tissues, a granulomatous reaction is provoked. It is, therefore, proposed that the distribution of lipid in the spleen is the result of a lymphatic spread and occurs as part of a generalized lymphatic involvement.

Summary

In 3 examples exhibiting lipidosis of the splenic follicles, lipid globules were observed in the adventitia of the splenic arteries and veins. The localization of the globules corresponded to that of carcinoma cells in instances of lymphogenous splenic metastases. The globules, as in the case of the carcinoma cells, were found in spaces identified as lymphatics constituting portions of a deep parenchymal lymphatic system in the spleen. It is suggested that lipid globules, which reach the pulp as the result of disruption of minute periarteriolar lymphatics, provoke the characteristic lipid granulomas which are observed.

REFERENCES

1. Goldberg, G. M. Metastatic carcinoma of the spleen resulting from lymphogenic spread. *Lab. Invest.*, 1957, 6, 383–388.
2. Goldberg, G. M. Lymphatics of the spleen in normal and pathological states. *Bull. Res. Council of Israel*, 1957, 6E, *Experimental Medicine*, p. 159.
3. Goldberg, G. M. Lymphatics of the spleen. *J. Anat.*, 1958, 92, 310–314.
4. Goldberg, G. M., and Ungar, H. The lymphatics of the spleen in leukemia with reference to so-called "infiltration of vascular walls." *Lab. Invest.*, 1958, 7, 146–151.
5. Wassiljeff, A. M. Über die Ablagerung von Fettsubstanzen und Eisenverbindungen in der Milzkapsel und den Trabekeln. *Virchows Arch. path. Anat.*, 1923–1924, 247, 640–649.

6. Kusunoki, M. Lipoidsubstanzen in der Milz und im Leichenblut. *Beitr. path. Anat.*, 1914, 59, 564–600.
7. Poscharisky, J. F. Zur Frage des Fettgehaltes der Milz. *Beitr. path. Anat.*, 1912, 54, 369–384.
8. Richter, M. N. The Spleen, Lymph Nodes and Reticuloendothelial System. In: Pathology. Anderson, W. A. D. (ed.). The C. V. Mosby Co., St. Louis, 1957, ed. 3, pp. 907–947.
9. Wiland, O. K., and Smith, E. B. Lipid globules in the lymphoid follicles of the spleen. *A.M.A. Arch. Path.*, 1957, 64, 623–628.
10. Stryker, W. A. Absorption of liquid petrolatum ("mineral oil") from the intestine. A histologic and chemical study. *Arch. Path.*, 1941, 31, 670–692.
11. Pinkerton, H., and Moragues, V. Paraffinoma of the lung with secondary tubercle-like lesions in the liver and spleen. *Arch. Path.*, 1940, 29, 691–699.
12. Lubarsch, O. Pathologische Anatomie der Milz. In: Handbuch der Speziellen Pathologischen Anatomie und Histologie. Vol. I., Part 2. Blut, Knochenmark, Lymphknoten, Milz. Henke, F., and Lubarsch, O. (eds.). Julius Springer, Berlin, 1927, pp. 373–774.

LEGENDS FOR FIGURES

All sections illustrated were stained with hematoxylin and eosin stain.

FIG. 1. Hilar artery and vein with vacuoles and mural slit. Note perivascular lymphorrhages. × 600.

FIG. 2. Trabecular artery. The slit in its wall contained sudanophilic vacuoles. × 200.

FIG. 3. A trabecular artery with carcinoma cells in lymphatics. To be compared with Figure 2. × 200.

FIG. 4. A follicular arteriole coursing in the white pulp. A sudanophilic vacuole is visible between the arteriolar wall and the white pulp. × 1,300.

FIG. 5. Follicular arteriole. Lymphatics are made visible by the presence of carcinoma cells. To be compared with Figure 4. × 1,300.

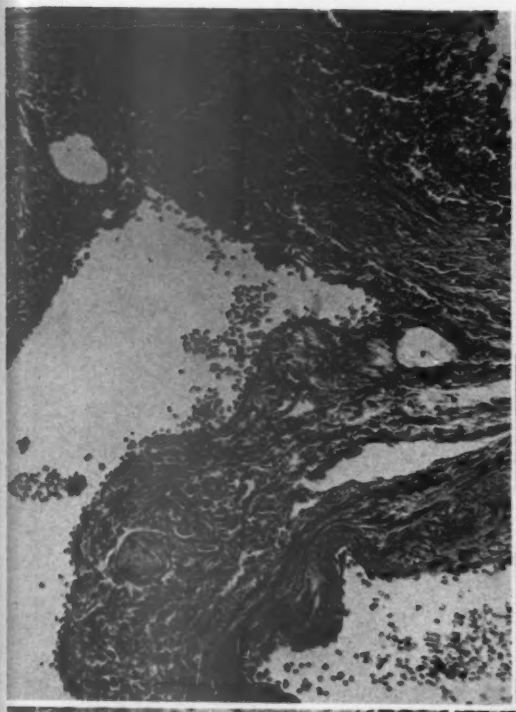

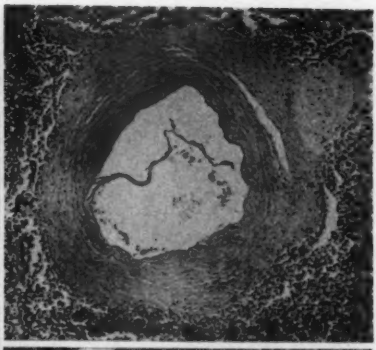

2

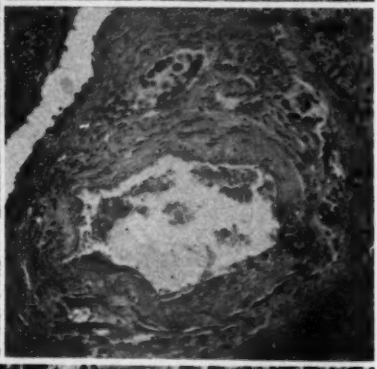

3

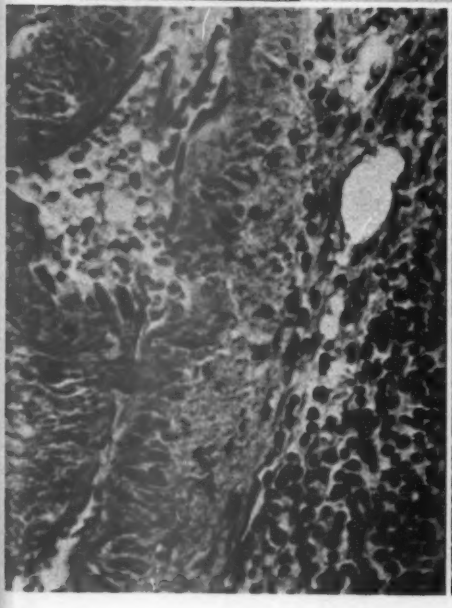

5

FIG. 6. Migration of vacuoles into adjoining red pulp. To be compared with Figure 7. × 600.

FIG. 7. Invasion by carcinoma cells which enter the surrounding white and red pulp from periarteriolar lymphatics. × 600.

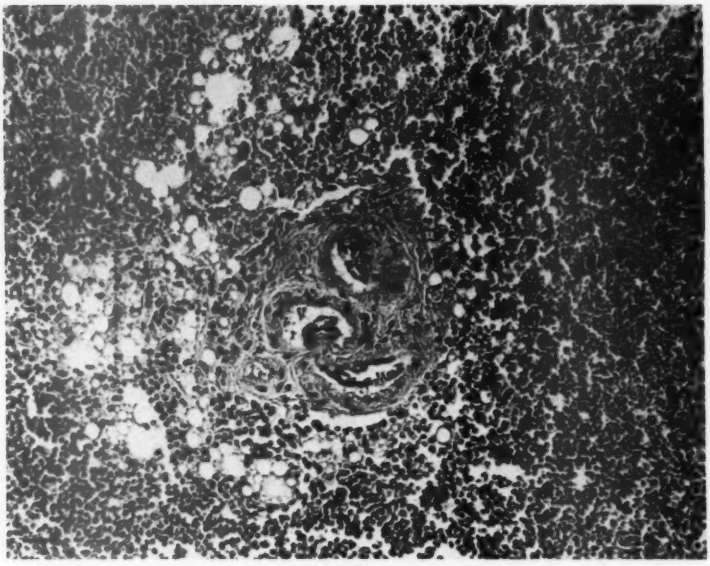

6

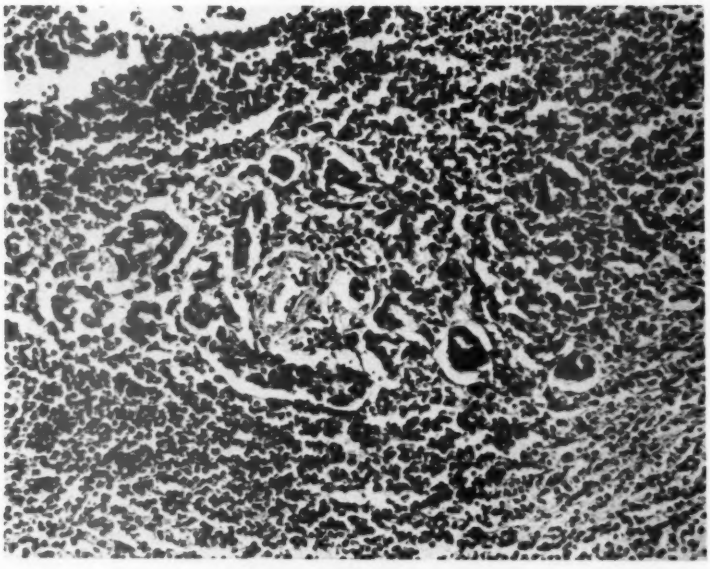

7

FIG. 8. A central arteriole in a malpighian follicle. Note the single vacuole with what appears to be an endothelial lining. To be compared with Figure 10. × 1,000.

FIG. 9. A central arteriole in a malpighian follicle. Coalescent multiple vacuoles are manifest. To be compared with Figure 10. × 1,200.

FIG. 10. A central arteriole in a malpighian follicle. Note lymphatics containing carcinoma cells. × 1,000.

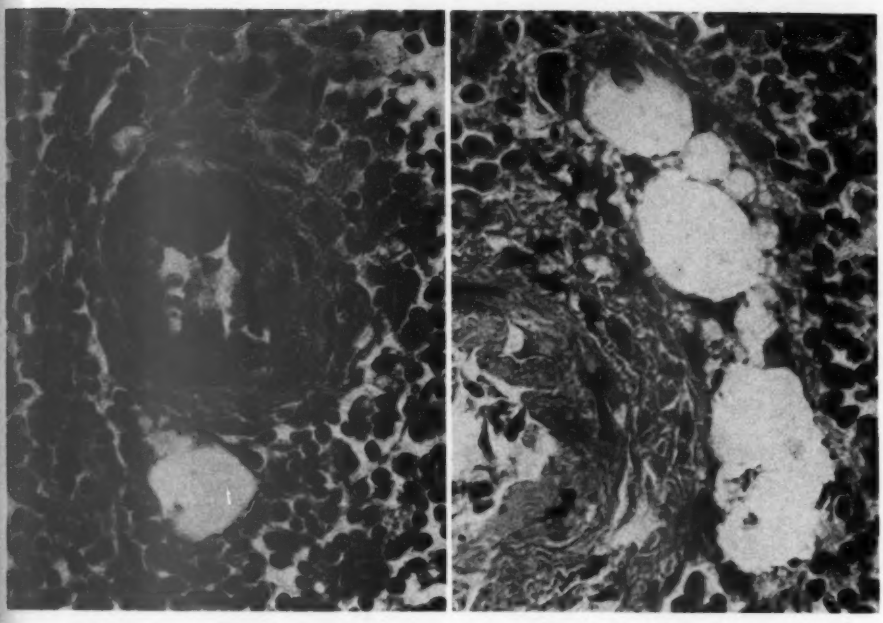

8 9

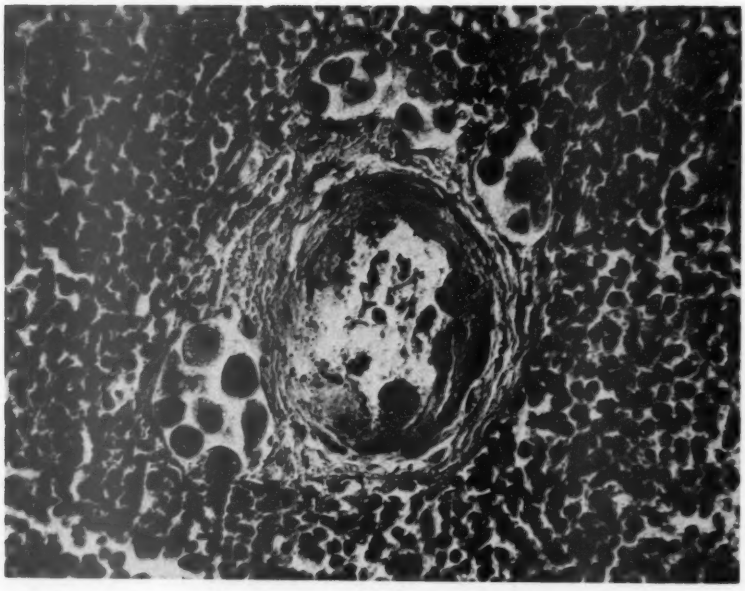

10

FIG. 11. Hilus of the spleen. Note vacuoles surrounded by lymphoid elements (lymphorrhages) in a vein wall. To be compared with Figure 12. × 1,040.

FIG. 12. Hilus of the spleen. Note lymphatic vessel in the vein wall, highlighted by the presence of carcinoma cells. × 1,040.

FIG. 13. A trabecular vein with vacuoles present in its wall. Note lymphorrhages around vacuoles. To be compared with Figure 14. × 600.

FIG. 14. A trabecular vein with tumor cells in intramural lymphatics. × 300.

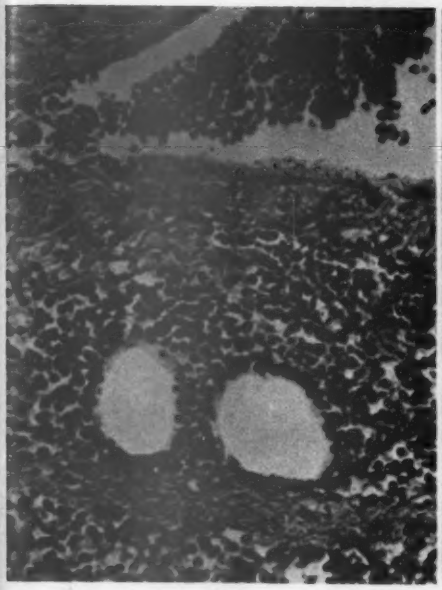

11

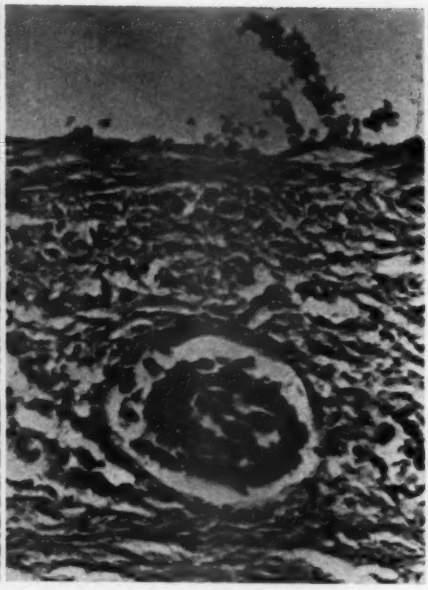

12

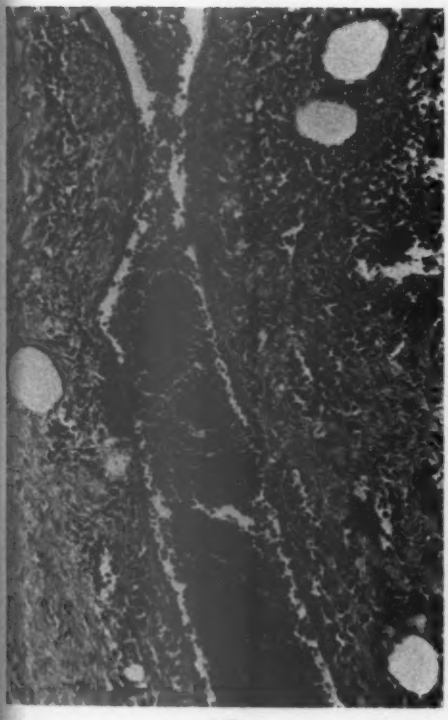

13

14

FIG. 15. Wall of a trabecular vein. Lymphoid elements in an intramural lymphatic cause bulging into the lumen of the vein. Also note minute vacuoles in a zone of mural lymphorrhage. × 600.

FIG. 16. Foreign body giant cell with large lipid vacuole located near an arteriole. × 1,000.

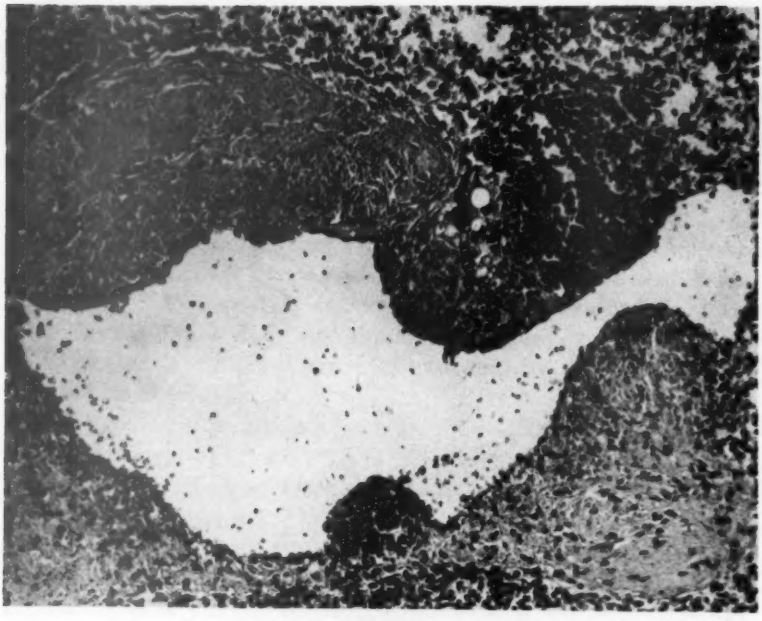

15

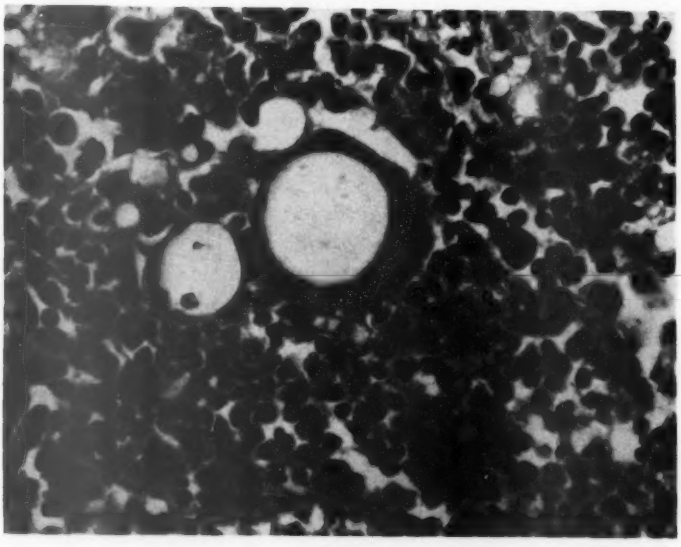

16

IRON STORAGE

I. The Influence of Time on the Redistribution of Excess Storage Iron *

Arne Sheden, Kem. Ing., and Phillip Sturgeon, M.D.
From the Hematology Research Laboratories, Children's Hospital, and the Department of Pediatrics, University of Southern California, School of Medicine, Los Angeles, Calif.

Iron in excess of that needed for the synthesis of hemoglobin and other functional iron compounds is stored primarily in the liver; under these circumstances the spleen and bone marrow iron is also increased in amount. This iron, often considered as reserve, is present in two physically different protein compounds. One, hemosiderin, is microscopically visible as discrete granules which give a positive Prussian blue reaction. The other, ferritin, is water soluble and is not demonstrable histochemically.

In the course of an earlier experiment[1] in which several rabbits were given large excesses (2,000 mg.) of iron parenterally over a relatively short period, the data indicated that the livers of the animals sacrificed 1 to 2 years after receiving injections had greater amounts of iron than those sacrificed 1 month after the last injection. The present investigation was undertaken to confirm this previous observation and to study, during the apparent process of redistribution of excess storage iron, the relationship between ferritin and hemosiderin in the liver and other organs.

Methods

New Zealand white rabbits, 6-month-old males, were given 2,000 mg. of iron intravenously in the form of saccharated iron oxide (Feojectin) over a period of 6 weeks. Two animals were sacrificed at 1 week, and 3, 6, 10, and 14 months after the last injection. The livers and other organs were analyzed for ferritin and hemosiderin by water extraction and centrifugation with an arbitrarily chosen force of gravity. The method has been described in detail.[2] Quantitative determination of iron was made, according to the method of Lorber.[3]

To eliminate hemoglobin iron from the water soluble extracts, the livers were perfused with 0.9 per cent saline immediately post mortem. In the extracts from other organs, the hemoglobin content was measured as reduced pyridine hemochromogen and the equivalent amount

* This investigation was supported in part by a grant from the United States Atomic Energy Commission, Contract #AT (04-3)-77, and in part by Lakeside Laboratories, Inc., Milwaukee, Wisc.
Received for publication, March 26, 1958.

of iron subtracted from the total iron determination.*[4] Calculations for the amount of hemoglobin in the presence of ferritin were carried out according to a modification of the method used by Borei and Shoden[5] for the determination of cytochrome C (hemochromogen) in bakers' yeast.

The light absorption curve of ferritin in the Beckman Model B spectrophotometer is close to a straight line in the region 540 to 580 mμ; this line is not parallel to the X-axis (Text-fig. 1). The slope of the curve varies with the ferritin concentration.

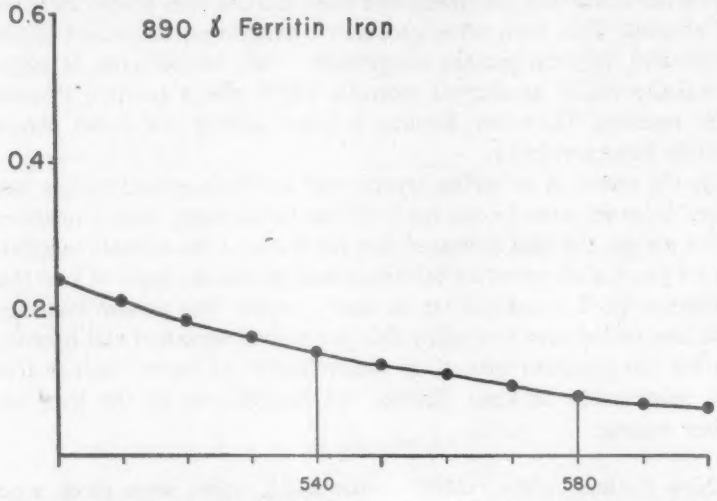

Text-figure 1. Ferritin. Light absorption in the region of 400 to 600 mμ. Beckman Model B spectrophotometer. Abscissa, λ; ordinate, optical density.

The hemochromogen curve was read at 540, 555, and 580 mμ (Text-fig. 2). An arbitrary base line for determination of the value R at 555 mμ was provided by readings taken at 540 and 580 mμ. The distance R (Text-fig. 2) represented a constant percentage of the total hemoglobin content of the sample. By calculating R from determinations on a pure hemoglobin solution of known concentration, the relation between R and the hemoglobin concentration was derived: mg. Hb. per ml. $= K \times R$; or, $K = \frac{\text{mg. Hb. per ml.}}{R}$.

In a sample containing ferritin and hemoglobin (or hemoglobin alone), the total light absorption at 555 mμ (r_{555}) may be looked upon

* The ammonia and pyridine can be added to a whole series of samples, but each sample is reduced separately with sodium hydrosulfite and read within one minute. The ferritin iron will start to precipitate as hydroxide after it is reduced, and the turbidity will interfere with the reading.

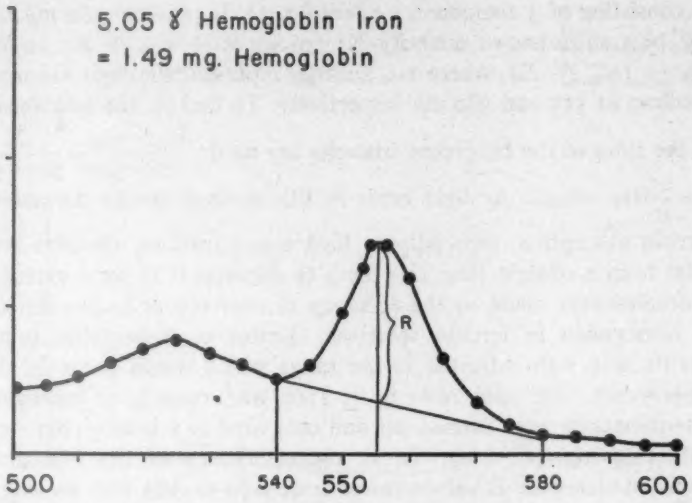

Text-figure 2. Hemoglobin. Light absorption in the region of 400 to 600 mμ. Beckman Model B spectrophotometer. Abscissa, λ; ordinate, optical density.

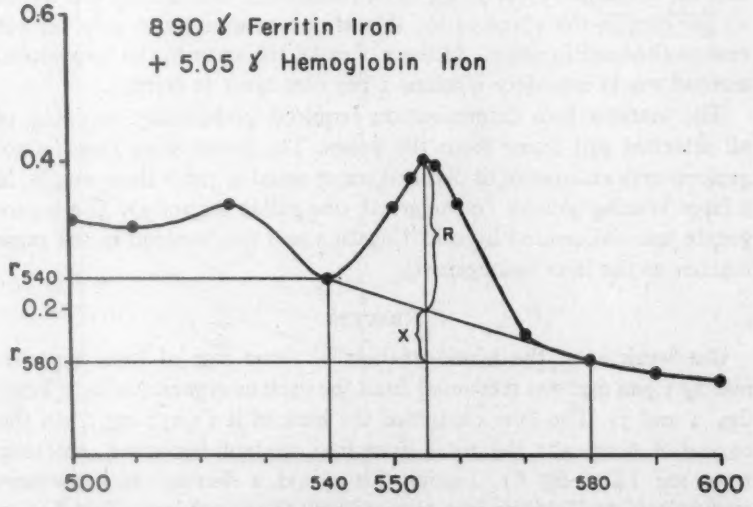

Text-figure 3. Ferritin and hemoglobin. Light absorption in the region of 400 to 600 mμ. Beckman Model B spectrophotometer. Abscissa, λ; ordinate, optical density.

as consisting of 3 components (Text-fig. 3), R plus the 580 mμ reading, plus an unknown quantity X; $r_{555} = R + r_{580} + X$; or $R = r_{555} - (r_{580} + X)$, where r_{555} and r_{580} represent the light absorption readings at 555 and 580 mμ respectively. To find X, the relationships of the sides of the congruent triangles are used: $\frac{r_{540}-r_{580}}{580-540}=\frac{X}{580-555}$; $X=\frac{25}{40}(r_{540}-r_{580})$. A slight error in this method results because the ferritin absorption, especially in high concentrations, deviates somewhat from a straight line; this tends to decrease R to some extent.

Studies were made on the accuracy of recovery of known amounts of hemoglobin in ferritin solutions. Ratios of hemoglobin iron to ferritin iron were adjusted to the range which would occur in these experiments. For each ratio (1:1, 1:10, and 1:100), 12 hemoglobin determinations were carried out and compared to a hemoglobin standard (1.49 mg. per ml.). In 12 determinations of the hemoglobin standard alone, the R values varied from .170 to .183 with an average of .177. The K value obtained from these figures was $\frac{1.49}{.177}= 8.4$. In a ratio of 1:1 (hemoglobin iron to ferritin iron), the R values were .180 to .190 (average .184). The R values in the 1:10 ratio were .168 to .186 (average .175); and in the 1:100 ratio, .127 to .156 (average .143). The hemoglobin recoveries were thus 104 per cent, 99 per cent, and 81 per cent respectively. It can be seen from these figures that the maximum error in the determination of hemoglobin was minus 19 per cent in the 1:100 ratio; this of course would add only .19 per cent to the ferritin value. At the 1:1 ratio, the error in the hemoglobin method would introduce a minus 4 per cent error in ferritin.

The marrow iron determination required preliminary scraping of all attached soft tissue from the bones. The bones were then homogenized with an amount of distilled water equal to twice their weight, in a large Waring blender (commercial, one gallon capacity). The homogenate was sedimented by centrifugation and fractionated in the same manner as the liver homogenates.

Results

One week after the administration of 2,000 mg. of iron, approximately 1,700 mg. was recovered from the various organs studied (Text-figs. 4 and 5). The liver contained the bulk of it (1,250 mg.). In the course of 6 months the total liver iron content increased, reaching 1,500 mg. (Text-fig. 6). During this period, a decrease in bone marrow, spleen, and kidney iron was evident (see total iron, Text-figs. 7 and 8). The spread of total iron values (Text-fig. 5) in the lungs pre-

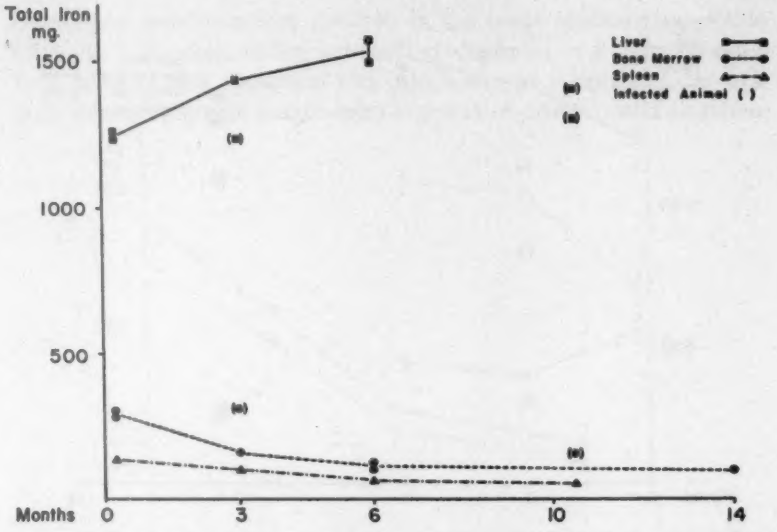

Text-figure 4. Redistribution, with time, of excess storage iron (2,000 mg.) in liver, bone marrow, and spleen. Brackets indicate infected animal.

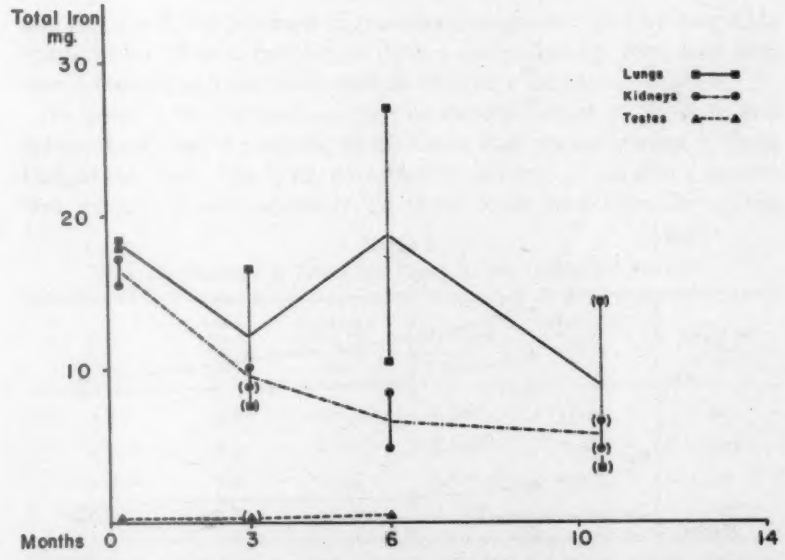

Text-figure 5. Redistribution, with time, of excess storage iron (2,000 mg.) in lung, kidney, and testis. Brackets indicate infected animal.

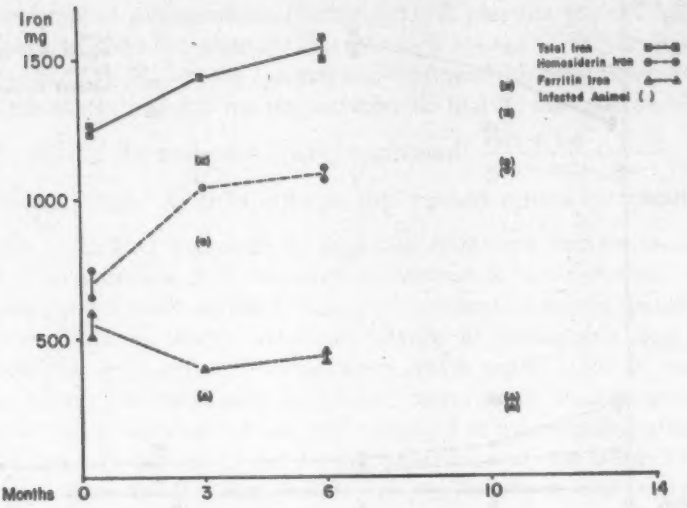

Text-figure 6. Redistribution, with time, of excess storage iron (2,000 mg.) in livers of rabbits. Comparison of ferritin to hemosiderin.

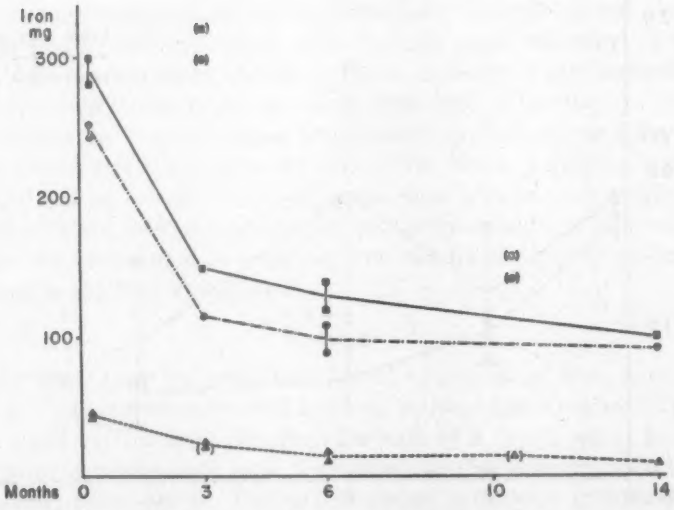

Text-figure 7. Redistribution, with time, of excess storage iron (2,000 mg.) in bone marrow of rabbits. Comparison of ferritin to hemosiderin.

cluded any interpretation; the iron in the testis appeared to remain constant. The points in brackets in Text-figures 4 to 8 were obtained from animals with obvious severe infections. In 2 instances, the animals lost considerable weight from diarrhea of 1 to 2 weeks' duration,

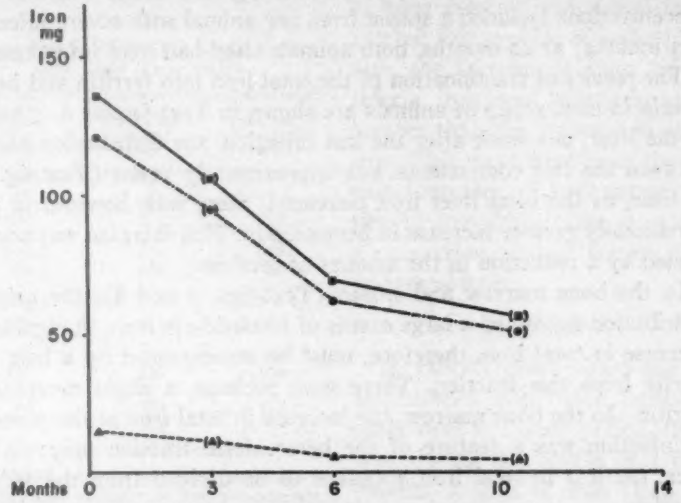

Text-figure 8. Redistribution, with time, of excess storage iron (2,000 mg.) in spleens of rabbits. Comparison of ferritin to hemosiderin.

and in a third, the presence of pneumonia was confirmed by histologic examination. It is of interest, in these 3 cases, that the total liver iron was decreased and the bone marrow showed a reciprocal increase.

In Table I the comparisons of iron concentrations in the liver and spleen show that the spleen, at all times, had approximately 3 times that of the liver. The liver, nevertheless, because of its much greater size, contained approximately 10 times more iron than the spleen

TABLE I

*Iron Concentration in Spleen and Liver of Iron Overloaded Rabbits**

Time after injection	Average wt. of spleen (gm.)	Average wt. total Fe in spleen (mg.)	Mg. Fe per 100 gm. of spleen	Average wt. total Fe in liver (mg.)	Mg. Fe per 100 gm. of liver
1 wk.	4.8	136.2	2,830	1,250	840
3 mos.	2.5	106.1	4,250†	1,285†	1,230†
6 mos.	2.1	69.0	3,270	1,535	1,180
10½ mos.	1.3	56.7	4,350†	1,350†	1,180†

* The two spleens from each group were pooled and run as one sample. For comparison, the average of values from two corresponding livers is tabulated.

† Includes infected animals.

(Text-fig. 4). It is apparent that the decrease in total spleen iron was paralleled by a decrease in weight of the spleen (Table I); the concentration, thus, remained approximately constant. It is also noteworthy that the determinations showing somewhat higher iron concentrations included a spleen from one animal with severe infection at 3 months; at 10 months, both animals cited had mild infections.

The results of fractionation of the total iron into ferritin and hemosiderin in each group of animals are shown in Text-figures 6, 7 and 8. In the liver, one week after the last injection, the distribution of iron between the two components was approximately equal (Text-fig. 6). In time, as the total liver iron increased, there was, however, a proportionately greater increase in hemosiderin. This increase was accompanied by a reduction in the amount of ferritin.

In the bone marrow and spleen (Text-figs. 7 and 8), the original distribution contained a large excess of hemosiderin iron. A significant decrease in total iron, therefore, must be accompanied by a loss, primarily from this fraction. There was, perhaps, a slight decrease in ferritin. In the bone marrow, the increase in total iron in the presence of infection was a feature of the hemosiderin fraction only; in the liver, the loss in total iron appeared to be derived from the ferritin fraction.

Discussion

The experimental approach employed in this and previous studies has made no allowance for the size of animals used or the weight of the organs studied. No practical way was found to predict the latter at the time of administering the iron. In these studies, all animals, irrespective of weight, were given equal doses of iron. Analyses were made for total iron or iron compounds per animal or organ. It was found in these and in previous experiments that agreement between duplicate animals or organs was very poor if the data were presented in terms of iron concentration (mg. per 100 gms. of tissue). On the other hand, when total iron was measured, there was good agreement. Table II lists the weights of 5 pairs of livers from animals given equal amounts of iron per pair, and compares the weight of iron content (mg. per 100 gm.) of the liver to the total iron in the liver. It illustrates that the agreement between members of each pair was much better when the data were recorded in terms of total iron per organ. This observation indicates, therefore, that the quantity of iron per organ in experiments of this nature was related to the total iron administered rather than to the weight of the organ.

These experiments, though complicated by infection in some of the animals, confirmed the observation noted in a previous study[1] that,

following iron overloading of rabbits, there was, with time, a redistribution of iron. The present experiments have shown that redistribution occurred for the most part in the first 3 to 6 months and was characterized by an increase in total liver iron and a decrease chiefly in bone marrow and spleen iron. During this process of redistribution, the increase in liver hemosiderin iron was proportionately greater than the increase in total iron. This must have been the result, therefore, of both accumulation of iron from other sites and a conversion of liver ferritin iron to hemosiderin.

TABLE II

*Comparison of Liver Iron Concentration with Total Liver Iron**

Wt. of liver (gm.)	Mg. Fe per 100 gm. tissue	Total iron in organ† (mg.)
68	467	319
106	275	293
121.5	714	868
85.5	982	840
165.5	660	1,090
116	912	1,060
166	747	1,240
133	950	1,260
144	1,080	1,572
116	1,295	1,501

* Paired experiments; both animals receiving same quantity of iron parenterally.

† Note close agreement in total iron, irrespective of differences in sizes of livers.

SUMMARY

In rabbits given 2,000 mg. of saccharated iron oxide intravenously over a 6-week period, there was, during the course of 3 to 6 months, a shift of iron from the spleen and bone marrow to the liver.

During this process of redistribution, the liver hemosiderin iron increased to a greater extent than the total liver iron. Thus, there was a concurrent decrease in liver ferritin iron.

These observations indicate that in states of iron overloading, the time interval between administration and observation is an important factor in considerations of the ultimate distribution of iron.

REFERENCES

1. Shoden, A.; Gabrio, B. W., and Finch, C. A. The relationship between ferritin and hemosiderin in rabbits and man. *J. Biol. Chem.*, 1953, 204, 823–830.
2. Gabrio, B. W.; Shoden, A., and Finch, C. A. A quantitative fractionation of tissue ferritin and hemosiderin. *J. Biol. Chem.*, 1953, 204, 815–821.
3. Lorber, L. Einfache micro-kolorimetrische Eisenbestimmungsmethode. *Biochem. Ztschr.*, 1927, 181, 391–394.
4. Flink, E. B., and Watson, C. J. A method for the quantitative determination of hemoglobin and related heme pigments in feces, urine and blood plasma. *J. Biol. Chem.*, 1942, 146, 171–178.
5. Borei, H., and Sjøden [Shoden], A. Züchtungsbedingte Veränderungen des Cytochrom-C Gehalts der Oberhefe. *Arkiv. Kemi. Mineral., Geol.*, 1943, 16A, No. 19, 1–17.

The authors wish to express their appreciation to Miss Royeta Peyton and Miss Marianne Lindgren for valuable technical assistance.

LIPOBLASTOMATOSIS: A TUMOR OF FETAL FAT DIFFERENT FROM HIBERNOMA

Report of a Case, with Observations on the Embryogenesis of Human Adipose Tissue *

Frank Vellios, M.D.; José Baez M., M.D.,† and Harris B. Shumacker, M.D.
From the Departments of Pathology and Surgery, Indiana University School of Medicine, Indianapolis, Ind.

Tumors of adipose tissue are varied, and no classification of them is generally accepted. The tumors include true neoplasms, the lipomas and liposarcomas, and non-neoplastic masses.[1] Benign neoplasms of fat, lipomas are usually composed of mature fat cells; each cell is distended with a large vacuole of lipid which displaces the nucleus and compresses it against the cytoplasmic membrane. The so-called hibernoma is a tumor of adipose tissue, the component elements of which are multivacuolated and contain varying amounts of eosinophilic cytoplasm. These tumors resemble the brown fat of hibernating animals; hence their name. Cox[2] has suggested that tumors of brown fat are composed of immature adipose tissue.

It is now generally agreed that the lipoblast is a specialized cell differing from the fibroblast.[3] According to Shaw,[4] this theory was proposed by Todd and Bowman, in 1845, and supported by Toldt, in 1870. Subsequently others have held that adipose tissue is derived from the fibroblast, which elaborates fat. It has been suggested that fat in different sites is not necessarily similar, the notable exception being the brown fat found especially in hibernating animals.[5-9] According to Rasmussen,[7] brown fat in animals forms a large mass in the superior mediastinum. It extends into the intermuscular septums in the cervical region, with large lobes in the lateral portions of the neck. A pair of dorsal lobes is situated between the scapulas, and there are also extensions into the abdominal cavity with prominent perirenal lobes. In the human, the white fat encountered in the fetal and infantile periods resembles brown fat histologically.

Recently, we observed an unusual tumor, resembling fetal adipose tissue, in an 8-month-old child. This tumor was located in the subcutaneous tissue of the anterior wall of the thorax, the right axilla, and the right suprascapular area. It differed from hibernoma clinically,

* This study was aided in part by funds from the Indiana Elks Association.
Received for publication, April 1, 1958.

† Dr. Baez was a Fellow of the Rockefeller Foundation at the time of this study. His present address is Laboratorio de Patologia, Hospital Central, Universidad de Leon, Leon, Guanajuato, Mexico.

grossly, and microscopically, but was also distinctly different from tumors of adult adipose tissue. Histologically, the lesion resembled fetal fat, and the term "lipoblastomatosis" is proposed for this reason. A study of the development of adipose tissue in human fetuses was undertaken in order to gain a better understanding of the nature of this lesion.

Case History

An 8-month-old white girl was admitted to the Pediatrics Service of the James Whitcomb Riley Hospital, Indiana University Medical Center, on July 26, 1955. Five weeks before admission, her parents noted enlargement of the right arm and forearm. Before that, she was in good health, ate well, and grew satisfactorily.

Physical Examination. The right upper extremity was somewhat larger than the left, but was not increased in length. There was a faint pink discoloration; no cyanosis was noted. A soft swelling occupied the pectoral region and the axilla on the right side. The swelling appeared to increase with crying. No definite mass could be palpated. There was no limitation of motion of the arm and no pain. The axillary and brachial pulses were equal on both sides. The femoral and aortic pulses were good. Examination of the chest and abdomen showed no other abnormalities.

Laboratory Studies. The hemogram and urinalysis were normal. A posteroanterior roentgenogram of the chest revealed deformity of the right first rib, which was fused with the second rib anteriorly at about the junction of the rib and the costal cartilage. The possibility of venous or lymphatic stasis secondary to the rib abnormality was considered. A venogram revealed no obstruction of the circulation.

Clinical Course. Operative exploration of the affected region demonstrated a diffuse tumor in the subcutaneous tissue of the anterior part of the thorax, the areolar tissue of the right axilla, and the right supraclavicular area. As much of this tissue as possible was removed. Another mass, which was fairly well encapsulated, was found surrounding the brachial artery and vein and the cords of the brachial plexus. This was dissected free without injuring the adjacent structures. The postoperative course was uneventful. There had been no recurrence of the lesion on February 7, 1958.

Pathologic Examination

The specimen (I.U. # 77452) consisted of two masses measuring 4.5 by 3 by 1.5 cm. and 7 by 5 by 3 cm. The tissue was composed of numerous small, soft, pale gray lobules, most of which were several millimeters in diameter; some were as large as 1 cm. Portions of the lesions were myxomatous. The cut surface was greasy.

Histologically, a lobular pattern was evident, the lobules being joined by loose connective tissue. The lesion was richly vascular, and each lobule had its major vessel which arborized in a plexiform manner (Fig. 1). Many of the cells were vacuolated, and in some of these there was a large single vacuole displacing the nucleus against the cytoplasmic membrane. Smaller cells were multivacuolated and contained more centrally placed, round nuclei (Fig. 2). In such cells a moderate amount of granular eosinophilic cytoplasm intervened be-

tween the vacuoles. The vacuoles proved to be sudanophilic in frozen sections of formalin-fixed tissue.

In some sites, spindle-shaped and stellate cells lay in an abundant pale-staining stroma. These appeared more frequently at the periphery of the lobules (Fig. 1), and in some marginal lobules the entire content was of this nature.

Although the histologic appearance of the lesion resembled myxoid liposarcoma, its lobular arrangement, circumscription, and the absence of invasion into surrounding tissues served to distinguish it from this neoplasm. The lobulated pattern of the tumor simulated that seen in hibernoma, but differed in that there were numerous spindle-shaped and few polyhedral cells with granular, eosinophilic cytoplasm.

Embryology of Adipose Tissue

Material

Thirteen human fetuses in good state of preservation were studied. Eleven were specimens procured from spontaneous abortions, one was the product of a premature stillbirth delivery, and one was a full-term, stillborn infant. Four fetuses were 10 cm. or less in crown-to-heel length; one was 13.5 cm., two were 20 cm., two were 23 cm., and one each was 27 cm., 28 cm., 41 cm., and 48 cm. Specimens were fixed in neutral formalin. Sections of tissues from various sites were examined, especially samples from the axillary, interscapular, and mediastinal regions, the perirenal area, the buccal fat pad, and subcutaneous tissues in various sites. Paraffin sections were prepared with hematoxylin and eosin, Mayer's mucicarmine, and Alcian blue-periodic acid-Schiff stains. Frozen sections of some specimens were stained with Sudan IV.

Observations

No significant differences were evident in the mode of formation of adipose tissue in the various sites. However, fat appeared earlier in some locations than in others. The sites of earliest appearance were the subcutaneous region, the buccal fat pad, and the axilla. Adipose tissue in the mediastinum and retroperitoneal regions made its appearance and matured later.

The first change detectable histologically was the appearance of capillaries in relatively acellular primitive mesenchyme (Fig. 3). This was seen earliest in the subcutaneous tissues of some, but not all, fetuses of about 9 cm. crown-to-heel length. Plump, spindle-shaped and stellate cells were found adjacent to the capillaries. These cells had large nuclei and well defined, somewhat basophilic cytoplasm.

Vacuoles were difficult to identify in hematoxylin and eosin preparations, but with Sudan IV stain, minute, sudanophilic cytoplasmic vacuoles were noted. In these regions in older fetuses, very vascular lobules were present (Figs. 4 to 6), each surrounded by compressed mesenchyme. The entire mass of lobules comprising the buccal fat pad was invested by a dense capsule (Fig. 6).

In fetuses 20 cm. in length, the adipose tissue was well defined. The vascularized lobules were relatively cellular. Some of the cells were spindle shaped; others had multiple small vacuoles; still others contained a few larger vacuoles, and many contained one large vacuole with the nucleus displaced to one side. The latter were the most abundant elements present. Multivacuolated cells were uncommon.

In the fetuses 23 to 28 cm. in length, fat tissue was well established. Lobules appeared in the gross as small flecks of yellow in myxomatous stroma. This was the case in the buccal, mediastinal, axillary, and retroperitoneal regions where the yellow aggregates were limited by delicate membranes. Isolated lobules of fat were found developing in the mesenchyme between muscle bundles, but these were not visible grossly. Histologically, the adipose tissue at this age was clearly lobulated, and the lobules now abutted on one another. The cells were mostly univacuolated, signet-ring forms. At the periphery of the lobules, the cells were occasionally moruloid or lacked detectable vacuoles in hematoxylin and eosin stained preparations. This arrangement suggested that the cells at the periphery of lobules and at some distance from the larger vascular branches were younger in point of development. The adipose tissue at this age was still recognizably richly vascular and possessed an organoid pattern.

In later stages of development, fat was recognizable grossly as gray or yellow lobulated tissue. In various areas it extended by insinuating itself into crevices between other supporting structures (muscle), in this respect resembling the growth of capillary hemangiomas of infancy. Eventually the various collections of adipose tissue joined to form continuous masses.

The microscopic appearance of the fat in the 41 cm. and 48 cm. fetuses varied in appearance in different areas, but the lobular pattern was manifest. In the buccal fat pad and in most of the subcutaneous tissue, it was composed of fully developed fat cells, each with only one large vacuole. Much of the adipose tissue in the axillary, mediastinal and retroperitoneal regions, however, was composed of fat cells with multiple vacuoles and abundant intervacuolar eosinophilic granular cytoplasm (Figs. 9 and 10). The nuclei were centrally placed. These cells resembled the brown fat of lower animals.

Discussion

A survey of fetal tissues indicates that fat is a specialized substance derived from lipoblasts which, in turn, arise from perivascular mesenchyme. Wasserman[10] considered the lipoblast to be closely allied to the reticuloendothelial system and especially to the hematopoietic organ. Stout[11] cautioned that it was safer to regard the lipoblast as a fat-forming mesenchymal cell which could on occasion produce a wide variety of different and complex tissues.

Our observations indicate that adipose tissue in the human fetus develops in similar fashion in various locations, but that in the axillary, mediastinal, and retroperitoneal areas it does not attain adult form at the time of birth. The manner of maturation in the various sites is in accord with the description of the development of the buccal fat pad recorded by Scammon.[12] This author pointed out that early growth consisted of the expansion of enclosed mesenchymal and pre-adipose tissues; later growth was principally by increase in fat content. The latter included increase in number of fat lobules, formation of new fat cells, and growth of individual fat cells. According to Scammon, the formation of lobules in the buccal fat pad ceased by the fifth fetal month, at which time there were between 250 and 350 lobules. He felt that formation of new fat cells in this region ceased in later fetal life, usually by the seventh fetal month.

Whether lobules continue to develop in other sites in the late fetal and postnatal periods is not clarified by our study. It seems reasonable to suppose that a halt in the development of new lobules occurs in this period but that lipoblasts continue to be formed. The lesion in our case appears to have resulted from continued proliferation not only of lipoblasts but also of new lobules of adipose tissue in the postnatal period.

The case reported by Van Meurs[13] as an embryonic lipoma is similar to ours. Van Meur's patient was a 5-month-old child who had 4 recurrences of the lesion during 20 months following repeated excisions. All 5 of the specimens were similar, but with later operations, the tumor assumed the appearance of mature adipose tissue, a feature which the author considered a transformation of an embryonic lipoma to a common lipoma.

The case reported by Cox[2] as a hibernoma may be another example of this type of lesion. This was a 6-week-old male infant who died from asphyxiation due to the tumor in the neck. The author noted the similarity of the lesion to immature fat and considered it to be a hibernoma because of the presence of cells with eosinophilic granular cytoplasm. The illustrations in this report are difficult to evaluate. It

is notable, however, that other recorded instances of hibernoma occurred in adults.[2,8,14-18]

We suggest that the hibernoma is a tumor of fat cells in which the enzyme systems are incompletely developed. This differs from lipoblastomatosis, essentially a tumor of embryonic adipose tissue.

Summary

An unusual tumor of embryonal fat tissue, designated lipoblastomatosis, is reported. This lesion appeared as a soft mass in the subcutaneous tissues of the anterior wall of the thorax and the areolar tissue of the axilla and supraclavicular regions of an 8-month-old girl. It was not encapsulated but infiltrated the area diffusely. It was composed of distinct lobules of embryonal adipose tissue; the fat content of the component cells varied. The tumor had not recurred after 30 months and was presumed to be benign.

A study of the embryogenesis of adipose tissue in human fetuses was undertaken in the light of this unusual neoplasm. Adipose tissue was first recognizable at certain locations in embryos at about 9 cm. in crown-to-heel length. Formation of fat lobules apparently ceases in the late fetal or early postnatal period, although formation of individual lipoblasts may continue. Fat cells in the axillary, mediastinal, and retroperitoneal regions may not attain adult form at the time of birth. Lipoblastomatosis apparently results from continued proliferation of lipoblasts and of new lobules of adipose tissue in the postnatal period.

References

1. Wells, H. G. Adipose tissue, a neglected subject. *J.A.M.A.*, 1940, 114, 2177–2183; 2284–2289.
2. Cox, R. W. "Hibernoma": the lipoma of immature adipose tissue. *J. Path. & Bact.*, 1954, 68, 511–518.
3. Murray, M. R., and Stout, A. P. Characteristics of a liposarcoma grown in vitro. *Am. J. Path.*, 1943, 19, 751–763.
4. Shaw, H. B. A contribution to the study of the morphology of adipose tissue. *J. Anat. & Physiol.*, 1902, 36, 1–13.
5. Hatai, S. On the presence in human embryos of an interscapular gland corresponding to the so-called hibernating gland of lower mammals. *Anat. Anz.*, 1902, 21, 369–373.
6. Bonnot, E. The interscapular gland. *J. Anat. & Physiol.*, 1908–1909, 43, 43–58.
7. Rasmussen, A. T. The so-called hibernating gland. *J. Morphol.*, 1923, 38, 147–193.
8. Inglis, K. The so-called interscapular gland and tumours arising therein. *J. Anat.*, 1927, 61, 452–466.
9. Remillard, G-L. Histochemical and microchemical observations on the lipids of the interscapular brown fat of the female vespertilionid bat *Myotis lucifugus*. *Ann. New York Acad. Sc.*, 1958, 72, 1–68.

10. Wassermann, F. Die Fettorgane des Menschen. Entwicklung Bau und systematische Stellung des sogenannten Fettgewebes. *Ztschr. f. Zellforsch. u. mikr. Anat.*, 1925–1926, **3**, 235–328.

11. Stout, A. P. Liposarcoma—the malignant tumor of lipoblasts. *Ann. Surg.*, 1944, **119**, 86–107.

12. Scammon, R. E. On the development and finer structure of corpus adiposum buccae. *Anat. Rec.*, 1918–1919, **15**, 267–287.

13. Van Meurs, D. P. The transformation of an embryonic lipoma to a common lipoma. *Brit. J. Surg.*, 1947, **34**, 282–284.

14. Brines, O. A., and Johnson, M. H. Hibernoma, a special fatty tumor; report of a case. *Am. J. Path.*, 1949, **25**, 467–479.

15. Kittle, C. F.; Boley, J. O., and Schafer, P. W. Resection of an intrathoracic "hibernoma." *J. Thoracic Surg.*, 1950, **19**, 830–836.

16. Sieber, W. K., and Heller, E. L. Hibernoma; unusual location in popliteal space. *Am. J. Clin. Path.*, 1952, **22**, 977–980.

17. Sutherland, J. C.; Callahan, W. P., Jr., and Campbell, G. L. Hibernoma: a tumor of brown fat. *Cancer*, 1952, **5**, 364–368.

18. Gross, S., and Wood, C. Hibernoma. *Cancer*, 1953, **6**, 159–163.

The authors are indebted to Dr. Arthur Purdy Stout for reviewing the case and for helpful comments on the manuscript. The histologic material was prepared by Mr. Antonio R. Villanueva, and the photomicrographs were prepared by Messrs. James F. Glore and Paris Johnson.

[*Illustrations follow*]

LEGENDS FOR FIGURES

All sections shown in the figures were stained with hematoxylin and eosin.

FIG. 1. Cells at the periphery of the tumor are immature, and those near the vascular pedicle contain large solitary vacuoles. × 100.

FIG. 2. A portion of the tumor in which almost all of the cells contain fat vacuoles of varied size. Some are multivacuolated. × 600.

FIG. 3. The earliest recognizable lobule of adipose tissue, in the subcutaneous tissue of an 8.5 cm. fetus. Some of the cells contain fat, demonstrable with Sudan IV, but not visible here. × 300.

FIG. 4. Adipose tissue in the subcutaneous tissue of a 20 cm. fetus. Some of the cells are vacuolated. × 150.

FIG. 5. Adipose tissue in the perinephric region of a 20 cm. fetus. × 150.

2

4

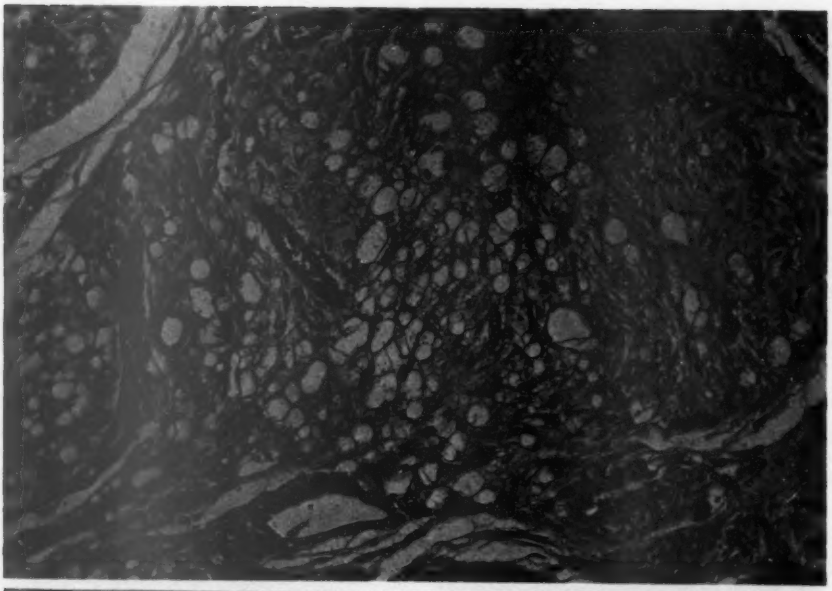

1

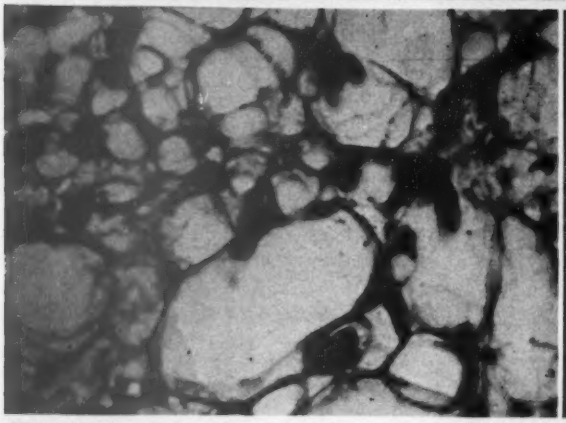

2

3

4

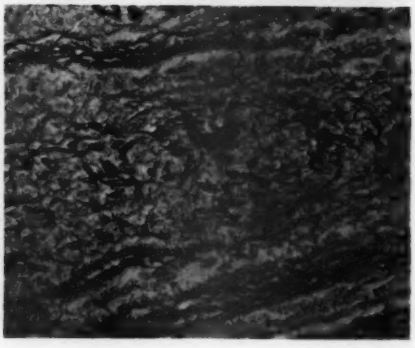

5

FIG. 6. Embryonal adipose tissue in the buccal fat pad of a 27 cm. fetus. Note the vascularity of the lobules. × 150.

FIG. 7. Adipose tissue in the buccal fat pad of a 23 cm. fetus. × 600.

FIG. 8. Adipose tissue in the perinephric region of a 28 cm. fetus. Note that it is not as well developed as that shown in Figure 7 from the buccal fat pad of a younger fetus. × 600.

FIG. 9. Axillary adipose tissue of a 41 cm. fetus. Cells contain multiple vacuoles separated by eosinophilic, granular cytoplasm. × 150.

FIG. 10. Adipose tissue in the perirenal region of a 48 cm. fetus. Many of the cells are multivacuolated, but the cytoplasm of a few is nonvacuolated and deeply eosinophilic. × 725.

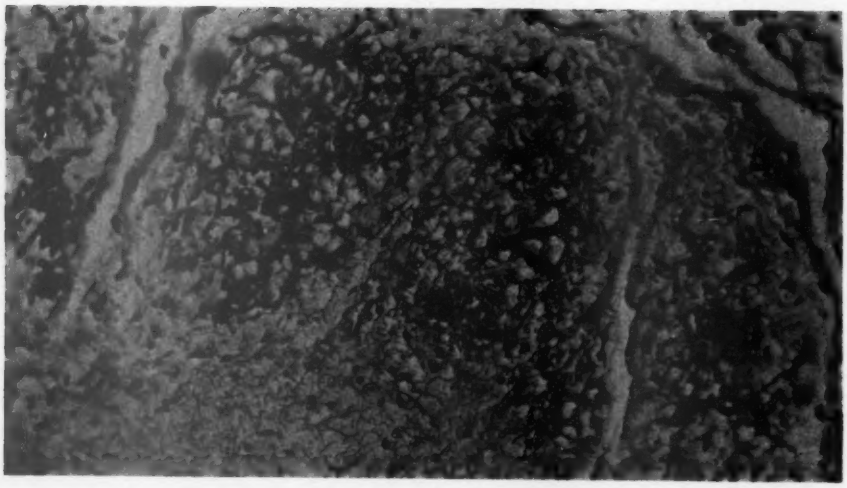

6

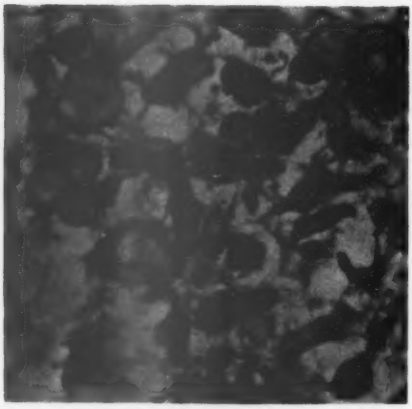

7

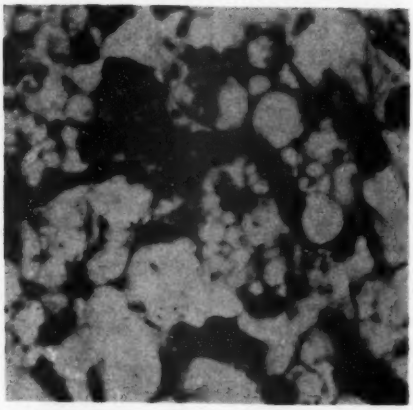

8

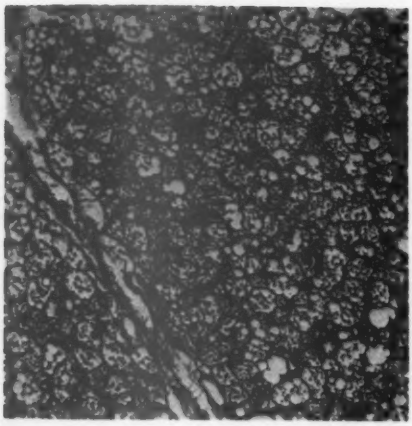

9

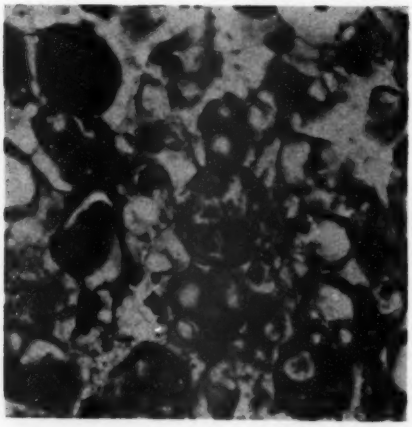

10

THE DIFFUSE ADRENAL LESION IN CUSHING'S DISEASE

Histologic Observations on Surgically Removed Adrenals in Four Cases *

C. T. Ashworth, M.D., and R. F. Garvey, M.D.

From the Departments of Pathology and Surgery, The University of Texas Southwestern Medical School, Dallas, Texas.

In spite of numerous observations on the clinical and physiologic aspects, and upon the pituitary lesions in Cushing's disease, the adrenal lesions have, from a pathologic standpoint, not been described in detail.[1] In most reports[2-4] the adrenals have been noted to contain an adenoma or carcinoma of the cortex, to be the seat of adenomatous hyperplasia, or to be of normal structure. The morphologic features of adenomatous hyperplasia in this disease have received only brief comment in case reports.

Since clinical and physiologic considerations indicate that the manifestations are largely those of hyperadrenocorticalism,[5] one would expect to find alterations in the adrenal cortex regularly. Examination of adrenal specimens from the 4 patients presented here revealed consistent and characteristic cortical changes of a diffuse nature. It is our purpose to describe these and to consider, insofar as possible, their apparent relationship to accepted principles of adrenocortical function. It appears that at least 60 per cent of patients with Cushing's disease have diffuse adrenal alterations while the remainder probably have an adenoma or a carcinoma of the cortex.[1] The structure of tumors of the cortex and their relationship to hyperadrenocorticalism have been well described, and are not the subject of this report.

Report of Cases

Case 1

A 44-year-old white female was seen on April 28, 1957. There was a 3 month history of increased facial hair, swelling of the feet and ankles, and marked fatiguability. She had also noted swelling of the face and abdomen and complained of low back pain.

Blood pressure was 170/110. There were moon facies, slight pedal edema, and a distribution of adipose tissue characteristic of Cushing's syndrome. Generalized purpura, with petechiae and ecchymoses, were found. There was dorsal kyphosis, and tenderness was noted over T8 and T9. The abdomen was protuberant, but no striae were seen.

The hemoglobin level was 12.4 gm. per 100 cc., and the blood urea nitrogen was 14 to 21 mg. Serum sodium value was 145 mEq/l; the serum potassium varied from 3.1 to 3.7 mEq/l. CO_2 was 28 mEq/l. A diabetic type of glucose tolerance curve was found. The blood eosinophils varied from 0 to 11 per mm.^{3} in the

* Received for publication, April 9, 1958.

fasting state. The urinary excretion of 17-ketosteroid ranged from 14.7 mg. to 29 mg. per 24 hours. A roentgenogram revealed 3 compression fractures of thoracolumbar vertebrae.

Radiation therapy was administered over the pituitary region. Because of rising blood pressure and blood urea nitrogen, however, a bilateral adrenalectomy was performed. Cortisone administration was begun approximately 24 hours before operation.

Case 2

A 26-year-old white female had increasing growth of hair on the face, pubic region, and extremities for two years. For 18 months menses had been very irregular and progressively scanty. She had gained 100 pounds in weight during the preceding 6 years. Decreased libido and increasing weakness had also been noted.

Blood pressure was 140/90. A buffalo hump type of obesity was observed. There were large purple striae in the skin of the abdomen, thighs and breasts. An acneiform eruption of the face was present.

The urinary 17-ketosteroid excretion varied from 29 to 36 mg. per 24 hours. The level fell to 15 mg. after 5 days of treatment with Meticorten.® The glucose tolerance test was normal.

Temporary improvement followed irradiation of the pituitary area. Later, there was evidence of increasing hair growth. Excretion of 17-ketosteroids again rose to abnormal levels, and moon facies became manifest. Bilateral adrenalectomy was then performed; cortisone therapy was instituted 24 hours prior to operation.

Case 3

A 20-year-old white female complained of weakness, acneiform eruption of the face, arms, chest and back, low back pain and amenorrhea. She had had a thyroidectomy two years previously for Graves's disease.

There were truncal obesity and moderate dorsal kyphosis. A severe acneiform eruption was observed. The pubic hair had a male distribution, and there was considerable growth of hair about the face. Blood pressure was 126/82.

Excretion of 17-ketosteroids varied from 23 to 28 mg., and 17-hydroxycorticosteroids ranged from 9 to 12 mg. per 24 hours. The 17-ketosteroid level fell to 11 mg. per 24 hours after the administration of fluorohydroxycortisone.

A bilateral adrenalectomy was performed.

Case 4

A 34-year-old white male exhibited obesity, hypertension, abdominal striae, and skin pigmentation in 1951. There were signs of mild cardiac failure and evidences of an old myocardial infarction. Clinical studies indicated Cushing's syndrome, and a subtotal left adrenalectomy was performed. This was followed by pituitary irradiation, but no change in the patient's status ensued. Thereupon, bilateral subtotal adrenalectomy was performed with some amelioration of symptoms. Adrenal insufficiency was controlled by cortisone administration.

During 1956 and 1957 the patient developed a recurrence of obesity with buffalo hump distribution, hypertension, skin pigmentation, and the 17-ketosteroid excretion increased to 24 mg. per 24 hours. Symptoms of mild cardiac failure with shortness of breath and ankle edema reappeared. Additional pituitary irradiation was given without benefit. Blood sugar level was found to be elevated, and the blood urea nitrogen was also slightly increased.

Abdominal exploration was then done, and about 10 gm. of nodular, yellowish tissue was removed from the retroperitoneal area. This had bilateral location and was near the original sites of the adrenals. Microscopic examination demonstrated the substance removed to be adrenocortical tissue which was markedly hyperplastic. The adrenal glands removed in 1951 were also available for study.

Post-operatively the 17-ketosteroid excretion fell to 3 to 7 mg. per 24 hours.

Observations on the Adrenal Glands

Because of the basic similarity of the gross and histologic abnormalities of the adrenal glands in these 4 cases, a composite description and discussion of the findings will be given. The specimens were compared with sections of normal adrenals removed surgically in the treatment of mammary carcinoma, and with necropsy material from patients who had died suddenly or rapidly with no known preceding disease.

The adrenals in the cases of Cushing's disease were found to be only slightly, though diffusely enlarged. None contained large adenomas or other evidence of tumor. The combined weights of the two glands in each case varied from 11 to 19 gm. Cortical architecture was maintained, and in most instances the pattern was considered to be normal at first glance. Further study, however, revealed some thickening of the cortex, which measured from 2 to 3 mm. (Fig. 1). The outer portion was bright yellow, while the inner portion was brownish-yellow. In some glands the outer yellow area was less prominent, and the darker, brownish-yellow portion seemed to comprise most of the thickness of the cortex. Contrary to most recorded observations, there was only slight nodularity, and certainly in 3 of the cases the term adenomatous hyperplasia would not be considered descriptive of their gross appearance. The medullas were not remarkable.

Microscopically there was moderate cortical thickening, involving especially the zona fasciculata. The cell cords in this region were thicker than normal, but the sinusoids remained patent. A very noticeable feature was the division of the zona fasciculata into two portions: a deeper zone composed of large, granular cells which stained darker with hematoxylin and eosin, and an outer zone of large, clear, pale-staining cells, containing a marked excess of lipid droplets. These were in contrast with cells of the fasciculata in the normal gland (Figs. 2, 3 and 4). The zones varied in thickness and prominence in different cases as well as in different portions of the same gland. The junction between the clear and the granular cortical cells was usually very sharp, with almost abrupt transition of the cell types. It was apparent, however, that the alteration affected cell cords of both the fasciculata and reticularis. The granular cell zone varied from one third to as much as three fourths of the entire thickness of the cortex.

The granular, dark-staining cells were characterized by abundant cytoplasm (Fig. 5). Lipid droplets were demonstrated by Sudan black, Nile blue sulphate, and oil red O stains. These were distinctly fewer than in the outer, clear-staining cells, and were also less prominent than in cells of the fasciculata of normal adrenals. The cells were characterized by increased cytoplasmic granularity and were relatively

opaque. The clear-staining cells in the outer portion of the fasciculata contained very little cytoplasmic granulation in comparison (Fig. 6). The lipid droplets were more numerous, more clearly demarcated, and seemed to be larger than those in the granular cell zone. The cytoplasmic membrane was thickened and appeared considerably more prominent than in the case of normal cortical cells and the granular cells of the zona fasciculata.

The zona glomerulosa was of particular interest. In many areas it was difficult to differentiate the zona glomerulosa from the zona fasciculata, but the reticulum stain was helpful in making this distinction (Fig. 4). The glomerulosa was often completely missing, and the lipid-filled, clear-staining cells of the fasciculata seemed to extend all the way to the capsule. Usually, however, the glomerulosa was still present but atrophic (Fig. 7). In some instances the cells of the glomerulosa appeared to be distended with lipid and resembled the clear staining cells of the outer fasciculata. The remnant of glomerulosa was usually quite small, and the cells themselves were decreased in size. They appeared to be distorted and focally were compressed by the swollen elements of the fasciculata so that their long axes were parallel to the capsule.

The zona reticularis was not markedly altered in appearance. In some regions it was difficult to differentiate it from the fasciculata, and the two zones appeared to be continuous (Fig. 4). The cells of the zona reticularis contained abundant cytoplasmic granules. There were few lipid droplets, and in general they resembled the granular cells of the deeper portion of the fasciculata (Fig. 8). Lipochrome pigment was somewhat increased in the reticularis cells. There also appeared to be a deposit of lipochrome pigment in some of the cells in the deeper portion of the fasciculata.

Although adenomatous nodules were not grossly manifest in 3 of the glands, adrenals in all cases contained several collections of cells in the fasciculata arranged in micronodular fashion on microscopic examination (Fig. 9). These foci measured up to 2 mm. in diameter. They were not encapsulated but were continuous with the surrounding cortical cell cords. In some of the nodules, the outer portions were comprised of large clear cells, while the deeper portions were composed of granular, dark-staining cells. As in the non-nodular portions of the cortex, the dividing line between these two zones was usually very distinct. Some of the cells in the nodules were hypertrophied. Their nuclei were hyperchromatic, larger than normal, and were considered indicative of polyploidy. An increased number of binucleated cells was observed, but there were no mitotic figures. Similar nuclear

changes were also encountered in the non-nodular portions of the cortex.

In the adrenocortical tissue removed from the retroperitoneal region after previous bilateral adrenalectomy in case 4, irregular collections of large, dark-staining cells and a few groups of clear, foamy cells were observed (Fig. 10).

In some of the glands there were infiltrations of small round cells resembling lymphocytes and plasma cells, and a few groups of large fat droplets similar to those described in fatty metamorphosis of the adrenal cortex abnormally stimulated by corticotropin.[6]

Discussion

There is a considerable similarity between the alterations observed in the adrenals of Cushing's disease and those produced by continued administration of adrenocorticotropic hormone, or noted in reactions to stress.[6,7] The occurrence of a prominent layer of large, dark-staining, granular cells in the zona fasciculata is particularly suggestive of corticotropin stimulation. However, the atrophic changes in the zona glomerulosa, the ballooned appearance of clear-staining cells in the outer part of the zona fasciculata, and the distinct dividing line between the clear and granular cells have not been described in association with corticotropin administration. These differences suggest that additional factors may contribute to the structural alterations observed in these cases.

A relationship between the concentration of sodium in the extracellular fluid, and the status of the zona glomerulosa has been demonstrated.[8-10] On this basis, overactivity of the adrenal cortex in Cushing's disease might lead to hypernatremia of such a degree as to cause decreased function and atrophy of the zona glomerulosa. On the other hand, the administration of corticotropin to monkeys does not produce any detectable change in the glomerulosa.[11] It is possible that atrophy of the glomerulosa might be due simply to compression by the markedly swollen cells of the outer portion of the fasciculata.

It is surmised that the granular cells in the inner, dark-staining zone are engaged in increased functional activity and elaboration of cortical hormones, while those of the outer, clear zone are in a state of lipid storage and decreased hormone synthesis. Cortisone will induce lipid storage and clarity of staining in adrenocortical cells,[12] although this would not appear to explain the zonation of clear-staining and granular cells. The patients in this study had received cortisone for an average of one day prior to adrenalectomy. Since we have not examined adrenal glands from patients with Cushing's disease, removed without

prior cortisone administration, an interpretation of the clear-staining cells in the outer zona fasciculata cannot be given at this time.

Failure of the adrenal cortex to convert 17-hydroxyprogesterone to 17-hydroxycorticosterone, resulting in the lack of pituitary inhibition by the latter, has been suggested as the primary disturbance accounting for the adrenogenital syndrome.[13] A similar type of defect might exist in the adrenal cortex in Cushing's disease. Since the clear-staining cells in the outer portion of the zona fasciculata appear to be in a state of diminished functional activity, it seems possible that this, or the atrophy of the glomerulosa, could induce a similar deficiency in production of a pituitary inhibitory substance. This mechanism could also explain the occasional occurrence of basophil adenoma and basophil hyperplasia of the pituitary in Cushing's disease, and probably parallels the appearance of mammotropic and adrenotropic pituitary adenomas following experimental ablation of the thyroid.[14] On the other hand, a primary pituitary or hypothalamic basis for the adrenotropic activity in Cushing's disease has certainly not been disproved.

It seems feasible at this time to locate the adrenal lesion of Cushing's disease, at least in part, in the fasciculata. There is evidence of hyperactivity of the cortical cells as well as an unexplained increase in lipid storage and an apparent decrease of cellular activity in the outer portion of the fasciculata. This is, to some degree, in accord with the concept of functional zonation[9] of the adrenal cortex. Since it appears most likely that cells of the glomerulosa produce aldosterone,[15] adenomas or hyperplasia of the glomerulosa might be expected to be the basis for hyperaldosteronism. The lesion responsible for the adrenogenital syndrome has been related to the zona reticularis.[16]

Summary

The adrenal glands removed from 4 patients with Cushing's disease exhibited a zone of large, clear-staining cells in the outer portion of the zona fasciculata, while the deeper portions of the fasciculata were composed of granular cells. These alterations were thought to be indicative of increased adrenocorticotropic stimulation with increased adrenocortical hormone synthesis. The zona glomerulosa was found to be atrophic and, in many areas, completely absent. This was interpreted to be compatible with a reduction in the normal inhibitory effect of adrenocortical hormone upon the pituitary, resulting, in turn, in an increased adrenocorticotropic effect. Since the patients had received cortisone prior to surgery, it was considered possible that increased lipid content of the cells in the outer portion of the fasciculata was attributable to this therapy.

REFERENCES

1. Cope, O., and Raker, J. W. Cushing's disease. The surgical experience in the care of 46 cases. *New England J. Med.*, 1955, **253**, 119–127; 165–172.
2. Hare, D. C.; Ross, J. M., and Crooke, A. C. Cortical carcinoma of the suprarenal with Cushing's basophil pituitary syndrome. *Lancet*, 1935, **2**, 118–122.
3. Calder, R. M., and Porro, F. W. Adenoma of adrenal cortex simulating pituitary basophilism (Cushing's syndrome). *Bull. Johns Hopkins Hosp.*, 1935, **57**, 99–110.
4. Forbus, W. D. Reaction to Injury. Pathology for Students of Disease. Williams & Wilkins Co., Baltimore, 1952, Vol. II, p. 493.
5. Albright, F.; Parson, W., and Bloomberg, E. Cushing's syndrome interpreted as hyperadrenocorticism leading to hypergluconeogenesis; results of treatment with testosterone propionate. *J. Clin. Endocrinol.*, 1941, **1**, 375–384.
6. Selye, H., and Stone, H. On the Experimental Morphology of the Adrenal Cortex. Charles C. Thomas, Springfield, Ill., 1950, 105 pp.
7. Symington, T.; Duguid, W. P., and Davidson, J. N. Effect of exogenous corticotropin on the histochemical pattern of the human adrenal cortex and a comparison with the changes during stress. *J. Clin. Endocrinol.*, 1956, **16**, 580–598.
8. Greep, R., and Deane, H. Cytology and cytochemistry of adrenal cortex. *Ann. New York Acad. Sc.*, 1949, **50**, 596–615.
9. Race, G. J.; Nickey, W. M.; Wolf, P. S., and Jordan, E. J. Studies on functional zonation of the adrenal cortex. *A.M.A. Arch. Path.*, 1957, **64**, 312–323.
10. Sarason, E. L. Morphological changes in the rat's adrenal cortex under various experimental conditions. *Arch. Path.*, 1943, **35**, 373–390.
11. Knobil, E.; Morse, A., and Greep, R. O. The morphological autonomy of the zona glomerulosa of the adrenal cortex in the rhesus monkey. (Abstract) *Anat. Rec.*, 1955, **121**, 324.
12. O'Donnell, W. M.; Fajans, S. S., and Weinbaum, J. G. Human adrenal cortex after administration of ACTH and cortisone. *A.M.A. Arch. Int. Med.*, 1951, **88**, 28–35.
13. Jailer, J. W. Virilism. *Bull. New York Acad. Med.*, 1953, **29**, 377–394.
14. Furth, J., and Clifton, K. H. Experimental pituitary tumors and the role of pituitary hormones in tumorigenesis of the breast and thyroid. *Cancer*, 1957, **10**, 842–853.
15. Gaunt, R.; Renzi, A. A., and Chart, J. J. Aldosterone—a review. *J. Clin. Endocrinol.*, 1955, **15**, 621–646.
16. Blackman, S. S. Concerning the function and origin of the reticular zone of the adrenal cortex. *Bull. Johns Hopkins Hosp.*, 1946, **78**, 180–217.

The photographs were prepared by Mr. Robert Sage of the Medical Art Department, The University of Texas Southwestern Medical School.

[*Illustrations follow*]

LEGENDS FOR FIGURES

FIG. 1. Adrenals from cases 1, 2, and 3. These reveal a moderate, diffuse, cortical thickening with an increased prominence of the brown cortical zone in cases 2 and 3, and very little gross evidence of an adenomatous nodular configuration. Hemorrhage in the medulla of the adrenal of case 1 is due to injury incident to surgical removal.

FIG. 2. Adrenal cortex in case 1. The zona glomerulosa is markedly atrophic while the zona fasciculata is thickened. The division of the fasciculata into outer, clear cells and inner, granular, dark-staining cells is well seen. Hematoxylin and eosin stain. × 72.

FIG. 3. Adrenal cortex in case 3. The cells of the zona glomerulosa are atrophic and seemingly compressed. In this area the granular cell layer of the zona fasciculata comprises most of the thickness of the cortex. Hematoxylin and eosin stain. × 55.

FIG. 4. Adrenal cortex in case 2, stained with reticulum stain. The atrophic zona glomerulosa is apparent. It is noted that most of the granular cell zone is in the deeper portion of the zona fasciculata, although the zona reticularis cells are continuous with the cells of the fasciculata. × 68.

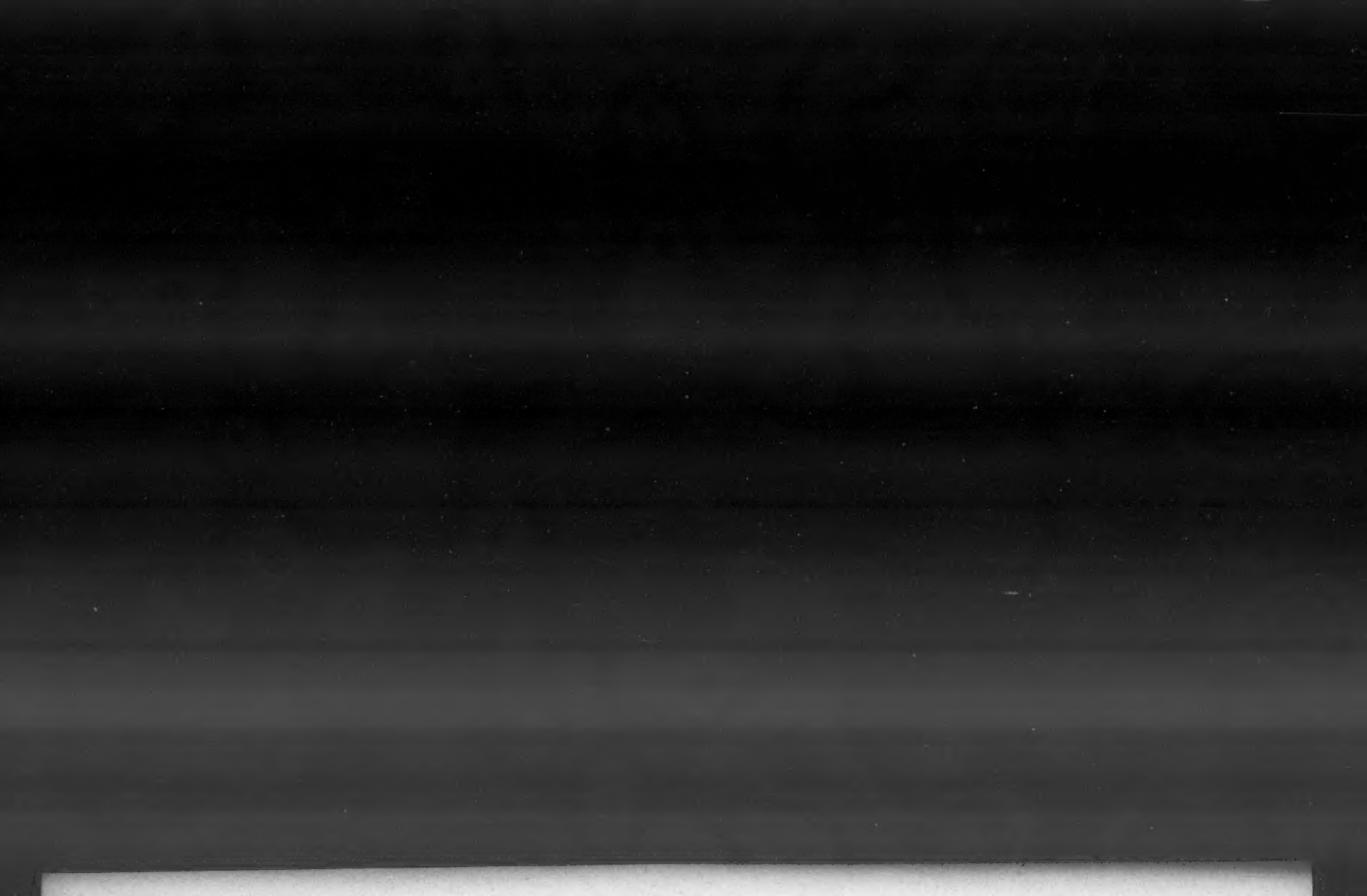

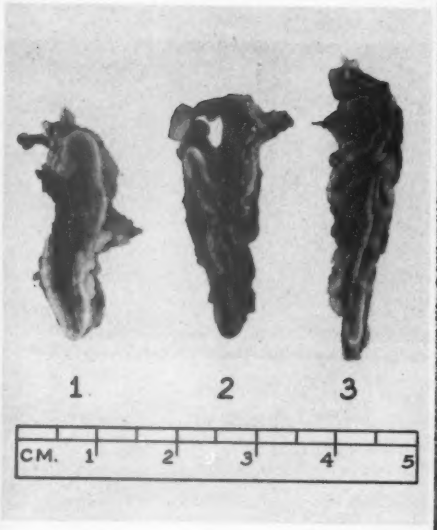

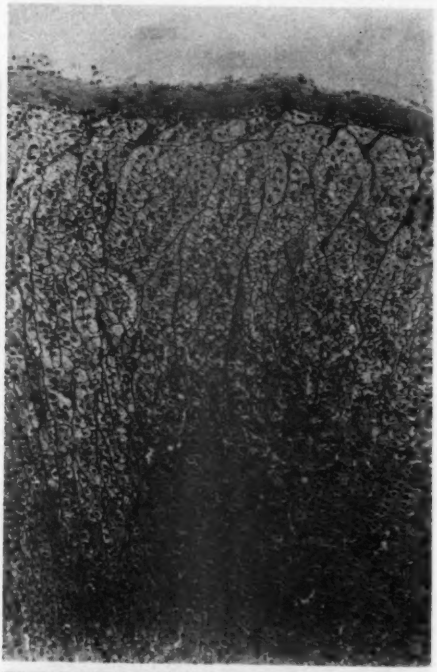

2

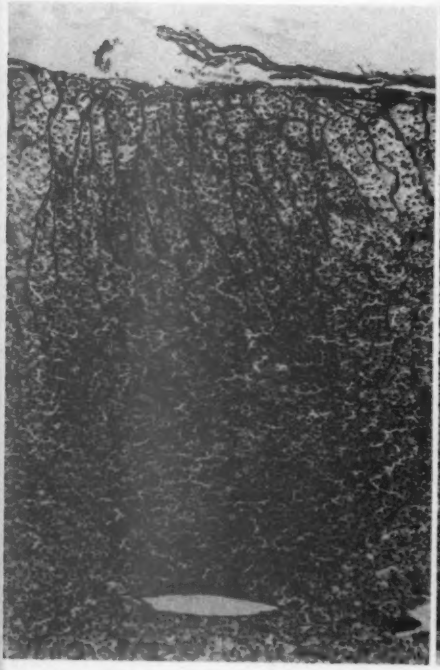

4

FIG. 5. Granular cells of the zona fasciculata in case 1. There is a marked reduction in the lipid droplets, and the cytoplasmic granular material is increased. Hematoxylin and eosin stain. × 350.

FIG. 6. In the outer, clear cells of the zona fasciculata (case 1), lipid droplets fill the cytoplasm, and the cytoplasmic granular material seems to be reduced. Hematoxylin and eosin stain. × 350.

FIG. 7. Zona glomerulosa, showing atrophic cells with small cytoplasmic mass. Scanty lipid material is present, and cytoplasmic granules are not prominent. Hematoxylin and eosin stain. × 350.

FIG. 8. Cells of the zona reticularis in case 2. These cells contain abundant cytoplasmic granular material, do not show atrophy as in the normal zona reticularis, and are quite similar to the cells of the deeper portion of the zona fasciculata. Hematoxylin and eosin stain. × 350.

FIG. 9. Adrenal cortex in case 1, showing a micronodule containing large granular cells of the fasciculata mainly, but small foci of clear cells may be seen also. Hematoxylin and eosin stain. × 55.

FIG. 10. Adrenocortical tissue removed from retroperitoneal area at second operation in case 4. Many large granular cells and a few clear cells resembling zona fasciculata may be seen. Hematoxylin and eosin stain. × 55.

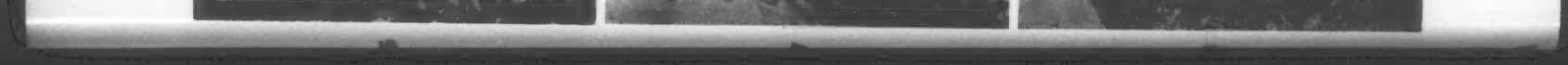

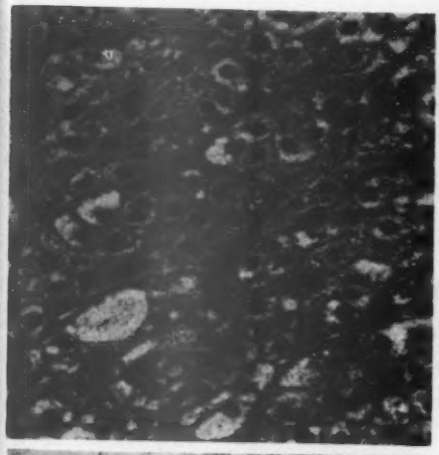

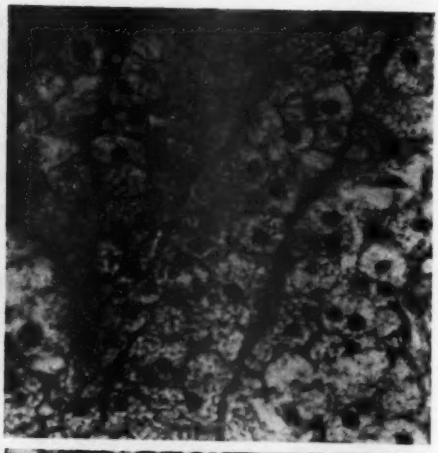

6

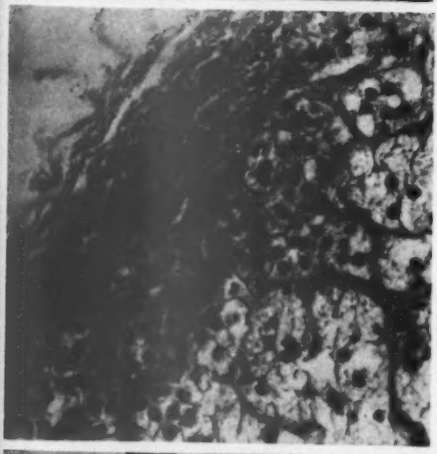

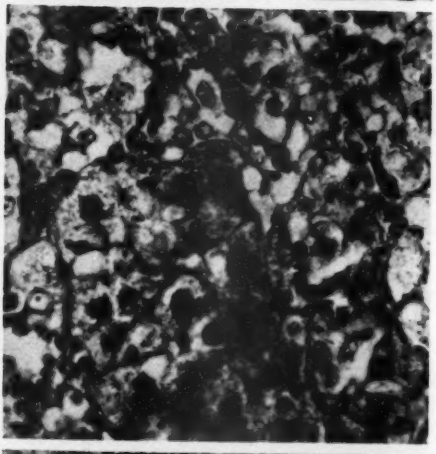

8

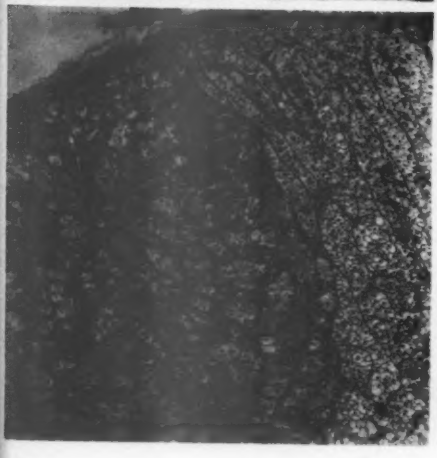

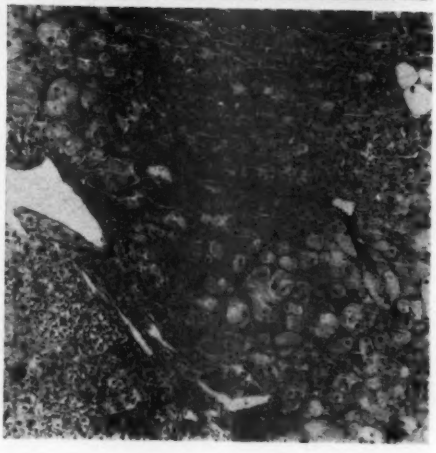

10

THE HISTOGENESIS OF ACUTE HEMORRHAGIC PANCREATITIS IN DOGS*

DAVID SAFADI, M.D.; ROBERT B. PFEFFER, M.D., and J. WILLIAM HINTON, M.D.
From the Department of Surgery, New York University Post-Graduate Medical School, New York, N.Y.

The past 50 years have seen numerous ingenious experiments designed to understand the perplexing phenomenon, acute hemorrhagic pancreatitis. A critical review of the data accumulated from the experiments of Opie,[1] Rich and Duff,[2] Smyth,[3] and Popper, Necheles and Russell[4] have failed to clarify many of the fundamental mechanisms of this entity. The numerous experiments designed by our group to arrive at a proper understanding of acute pancreatitis made it mandatory to study the sequential morphologic events in the development of this process.

This study was made difficult by the lack of a suitable technique which could repeatedly induce hemorrhagic pancreatitis. Some of the other methods for the production of this lesion, described in the literature, were not effective in any large percentage of animals in our laboratory. Among the many techniques we have used were: injection of bile into the main pancreatic duct with or without ligation of the duct; injection of trypsin or a combination of trypsin and bile into the main pancreatic duct; injection of bile or trypsin following trauma to the gland; and vagal stimulation following feeding of animals, with or without ligation of both pancreatic ducts. Six dogs were used in each of the foregoing experiments (a total of 24), and time of sacrifice in each instance was 72 hours.

It became apparent that the technique of Pfeffer, Stasior and Hinton,[5] employing a closed duodenal loop obstruction, would regularly produce acute hemorrhagic pancreatitis in dogs (12 dogs were utilized). Fortified by this new technique, we intended to study the sequential morphologic alterations in the course of the development of hemorrhagic pancreatitis as part of a new concept of its pathogenesis. This paper deals with the histologic alterations; correlative concomitant studies will be reported elsewhere.

METHOD

Twelve mongrel dogs, weighing 11 to 20 kg., were used. The animals were fasted for 24 hours preoperatively and given 600,000 units of penicillin. A midline, upper abdominal incision was made, and the

* This work was supported by grants from the John H. Hartford Foundation, Inc., and the U.S. Public Health Service.
Received for publication, March 14, 1958.

duodenum was divided just beyond the pylorus and again beyond the reflection of the pancreas onto the dorsal mesentery. Both ends of the duodenum were inverted, thus creating a closed loop approximately 7 to 10 cm. in length into which the pancreatic ducts drained.

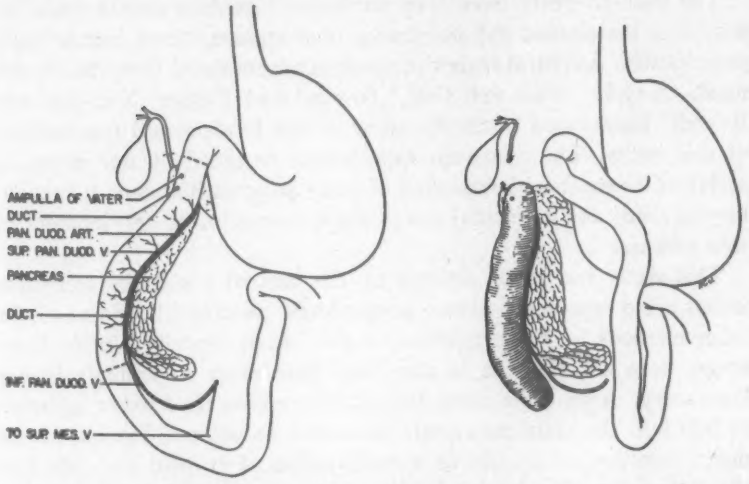

Text-figure 1. On the left, the normal anatomy of the pancreatic region in the dog. On the right, the completed operation, showing the closed duodenal loop and the division and ligation of the common bile duct. (Reproduced with permission from Surgical Forum,[5] p. 249.)

Bile was prevented from entering the duodenal segment by dividing and ligating the common bile duct (Text-fig. 1). Prior to closure of the duodenal loop, irrigation with 150 cc. of warm sterile saline was carried out, and the washings were cultured.

The 12 dogs were sacrificed at hourly intervals (from 0 to 11 hours) by means of an overdose of intravenous Nembutal,® and the gross alterations were observed. Tissue specimens were taken from the head, body, and tail of the pancreas. The tissues were fixed in formalin, and sections prepared from them were stained with hematoxylin and eosin. Cultures were again procured from the fluid content of the closed duodenal loop. Serial photographs were made of each animal in order to record the progression of the lesion. Serum amylase and lipase values were determined preoperatively and at the time of necropsy. In addition, amylase and lipase determinations were made on the fluid in the duodenal loop and the peritoneal fluid when it was present. The histologic studies were carried out without any knowledge of the type of procedure performed, the gross findings, and the hour at which the animal was sacrificed. The independent evaluation of tissue alterations,

the chemical values, and the gross observations were correlated and integrated at a subsequent time. This procedure was employed in all phases of our group studies to avoid any subconscious prejudice or influence upon the findings.

Results

The earliest gross manifestations of pancreatitis were evident at 4 hours. Edema was present in the head and body of the gland, and approximately 30 cc. of hemorrhagic peritoneal fluid appeared (Fig. 1). There was little distinct change in this process during the next 4 hours. The amount of hemorrhagic peritoneal fluid increased consistently, however, and at 9 hours a small hemorrhagic zone appeared in the head of the pancreas. From this point on, progression of the lesion was rapid. At 10 hours the head and body of the pancreas were enveloped by the apoplectic reaction. Finally, at 11 hours, the entire pancreas became a hemorrhagic mass, and the bloody peritoneal fluid had increased to 125 cc. (Fig. 2).

Microscopic alterations were present within one hour following the surgical procedure. There was moderate interlobular edema separating the pancreatic parenchyma, but no inflammatory cells were evident. A few inflammatory elements were present only in the peripancreatic tissue. At 2 hours the edema was accompanied by focal congestion of small non-muscular blood vessels. Throughout this period the pancreatic parenchyma appeared otherwise normal, and the acinar architecture remained intact (Fig. 3). At 4 hours minute foci of extravasated red blood cells could be seen within scattered acini if searched for meticulously. The bulk of the pancreatic parenchyma remained ostensibly "normal" (Fig. 4). The hemorrhagic acini showed slight tinctorial alterations when compared with the neighboring unaffected glands. These lesions were definite and distinct by 5 hours. The hemorrhagic extravasation was now more pronounced, and larger foci were affected (Fig. 5). The lesions were characterized by subtle tinctorial alterations, loss of cellular polarity, disruption of lobular and acinar architecture, and indistinct cellular and nuclear membranes.

The changes in subsequent hours were those of degree and amount. With time, larger areas of parenchyma were increasingly affected without any extension into the edematous interstitial connective tissue. At 8 hours hemorrhagic zones were found in the interstitial tissue; these progressed rapidly until the 11 hour period when extensive hemorrhagic involvement of both parenchyma and interstitial connective tissue became manifest (Fig. 6).

There were no lesions in the branches of the pancreatic ducts or in the large muscular vessels. The latter were free of thrombosis. The

ductal mucosa was intact, and the duct walls were free of necrosis or acute inflammatory cells. The absence of inflammatory cells in the parenchyma and interstitial tissue is a noteworthy feature (Fig. 7). Sections of the closed loop of the duodenum were essentially free of significant intrinsic alterations during the entire 11 hour period, except for evidence of peritonitis. Eventually, if allowed to continue unchecked, the changes which occurred were those ordinarily found in advanced obstruction of the small intestine.

Discussion

Through a preliminary series of dog experiments, it became evident that a closed duodenal loop obstruction would consistently produce an acute hemorrhagic pancreatitis. After this work was concluded, it was discovered that Seidel[6] in 1910 observed a similar lesion produced by means of a closed duodenal loop.

The following were considered important factors in this investigation: The end result of the procedure was a regularly induced acute hemorrhagic pancreatitis; the exclusion of the common bile duct eliminated bile as a causative agent; the operation, as devised, required minimal handling of the pancreas; and immediate examination of the experimental animal after sacrifice avoided tissue autolysis. More significant than these was the anatomic knowledge that the duodenal loop and the head and body of the pancreas shared a common blood supply, the superior pancreatico-duodenal artery. Thus the duodenum served as an excellent monitor, indicating that no interference with the major blood supply of the pancreas had occurred. This last point was a vital key in the hourly study. The results indicated that throughout the development of the pancreatic lesion, the duodenum maintained an adequate blood supply.

In the pancreas the progressive lesion induced had salient characteristics. The earliest lesion noted was a focal extravasation of blood cells into the parenchyma. This was thought to interfere with the acinar nutrition and to lead to parenchymal destruction. The rapidly progressive extension of the lesion, with no evidence of acute inflammatory exudate, was considered indicative of interference with local blood supply. The progressive necrosis and absence of acute inflammatory cells is a feature of a hemorrhagic apoplexy.

The inference that the earliest morphologic alteration was a vascular lesion has been substantiated by the experiments of Reid, Challis, Paulette and Hinton.[7,8] These workers showed that the reflux of bile and of trypsin was not provocative of hemorrhagic pancreatitis although present-day thinking and teaching continue to be dominated

by such concepts. The morphologic sequences observed would seem to justify the belief that a vascular lesion initiates the fulminating pancreatic apoplexy in a short period of time.

Summary

A closed duodenal loop obstruction was used to produce acute hemorrhagic pancreatitis. Sequential histologic studies showed the earliest lesion to be the extravasation of red blood cells which caused disruption and interference with the nutrition of the parenchyma at the acinar level. The histologic lesions of the rapidly progressive apoplectic phenomenon appeared to indicate a response to local vascular lesions.

REFERENCES

1. Opie, E. L. The etiology of acute hemorrhagic pancreatitis. *Bull. Johns Hopkins Hosp.*, 1901, **12**, 182–188.
2. Rich, A. R., and Duff, G. L. Experimental and pathological studies on the pathogenesis of acute haemorrhagic pancreatitis. *Bull. Johns Hopkins Hosp.*, 1936, **58**, 212–259.
3. Smyth, C. J. Etiology of acute hemorrhagic pancreatitis with special reference to the vascular factors. *Arch. Path.*, 1940, **30**, 651–669.
4. Popper, H. L.; Necheles, H., and Russell, K. C. Transition of pancreatic edema into pancreatic necrosis. *Surg. Gynec. & Obst.*, 1948, **87**, 79–82.
5. Pfeffer, R. B.; Stasior, O., and Hinton, J. W. Hourly Observations of the Sequential Development of Acute Hemorrhagic Pancreatitis in the Dog. Surgical Forum. Proceedings of the Forum Session, 43rd Clinical Congress of the American College of Surgeons, Vol. VIII, 1957, pp. 248–251.
6. Seidel, H. Bemerkungen zu meiner Methode der experimentellen Erzeugung der akuten hämorrhagischen Pankreatitis. *Zentralbl. Chir.*, 1910, **37**, 1601–1604.
7. Reid, L. C.; Challis, T. W.; Paulette, R. E., and Hinton, J. W. The Role of Propylthiouracil in Pancreatitis. Surgical Forum. Proceedings of the Forum Session, 42nd Clinical Congress of the American College of Surgeons, Vol. VII, 1956, pp. 445–448.
8. Reid, L. C.; Paulette, R. E.; Challis, T. W., and Hinton, J. W. The mechanism of the pathogenesis of pancreatic necrosis and the therapeutic effect of propylthiouracil. *Surgery*, 1958, **43**, 538–549.

[*Illustrations follow*]

LEGENDS FOR FIGURES

FIG. 1. Necropsy at 4 hours. Early distension of closed duodenal loop with edema of head and body *in situ*. Small amount of hemorrhagic peritoneal fluid at left of liver edge. (1) Pancreas. (2) Duodenum. (3) Peritoneal fluid. (4) Liver. (5) Gall bladder.

FIG. 2. Necropsy at 11 hours. Marked distension of closed duodenal loop. Hemorrhagic pancreatitis present in entire gland. Hemorrhagic peritoneal fluid may be seen between loops of intestine. (1) Pancreas. (2) Duodenum. (3) Peritoneal fluid. (4) Liver. (5) Gall bladder.

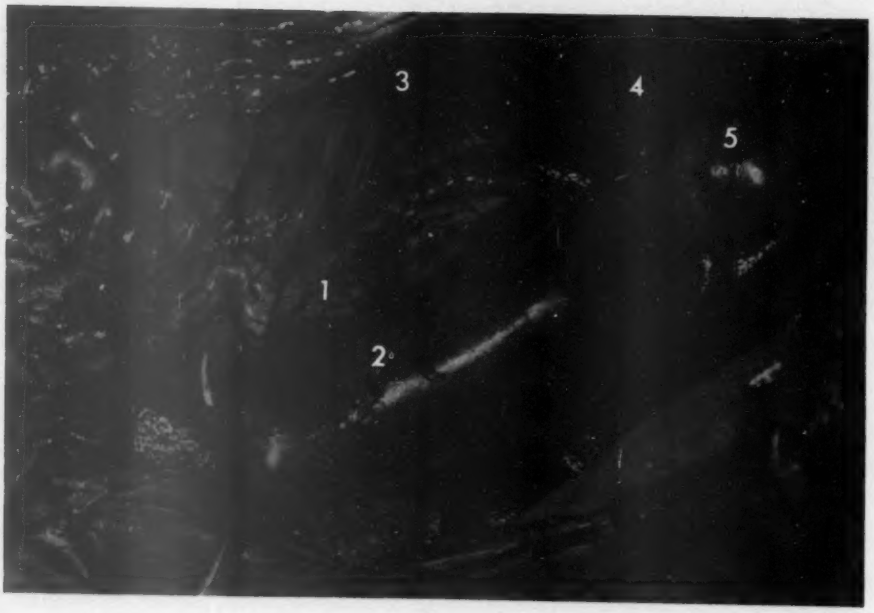

1

2

FIG. 3. Pancreatic architecture is maintained, but acini are separated by a minimal intralobular and intracinar edema. The duct is normal. Hematoxylin and eosin stain. × 65.

FIG. 4. At 4 hours red blood cells are seen between the acinar units. Inflammatory cells are absent. Hematoxylin and eosin stain. × 225.

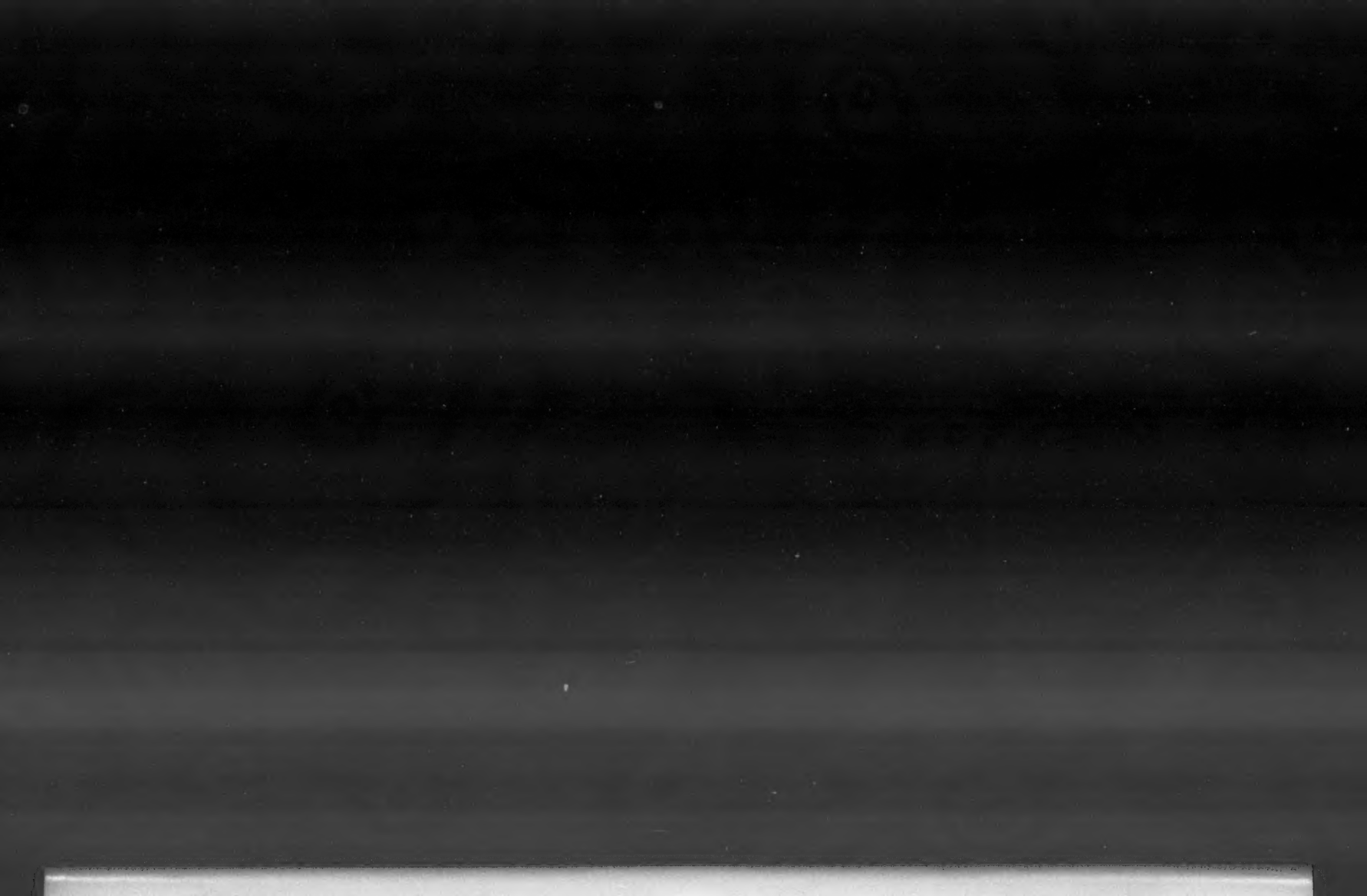

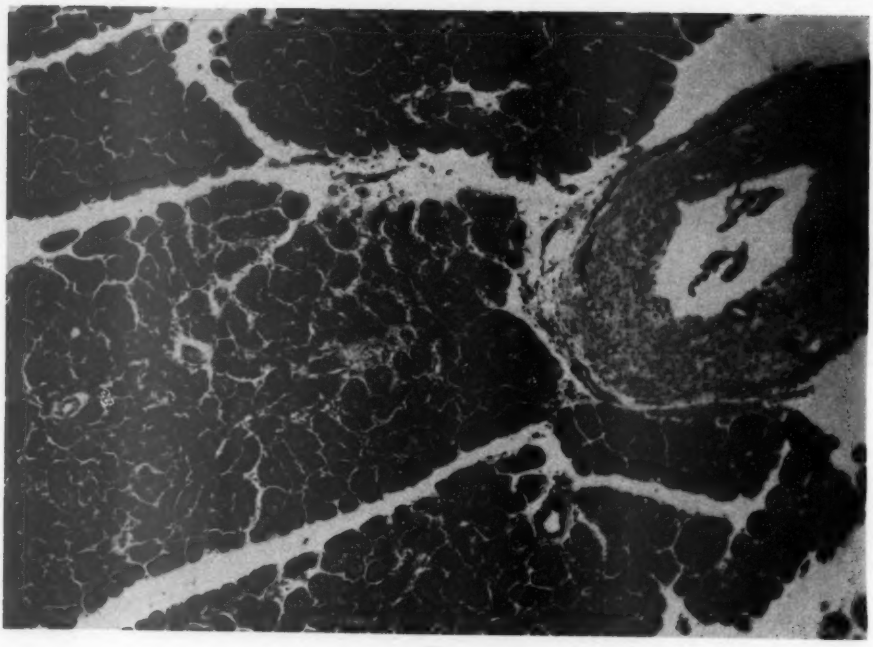

3

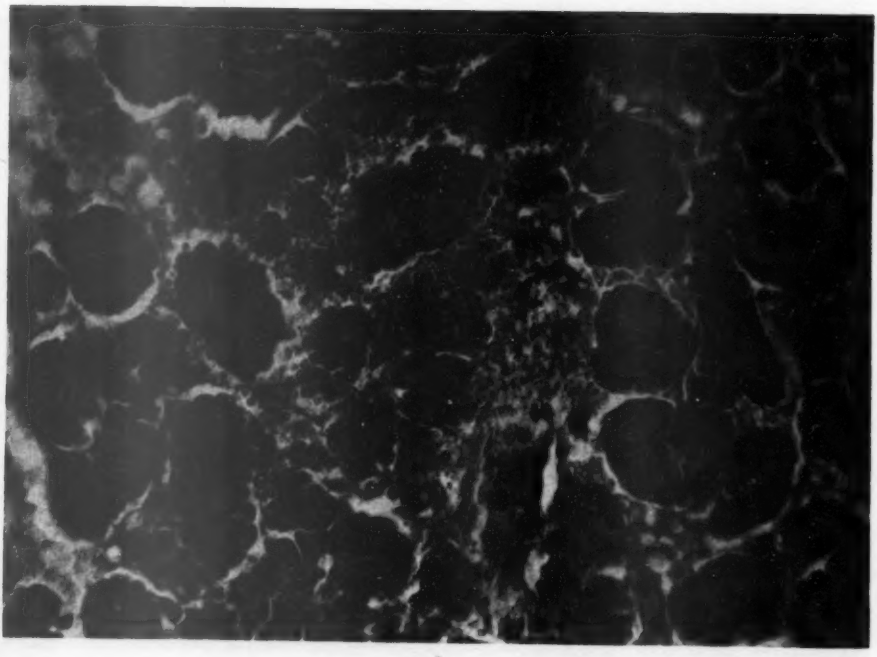

4

FIG. 5. Higher magnification, showing red blood cells separating the pancreatic acini. Hematoxylin and eosin stain. × 600.

FIG. 6. A massive hemorrhage, replacing a large pancreatic lobule. A rim of parenchyma can be seen separating the zone of intralobular hemorrhage from the adjacent interstitial lesion. Hematoxylin and eosin stain. × 65.

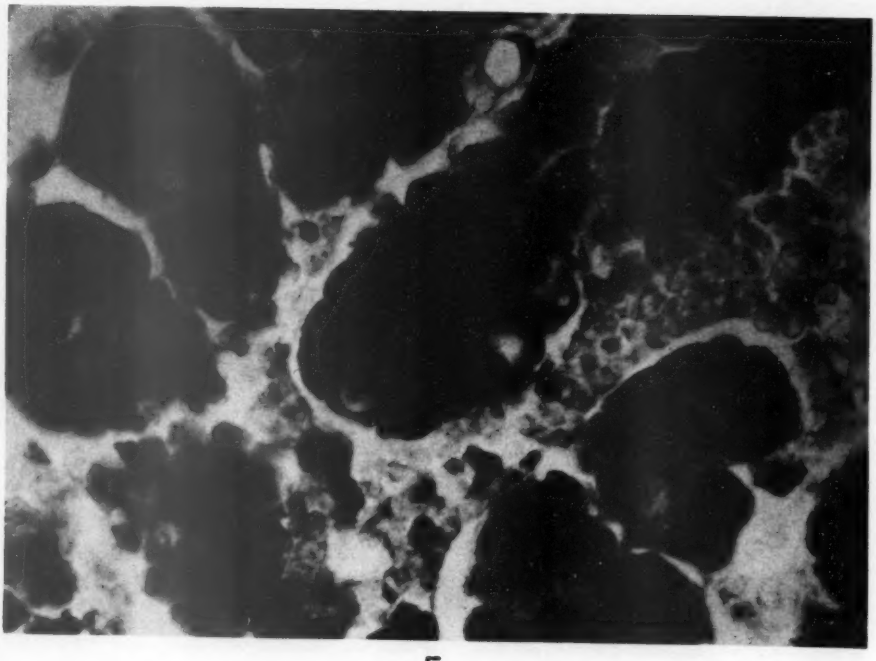

5

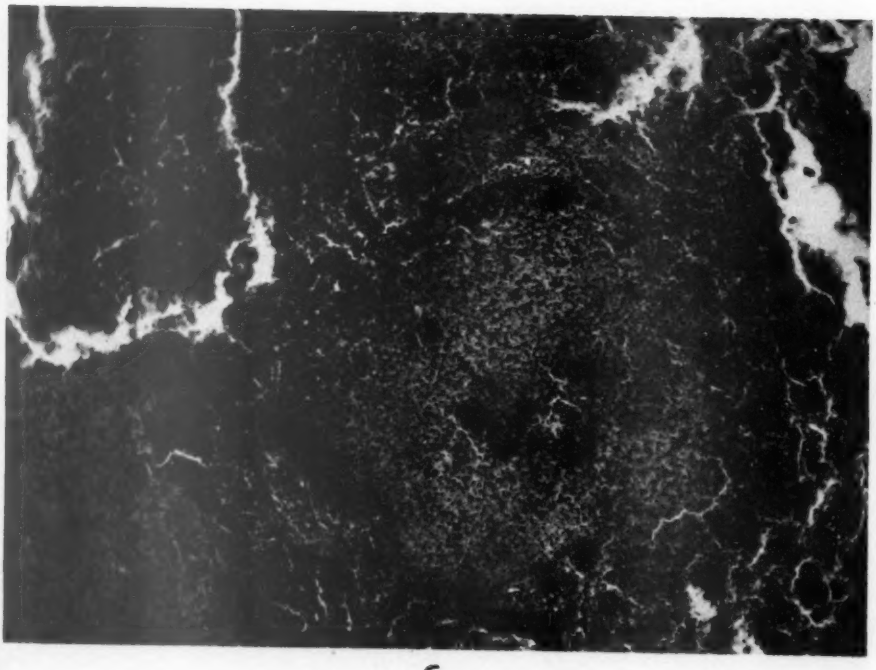

6

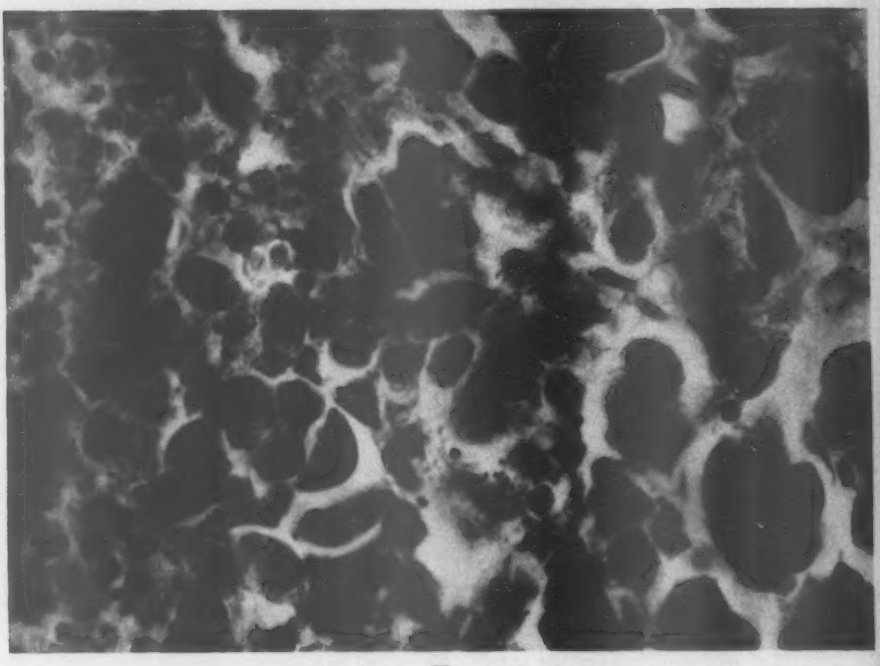

7

FIG. 7. Complete disorganization of pancreatic acini with cellular degenerative changes. Red blood cells are present between the cells. Hematoxylin and eosin stain. × 600.

INDEX TO VOLUME XXXIV

1958

INDEX OF SUBJECTS

Acanthamoeba (Castellani) . . 592*
Adenovirus—tissue culture . . . 789
Adipose tissue—embryogenesis . . 1149
Adrenal—Cushing's disease . . . 1161
——heart-lung preparation . . . 717
——hormone 717
——myelolipoma 487
——newborn 137
——plasma sodium . 557*; 602*; 863
——zona glomerulosa . . . 557*; 863
Age—aorta 1023
——cancer 552*
——cardiac amyloid 593*
——diaphragm tendon 567*
——heart 583*
——infection 573*
Alloxan diabetes 575*
Altitude 583*
Alveolar proteinosis 584*
Amebiasis—experimental . . . 592*
Aminonucleoside—nephrosis 558*; 559*
Amniotic fluid embolism . . . 594*
Amyloid—cardiac 593*
——mycobacterial infection . . . 586*
Anastomosis—uretero-caval . . 561*
Anemia—cardiac hypertrophy . . 149
——heart weight 578*
Anencephaly 169
Anthrax—experimental 573*
Antibiotic agent—aspergillosis . . 585*
Antibody—glomerulus 557*
Antihypertensive treatment 817; 1011
Anti-kidney duck serum . . . 835
Anti-rabbit-kidney duck serum . 557*
Anti-rat-lung serum 558*
Aorta—aging 1023
——atheroma 209; 731; 897
——injury 579*
——polysaccharide 580*
Artery—arteritis 817
——cerebral 631
——hypertension 817
Aspergillosis—experimental . . 585*
Atheroma—aorta 209; 731
——coronary 578*
——Costa Rica 731
——experimental . . 579*; 580*; 897
——Guatemala 578*; 731
——New Orleans . . 209; 578*; 731
Atresia—biliary 565*
——mitral 582*
Atrophy—heart 745
——optic 185
——renal tubules 556*

Bacteria—anthrax 573*
——capsule 595*
——frostbite 575*
——infection 578*
——*Malleomyces pseudomallei* . . 1099
——mycobacteria 586*; 597*
——polysaccharide 551*
——resistance to 578*
Beta mercaptoethylamine . . . 562*
Biliary atresia 565*
Biometry—cervix 555*
Biopsy—renal 556*
Blood-brain barrier 631
Blood dyscrasia—central nervous system 349
——infectious mononucleosis . . 586*
Bone—beta mercaptoethylamine . 562*
——chemodectoma 293
——chondrosarcoma 551*
——fluoride rickets 25
——hyperostosis 562*
——Osgood-Schlatter's disease . . 803
Bone marrow—erythropoiesis . . 570*
——injection 571*
——radiation 571*
Bovine globulin 589*
Brain—blood-brain barrier . . . 631
——infection 577*
——myelin forms 590*
——radiation 588*
Brain filtrate—cell free 600*
——lymphoblastoma 600*
Breast—mucopolysaccharides . . 993
——tumors, mouse 599*
Bronchiolitis obliterans—experimental 600*
Bronchus—bronchiolitis obliterans 600*
——carcinoma, experimental . . 554*
——cigarette smoke 601*
——muco-epidermoid tumor . . 671
——tuberculosis 597*

Calcification—hypervitaminosis D . . . 37; 395
——nephrotoxic 581*
Cancer—age 552*
——lymph node reactivity . . . 589*
"Cancer eye" 602*
Capillary proliferation 1033
Carbon$_{14}$ 551*
Carcinoma—bronchogenic . . . 554*
——cervix 555*
——experimental . . 554*; 555*; 911
——intraepithelial 555*
——mesonephric 603*
——ovary 603*
——squamous 602*
——stomach 531; 554*
——thyroid 552*; 553*
Cardiomegaly—infantile . . 584*; 745
Carotid body tumor 293
Carrageenin 569*
Cat—sodium deficiency 602*
Cataract—dog 965
Cell—chemical mediators . . . 921
——inflammation 921
Central nervous system—anencephaly 169
——demyelinating disease . . . 375
——ground substance 363
——leukemia 349
——myelin forms 590*
——Parkinson's disease 592*
——radiation 588*
Cerebellum—radiation 588*

* Abstract of paper presented at the meeting of the American Association of Pathologists and Bacteriologists held at Cleveland, Ohio, April 24, 25, and 26, 1958.

Cervix 555*
Chemical mediators 921
Chemodectoma 293
Chick embryo 77
Children 552*; 563*; 599*
Cholesterol feeding 579*
Chondroitin sulfate—systemic effects 61
Chondrosarcoma 551*
Chorionic tissue—atypical . . . 601*
Cigarette smoke 601*
Cirrhosis—experimental 568*; 598*; 603*
Clot 591*
Clubbing 237
Collagen disease—lung 585*
"Collecting veins" 556*
Conduction system 588*
Congenital anomaly . 565*; 582*; 965
Congenital heart disease—mitral atresia 582*
Conjoined monster 169
Coronary artery—atheroma . . 578*
Corticosteroid—urinary 561*
Corticosterone—hypertension . . 560*
Corticotropin zinc 121
Cortisone—aortic repair 579*
——aspergillosis 585*
——fibrosis 569*
Costa Rica—atheroma 731
Coxsackie virus 587*
Cow—"cancer eye" 602*
Cross resistance 577*
Cryptococcosis—capsule . . . 595*
——experimental 517
Cushing's disease 1161
Cutaneous tuberculosis 337
Cystic fibrosis of pancreas—myopathy 565*
Cytoplasmic bodies—Parkinsonism 592*
Cytotoxic action of normal human serum 576*

Dehydrogenase—hepatic . . . 568*
Demyelinating disease 375
Deoxyribose nucleic acid—bone marrow 571*
——intestine 572*
——radioautograph 572*
Dermatomyositis 607
Diabetes 121; 575*
Diabetogenic hormone 121
Diaphragm tendon 567*
Diet—cirrhosis 603*
——lipogranuloma 263
——thrombosis 581*
Dihydrocholesterol—cirrhosis . . 598*
Dog—cataract 965
——conduction system 588*
——hydronephrosis 560*
——hypertension 561*
——pancreatitis 1173
——sodium deficiency 602*
——thyroiditis 564*
Dorsal root ganglion—lymphoma 349
Duck serum—anti-kidney . 557*; 835
——anti-lung 558*
Duodenum 591*
Dysgenesis—gonadal 563*
Dysplasia—cervix 555*

——mammary 993

Ear chamber—metastases . . . 576*
Electron microscopy—aortic atheroma 897
——cerebellum 588*
——glomerulus 559*; 885
——nephrosis 559*
——pseudoxanthoma elasticum 566*; 977
——salivary gland virus 604*
——squamous carcinoma 602*
Embolism—amniotic fluid . . . 594*
Embryo—chick 77
Embryogenesis—adipose tissue . 1149
Endobronchitis—tuberculous . . 597*
Endocardium—aging 583*
——fibroelastosis 745
Endocervical smears 555*
Endocrine gland—pituitary injury 433
——postnephrectomy 563*
Endometrium—pregnancy . . . 601*
Endothelium—salivary gland virus 1069
Endotoxin—gram-negative . 589*; 631
Enteric virus 943
Epidermis—aspirated 161
Erythrocytosis—uterine 598*
Erythropoiesis—iron storage . . 570*
Escherichia coli 471
Esophagus—ring 595*
Ethionine 565*; 569*
Excess iron 1139
Extraovarian thecoma 554*
Eye—carcinoma, bovine 602*
——cataract 965
——optic atrophy 185

"Farmers' lung" 585*
Fibroelastosis—endocardial . . . 745
Fibrosis—carrageenin 569*
——hepatic 569*
Fibrous mesothelioma 554*
Finger—clubbing 237
Fluorescent antigen 1081
Fluoride rickets 25
Flying spot microscope 591*
Frostbite 575*
Fungus disease—aspergillus . . 585*
——cryptococcus 517
——mucormycosis 575*

Gamma globulin 604*
Ganglion 349
Gardner lymphosarcoma . 767; 911
Gastric osteodystrophy 285
Gaucher's disease 566*
Globulin—bovine 589*
——inflammation 604*
Glomerulonephritis—experimental 835
——post streptococcal 556*
Glomerulus—electron microscopy . 885
——proteinuria 559*
Glomus jugulare tumor 293
Glucagon—pancreas 565*
Glycogen 566*
Goat—pituitary 433
Gonadal dysgenesis 563*
Gram-negative endotoxin . 589*; 631
Granuloma—mucormycosis . . . 575*
Ground substance 363

Growth hormone 121
Guatemala—atheroma 731
——coronary disease 578*
Guinea pig—high altitude . . . 583*
——thyroiditis 564*
——urinary corticosteroids . . . 561*

Hair—in lung 161
Hamster—melioidosis 1099
——mycobacteria 586*; 597*
Healing—wound 574*
Heart—aging 583*
——amyloid 593*
——anemia 149
——atrophy 584*; 745
——conduction system 588*
——coronary disease 578*
——high altitude 583*
——hyperplasia 584*; 745
——hypertrophy 149
——mitral atresia 582*
——valvular lesions 595*
——weight 578*
Heart-lung preparations . . . 717
Hemangioblastomyxoma . . . 599*
Hematopoiesis—mechanism . . 571*
Hematopoietin 571*
Hematoxylin bodies 1
Hemochromatosis—secondary . . 570*
Hepatectomy—partial 568*
Hepatic fibrosis 569*
Hepatitis—rat 570*
Heredity—cataract 965
——hyperostosis 562*
——optic atrophy 185
——pseudoxanthoma elasticum 566*; 977
Hibernoma 1149
High altitude 583*
Hiroshima—gastric carcinoma . . 531
Histochemistry—aorta 580*
——brain 363
——breast 993
——chemodectoma 293
——deoxyribonucleic acid . . . 607
——glomerulonephritis 835
——hepatectomy 568*
——leiomyometaplasts 273
——lupus erythematosus . . . 1; 607
——mucopolysaccharides 993
——periodic acid-Schiff reaction . 566*
——pseudoxanthoma elasticum 566*; 977
——renal tubules 556*
——wound healing 574*
Hormone—adrenal 717
——mycobacterial infection . . . 586*
Human cells 576*
Hyalin—"alcoholic" 603*
Hyaline membrane disease . . 604*
Hydralazine 817
Hydrocortisone acetate 121
Hydronephrosis—experimental . 560*
Hypercholesterolemia—experimental 579*; 897
Hyperostosis 562*
Hyperplasia—gastric mucosa . . 554*
——myocardium 584*; 745
Hypertension—
experimental . . 560*; 561*; 817
——heart weight 578*
——malignant 579*; 1011
——renal artery obstruction . . . 582*
——renal biopsy 685
——renal lesions 1011
——renal lipids 579*
——treated 817
——vascular lesions 817
Hypertrophy—heart . 149; 584*; 745
Hypervitaminosis D 37; 395
Hypoglycemia—mesothelium . . 554*

Immunity—anthrax 573*
——bacterial 578*
——fluorescence 1081
——globulin 589*
——histochemistry 607
——immunization 564*
——influenza 577*
——leukocyte 574*
——melioidosis 1099
——natural 578*
——properdin 471; 588*
——*Schistosoma mansoni* . . . 577*
——serum 1081
——thyroiditis 564
——trichinosis 596*
——typhoid 577*
Inclusion body—Parkinsonian state 592*
——salivary gland virus 775
Infant 137; 169; 563*; 584*; 587*; 745
Infantile cardiomegaly . . 584*; 745
Infection—amebiasis 592*
——anthrax 573*
——bacterial 578*
——Coxsackie virus 587*
——frostbite 575*
——influenza 577*
——mycobacteria 586*
——properdin 471; 588*
——streptococcus 556*
——typhoid 577*
Infectious mononucleosis . . . 586*
Inflammation—chemical mediators 921
——neutrophil 645
——serum globulin 604*
——skin window 574*
Influenza 577*
Inoculation—tuberculosis . . . 337
Intestine—deoxyribose nucleic acid 572*
——epithelial proliferation . . . 572*
——*Trichinella spiralis* 596*
Iron storage 570*; 1139
Isothiocyanate compounds . . . 1081

Juvenile melanomas 552*
Juxtaglomerular apparatus
. . . . . 557*; 602*; 863

Kidney—
aminonucleoside nephrosis 558*; 559*
——biopsy 685
——"collecting veins" 556*
——electron microscopy . . 559*; 885
——glomerulus 885
——glomerulonephritis 556*
——hydronephrosis 560*
——hypertension 579*; 685
——juxtaglomerular apparatus
. . . . . 557*; 602*; 863

——lipids 579*
——malignant hypertension . . . 1011
——nephritis, experimental . 557*; 558*
——nephrosis 554*
——proteinuria 556*; 559*
——subtotal nephrectomy . . . 563*
——tubular atrophy 556*
——uretero-caval anastomosis . . 561*
——vascular lesions 581*
Klebsiella pneumoniae 471

Leber's disease 185
Leiomyometaplasts 273
Leukemia—central nervous system 349
——mast cell 567*
Leukocytes—chemical mediators . 921
——inflammation 645
——skin window 574*
Lipid—renal 579*
——splenic 1123
Lipoblastomatosis 1149
Lipogranuloma 263
Liquoid 589*
Liver—carrageenin 569*
——cirrhosis, experimental 568*; 598*; 603*
——fibrosis 569*
——hepatectomy 568*
——hepatitis, mouse 570*
——histochemistry 566*
Lung—alveolar proteinosis . . . 584*
——aspergillosis 585*
——capillary proliferation . . . 1033
——cigarette smoke 601*
——collagen disease 585*
——"farmers' lung" 585*
——foreign body 161
——hyaline membrane disease . . 604*
——muco-epidermoid tumor . . . 671
——oxygen therapy 1033
——pneumonitis, experimental . . 1051
——schistosomiasis 577*
——tuberculous endobronchitis . . 597*
Lupus erythematosus . 1; 585*; 607
Lymph glands 586*; 589*
Lymph node—infectious mononucleosis 586*
——reactivity to cancer 589*
Lymphatic—intrasplenic 1123
Lymphoma—central nervous system 349
——experimental 551*; 600*; 767; 911
——plasma cell 599*
——stomach 553*
Lymphosarcoma . . 551*; 767; 911

Macroglobulinemia 592*
Malformations—anencephaly . . 169
——cerebrovascular 169
——double monster 169
——eye 965
——gonadal dysgenesis 563*
——mitral atresia 582*
——selenium 77
Malleomyces pseudomallei . . . 1099
Mammary tumor—mouse . . . 599*
Marrow 570*; 571*
Mast cell leukemia 567*
Mastocytoma 567*
Melanoma—juvenile 552*
Melioidosis 1099
Mercaptoethylamine 562*
Mesenchymoma 599*
Mesonephric carcinoma—ovary . 603*
Mesothelioma 554*
Metabolism—iron storage . . . 1139
Metaplasia—cervix 555*
Metastasis—ear chamber 576*
Microscope—flying spot television 591*
Mitral atresia—congenital . . . 582*
Monkey—cutaneous tuberculosis . 337
——hypervitaminosis D 37
——schistosomiasis 577*
Monster 169
Mouse—bronchial epithelium . . 601*
——cirrhosis 603*
——hair in lung 161
——hepatitis 570*
——lymphoma . . . 600*; 767; 911
——mammary tumor 599*
——melioidosis 1099
——trichinosis 596*
Muco-epidermoid tumor . . . 671
Mucopolysaccharide—atheroma . 580*
——breast 993
——hydration 595*
Mucormycosis 575*
Multiple myeloma—central nervous system 349
Myasthenia gravis 563*
Mycobacteria—photochromogenic . 586*
——virulence 597*
Myelin—demyelinating disease . . 395
Myeloadipose structures—adrenal 487
Myelolipoma 487
Myeloma 349
Myopathy—tocopherol deficiency . 565*

Necrosis—selenium 77
Neoplasm—rat 311
Nephrectomy—experimental . . 563*
Nephritis—experimental . . . 557*; 558*; 835
Nephrosclerosis—malignant . . 1011
——treatment 1011
Nephrosis—aminonucleoside 558*; 559*
——mesothelioma 554*
Nephrotoxic renal disease . . 581*
Nerve—leukemia 349
Neuron—cytoplasmic body . . . 592*
Neurotoxin—influenza 577*
Neutrophil—inflammation . . . 645
New Orleans—atheroma . 209; 731
——coronary disease 578*
Newborn—adrenal 137
——Coxsackie virus 587*
Nuclear changes—cirrhosis . . . 568*
Nucleic acid—spleen 571*
Nutrition—hepatitis 570*

Obstruction—renal artery . . . 582*
Ocular defects 185; 965
Optic atrophy 185
Osgood-Schlatter's disease . . 803
Osteodystrophy 285
Ovary—mesonephric carcinoma . 603*
Oxygen therapy—capillary proliferation 1033

Pancreas—cystic fibrosis . . . 565*
——diabetogenic hormone . . . 121
——feeding 565*
——glucagon 565*
——islets 565*
——pancreatitis 1173
Pancreatin 565*
Papain 61
Papillary carcinoma 553*
Parakeet 562*
Parasite—acanthamoeba . . . 592*
——schistosoma 577*
Parkinsonian state 592*
Patella 803
Permeability—blood-brain . . . 631
Pig 25
Pituitary—histochemistry . . . 566*
——stalk section 433
Placenta—dysfunction 137
——trophoblast 555*
Plasma—hematopoietin 571*
——proteolysin 572*
Plasma cell lymphoma 599*
Plasma sodium—juxtaglomerular apparatus 557*; 863
——zona glomerulosa . . . 557*; 863
Plasmocytoma 599*
Pneumococcus—capsule 595*
Pneumonitis—experimental . . . 1051
——staphylococcal toxin 1051
Polysaccharide—aorta 580*
——atheroma 580*
——breast 993
——Carbon$_{14}$ 551*
Post-term infant 137
Pregnancy—atypical endometrium 601*
——trophoblastic cells 555*
Profibrinolysin 572*
Properdin—infection . . . 471; 588*
——lymphosarcoma 911
Protein 1; 559*; 607
Proteinosis—alveolar 584*
Proteinuria—experimental . . . 559*
——tubular atrophy 556*
Proteolysin 572*
Pseudoxanthoma elasticum 566*; 977

Rabbit—alloxan diabetes 575*
——atheroma . . . 579*; 580*; 897
——bone marrow 571*
——chondroitin sulfate 61
——cirrhosis 598*
——ear chamber 576*
——endotoxin 589*
——frostbite 575*
——glomerulus 559*
——glucagon 565*
——mucormycosis 575*
——nephritis 557*; 835
——pancreas 121
——papain 61
——pneumonitis 1051
——thyroiditis 564*
Radiation—bone marrow 571*
——bronchogenic carcinoma . . . 554*
——cerebellum 588*
——deoxyribose nucleic acid . . 571*
——nucleic acid 571*
——stomach 105
——*Trichinella spiralis* 596*
Radioautograph—chondrosarcoma 551*
——deoxyribose nucleic acid . . 572*
Rat—aminonucleoside nephrosis . 558*
——anthrax 573*
——beta mercaptoethylamine . . 562*
——bronchogenic carcinoma . . . 554*
——carrageenin 569*
——cirrhosis 568*; 603*
——ethionine 565*
——hypertension 560*; 817
——lipogranuloma 263
——lymphosarcoma 551*
——neoplasm 311
——nephrectomy 563*
——nephritis 558*
——radiation 571*
——renal disease 581*
——sodium deficiency 602*
——thrombosis 581*
Reactivity—lymph node 589*
Renal artery—obstruction . . . 582*
Renal function—hydronephrosis . 560*
Retroperitoneal region—chemodectoma 293
Rickets—fluoride 25
Ring—esophagus 595*
Roentgenogram—heart 583*

Salivary gland virus—electron microscopy 604*
——endothelium 1069
——tissue culture 775
Sarcoid—mycobacterial infection . 586*
Schaumann bodies 586*
Schistosoma mansoni 577*
Scleroderma 607
Sebaceous gland 567*
Selenium—in embryo 77
Senile cardiac amyloidosis . . . 593*
Sensitization 607
Serum—cytotoxicity 576*
——immune 1081
——lymphosarcoma 767
Serum globulin—inflammation . 604*
——macroglobulinemia 592*
Sex-linked hyperostosis . . . 562*
Skin—pseudoxanthoma elasticum 566*; 977
——tuberculosis 337
——window 574*
Smear—vaginal, cervical 555*
Smoke—bronchial epithelium . . 601*
Smooth muscle—leiomyometaplasts 273
Sodium deficiency . . . 602*; 863
Sodium fluoride 25
Spleen—lipidosis 1123
Spontaneous tumor 311
Squamous carcinoma 602*
Staphylococcal toxin 1051
Steroids—aortic repair 579*
——carrageenin fibrosis 569*
——diabetogenic 121
Stomach—carcinoma . . . 531; 554*
——fistula 285
——hyperplasia 554*
——lymphoma 553*
——radiation 105
Streptococcus 556*

Stroma—reactivity in cancer . . 589*
Succinic dehydrogenase . . . 568*
Sulfur$_{35}$—chondrosarcoma . . . 551*
Surface-active substance . . . 590*
Swelling—tendon 567*
Syndrome—placental dysfunction . 137

Technique—bacterial capsule . . 595*
——tetrahydrofuran 596*
Television—ultraviolet flying spot microscope 591*
Temporal bone 293
Tendon—diaphragm 567*
Tetrahydrofuran 596*
Thecoma 554*
Thrombus—experimental 581*; 591*; 594*
——*in vitro* 594*
Thymoma 563*
Thymus—myasthenia gravis . . 563*
Thyroid—carcinoma . . . 552*; 553*
——histochemistry 566*
——thyroiditis 564*
Tibial tuberosity 803
Tissue culture—adenovirus . . . 789
——bovine ocular carcinoma . . 602*
——human cells 576*
——enteric virus 943
——salivary gland virus . . 604*; 775
——simian virus 789
Tocopherol deficiency 565*
Toxin—staphylococcal 1051
Trichinella spiralis 596*
Trophoblastic cells 555*
Trypsin 565*
Tuberculosis—bronchus 597*
——cutaneous 337
Tubular atrophy—renal . . . 556*
Tumor—muco-epidermoid . . . 671
——rat 311
Typhoid 577*

Ultraviolet—flying spot microscope 591*
Uretero-caval anastomosis . . 561*
Urinary corticosteroids . . . 561*
Uterus—biometry, cervix . . . 555*
——carcinoma, cervix 555*
——erythrocytosis 598*
——pregnancy 601*

Vaginal smear 555*
Valvular lesions—experimental . 595*
Vascular system—anomaly . . . 169
——thrombosis 581*
Vein—renal collecting 556*
——vertebral plexus 591*
Vertebra—vein 591*
Viosterol 395
Virus—adenovirus 789
——Coxsackie 587*
——enteric 943
——hepatitis, mouse 570*
——influenza 577*
——salivary gland . 604*; 775; 1069
——simian 789
——tissue culture 789; 943
Vitamin D 37; 395

Waldenström—macroglobulinemia 592*
Window—skin 574*
Wound healing 574*

Zona glomerulosa . . . 557*; 863
Zymosan 471; 588*

INDEX OF AUTHORS

Adams, R. B. See Dominguez and Adams (May-June) 560*
Allen, A. C. Juvenile melanomas of children and adults and melanocarcinomas of children. (May-June) 552*
Allen, A. M., and Kinard, R. F. Primary cutaneous inoculation tuberculosis in the *Macaca mulatta* monkey. (March-April) 337
Altschuler, B. See Kuschner, Laskin, Nelson, and Altschuler (May-June) . . 554*
Andersen, A. C., and Shults, F. T. Inherited (congenital) cataract in the dog. (September-October) 965
Andrews, J. R. See Swarm, Andrews, Rubin, Schlachter, Brace, and Miller (May-June) 551*
Angrist, A.; Oka, M.; Nakao, K., and Marquiss, J. The production of valvular lesions by mechanisms which eliminate sensitivity factor. (May-June) . . 595*
Appel, L. L. See Valdivia and Appel (May-June) 583*
Arey, J. B., and DiGeorge, A. Gonadal dysgenesis in infants and children. (May-June) 563*
Arias-Stella, J. On the importance of the atypical endometrial changes associated with the presence of chorionic tissue in the diagnosis of pregnancy. (May-June) 601*
Ashworth, C. T., and Garvey, R. F. The diffuse adrenal lesion in Cushing's disease. Histologic observations on surgically removed adrenals of four cases. (November-December) 1161
Atamer, M. A. See Steinberg, Dietz, Martin, and Atamer (May-June) . . . 571*
Attwood, H. D. The histologic diagnosis of amniotic fluid embolism. (May-June) 594*
Ayres, W. W. Formation of myelin forms from brain tissue by means of surface active substances. (May-June) 590*

Baez, J. See Vellios, Baez, and Shumacker (November-December) 1149
Bahn, R. C.; Ross, G. T., and Schmit, R. W. Comparative histochemical properties of the periodic acid-Schiff (PAS) reactive material of anterior pituitary basophils, Gaucher cells, thyroid colloid and hepatic glycogen. (May-June) 566*
Banson, B. B. See Grisham and Banson (May-June) 568*
Bardawil, W. A.; Toy, B. L.; Galins, N., and Bayles, T. B. Disseminated lupus erythematosus, scleroderma, and dermatomyositis as manifestations of sensitization to DNA-protein. I. An immunohistochemical approach. (July-August) 607
Barest, H. D. See Kwittken and Barest (January-February) 185
Barr, R. See Gore and Barr (May-June) 580*
Barron, A. L. See Shaver, Barron, and Karzon (September-October) 943
Bauer, H. See Sheldon and Bauer (May-June) 575*
Bayles, T. B. See Bardawil, Toy, Galins, and Bayles (July-August) 607
Bechtold, E. See Prior, Bechtold, and Reicher (May-June) 555*
Beher, W. T. See Hartmann, Sieracki, Beher, and Horn (May-June) 598*
Béland, J. E. See McCormack, Béland, Schneckloth, and Corcoran (November-December) 1011
Bélanger, L. F.; Visek, W. J.; Lotz, W. E., and Comar, C. L. Rachitomimetic effects of fluoride feeding on the skeletal tissues of growing pigs. (January-February) 25
Benirschke, K.; Kibrick, S., and Craig, J. M. The pathology of fatal Coxsackie infection in the newborn. (May-June) 587*
Benson, R. E. See Kent, Vawter, Dowben, and Benson (January-February) . 37
Berenbom, M. See Iammarino and Berenbom (May-June) 571*
Bevans, M. See Seegal, Bevans, Hsu, and Rothenberg (May-June) 557*
Bigler, F. C. The morphology of clubbing. (March-April) 237
Black, M. M., and Speer, F. D. Naturally occurring lymph node and stromal reactivity of prognostic significance in human cancer. (May-June) . . . 589*
Black-Schaffer, B., and Turner, M. E. Hyperplastic infantile cardiomegaly; a form of "idiopathic hypertrophy" with or without endocardial fibroelastosis; and a comment on cardiac "atrophy." (July-August) 745
——, and ——. Infantile hyperplastic cardiomegaly. (May-June) 584*
Blundell, G. P. See Taylor, Kennedy, and Blundell (May-June) 573*
Bolande, R. P. Adrenal changes in post-term infants and the placental dysfunction syndrome. (January-February) 137
——. The cytotoxic action of normal human serum on certain human cells propagated *in vitro*. (May-June) 576*
Bond, V. P. See Brecher, Cronkite, Quastler, and Bond (May-June) 572*
Bonner, W. A. See Montgomery and Bonner (May-June) 591*
Boughton, G. A. See Sommers and Boughton (May-June) 554*
Brace, K. See Swarm, Andrews, Rubin, Schlacter, Brace, and Miller (May-June) 551*

* Abstract of paper presented at the meeting of the American Association of Pathologists and Bacteriologists held at Cleveland, Ohio, April 24, 25, and 26, 1958.

Bramhall, J. See Ruebner and Bramhall (May-June) 570*
Braunstein, H. A histochemical study of the polysaccharides of the aorta. (May-June) 580*
——. See Buerger and Braunstein (May-June) 593*
Brecher, G.; Cronkite, E. P.; Conard, R. A., and Smith, W. W. Gastric lesions in experimental animals following single exposures to ionizing radiations. (January-February) 105
——; ——; **Quastler, H., and Bond, V. P.** Study of dynamics of gastrointestinal epithelial proliferation by DNA radioautographs. (May-June) 572*
Brunson, J. G. See Eckman, King, and Brunson (July-August) 631
——. See Fehr and Brunson (May-June) 589*
——. See Nahas, Brunson, King, and Cavert (July-August) 717
Bryant, J. H. See Spicer and Bryant (January-February) 61
Bubelis, I. See Zak, Bubelis, and Paronetto (May-June) 569*
Buck, R. C. The fine structure of the aortic endothelial lesions in experimental cholesterol atherosclerosis of rabbits. (September-October) 897
Buerger, L., and Braunstein, H. Senile cardiac amyloidosis. (May-June) . . 593*
Burckhalter, J. H. See Riggs, Seiwald, Burckhalter, Downs, and Metcalf (November-December) 1081

Camp, F. A. See Prior, Rohner, Camp, and Rustad (May-June) 579*
Campagna-Pinto, D., and Sherwin, R. P. Lymphoma of plasma cell lineage (exclusive of multiple myeloma). (May-June) 599*
Castleman, B. See Rosen, Castleman, and Liebow (May-June) 584*
Cavert, H. M. See Nahas, Brunson, King, and Cavert (July-August) 717
Chandler, A. B. A method for producing a thrombus *in vitro*. (May-June) . . 594*
Chason, J. L. See Dickenman and Chason (March-April) 349
Chesky, V. E. See Hellwig, Chesky, and Welch (May-June) 553*
Clark, R. L., Jr. See Russell, Clark, Ibanez, and White (May-June) 552*
Cohen, H. K. See Culbertson, Smith, Cohen, and Minner (May-June) . . . 592*
Comar, C. L. See Bélanger, Visek, Lotz, and Comar (January-February) . . . 25
Conard, R. A. See Brecher, Cronkite, Conard, and Smith (January-February) . 105
Corcoran, A. C. See Masson, McCormack, Dustan, and Corcoran (September-October) 817
——. See McCormack, Béland, Schneckloth, and Corcoran (November-December) 1011
Cox, A. J., Jr., and DeEds, F. Dietary production of lipogranuloma in rats. (March-April) 263
Cox, F. H. See Lukes and Cox (May-June) 586*
Craig, J. M. See Benirschke, Kibrick, and Craig (May-June) 587*
Crain, R. C. Spontaneous tumors in the Rochester strain of the Wistar rat. (March-April) 311
Cronkite, E. P. See Brecher, Cronkite, Conard, and Smith (January-February) 105
——. See Brecher, Cronkite, Quastler, and Bond (May-June) 572*
Culbertson, C. G.; Smith, J. W.; Cohen, H. K., and Minner, J. R. *Acanthamoeba* (Castellani); Experimental infection in laboratory animals. (May-June) 592*

Dammin, G. J. See Kulka, Hardison, Fremont-Smith, and Dammin (May-June) 575*
Daniel, P. M., and Prichard, M. M. L. The effects of pituitary stalk section in the goat. (May-June) 433
Dannenberg, A. M., Jr., and Scott, E. M. Melioidosis: pathogenesis and immunity in mice and hamsters. II. Studies with avirulent strains of *Malleomyces pseudomallei*. (November-December) 1099
Dawkins, W. A. See Lumb, Shacklett, and Dawkins (May-June) 588*
DeEds, F. See Cox and DeEds (March-April) 263
Deitch, A. D. See Godman, Deitch, and Klemperer (January-February) . . . 1
Dickenman, R. C., and Chason, J. L. Alterations in the dorsal root ganglia and adjacent nerves in the leukemias, the lymphomas and multiple myeloma. (March-April) 349
Dietz, A. A. See Steinberg, Dietz, Martin, and Atamer (May-June) 571*
DiGeorge, A. See Arey and DiGeorge (May-June) 563*
Dmochowski, L.; Sykes, J. A.; Wynne, E. S., and Russell, W. O. Bovine ocular squamous carcinoma ("cancer eye") and its benign precursor lesions in the light of recent tissue culture and electron microscope studies. (May-June) 602*
Dominguez, R., and Adams, R. B. Renal function during and after acute hydronephrosis in the dog. (May-June) 560*
Donati, E. J. See Innes, Donati, and Yevich (January-February) 161
Dowben, R. M. See Kent, Vawter, Dowben, and Benson (January-February) . 37
Downs, C. M. See Riggs, Seiwald, Burckhalter, Downs, and Metcalf (November-December) 1081

Dustan, H. P. See Masson, McCormack, Dustan, and Corcoran (September-October) 817
Dutcher, T. F., and Fahey, J. The histology of the macroglobulinemia of Waldenström. (May-June) 592*

Earle, D. P., Jr. See Jennings and Earle (May-June) 556*
Eckman, P. L.; King, W. M., and Brunson, J. G. Studies on the blood brain barrier. I. Effects produced by a single injection of gram-negative endotoxin on the permeability of the cerebral vessels. (July-August) 631
Ellis, J. T. Glomerular lesions in rabbits with experimentally induced proteinuria as disclosed by electron microscopy. (May-June) 559*
Eyler, W. R. See Sieracki, Horn, and Eyler (May-June) 585*

Fahey, J. See Dutcher and Fahey (May-June) 592*
Fazekas, G., and Schwarz, J. Histology of experimental murine cryptococcosis. (May-June) 517
Fehr, P. E., and Brunson, J. G. Influence of subcutaneously administered bovine globulin on the response of rabbits to intravenous gram-negative endotoxin or Liquoid. (May-June) 589*
Fisher, E. R.; Rodnan, G. P., and Lansing, A. I. Identification of the anatomic defect in pseudoxanthoma elasticum (PXE). (September-October) . . . 977
——; ——, and ——. Identification of the anatomic defect in pseudoxanthoma elasticum (PXE). (May-June) 566*
Foraker, A. G. Comparison of nuclear mass and allied phenomena in uterine cervical squamous mucosa: normal exocervix, metaplasia, dysplasia, intraepithelial carcinoma and invasive carcinoma. (May-June) 555*
Fremont-Smith, P. See Kulka, Hardison, Fremont-Smith, and Dammin (May-June) 575*
Frenkel, J. K. Hormonal effects on a sarcoid-like response with Schaumann bodies and amyloid in golden hamsters infected with photochromogenic mycobacteria. (May-June) 586*
Friedman, L. See Sidransky and Friedman (May-June) 585*
Friedman, N. B. See Nevius and Friedman (May-June) 554*
Frumin, A. M. See Niedzewiedz, Frumin, and Meranze (May-June) 598*
Furth, J. See Ono, Furth, Zompetti, and Hagen (May-June) 567*

Galins, N. See Bardawil, Toy, Galins, and Bayles (July-August) 607
Garvey, R. F. See Ashworth and Garvey (November-December) 1161
Geer, J. C. See Holman, McGill, Strong, and Geer (March-April) 209
Genkins, G. See Mendelow and Genkins (May-June) 563*
Ghosh, H. The mechanisms of formation of various histologic patterns as observed in mammary tumors of mice. (May-June) 599*
Gibbons, R. J. See Jackson, Gibbons, and Magner (November-December) . . 1051
Godman, G. C.; Deitch, A. D., and Klemperer, P. The composition of LE and hematoxylin bodies of systemic lupus erythematosus. (January-February) . 1
Goldberg, G. M., and Saphir, O. Follicular lipidosis of the spleen (a study of the mode of lipid transport with reference to the lymphatics of the spleen. (November-December) 1123
Good, R. A. See Page and Good (July-August) 645
Gordon, H. H. See Weinberg, Gordon, Oppenheimer, and Nitowsky (May-June) 565*
Gordon, J. See Morrison, Robbins, and Gordon (May-June) 563*
Gore, I., and Barr, R. Mucopolysaccharides and experimental atherosclerosis in rabbits. (May-June) 580*
Grand, N. G. Production of salivary gland virus inclusions in cultures of mouse salivary gland. (July-August) 775
Green, R. See Pearson, Grose, and Green (May-June) 568*
Grisham, J. W., and Banson, B. B. Nuclear changes in the liver of the rat associated with developing cirrhosis. (May-June) 568*
Grose, F. See Pearson, Grose, and Green (May-June) 568*
Gruenwald, P. Malformations caused by necrosis in the embryo, illustrated by the effect of selenium compounds on chick embryos. (January-February) . . 77

Hackel, D. B., and Heymann, W. Calcific and lipid-containing vascular lesions in rats with nephrotoxic renal disease. (May-June) 581*
——. See Wilson, Hackel, and Heymann (May-June) 558*
Hagen, P. See Ono, Furth, Zompetti, and Hagen (May-June) 567*
Hardison, W. G. M. See Kulka, Hardison, Fremont-Smith, and Dammin (May-June) 575*
Harkin, J. C., and Recant, L. The earliest lesion in aminonucleoside nephrosis: an electron microscopic study. (May-June) 559*

Hartmann, W. H.; Sieracki, J. C.; Beher, W. T., and Horn, R. C., Jr. Dihydrocholesterol-induced lapin cirrhosis. (May-June) 598*
Hartroft, P. M.; Newmark, L., and Pitcock, J. A. Further observations on the effects of dietary sodium deficiency on renal juxtaglomerular cells and adrenal cortex (rat, dog, cat). (May-June) 602*
——. See Pitcock and Hartroft (May-June) 557*
——. See Pitcock and Hartroft (September-October) 863
Hartroft, W. S. Intracellular ("pseudo-alcoholic") hyalin in experimental dietary cirrhosis of rats and mice. (May-June) 603*
——. See O'Neal, Hartroft, and Thomas (May-June) 581*
Hass, G. M.; Trueheart, R. E.; Taylor, C. B., and Stumpe, M. An experimental histologic study of hypervitaminosis D. (May-June) 395
Haust, M. D. See Kipkie and Haust (May-June) 599*
——. See Movat, More, and Haust (November-December) 1023
——; **More, R. H., and Kipkie, G. F.** The application of tetrahydrofuran (THF) to necropsy and surgical pathology tissue. (May-June) 596*
Hays, J. W. See Paplanus, Zbar, and Hays (January-February) 149
Hazard, J. B. See McCormack, Hazard, and Poutasse (May-June) 582*
Hellstrom, H. R. See Moran and Hellstrom (May-June) 600*
Hellwig, C. A.; Chesky, V. E., and Welch, J. W. Follicular and papillary carcinoma of the thyroid: analysis of 77 cases. (May-June) 553*
Helwig, E. B. See Smith and Helwig (May-June) 553*
Herbut, P. A., and Kraemer, W. H. The effects of animal serums on lymphosarcoma 6C3HED in C3H mice. (July-August) 767
——, and ——. The properdin system in transplantable cancer (Gardner lymphosarcoma 6C3HED). (September-October) 911
Heymann, W. See Hackel and Heymann (May-June) 581*
——. See Wilson, Hackel, and Heymann (May-June) 558*
Hilgar, A. C. See Nadel, Young, and Hilgar (May-June) 561*
Hinton, J. W. See Safadi, Pfeffer, and Hinton (November-December) . . . 1173
Hoge, R. H. See Kay and Hoge (May-June) 603*
Holman, R. L. See Strong, McGill, Tejada, and Holman (July-August) . . . 731
——. See Strong, Tejada, McGill, and Holman (May-June) 578*
——; **McGill, H. C., Jr.; Strong, J. P., and Geer, J. C.** The natural history of atherosclerosis: the early aortic lesions as seen in New Orleans in the middle of the 20th century. (March-April) 209
Hook, E. W. See Wagner and Hook (May-June) 577*
Horn, R. C., Jr. See Hartmann, Sieracki, Beher, and Horn (May-June) . . . 598*
——. See Sieracki, Horn, and Eyler (May-June) 585*
Hosier, D. M. See Newton and Hosier (May-June) 587*
Hsu, K. C. See Seegal, Bevans, Hsu, and Rothenberg (May-June) 557*
——. See Triedman, Metzger, Hsu, and Urquhart (May-June) 558*

Iammarino, R. M., and Berenbom, M. Effect of bone marrow injections on splenic nucleic acids of x-irradiated rats. (May-June) 571*
Ibanez, M. L. See Russell, Clark, Ibanez, and White (May-June) 552*
Innes, J. R. M.; Donati, E. J., and Yevich, P. P. Pulmonary lesions in mice due to fragments of hair, epidermis and extraneous matter accidentally injected in toxicity experiments. (January-February) 161

Jackson, J. R.; Gibbons, R. J., and Magner, D. The effects of staphylococcal toxin on the lungs of rabbits. (November-December) 1051
Jennings, R. B., and Earle, D. P., Jr. Biopsy studies of post streptococcal acute glomerulonephritis. (May-June) 556*
Jones, R. S. Lymphosarcoma in the rat and C^{14}-labeled bacterial polysaccharide. (May-June) 551*

Karzon, D. T. See Shaver, Barron, and Karzon (September-October) 943
Kaufman, N. See Klavins, Kaufman, and Kinney (May-June) 565*
Kay, S., and Hoge, R. H. Mesonephric carcinoma of the ovary. (May-June) . 603*
Kennedy, G. H. See Taylor, Kennedy, and Blundell (May-June) 573*
Kent, G. See Thompson and Kent (May-June) 597*
——, **and Popper, H.** Relationship of the increased iron storage in secondary hemochromatosis to marrow erythropoiesis. (May-June) 570*
Kent, S. P. The distribution of renal lipids in benign and malignant hypertension. (May-June) 579*
——; **Vawter, G. F.; Dowben, R. M., and Benson, R. E.** Hypervitaminosis D in monkeys: a clinical and pathologic study. (January-February) . . . 37
Kibrick, S. See Benirschke, Kibrick, and Craig (May-June) 587*

Kinard, R. F. See Allen and Kinard (March-April) 337
King, W. M. See Eckman, King, and Brunson (July-August) 631
——. See Nahas, Brunson, King, and Cavert (July-August) 717
Kinney, T. D. See Klavins, Kaufman, and Kinney (May-June) 565*
Kipkie, G. F. See Haust, More, and Kipkie (May-June) 596*
——, and **Haust, M. D.** Malignant mesenchymoma (of the hemangioblastomyxomatous variety) in a five-year-old boy. (May-June) 599*
Klavins, J. V.; Kaufman, N., and Kinney, T. D. The effect of feeding pancreas, pancreatin and trypsin in rats fed ethionine. (May-June) 565*
Klemperer, P. See Godman, Deitch, and Klemperer (January-February) . . . 1
Kohn, R. R. Relationship of age to swelling properties of human diaphragm tendon. (May-June) 567*
Kraemer, W. H. See Herbut and Kraemer (July-August) 767
——. See Herbut and Kraemer (September-October) 911
Kulka, J. P.; Hardison, W. G. M.; Fremont-Smith, P., and Dammin, G. J. The course of natural bacterial infection in experimental frostbite of rabbits. (May-June) 575*
Kuschner, M.; Laskin, S.; Nelson, N., and Altschuler, B. Radiation induced bronchogenic carcinoma in rats. (May-June) 554*
Kwittken, J., and Barest, H. D. The neuropathology of hereditary optic atrophy (Leber's disease): the first complete anatomic study. (January-February) . 185

Ladewig, P. P. Anatomy of the "collecting veins" of the kidney (with consideration of functional aspects). (May-June) 556*
Lange, K. See Wachstein and Lange (May -June) 556*
——. See Wachstein and Lange (September-October) 835
Lansing, A. I. See Fisher, Rodnan, and Lansing (May-June) 566*
——. See Fisher, Rodnan, and Lansing (September-October) 977
Larsh, J. E., Jr., and Race, G. J. A histologic study of the upper small intestine of mice immunized with pre-adult irradiated *Trichinella spiralis* larvae. (May-June) 596*
Laskin, S. See Kuschner, Laskin, Nelson, and Altschuler (May-June) 554*
Lazarus, S. S. See Volk and Lazarus (January-February) 121
——. See Volk and Lazarus (May-June) 565*
LaZerte, G. D., and Rapp, I. H. Pathogenesis of Osgood-Schlatter's disease. (July-August) 803
LeBeau, R. W. See Prier and LeBeau (July-August) 789
Lending, M. See Ozzello, Lending, and Speer (March-April) 363
Leuchtenberger, C. See Uyeki, Leuchtenberger, and Salerno (May-June) . . . 571*
——; **Leuchtenberger, R.; Zebrun, W., and Shaffer, P.** Changes in the bronchial epithelium of mice after exposure to cigarette smoke. (A correlated histologic, cytologic and cytochemical study). (May-June) 601*
Leuchtenberger, R. See Leuchtenberger, Leuchtenberger, Zebrun, and Shaffer (May-June) 601*
Lev, M. See McMillan and Lev (May-June) 583*
Leventhal, M. L. See Saphir and Leventhal (May-June) 555*
Lichtenberg, F. V., and Ritchie, L. S. Trapping of "schistosomula" in the lung of *Macaca mulatta* with experimentally induced resistance to *Schistosoma mansoni* infection; pathologic study. (May-June) 577*
Liebow, A. A. See Rosen, Castleman, and Liebow (May-June) 584*
Lipkin, L. E. The relation of neuronal cytoplasmic bodies to Parkinsonian states. (May-June) 592*
Lotz, W. E. See Bélanger, Visek, Lotz, and Comar (January-February) . . . 25
Lukes, R. J., and Cox, F. H. Clinical and morphologic findings in 30 fatal cases of infectious mononucleosis. (May-June) 586*
Lumb, G.; Shacklett, R. S., and Dawkins, W. A. Conduction tissue studies in human and canine hearts. (May-June) 588*
Lupton, C. H. See McManus and Lupton (May-June) 574*
Luse, S. A., and Smith, M. G. Electron microscopy of the growth cycle of human strain of salivary gland virus grown in tissue culture. (May-June) . . . 604*

MacMahon, H. E., and Schatzki, R. The pathology of the lower esophageal ring. (May-June) 595*
Magner, D. See Jackson, Gibbons, and Magner (November-December) . . 1051
Marquiss, J. See Angrist, Oka, Nakao, and Marquiss (May-June) 595*
Martin, R. A. See Steinberg, Dietz, Martin, and Atamer (May-June) 571*
Masson, G. M. C.; McCormack, L. J.; Dustan, H. P., and Corcoran, A. C. Hypertensive vascular disease as a consequence of increased arterial pressure. Quantitative study in rats with hydralazine-treated renal hypertension. (September-October) 817

McBroom, R. D. See Norman and McBroom (May-June) 578*
McCormack, L. J. Idiopathic demyelinating disease in youth: a study of three cases. (March-April) 375
——. See Masson, McCormack, Dustan, and Corcoran (September-October) . . 817
——; **Béland, J. E.; Schneckloth, R. E., and Corcoran, A. C.** Effects of antihypertensive treatment on the evolution of the renal lesions of malignant nephrosclerosis. (November-December) 1011
——; **Hazard, J. B., and Poutasse, E. F.** Obstructive lesions of the renal artery associated with remediable hypertension. (May-June) 582*
McGill, H. C., Jr. See Holman, McGill, Strong, and Geer (March-April) . . 209
——. See Strong, McGill, Tejada, and Holman (July-August) 731
——. See Strong, Tejada, McGill, and Holman (May-June) 578*
McManus, J. F. A., and Lupton, C. H. The healing wound as a chemical system: a histochemical study. (May-June) 574*
McMillan, J. B., and Lev, M. The aging heart. I. Endocardium. (May-June) 583*
McNeil, C. Changes in serum globulins during inflammatory processes. (May-June) 604*
Mendelow, H., and Genkins, G. The thymoma and myasthenia gravis. (May-June) 563*
Menkin, V. Chemical mediators in relation to cytologic constituents in inflammation. (September-October) 921
Meranze, D. R. See Niedzewiedz, Frumin, and Meranze (May-June) 598*
Mescon, H. See Strauss and Mescon (May-June) 567*
Metcalf, T. G. See Riggs, Seiwald, Burckhalter, Downs, and Metcalf (November-December) 1081
Metzger, H. See Triedman, Metzger, Hsu, and Urquhart (May-June) 558*
Miller, E. See Swarm, Andrews, Rubin, Schlachter, Brace, and Miller (May-June) 551*
Minner, J. R. See Culbertson, Smith, Cohen, and Minner (May-June) . . . 592*
Monaghan, E. A. See Rebuck, Monto, and Monaghan (May-June) 574*
Montgomery, P. O., and Bonner, W. A. The ultraviolet flying spot television microscope. (May-June) 591*
Monto, R. W. See Rebuck, Monto, and Monaghan (May-June) 574*
Moran, T. J. See Totten and Moran (May-June) 585*
——, **and Hellstrom, H. R.** The pathogenesis of experimental bronchiolitis obliterans. (May-June) 600*
More, R. H. See Haust, More, and Kipkie (May-June) 596*
——. See Movat, More, and Haust (November-December) 1023
Morrison, A. B.; Robbins, T., and Gordon, J. Subtotal (5/6) nephrectomy on weanling rats and the long term changes in the bones and endocrine organs. (May-June) 563*
Movat, H. Z.; More, R. H., and Haust, M. D. The diffuse intimal thickening of the human aorta with aging. (November-December) 1023
Mowry, R. W. The value of mucopolysaccharide hydration in the demonstration of microbial capsules in paraffin sections: with special reference to *Cryptococcus neoformans* and pneumococci. (May-June) 595*
Muirhead, E. E., and Stirman, J. A. Dietary protein and hypertension of dog; protection by uretero-caval anastomosis with a study of kidneys so treated. (May-June) 561*
Mulligan, R. M. Necropsy study of 257 persons with cancer and 70 years of age and older. (May-June) 552*
Murphy, E. S., and Yasuda, A. Carcinoma of the stomach in Hiroshima, Japan. (May-June) 531
Murray, M. A study of the alterations in proteolytic and profibrinolytic activity of the plasma in various disease entities. (May-June) 572*

Nadel, E .M.; Young, B. G., and Hilgar, A. C. Urinary corticosteroids in Hartley strain 2 and strain 13 guinea pigs. (May-June) 561*
Nahas, G. G.; Brunson, J. G.; King, W. M., and Cavert, H. M. Functional and morphologic changes in heart lung preparations following administration of adrenal hormones. (July-August) 717
Nakao, K. See Angrist, Oka, Nakao, and Marquiss (May-June) 595*
Nelson, N. See Kuschner, Laskin, Nelson, and Altschuler (May-June) . . . 554*
Nevius, D. B., and Friedman, N. B. Fibrous mesotheliomas, extraovarian thecomas and physiologic effects of mesotheliomas including hypoglycemic and nephrotic syndromes. (May-June) 554*
Newmark, L. See Hartroft, Newmark, and Pitcock (May-June) 602*
Newton, W. A., Jr., and Hosier, D. M. Coxsackie infection in infants and children: focal and disseminated; fatal and nonfatal. (May-June) 587*

Niedzwiedz, A.; Frumin, A. M., and Meranze, D. R. Uterine erythrocytosis. (May-June) 598*
Nitowsky, H. M. See Weinberg, Gordon, Oppenheimer, and Nitowsky (May-June) 565*
Norman, T. D., and McBroom, R. D. The effect of anemia, hypertension, and anemia with hypertension upon heart weight. (May-June) 578*

Oka, M. See Angrist, Oka, Nakao, and Marquiss (May-June) 595*
O'Neal, R. M.; Hartroft, W. S., and Thomas, W. A. Anatomic features of thrombosis induced in rats by dietary means alone. (May-June) 581*
Ono, S.; Furth, J.; Zompetti, L., and Hagen, P. Relation of blood mast cells to tissue mast cells; of mastocytoma to mast cell leukemia. (May-June) . . 567*
Oppenheimer, E. H. See Weinberg, Gordon, Oppenheimer, and Nitowsky (May-June) 565*
Ozzello, L.; Lending, M., and Speer, F. D. The ground substance of the central nervous system in man. (March-April) 363
——, and Speer, F. D. The mucopolysaccharides in the normal and diseased breast; their distribution and significance. (September-October) 993

Page, A. R., and Good, R. A. A clinical and experimental study of the function of neutrophils in the inflammatory response. (July-August) 645
Pak Poy, R. K. F. Electron microscopy of the mammalian renal glomerulus; the problems of intercapillary tissue and the capillary loop basement membrane. (September-October) 885
Paplanus, S. H.; Zbar, M. J., and Hays, J. W. Cardiac hypertrophy as a manifestation of chronic anemia. (January-February) 149
Paronetto, F. See Popper, Paronetto, and van der Noen (May-June) . . . 569*
——. See Zak, Bubelis, and Paronetto (May-June) 569*
Pearson, B.; Grose, F., and Green, R. Histochemical changes in liver succinic dehydrogenase during rapid growth following partial hepatectomy. (May-June) 568*
Pfeffer, R. B. See Safadi, Pfeffer, and Hinton (November-December) . . . 1173
Pitcock, J. A. See Hartroft, Newmark, and Pitcock (May-June) 602*
——, and Hartroft, P. M. Correlation of the degree of granulation of juxtaglomerular cells of man with the level of plasma sodium and with the width of the zona glomerulosa of the adrenal cortex. (May-June) 557*
——, and ——. The juxtaglomerular cells in man and their relationship to the level of plasma sodium and to the zona glomerulosa of the adrenal cortex. (September-October) 863
Plaut, A. Myelolipoma in the adrenal cortex (myeloadipose structures). (May-June) 487
Pollak, A. The variation in virulence for golden hamsters of different strains of mycobacteria. (May-June) 597*
Popper, H. See Kent and Popper (May-June) 570*
——; Paronetto, F., and van der Noen, H. Studies on mechanism of hepatic fibrosis. (May-June) 569*
Poutasse, E. F. See McCormack, Hazard, and Poutasse (May-June) 582*
Pratt, P. C. Pulmonary capillary proliferation induced by oxygen inhalation. (November-December) 1033
Prichard, M. M. L. See Daniel and Prichard (May-June) 433
Prier, J. E., and LeBeau, R. W. Cellular lesions in monkey kidney epithelium induced by adenoviruses and viruses of simian origin. (July-August) . . 789
Prior, J. T.; Bechtold, E., and Reicher, N. B. Trophoblastic cells in vaginal and endocervical smears: problems concerned with their recognition and interpretation. (May-June) 555*
——; Rohner, R. F.; Camp, F. A., and Rustad, H. The effects of cortisone upon aortic intimal repair in the hypercholesterolemic rabbit. (May-June) . . 579*

Quastler, H. See Brecher, Cronkite, Quastler, and Bond (May-June) . . . 572*

Race, G. J. See Larsh and Race (May-June) 596*
Ramamurti, P., and Taylor, H. E. Skeletal lesions caused by beta mercaptoethylamine in rats. (May-June) 562*
Rapp, I. H. See LaZerte and Rapp (July-August) 803
Rebuck, J. W.; Monto, R. W., and Monaghan, E. A. Defects in leukocytic defenses in skin windows in disease. (May-June) 574*
Recant, L. See Harkin and Recant (May-June) 559*
Reicher, N. B. See Prior, Bechtold, and Reicher (May-June) 555*
Relman, A. S. See Sommers, Relman, and Smithwick (July-August) 685

Riggs, J. L.; Seiwald, R. J.; Burckhalter, J. H.; Downs, C. M., and Metcalf, T. G. Isothiocyanate compounds as fluorescent labeling agents for immune serum. (November-December) 1081
Ritchie, L. S. See Lichtenberg and Ritchie (May-June) 577*
Robbins, L. L. See Sniffen, Soutter, and Robbins (July-August) 671
Robbins, T. See Morrison, Robbins, and Gordon (May-June) 563*
Rodnan, G. P. See Fisher, Rodnan, and Lansing (May-June) 566*
——. See Fisher, Rodnan, and Lansing (September-October) 977
Rohner, R. F. See Prior, Rohner, Camp, and Rustad (May-June) 579*
Rose, N. R. See Terplan, Witebsky, and Rose (May-June) 564*
Rosen, S. H.; Castleman, B., and Liebow, A. A. Alveolar proteinosis. (May-June) 584*
Ross, G. T. See Bahn, Ross, and Schmit (May-June) 566*
Ross, Oscar A. Experimental studies of the *in vivo* relationships of the properdin system to resistance to infection. (May-June) 471
——. Experimental studies of the *in vivo* relationships of the properdin system to resistance to infection. (May-June) 588*
Rothenberg, M. S. See Seegal, Bevans, Hsu, and Rothenberg (May-June) . . 557*
Rubin, P. See Swarm, Andrews, Rubin, Schlachter, Brace, and Miller (May-June) 551*
Ruebner, B., and Bramhall, J. The effect of nutritional factors on experimental virus hepatitis in mice. (May-June) 570*
Russell, W. O. See Dmochowski, Sykes, Wynne, and Russell (May-June) . . 602*
——; **Clark, R. L., Jr.; Ibanez, M. L., and White, E. C.** Intraglandular distribution of thyroid carcinoma as shown by whole organ subserial sections; pathologic study of 47 cases. (May-June) 552*
Rustad, H. See Prior, Rohner, Camp, and Rustad (May-June) 579*

Safadi, D.; Pfeffer, R. B., and Hinton, J. W. The histogenesis of acute hemorrhagic pancreatitis in dogs. (November-December) 1173
Salerno, P. R. See Uyeki, Leuchtenberger, and Salerno (May-June) 571*
Saphir, O. See Goldberg and Saphir (November-December) 1123
——, **and Leventhal, M. L.** Production of lesions resembling carcinoma *in situ* of the cervix uteri. (May-June) 555*
Schatzki, R. See MacMahon and Schatzki (May-June) 595*
Schlachter, L. See Swarm, Andrews, Rubin, Schlachter, Brace, and Miller (May-June) 551*
Schlumberger, H. G. Sex-linked hyperostosis in the parakeet. (May-June) . . 562*
Schmit, R. W. See Bahn, Ross, and Schmit (May-June) 566*
Schneckloth, R. E. See McCormack, Béland, Schneckloth, and Corcoran (November-December) 1011
Schoolman, H. M. See Szanto, Schwartz, Schoolman, and Spurrier (May-June) 600*
Schwartz, R. D. See Yesner, Schwartz, and Spiro (May-June) 591*
Schwartz, S. O. See Szanto, Schwartz, Schoolman, and Spurrier (May-June) . 600*
Schwarz, J. See Fazekas and Schwarz (May-June) 517
Scott, E. M. See Dannenberg and Scott (November-December) 1099
Seegal, B. C.; Bevans, M.; Hsu, K. C., and Rothenberg, M. S. Immediate nephritis produced in rabbits by duck anti-rabbit-kidney serum: localization of the antibody in the glomeruli. (May-June) 557*
Seiwald, R. J. See Riggs, Seiwald, Burckhalter, Downs, and Metcalf (November-December) 1081
Selye, H. Gastric osteodystrophy. (March-April) 285
Shacklett, R. S. See Lumb, Shacklett, and Dawkins (May-June) 588*
Shaffer, P. See Leuchtenberger, Leuchtenberger, Zebrun, and Shaffer (May-June) 601*
Shaver, D. N.; Barron, A. L., and Karzon, D. T. Cytopathology of human enteric viruses in tissue culture. (September-October) 943
Sheldon, W. H., and Bauer, H. Activation of quiescent mucormycotic granulomas in rabbits by induction of acute alloxan diabetes. (May-June) 575*
Sherwin, R. P. See Campagna-Pinto and Sherwin (May-June) 599*
Shoden, A., and Sturgeon, P. Iron storage. I. The influence of time on the redistribution of excess storage iron. (November-December) 1139
Shultz, F. T. See Andersen and Shultz (September-October) 965
Shumacker, H. B. See Vellios, Baez, and Shumacker (November-December) . 1149
Sidransky, H., and Friedman, L. Pulmonary aspergillosis associated with cortisone and antibiotic administration; human and experimental studies. (May-June) 585*
Sieracki, J. C. See Hartmann, Sieracki, Beher, and Horn (May-June) 595*
——; **Horn, R. C., Jr., and Eyler, W. R.** Pulmonary changes in the so-called "collagen diseases." (May-June) 585*

Skelton, F. R. Production and inhibition of hypertensive vascular disease in the rat by corticosterone. (May-June) 560*
Smith, J. L., Jr., and Helwig, E. B. Malignant lymphoma of the stomach; its diagnosis, distinction and biologic behavior. (May-June) 553*
Smith, J. W. See Culbertson, Smith, Cohen, and Minner (May-June) . . . 592*
Smith, M. G. See Luse and Smith (May-June) 604*
Smith, W. W. See Brecher, Cronkite, Conard, and Smith (January-February) . 105
Smithwick, R. H. See Sommers, Relman, and Smithwick (July-August) . . . 685
Sniffen, R. C.; Soutter, L., and Robbins, L. L. Muco-epidermoid tumors of the bronchus arising from surface epithelium. (July-August) 671
Sommers, S. C., and Boughton, G. A. Relation of gastric epithelial hyperplasia to carcinoma. (May-June) 554*
——; **Relman, A. S., and Smithwick, R. H.** Histologic studies of kidney biopsy specimens from patients with hypertension. (July-August) 685
Soutter, L. See Sniffen, Soutter, and Robbins (July-August) 671
Speer, F. D. See Black and Speer (May-June) 589*
——. See Ozzello and Speer (September-October) 993
——. See Ozzello, Lending, and Speer (March-April) 363
Spicer, S. S., and Bryant, J. H. Systemic effects in rabbits receiving injections of papain and chondroitin sulfate. (January-February) 61
Spiro, H. M. See Yesner, Schwartz, and Spiro (May-June) 591*
Spurrier, W. See Szanto, Schwartz, Schoolman, and Spurrier (May-June) . . 600*
Steinberg, B.; Dietz, A. A.; Martin, R. A., and Atamer, M. A. Mechanism of hematopoiesis: hemopoietins in normal human plasma. (May-June) . . . 571*
Stirman, J. A. See Muirhead and Stirman (May-June) 561*
Strauss, J. S., and Mescon, H. Histologic reaction patterns of the human sebaceous gland. (May-June) 567*
Strong, J. P. See Holman, McGill, Strong, and Geer (March-April) 209
——; **McGill, H. C., Jr.; Tejada, C., and Holman, R. L.** The natural history of atherosclerosis; comparison of the early aortic lesions in New Orleans, Guatemala, and Costa Rica. (July-August) 731
——; **Tejada, C.; McGill, H. C., Jr., and Holman, R. L.** Coronary atherosclerosis in New Orleans versus Guatemala. (May-June) 578*
Stumpe, M. See Hass, Trueheart, Taylor, and Stumpe (May-June) 395
Sturgeon, P. See Shoden and Sturgeon (November-December) 1139
Swarm, R. L.; Andrews, J. R.; Rubin, P.; Schlachter, L.; Brace, K., and Miller, E. Radioautographic demonstration of sulfur^{35} in neoplastic and certain other biopsied tissues of a patient with chondrosarcoma. (May-June) . 551*
Sykes, J. A. See Dmochowski, Sykes, Wynne, and Russell (May-June) . . . 602*
Szanto, P. B.; Schwartz, S. O.; Schoolman, H. M., and Spurrier, W. The pathogenesis of experimental lymphoblastoma induced in C_3HEB mice by means of cell-free brain filtrates. (May-June) 600*

Tannenberg, J. The hyaline membrane syndrome or disease: a dangerous misnomer. (May-June) 604*
Taylor, C. B. See Hass, Trueheart, Taylor, and Stumpe (May -June) 395
Taylor, H. E. See Ramamurti and Taylor (May-June) 562*
Taylor, M. J.; Kennedy, G. H., and Blundell, G. P. The correlation in the rat of age with its degree of resistance to anthrax. (May-June) 573*
——. See Strong, McGill, Tejada, and Holman (July-August) 731
——. See Strong, Tejada, McGill, and Holman (May-June) 578*
Terplan, K. L.; Witebsky, E., and Rose, N. R. Experimental thyroiditis in rabbits, guinea pigs, and dogs, following immunization with species specific thyroid extract. (May-June) 564*
Thomas, W. A. See O'Neal, Hartroft, and Thomas (May-June) 581*
Thompson, J. R., and Kent, G. Occult tuberculous endobronchitis in surgically resected lung specimens. (May-June) 597*
Thompson, S. W. II. Leiomyometaplasts, particles of unknown significance in smooth muscle cells. (March-April) 273
Totten, R. S., and Moran, T. J. The histology of "farmers' lung." (May-June) 585*
Toy, B. L. See Bardawil, Toy, Galins, and Bayles (July-August) 607
Triedman, R. S.; Metzger, H.; Hsu, K. C., and Urquhart, F. E. Localization of duck anti-rat-lung serum in rat glomeruli associated with the occurrence of immediate nephritis. (May-June) 558*
Trueheart, R. E. See Hass, Trueheart, Taylor, and Stumpe (May-June) . . . 395
Turner, M. E. See Black-Schaffer and Turner (May-June) 584*
——. See Black-Schaffer and Turner (July-August) 745

Urquhart, F. E. See Triedman, Metzger, Hsu, and Urquhart (May-June) . . 558*
Uyeki, E. M.; Leuchtenberger, C., and Salerno, P. R. Changes in the deoxyribose nucleic acid (DNA) synthesis of bone marrow from rabbits after x-irradiation (a microspectrophotometric study). (May-June) 571*

Valdivia, E., and Appel, L. L. Radiologic study of the heart in guinea pigs living at simulated high altitude. (May-June) 583*
Van der Noen, H. See Popper, Paronetto, and van der Noen (May-June) . . 569*
Vawter, G. F. See Kent, Vawter, Dowben, and Benson (January-February) . . 37
——. Congenital mitral atresia. (May-June) 582*
Vellios, F.; Baez, J., and Shumacker, H. B. Lipoblastomatosis: a tumor of fetal fat different from hibernoma. Report of a case with observations on the embryogenesis of human adipose tissue. (November-December) 1149
Visek, W. J. See Bélanger, Visek, Lotz, and Comar (January-February) . . . 25
Vogel, F. S. The association of vascular anomalies with anencephaly: a postmortem study of nine cases in one of which unilateral anencephaly was present in a conjoined double monster. (January-February) 169
——. Changes in the fine structure of cerebellar neurons following ionizing radiation. (May-June) 588*
——. Enhanced susceptibility of proliferating endothelium to salivary gland virus under naturally occurring and experimental conditions. (November-December 1069
Volk, B. W., and Lazarus, S. S. The effect of various diabetogenic hormones on the structure of the rabbit pancreas. (January-February) 121
——, and ——. The pancreatic islets of rabbits after glucagon administration. (May-June) 565*

Wachstein, M., and Lange, K. Histologic and histochemical studies of the rabbit glomerulonephritis produced by specific anti-kidney duck serum. (September-October) 835
——, and ——. The relationship of proteinuria to tubular atrophy as studied by enzymatic histochemistry. (May-June) 556*
Wack, J. P., and Wyatt, J. P. The role of the vertebral venous plexus in the dissemination of labeled blood clots. (May-June) 591*
Wagner, R. R., and Hook, E. W. Cross resistance to cerebral typhoid infection and influenza virus neurotoxicity. (May-June) 577*
Weinberg, T.; Gordon, H. H.; Oppenheimer, E. H., and Nitowsky, H. M. Myopathy in association with tocopherol deficiency in cases of congenital biliary atresia and cystic fibrosis of the pancreas. (May-June) 565*
Welch, J. W. See Hellwig, Chesky, and Welch (May-June) 553*
White, E. C. See Russell, Clark, Ibanez, and White (May-June) 552*
Wilson, S. G. F.; Hackel, D. B., and Heymann, W. Aminonucleoside nephrosis in rats. (May-June) 558*
Witebsky, E. See Terplan, Witebsky, and Rose (May-June) 564*
Wood, S., Jr. Pathogenesis of metastasis formation observed *in vivo* in the rabbit ear chamber. (May-June) 576*
Wood, W. B., Jr. Natural and acquired resistance to bacterial infections: some comments on principles. (May-June) 578*
Wyatt, J. P. See Wack and Wyatt (May-June) 591*
Wynne, E. S. See Dmochowski, Sykes, Wynne, and Russell (May-June) . . . 602*

Yasuda, A. See Murphy and Yasuda (May-June) 531
Yesner, R.; Schwartz, R. D., and Spiro, H. M. Studies in histology of the duodenum. (May-June) 591*
Yevich, P. P. See Innes, Donati, and Yevich (January-February) 161
Young, B. G. See Nadel, Young, and Hilgar (May-June) 561*

Zacks, S. I. Chemodectomas occurring concurrently in the neck (carotid body), temporal bone (glomus jugulare) and retroperitoneum; report of a case with histochemical observations. (March-April) 293
Zak, F. G.; Bubelis, I., and Paronetto, F. Experimental fibroplasia in the liver induced by carrageenin in the normal rat and under the influence of cortisone and ethionine. (May-June) 569*
Zbar, M. J. See Paplanus, Zbar, and Hays (January-February) 149
Zebrun, W. See Leuchtenberger, Leuchtenberger, Zebrun, and Shaffer (May-June) 601*
Zompetti, L. See Ono, Furth, Zompetti, and Hagen (May-June) 567*